Identification of Gcn1 binding proteins and characterization of their effect on Gcn2 function

A thesis submitted in partial fulfillment of the requirements for the degree Doctor of Philosophy in Biochemistry

Massey University, Albany
New Zealand

Renuka Shanmugam
ID – 09202463

2015

Abstract

All cells must have the ability to deal with a variety of environmental stresses. Failure to adapt and protect against adverse stress conditions can lead to cell death. One important stress that affects all cells is amino acid limitation. Amino acids are building blocks of proteins. Gcn2 is a protein kinase, activated under conditions of amino acid limitation and the active Gcn2 reduces the general protein synthesis and specifically increases the synthesis of a protein called Gcn4, a transcription factor of stress response genes.

Gcn2 is found in virtually all eukaryotes. In addition to the amino acid limitation it protects cells to a large array of stress conditions such as glucose and purine limitation, high salt, reactive oxygen species and UV irradiation. Interestingly, Gcn2 has been found to have acquired additional functions in higher eukaryotes such as cell cycle regulation, viral defense and memory formation. Not surprisingly, Gcn2 has been implicated in diseases and disorders such as abnormal feeding behaviour, cancer, Alzheimer's disease, impaired immune response, congestive heart failure, and susceptibility to viruses including HIV. Despite of its medical relevance, so far it is unknown how the cell ensures proper Gcn2 function.

Yeast studies have uncovered that for almost all Gcn2 functions Gcn2 must bind to its positive effector protein Gcn1. Gcn1 is proposed to be a scaffold protein, strongly suggesting that it serves as a platform for recruiting other proteins close to Gcn2 to fine-tune its activity. For this reason, in this study, we set out to comprehensively identify all proteins binding to Gcn1, i.e. generate the **Gcn1 interactome**, using a procedure that allowed us to also identify proteins that only weakly or transiently contact Gcn1 (a typical property of regulatory proteins). We have identified several potential Gcn1 binding proteins from published and *in house* data. Sixty six of these were further analyzed using the respective deletion strains. Ten of these deletion strains were unable to grow under amino acid starvation conditions. Five of these showed reduced eIF2α phosphorylation, strongly suggesting that they are positive effectors of Gcn2. Using plasmids from the Yeast Genome Tiling Collection, we were able to rescue the Gcn2 function of three deletion strains (*kem1*Δ, *msn5*Δ and *sin3*Δ), indicating that the defect was due to the deletion of the respective gene. In addition, some of these proteins were confirmed to reciprocally bind to Gcn1. Finally, we show that Kem1 partially facilitates activation of Gcn2 via Gcn1 and it may play a role as a positive regulator of Gcn2. Furhther the interactions were validated by reciprocal immunoprecipitation. Taken together, this study sheds light on novel Gcn1 binding proteins regulating Gcn2.

Acknowledgements

I am extremely thankful and deeply indebted to my research guide Dr. Evelyn Sattlegger. You have been a phenomenal mentor for me. I would like to thank you for your invaluable advice, encouragement and continuous support which helped me a lot to come across the obstacles that I had in the last four years. Thank you very much for your continuous encouragement in every step right from the preliminary stage to the final stage of this research. I would also like to thank you for your patience in proof reading my thesis over and over again and helping me to improve my English writing skills in addition to getting my thesis done.

I would like to thank my research co-supervisor Dr. Mark Patchett.

Further, I would like to extend my thanks to my laboratory colleagues and friends Su Jung Lee, Viviane Jochmann and Rashmi Ramesh.

My special thanks go to my laboratory colleague and friend Michael Bolech. Thank you very much for being there always for me.

I am very grateful to Hayley Prescott, Paulina Hanson Manful and Kay Evans, for proof reading my thesis and making it to read well.

I am thankful to my interns Tina Fritzsche, Hayley Prescott, Katharina Dahlmann and Katja Dammann for helping me to get the screening done.

Table of Contents

Table of Figures

Table of Tables

Abbreviations

The following abbreviations are used in addition to the chemical symbols from the periodic table of elements and the International System of Units (SI)

3AT	3-Amino-1, 2, 4-triaxole
ABC	ATP Binding Cassette
APS	Ammonium PerSulphate
ATP	Adenosine tri phosphate
BSA	Bovine Serum Albumin
DNA	Deoxyribonucleic acid
EDTA	Ehtylenediamine tetra acetic acid
Co-IP	Co-Immunoprecipitation
DMSO	Dimethylsulfoxide
EDTA	Ethylene Diamine Tetra acetic Acid
eEF3	Eukaryotic Elongation Factor 3
eIF2	Eukaryotic Initiation Factor 2
eIF2α-P	Eukaryotic Initiation Factor 2 phosphorylated alpha subunit
eIF2B	Guanine nucleotide exchange factor
EtBr	Ethidium Bromide
GAAC	General Amino Acid Control
Gcn1	General control non-derepressible 1
Gcn2	General control non-derepressible 2
Gcn3	General control non-derepressible 3
Gcn4	General control non-derepressible 4
HIV	Human immunodeficiency virus
kDa	Kilo Dalton
LB	Luria- Bertani
mRNA	Messenger ribonucleic acid
NaCl	Sodium Chloride
NaOH	Sodium hydroxide

OD	Optical Density
ORF	Open Reading Frame
p	Plasmid
PAGE	Polyacrylamide Gel Electrophoresis
PEG	Polyethylene glycol
Pgk1	3-Phosphoglycerate kinase
PVDF	Polyvinylidine Difluoride
RNase	Ribonuclease
rpm	Revolutions per minute
RT	Room Temperature
SD	Synthetic Dextrose
SDS	Sodium Dodecyl Sulphate
SM	Sulfometuron Methyl
SM^S	Sensitivity to sulfometuron methyl
ss	Single strand
Slg-	Slow growth
TAE	Tris-Acetate EDTA
TBS	Tris-Buffered Saline
TBS-T	TBS-Tween
TC	Tertiary Complex
TEMED	N, N, N, N- Tetramethylethylenediamine
Y2H	Yeast Two Hybrid
YPD	Yeast extract Peptone Dextrose
YPG	Yeast extract Peptone Glycerol

Chapter 1 Introduction

Every living organism undergoes various challenges from the changing environmental conditions. All organisms have evolved with the ability to respond to changing environmental conditions by reprogramming their gene expression profile, metabolic activities and adjusting the translation rate. Such rapidly acting mechanisms are important for the survival of cells under sudden environmental changes. The environmental conditions that are not favouring optimal cell growth are called stresses. Stresses can be of physical, chemical or biological in nature; temperature, pH, salt, chemicals and nutrient availability. The molecular mechanism that operates in the budding yeast (*Saccharomyces cerevisiae*) cells to recognize and respond to amino acid limitation is known as the General Amino Acid Control (GAAC) (*1*).

1.1 Overview of the General Amino Acid Control (GAAC)

According to the current working model of the GAAC that was proposed by Sattlegger et al. (2000) (Figure 1.1), uncharged tRNAs (tRNAs not conjugated with amino acids) that accumulate under amino acid limiting conditions occupy the A-site of translating ribosomes and then are transferred to Gcn2 by the Gcn1-Gcn20 complex. It appears that Gcn1 may function by facilitating the entry of uncharged tRNAs to the A-site or by transferring them from the A-site to Gcn2 (*2-4*). The binding of uncharged tRNAs to the HisRS like region of Gcn2 results in activation of Gcn2 that is in a latent state under replete conditions (*5, 6*). Active Gcn2 phosphorylates the serine 51 residue in the alpha subunit of eukaryotic initiation factor (eIF2), resulting in a phosphorylated eukaryotic initiation factor (eIF2α-P) (*7*). The phosphorylated form of eIF2 is unable carry out the translation initiation process (*8*) thereby leading to reduced global protein synthesis. In parallel to this, the synthesis of a protein called Gcn4 is elevated, which is a transcription factor for many stress response genes (*9*).

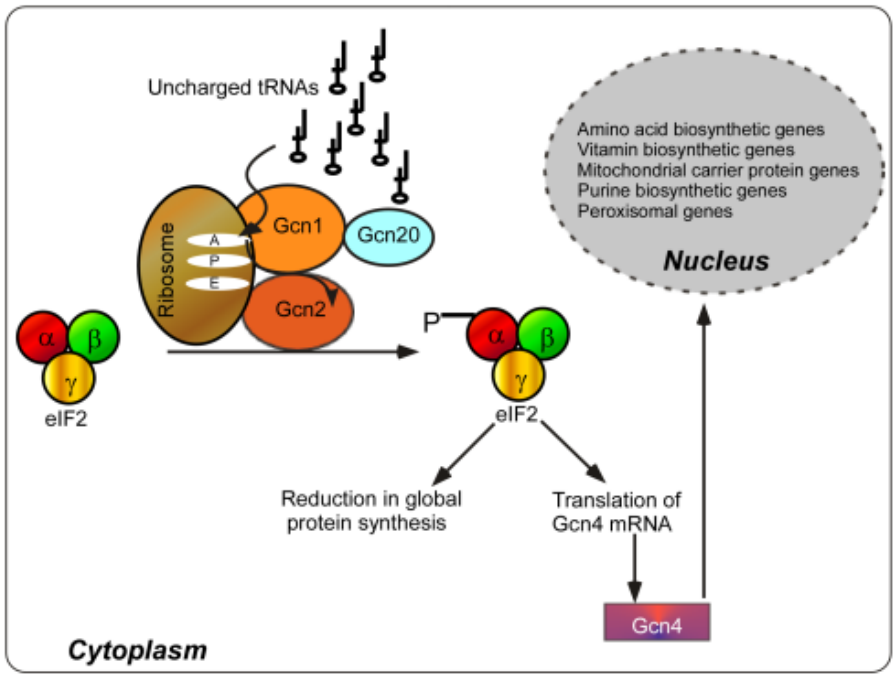

Figure 1.1. Overview of the GAAC. The uncharged tRNA pool is increased under amino acid limiting conditions. The uncharged tRNAs are delivered to Gcn2 by the Gcn1/Gcn20 complex on the ribosome. Binding of uncharged tRNAs to Gcn2 results in activation of the kinase, which in turn phosphorylates eIF2α. Phosphorylation of eIF2 results in reduction of global protein synthesis in parallel to increased translation of Gcn4 mRNA. Gcn4 is a transcription factor for genes involved in amino acid biosynthesis, vitamin biosynthesis, purine biosynthesis and mitochondrial carrier proteins.

The genes targeted by Gcn4 are involved in various biosynthetic pathways, including but not limited to amino acid biosynthesis, amino acid precursor biosynthesis, vitamin biosynthesis, peroxisome biogenesis and purine biosynthesis (*9*). Thus, by activating Gcn2 under amino acid starvation conditions the cells conserve its resources by reducing the general protein synthesis and redirect them for the synthesis of critical stress response proteins. The roles of each molecular player in the GAAC pathway are discussed below.

1.1.1 Gcn2 (General Control Nonderepressible 2)

Gcn2 is a multi-domain serine/threonine protein kinase. It contains an N-terminal domain that binds to the Gcn1/Gcn20 complex, a pseudo kinase domain with no enzymatic function, a kinase catalytic domain, a domain with sequence similarity to Histidyl-tRNA Synthetase (His-RS related domain) and a C-terminal ribosome binding or dimerization domain (Fig 1.2) (*10*).

The N-terminal domain of Gcn2 was called GI domain as it was found in Gcn2 and IMPACT (*11*). This domain is now known as the RWD domain because of its presence in RING finger protein, WD repeat proteins and DEAD like helicase (*12*).

Gcn2 is held inactive via several auto-inhibitory molecular interactions until it is exposed to an activation signal (*5, 6*). It is widely accepted that uncharged tRNAs that accumulate under amino acid starvation conditions are transferred to Gcn2 by the Gcn1-Gcn20 complex and the delivered tRNAs then bind to the HisRS-like domain of Gcn2 that resembles Histidyl-tRNA Synthetase (HisRS) (*5, 13, 14*). All forms of uncharged tRNAs investigated so far can bind to the HisRS domain of Gcn2 (*5*). The interaction of uncharged tRNAs to the HisRS related domain of Gcn2 brings about a conformational change in the protein kinase and C-terminal domain resulting in activation of Gcn2 (*5*). The highly conserved N-terminal RWD domain of Gcn2 binds to the Gcn1-Gcn20 complex (*13*). Overexpression of the Gcn2-RWD domain or Gcn1 (2052-2383) fragment impaired Gcn2 activation under amino acid limiting conditions (*4, 11, 13*). Furthermore, mutational studies revealed that Arg-2259 present in the conserved Gcn1 sequence (2052-2383) was essential for Gcn1-Gcn2 interaction and for Gcn2 function *in vivo*, suggesting that Gcn1-Gcn2 interaction via these regions is required for Gcn2 activation (*4*). The C-terminal region of Gcn2 binds to the ribosome (*3*) that also facilitates dimerization of Gcn2 (*15-17*). The ability of Gcn2 to dimerize and bind to the ribosome is required for Gcn2 activation (*18*).

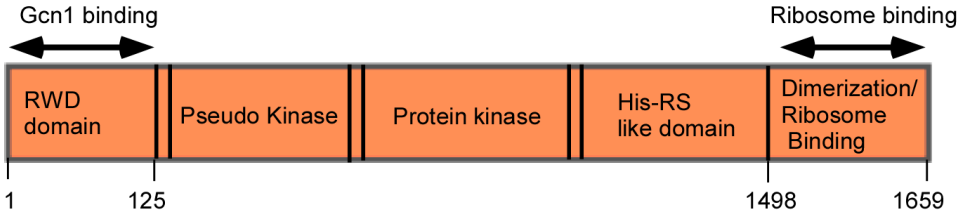

Figure 1.2. Representation of domains in Gcn2. Regions denoted with a double headed arrow are required for binding to the ribosome or Gcn1.

1.1.2 Gcn1/Gcn20 complex

Gcn1 is a large cytoplasmic protein with a molecular mass of 296 kDa and the first protein reported as a positive effector of Gcn2 (*2, 19*). Studies suggest that Gcn1 consists of regions for binding to Gcn2 (*4, 13*), Gcn20 (*20*), and the ribosome (*4*) (Figure 1.3). In addition, sequence analysis of Gcn1 suggests that it has more than twenty HEAT repeats spread throughout the protein (Figure 1.3B). The name HEAT was derived from proteins in which the repeats were first identified; **H**untington, **E**longation factor 3, Protein phosphatase 2**A** and **T**OR (PI3 kinase) (*21*).

The HEAT repeats are tandemly repeated, 37-47 amino acid long repeats (*22*). In HEAT repeat proteins, neighbouring repeats stack together into a single domain with a continuous core, forming an elongated super helix (*22*) (Figure 1.3C) that function as protein-protein interaction surfaces (*22*). The structure of HEAT repeats present in Gcn1 has not been resolved yet. The structure of HEAT repeats found in the PR65/A subunit of human protein phosphatase 2A is shown (Figure 1.3C).

Proteins containing HEAT repeats are usually large and known to interact with a wide variety of proteins (*21, 22*). Proteins with HEAT repeats may function as scaffold proteins by forming a platform on which signalling molecules can assemble in order to make a multiprotein complex (*23*). In addition, scaffold proteins function by localizing signalling molecules at specific sites in the cell or by protecting activated molecules from inactivation. The fact that Gcn1 is large,

having several HEAT repeats, suggests that it functions as a scaffold protein. In agreement with the idea that Gcn1 may act as a scaffold protein, it was found in a complex with many other proteins (*24-27*).

The steady state level of Gcn20 was found to be dependent on Gcn1 as the amount of Gcn20 was reduced in *gcn1*Δ strain compared to that of the wild type (*2*). The 85 kDa Gcn20 protein contains two regions that are highly similar to ATP binding cassettes (ABCs) (*2*). ABCs couple the energy of ATP hydrolysis to transport a wide a variety of molecules (metabolic products, lipids, sterols and drugs) across intra and extracellular membranes (*28*). Gcn1 was localized throughout the cytoplasm and did not show any obvious association with plasma or vacuolar membranes and these findings made it unlikely that Gcn1-Gcn20 complex function as an amino acid transporter. However, in the presence of ATP, the Gcn1-Gcn20 complex has an increased affinity for ribosomes than either Gcn1 or Gcn20 alone and the ATP stimulated ribosome binding of Gcn1-Gcn20 complex was dependent on the ABCs of Gcn20, suggesting that Gcn20 contribute to the interaction of Gcn1-Gcn20 to the ribosome (*2*). However ABCs of Gcn20 are not necessary for promoting Gcn2 activation *in vivo*, thus ATP stimulated Gcn1-polysome interaction is dispensable for sensing amino acid starvation. These observation lead to a model in which, under stress conditions such as carbon starvation or heat shock where uncharged tRNAs would not be expected to accumulate, the increased ribosome binding of the Gcn1-Gcn20 complex may facilitate activation of Gcn2 (*2*).

The middle portion of Gcn1 (amino acids 1330-1641) has sequence similarity to the N-terminal HEAT domain of eEF3 (eukaryotic elongation factor 3) (*19*), which is involved in translation elongation (*29*). In each round of translation elongation, eEF3 promotes the binding of charged tRNAs to the ribosomal acceptor site (A-site) and release of uncharged tRNAs from the exit site (E-site) (*29*). Due to the sequence similarity between Gcn1 and eEF3 it has been proposed that Gcn1 functions on the ribosome at the A-site in an eEF3-like manner to transfer the uncharged tRNAs from the ribosomal A site to Gcn2 (*2*).

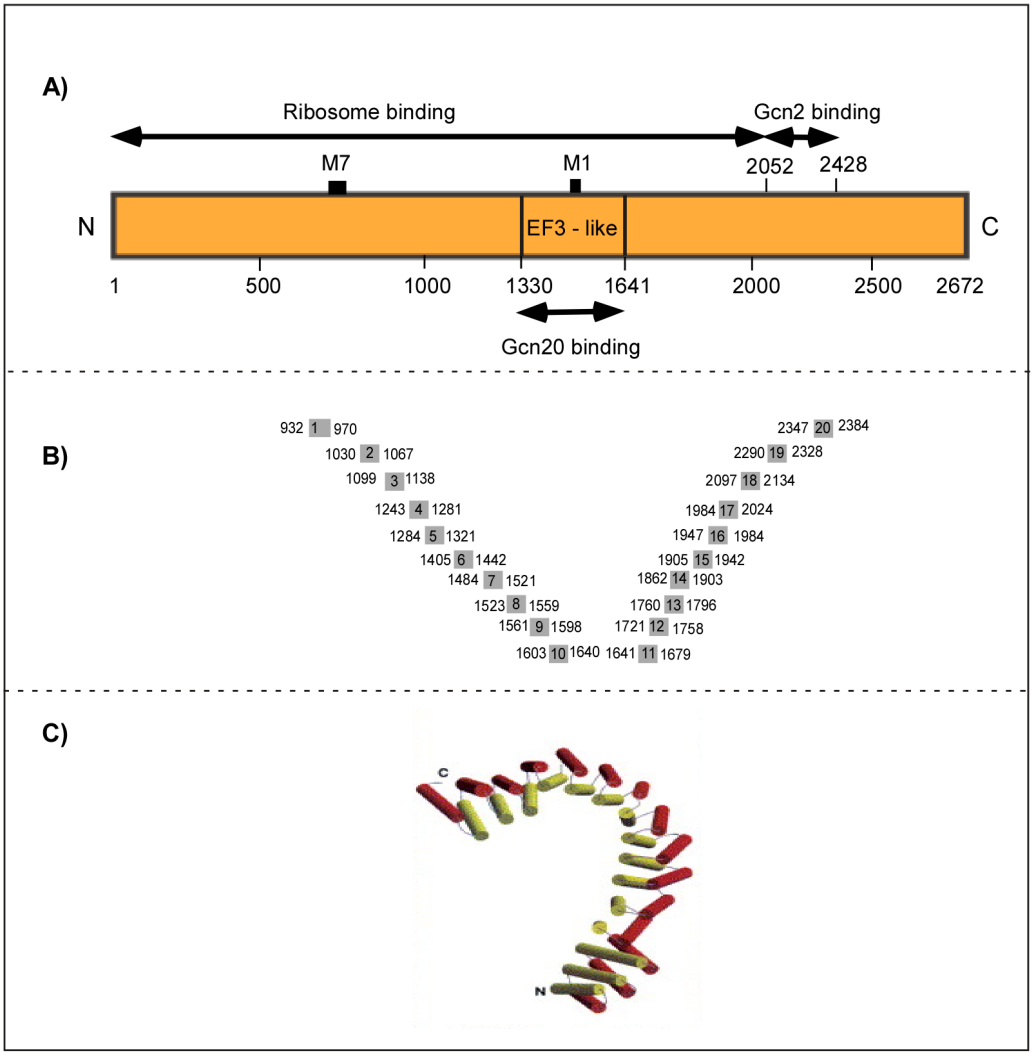

Figure 1. 3 A) Schematic representation of segments in Gcn1. Regions denoted with double headed arrows are required for ribosome, Gcn2 or Gcn20 binding. The Gcn20 binding region of Gcn1 has sequence homology to eEF3. M1 and M7 are the regions required for efficient ribosome binding. B) The 20 HEAT repeats of Gcn1 and their amino acid sequence range (data obtained from Swiss-Prot). C) The structural arrangement of HEAT repeats in PR65/A subunit of human protein phosphatase 2A (Picture taken from Andrade et al. (2001)).

In conjunction with the idea that Gcn1 is required for the transfer of the starvation signal to Gcn2, the kinase activity of Gcn2 was not affected in the cell extract obtained from the *gcn1*Δ strain; however the strain was unable to activate Gcn2 under amino acid starvation conditions (*19*). In addition, it has been demonstrated that the N-terminal three quarters of Gcn1 (residues 1-2052) is

required for its interaction with the translating ribosomes (polysomes) indicating that the sensing of starvation signal occurs on the ribosome and that the Gcn1-ribosome interaction is essential for Gcn2 function (*4, 30*).

In line with this idea that the Gcn1-ribosome interaction is essential for Gcn2 function, mutations in two different areas (M1 and M7) in the ribosome binding region of Gcn1 that have sequence similarity to eEF3 have reduced Gcn1-ribosome binding, associated with impaired Gcn2 activity (*30*). The region of Gcn1 that has sequence similarity to eEF3 binds to Gcn20 (Figure 1.3A) (*20*). Similarly to Gcn1, Gcn20 also has sequence similarity to eEF3 (*20*) and ribosome biding activity (*2*). Deletion of Gcn1 abolished eIF2α phosphorylation by Gcn2 (*19*) while deletion of Gcn20 reduced eIF2α phosphorylation by Gcn2 (*20*) suggesting that Gcn20 is required to co-operate with Gcn1 in mediating activation of Gcn2 (*20*).

1.1.3 eIF2 (eukaryotic Initiation Factor 2)

The only known substrate of active Gcn2 in *Saccharomyses cerevisiae* is the eukaryotic initiation factor 2 (eIF2). It is a hetero trimer consisting of three subunits (α, β and γ) and is involved in translation initiation. In the first step of translation initiation, eIF2 delivers the charged methionyl initiator tRNA (Met-tRNAi^{Met}) to the small 40S ribosomal subunit. In order to do this, eIF2 binds to the 40S subunit as a trimeric complex containing Met-tRNAi^{Met} and GTP; once initiation is completed it is subsequently released as an inactive eIF2-GDP binary complex. This eIF2-GDP is recycled to eIF2-GTP by the guanine nucleotide exchange factor eIF2B to participate in another round of translation initiation (Figure 1.4A).

This recycling of eIF2-GDP to eIF2-GTP can only happen if eIF2 is not phosphorylated, since phosphorylated eIF2 has a stronger affinity to eIF2B. Due to its stronger binding to eIF2B, phosphorylated eIF2 prevents the GDP in eIF2 exchanged for a GTP, leading to reduced eIF2-Met-tRNAi-GTP complex (ternary complex). Reduced ternary complex formation impairs translation initiation

thereby decreasing global protein synthesis, thus reducing the consumption of cell resources and to an increased expression of Gcn4.

1.1.4 Gcn4 (General Control Nonderepressible 4)

Gcn4 translation is regulated at the mRNA level (*10*). Under starvation conditions Gcn4 expression is induced without any change in the Gcn4 mRNA level. The leader sequence of Gcn4 mRNA contains a 590bp un-translated region with four uORFs (upstream open reading frames) called uORF1, 2, 3 and 4 respectively (*31*). As described in Figure 1.4A, under replete conditions eIF2B, a guanine nucleotide exchange factor recycles eIF2-GDP to eIF2-GTP, leading to high levels of eIF2-GTP-Met-tRNAi (ternary complex) formation. These ternary complexes together with the 40S ribosomes translate the uORF1 of *GCN4* mRNA. Almost 50% of the ribosomes do not disintegrate from the *GCN4* mRNA after translating uORF1 and continue scanning. The high levels of ternary complexes allow the scanning 40S ribosomes to rebind a ternary complex and translate uORF2, 3 and 4. Following uORF4 translation, no initiation takes place at the *GCN4* start site, presumably because most ribosomes dissociate from the mRNA.

Therefore, the expression of Gcn4 is constitutively repressed under replete conditions by the uORFs.

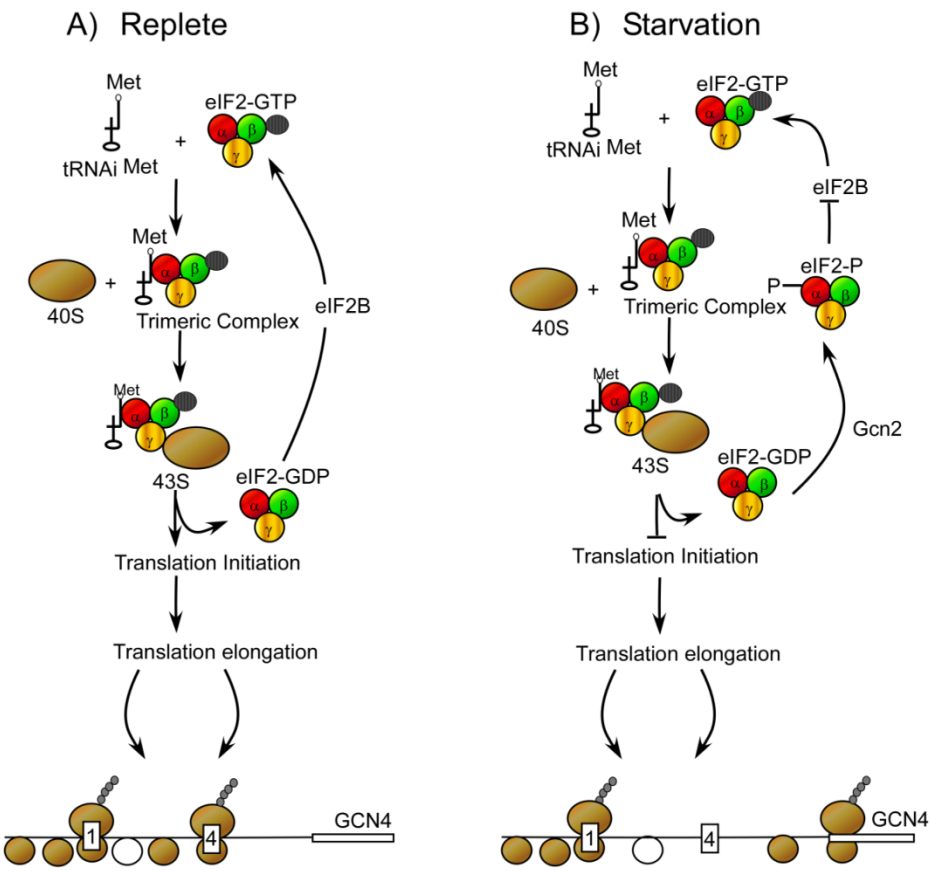

Figure 1.4. Schematic representation of translation initiation and Gcn4 expression under replete (A) and starvation (B) conditions. A) Met-tRNAi-GTP-eIF2 complex binds to the 40S subunit, builds the 43S pre-initiation complex that delivers the Met-tRNAi to initiate translation. During this process eIF2-GTP is converted into eIF2-GDP. In order to participate in another round of initiation process eIF2-GDP needs to be recycled by eIF2B. Under replete conditions when the levels of ternary complex are high, upon finding the first AUG codon the pre-initiation complex forms an 80S initiation complex to translate the uORF1 of *GCN4*. Most ribosomes that translate uORF1 do not dissociate from the mRNA immediately instead they continue scanning the mRNA as 40S subunits (indicated as empty circles) that is lacking a ternary complex and reinitiate translation at the next AUG codon after binding to another ternary complex. However the 80S ribosomes that translate uORF2, 3 or 4 dissociate from the mRNA and fail to reach the *GCN4* start codon. B) Under conditions of amino acid starvation phosphorylation of eIF2 by Gcn2 reduces the ternary complex formation. Similar to replete conditions, after translating uORF1 of *GCN4* the 40S subunits continue scanning the mRNA. However, reduced levels of ternary complex will result in 40S subunit to continue scanning uORF2, 3 or 4 without rebinding any ternary complex. The long stretch of RNA between uORF4 and AUG of *GCN4* increases the chance for the ribosomes to acquire a ternary complex and initiate translation of *GCN4*. For simplicity uORF2 and 3 were omitted.

1.1.5 GAAC is conserved from yeast to mammals

In *Saccharomyces cerevisiae* Gcn2 is the sole eIF2α kinase. In contrast to yeast, mammals have 4 different eIF2α kinases; GCN2, PKR like endoplasmic reticulum kinase (PERK/PEK), heme regulated inhibitor (HRI) and RNA dependent protein kinase (PKR). In mammals GCN2, PERK, HRI and PKR respond to nutritional stress, endoplasmic reticulum stress, heme deprivation in erythroid cells and viruses respectively by phosphorylating eIF2α subunit at ser-51 (Figure 1.5) (*32-35*).

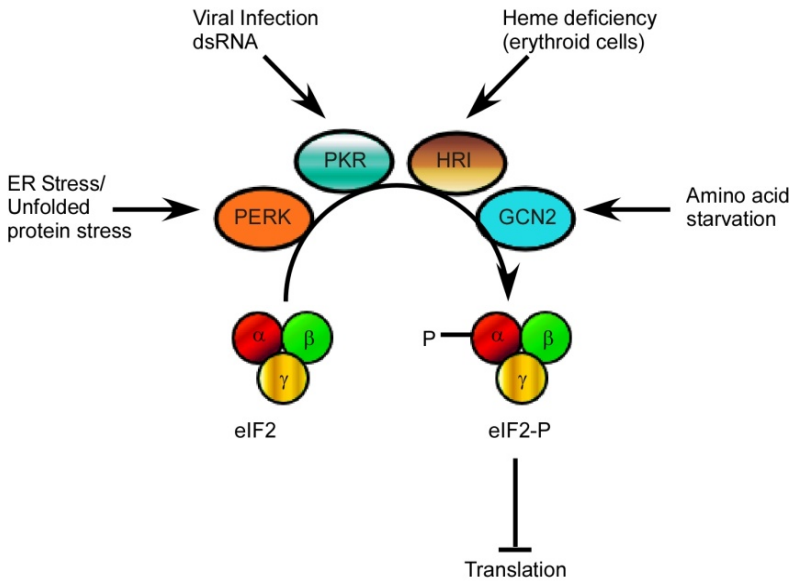

Figure 1.5. Representation of different eIF2α kinases in mammals and the different stress conditions that mediate phosphorylation of eIF2α.

Though higher eukaryotes contain more than one eIF2α kinase it has been shown that under amino acid starvation mammalian Gcn2 is activated by a mechanism resembling the one in yeast (*36, 37*). Homologs of yeast *GCN1* (*GCN1L1*) and *GCN4* (*ATF4*) have been identified in mammals and similarly to Gcn4, expression of *ATF4* is regulated by its uORFs (*38*). Since *ATF4* is the common downstream target of the various eIF2α kinases in mammals the eIF2-ATF4 pathway is being referred as the integrated stress response (ISR) (*39*).

1.2 Gcn1 dependent activation of Gcn2 under other nutrient stress conditions

In addition to the amino acid limitation, in yeast Gcn1 mediated activation of Gcn2 has been implicated in many other nutrient stresses, such as glucose (*40*) and purine limitation (*41*). Lack of glucose activates Gcn2 and results in increased phosphorylation of eIF2α. Gcn2 activation under glucose limiting condition is dependent on Gcn1, Gcn20, HisRS domain and ribosome association of Gcn2 (*40*). In addition to amino acid and glucose limitation, limitation for the nucleotide purine also activates Gcn2 (*41*). Purine limitation increases phosphorylation of eIF2α by Gcn2 and it is dependent on Gcn1 (*41*). As described before (Section 1.1.5) the molecular mechanism sensing the availability of nutrients operates from yeast to mammals. It has been reported that a diet deficient in essential amino acids activates Gcn2 in the mouse anterior perform cortex (APC) by an uncharged tRNA dependent manner (*42, 43*).

Under amino acid limiting conditions Gcn2 mediated regulation of fatty acid synthesis has been reported by Guo et al. (2007). The mice that had Gcn2, reduced triglyceride synthesis in the liver, coupled with enhanced mobilization of triglycerides from adipose tissue, when grown on a leucine missing diet. The mice that did not have Gcn2 have failed to reduce liver lipogenesis under the conditions of amino acid limitation and developed liver steatosis, suggesting that Gcn2 regulates fatty acid synthesis under amino acid starvation conditions (*44*).

In addition to nutrient limitation in yeast Gcn2 recognises many other forms of stresses. Stress conditions such as high salinity (*45*), intracellular acidic condition (*46*), accumulation of methylglyoxal (*47, 48*), boron (*49*), hydroxy urea, rapamycin (*50*), oxidative stress (*51*) and heterologous protein production (*52*) activate Gcn2.

1.3 Proteins regulating Gcn2 by disrupting the Gcn1-Gcn2 interaction

Proteins with sequence homology to the N-terminus of Gcn2 (a region known to bind to Gcn1) have been shown to regulate Gcn2; those are Yih1 and Gir2 (*53, 54*).

1.3.1 Yih1 (Yeast Impact Homologue)

Yih1 is a yeast homolog of mouse IMPACT (imprinted gene with ancient domain) gene (*11*).

Similarly to Gcn2, Yih1 contains an N-terminal RWD domain. It has been shown that over expressed Yih1 binds to Gcn1 but not Gcn2 and reduces the cellular level of Gcn1-Gcn2 interaction, resulting in reduced Gcn2 mediated phosphorylation of eIF2α (*53*). Furthermore, it has been demonstrated that overexpression of the Yih1-RWD domain is sufficient to impair cell growth under amino acid limiting conditions (*11*) and this was rescued by over expressing Gcn2. Based on the finding that the RWD domain of Gcn2 binds to Gcn1 (*4*), it was proposed that Yih1 regulates Gcn2 by competing with Gcn2 for Gcn1 binding (*53*). Furthermore, purified Gcn1 (2052-2428) is able to bind to purified Yih1 *in vitro* and similar to the Gcn1-Gcn2 interaction, this interaction is mediated by the Arg-2259 residue of Gcn1, as found for Gcn2 (*53*).

Endogenous and overexpressed Yih1 binds to translating ribosomes in a Gcn1 dependent manner and the overexpression of Yih1 does not have any effect on the Gcn1 or Gcn2 interaction with the polyribosome, indicating that Gcn1, Gcn2 and Yih1 bind to the ribosome independently of each other (*55*). Native Yih1 forms a complex with monomeric actin in a 1:1 ratio (*53*). The interaction of Yih1 with actin does not require Gcn1 and the interaction of Yih1 with Gcn1 does not require actin. The facts that endogenous Yih1 interacts with actin and not with Gcn1 and deletion of Yih1 does not have any effect on Gcn2 function and overexpressed Yih1 acts as a competitive inhibitor of Gcn2, led to a model where Yih1 resides in a Yih1-actin complex, and when released from actin under certain cellular conditions it then inhibits Gcn2 (*53*).

1.3.2 Gir2 (Genetically Interacts with Ribosomal genes 2)

Gir2 contains an N-terminal RWD domain that interacts with Gcn1 when overexpressed (*56*). The interaction between Gcn1 and Gir2 is also mediated by Gcn1-Arg-2259 as found for Gcn2 and Yih1. Similarly to Yih1, overexpression of Gir2 diminishes Gcn2 function, which can be reversed by overexpression of Gcn2, suggesting that the over expressed Gir2 competes with Gcn2 for Gcn1 binding thereby inhibiting Gcn2 activation. Similarly to Yih1, deletion of Gir2 does not lead to increased Gcn2 activity, suggesting that Gir2 is not a general inhibitor of Gcn2 (*56*).

A portion of Gir2 associates with ribosomes and the C-terminus of Gir2 binds to Rbg1 and Rbg2 (Ribosome interacting GTPase) (*56, 57*). Unlikely Yih1, the association of Gir2 with ribosome is partially dependent on Gcn1 (*56*).

Similarly to Gir2, a small fraction of Rbg2 associates with translating ribosomes (*56*). Complex formation between Gir2 and Rbg2 is increased in the presence of GTP and it is dependent on the GTP binding domain of Rbg2 which reflects the cellular energy level (*57*). Furthermore a role for Gir2-Rbg2 complex under amino acid starvation condition has been proposed recently. Strains lacking Gir2, Rbg2 or both, had increased doubling time under amino acid starvation conditions suggesting that the Gir2-Rbg2 complex is necessary to regulate cell division under starvation conditions (*57*)

Though Rbg2 was found associated with ribosomes (*56*), the Gir2-Rbg2 complex has not been found associating with the polysomes (*57*). The stabilization of the Gir2-Rbg2 complex is increased under amino acid starvation condition and the Gir2-Rbg2 complex binds to Gcn1. The complex formation between Gir2-Rbg2 and Gcn1 is increased in an amino acid starvation-dose dependent manner and the complex formation between Gir2 and Rbg2 is independent of Gcn1. The fact that the Rbg2/Gir2 complex was not associated with the ribosomes and overexpressed Gir2 acts as a competitive inhibitor of Gcn2, lead to the idea that the non-polysomal Rbg2/Gir2 complex can bind to Gcn1 that are not bound to the polysomes, to sequester any Gcn1 that can't

function at the A-site; or the non-polysomal Gir2-Rbg2 complex can bind to translating ribosome upon receiving a signal of starvation and bind to Gcn1 to prevent further activation of Gcn2 (*57*)

Although Gcn1 was found associated with ribosomes, it has been proposed that a fraction of Gcn1 may not be binding to ribosomes (*57*). This idea is further supported by the fact that a mutant form of Gcn20 was predominantly found in the non-polysomal fraction and it was still able to carry out the regulatory function under amino acid starvation conditions (*2*).

1.4 Hypothesis and aim of research

Gcn2 is involved in many essential functions in the cell. Gcn2 needs Gcn1 for its function (*38*). The known Gcn2 regulating proteins exert their function by binding to Gcn1 (*2, 20, 53, 56*). Gcn1 is a large HEAT repeat containing protein, HEAT repeats are proposed to serve as interaction surfaces for other proteins (*21, 22*), suggesting that Gcn1 may bind to several proteins. In line with this idea, protein-protein interaction studies suggest that Gcn1 interacts with more proteins than the ones identified so far (*24-27*). Large scale protein-protein interaction studies carried out on yeast did not consistently identify the known Gcn1 binding partners of Gcn1 (Gcn2, Gcn20, Yih1 and Gir2). Therefore, I hypothesize that Gcn1 may bind to more proteins than those known so far, and that these are involved in regulating Gcn2.

To test this hypothesis, the aim of this study was to:

- Comprehensively identify proteins that are in a complex with Gcn1, these will be called Gcn1 binding proteins (Gcn1 BPs)
- Identify Gcn1BPs that are required for promoting Gcn2 function

1.5 Scope of this study

Gcn2 is involved in key functions such as amino acid homeostasis, fatty acid homeostasis (*44*), memory formation (*58*) and feeding behaviour (*59*). It appears that deficiency of amino acids and glucose in tumour microenvironments results in activation of Gcn2 which in turn results in cancer cell survival and proliferation (*60, 61*). In addition, activation and function of Gcn2 have been reported under many stress conditions, including but not limited to nutrient limitation, salt stress (*45*), DNA damage (*62*), acid stress (*46*), and viral infection (*63, 64*). Though several studies were successful in deciphering the function of Gcn2 in such diverse conditions, very little is known about Gcn2 activation. The current working model for Gcn2 activation suggests that under starvation conditions Gcn1 is required for the delivery of the starvation signal to Gcn2 (*4*), or because Gcn1 has scaffold protein properties, it is possible that Gcn1 possibly positions Gcn2 on the ribosome in order to receive the starvation signal (*38*). Several proteins have been reported to regulate Gcn2 function under different conditions and many proteins have been found associated with Gcn2 regulatory proteins, suggesting that a complex protein network is involved in regulating Gcn2 (*38*). To help understand the complex Gcn2 regulatory network this study will investigate proteins binding to Gcn1 and their effect on Gcn2 function under amino acid limiting conditions.

Chapter 2 Materials and Methods

2.1 Biological Materials

The plasmids and strains used in this study are listed in table 2.1 and table 2.2.

Table 2. 1 Plasmids used in this study

Plasmid	Gene	Relevant features	Vector	Source
p2367	*GCN1*-Myc	Amp, URA3, CEN/ARSH4	pRS316	(*2*)
pRS316	*URA3*	Amp, URA3, CEN/ARSH4	pBLUESCRIPT	(*65*)
p1830	*URA3*	Amp, URA3	pRS316	(*2*)
p1834	*GCN1*-Myc	Amp, URA3, 2µ	pRS426	(*4*)
pDH114	*GCN2-FL-(cE803V)-FLAG-6XHis-FL-*	Amp, URA3, 2µ	pDH103	(*5*)
pHQ1213	*FLAG-6XHIS-PK (591-1010) hyper R794G,F842L*	Amp, URA3, 2µ	pEMBLyex4	(*66*)
p426GAL	*GAL1-URA3*	Amp, URA3, 2µ	P426GAL	Leos Valasek, Unpublished
pRS1	*KEM1*	Amp, URA3, CEN/ARSH4	pRS316	This study
YGPM3f19 (6H4)	*[MPT5], [YGL177W], [YGL176C], SAE2, BUD13, [KEM1]*	Kan, LEU2, 2µ	pGP564	OPEN BIOSYSTEMS
YGPM33c11 (6A5)	*[BUD13], KEM1, NUP49, ROK1, SPO74, tk(CUU)G2, [SUA5]*	Kan, LEU2, 2µ	pGP564	OPEN BIOSYSTEMS
YGPM3c22 (14D12)	*[TOP1], RPB11, SIN3, [YOL003C]*	Kan, LEU2, 2µ	pGP564	OPEN BIOSYSTEMS
YGPM31i12 (14E12)	*[SIN3], YOL003C, IZH2, PHO80, [RRP6]*	Kan, LEU2, 2µ	pGP564	OPEN BIOSYSTEMS
YGPM3n08 (4D6)	*[YDR333C], SWR1, MSN5, YDR3336W, MRPS28, [YDR338C]*	Kan, LEU2, 2µ	pGP564	OPEN BIOSYSTEMS
YGPM15n19 (4C6)	*[YDR332W], YDR333C, SWR1, [MSN5]*	Kan, LEU2, 2µ	pGP564	OPEN BIOSYSTEMS

Table 2.2 Yeast (*Saccharomyces cerevisiae*) strains used in this study

Strain	Genotype	Source
H1511	MATα ura3–52 trp1–63 leu2-112 GAL2	(*67*)Ref.15
H2556	H1511, and *GCN1* deletion	Vazquez de Aldana and Alan Hinnebusch, unpublished
BY4741	MATa *his3*Δ1 *leu2*Δ0 *met15*Δ0 *ura3*Δ0	Thermo Fisher
YDR283C	Same as BY4741 with *gcn2*Δ::KanMX4	Thermo Fisher
YGL173C	Same as BY4741 with *kem1*Δ::KanMX4	Thermo Fisher
YER070W	Same as BY4741 with *rnr1*Δ::KanMX4	Thermo Fisher
YDR335W	Same as BY4741 with *msn5*Δ::KanMX4	Thermo Fisher
YOL004W	Same as BY4741 with *sin3*Δ::KanMX4	Thermo Fisher
YKR001C	Same as BY4741 with *vps1*Δ::KanMX4	Thermo Fisher
YKL006W	Same as BY4741 with *rpl14A*Δ::KanMX4	Thermo Fisher
YJR145C	Same as BY4741 with *rps4A*Δ::KanMX4	Thermo Fisher
YDL229W	Same as BY4741 with *ssb1*Δ::KanMX4	Thermo Fisher
YHR025W	Same as BY4741 with *thr1*Δ::KanMX4	Thermo Fisher
YBR127C	Same as BY4741 with *vma2*Δ::KanMX4	Thermo Fisher
YER086W	Same as BY4741 with *ilv1*Δ::KanMX4	Thermo Fisher
YDL160C	Same as BY4741 with *dhh1*Δ::KanMX4	Thermo Fisher
YLR357W	Same as BY4741 with *rsc1*Δ::KanMX4	Thermo Fisher
YLR447C	Same as BY4741 with *vma6*Δ::KanMX4	Thermo Fisher
YBR097W	Same as BY4741 with *vps15*Δ::KanMX4	Thermo Fisher
YOR036W	Same as BY4741 with *pep12*Δ::KanMX4	Thermo Fisher
YGR167W	Same as BY4741 with *clc1*Δ::KanMX4	Thermo Fisher
YDR195W	Same as BY4741 with *ref2*Δ::KanMX4	Thermo Fisher
YGR134W	Same as BY4741 with *caf130*Δ::KanMX4	Thermo Fisher
YNL030W	Same as BY4741 with *hhf2*Δ::KanMX4	Thermo Fisher
YOL041C	Same as BY4741 with *nop12*Δ::KanMX4	Thermo Fisher
YLR398C	Same as BY4741 with *ski2*Δ::KanMX4	Thermo Fisher

YDL052C	Same as BY4741 with *slc1*Δ::KanMX4	Thermo Fisher
YGR234W	Same as BY4741 with *yhb1*Δ::KanMX4	Thermo Fisher
YMR163C	Same as BY4741 with *inp2*Δ::KanMX4	Thermo Fisher
YMR092C	Same as BY4741 with *aip1*Δ::KanMX4	Thermo Fisher
YBR020W	Same as BY4741 with *gal1*Δ::KanMX4	Thermo Fisher
YGL008C	Same as BY4741 with *pma1*Δ::KanMX4	Thermo Fisher
YJL047C	Same as BY4741 with *rtt101*Δ::KanMX4	Thermo Fisher
YOL055C	Same as BY4741 with *thi20*Δ::KanMX4	Thermo Fisher
YGL179C	Same as BY4741 with *tos3*Δ::KanMX4	Thermo Fisher
YHR199C	Same as BY4741 with *aim46*Δ ::KanMX4	Thermo Fisher
YLR059C	Same as BY4741 with *rex2*Δ::KanMX4	Thermo Fisher
YBR126C	Same as BY4741 with *tps1*Δ::KanMX4	Thermo Fisher
YLL040C	Same as BY4741 with *vps13*Δ::KanMX4	Thermo Fisher
YGR240C	Same as BY4741 with *pfk1*Δ::KanMX4	Thermo Fisher
YHL030W	Same as BY4741 with *ecm29*Δ::KanMX4	Thermo Fisher
YER110C	Same as BY4741 with *kap123*Δ::KanMX4	Thermo Fisher
YNL085W	Same as BY4741 with *mkt1*Δ::KanMX4	Thermo Fisher
YBR028C	Same as BY4741 with *ypk3*Δ::KanMX4	Thermo Fisher
YDR138W	Same as BY4741 with *hpr1*Δ::KanMX4	Thermo Fisher
YBR189W	Same as BY4741 with *rps9*BΔ::KanMX4	Thermo Fisher
YHL011C	Same as BY4741 with *prs3*Δ::KanMX4	Thermo Fisher
YPR164W	Same as BY4741 with *kim3*Δ::KanMX4	Thermo Fisher
YDR216W	Same as BY4741 with *adr1*Δ::KanMX4	Thermo Fisher
YKL205W	Same as BY4741 with *los1*Δ::KanMX4	Thermo Fisher
YGL241W	Same as BY4741 with *kap114*Δ::KanMX4	Thermo Fisher
YLR289W	Same as BY4741 with *guf1*Δ::KanMX4	Thermo Fisher
YNL037C	Same as BY4741 with *idh1*Δ::KanMX4	Thermo Fisher
YCL050C	Same as BY4741 with *apa1*Δ::KanMX4	Thermo Fisher
YHR200W	Same as BY4741 with *rpn10*Δ::KanMX4	Thermo Fisher
YNL271C	Same as BY4741 with *bni* Δ::KanMX4	Thermo Fisher
YOR001W	Same as BY4741 with *rrp6*Δ::KanMX4	Thermo Fisher

YOR035C	Same as BY4741 with *she4*Δ::KanMX4	Thermo Fisher
YMR116C	Same as BY4741 with *asc1*Δ::KanMX4	Thermo Fisher
YML124C	Same as BY4741 with *tub3*Δ::KanMX4	Thermo Fisher
YKL092C	Same as BY4741 with *bud2*Δ::KanMX4	Thermo Fisher
YOR035C	Same as BY4741 with *eaf3*Δ::KanMX4	Thermo Fisher
YMR012W	Same as BY4741 with *clu1*Δ::KanMX4	Thermo Fisher
YMR186W	Same as BY4741 with *hsc82*Δ:KanMX4	Thermo Fisher
YBR208C	Same as BY4741 with *dur1,2*Δ::KanMX4	Thermo Fisher
YAL021C	Same as BY4741 with *vps13*Δ::KanMX4	Thermo Fisher
YKL130C	Same as BY4741 with *she2*Δ::KanMX4	Thermo Fisher
YDR395W	Same as BY4741 with *sxm1*Δ::KanMX4	Thermo Fisher
YMR246W	Same as BY4741 with *faa4*Δ::KanMX4	Thermo Fisher
YLR059C	Same as BY4741 with *rex2*Δ::KanMX4	Thermo Fisher
YLR429W	Same as BY4741 with *crn1*Δ::KanMX4	Thermo Fisher
YGL195W	BY4741 containing *gcn1*::GFP-*HIS*	Life Technologies
YDR283C	BY4741 containing *gcn2*::GFP-*HIS*	Life Technologies
YFR009W	BY4741 containing *gcn20*::GFP-*HIS*	Life Technologies
YCR012W	BY4741 containing *pgk1*::GFP-*HIS*	Life Technologies
YGL173C	BY4741 containing *kem1*::GFP-*HIS*	Life Technologies
YKL182W	BY4741 containing *fas1*::GFP-*HIS*	Life Technologies
YPL231W	BY4741 containing *fas2*::GFP-*HIS*	Life Technologies
YER110C	BY4741 containing *kap123*::GFP-*HIS*	Life Technologies
YNR016C	BY4741 containing *acc1*::GFP-*HIS*	Life Technologies
YJL130C	BY4741 containing *ura2*::GFP-*HIS*	Life Technologies
YDR335W	BY4741 containing *msn5*::GFP-*HIS*	Life Technologies
YKR001C	BY4741 containing *vps1*::GFP-*HIS*	Life Technologies
YER070W	BY4741 containing *rnr1*::GFP-*HIS*	Life Technologies

2.2 Plasmid constructions

The *KEM1* fragment was excised using *Xho1* and *Xba1* from the plasmid YGPM33c11 (p6A5) (refer to Table 2.1), such that it has its endogenous promoter. The completion of restriction digestion was checked by agarose gel electrophoresis. The DNA fragment was extracted and purified from the agarose gel and then introduced into pRS316 which was also digested by *Xho1* and *Xba1*. The recombinant plasmid was verified by restriction digestion (Appendix-A.1).

2.3 Media

Media for bacterial and yeast cultures were prepared using MilliQ water and sterilized by autoclaving at 121°C for 20 minutes. Liquid media were cooled down to room temperature. Supplements were added to the cooled media and were stored at room temperature. Media containing light sensitive supplements were stored in amber colored bottle or covered by aluminium foil and stored at 4°C. Solid media were prepared by adding agar to a final concentration of 2% (W/V). After sterilization media were cooled down to 55°C and then supplements were added, mixed and poured into Petri plates. The plates were left at room temperature to solidify and stored at 4°C. Heat sensitive supplements were filter sterilized through 0.22 μm Millipore express® membrane filters. Carbon sources (glucose or galactose) were sterilized separately and added to media prior to use.

Yeast Media

Yeast media were prepared as outlined in Evans et al. (1996).

Yeast extract Peptone Dextrose (YPD)
1% (w/v) yeast extract (Formedium)
2% (w/v) peptone (Formedium)
2% (w/v) glucose (Formedium)

Yeast extract Peptone Glycerol (YPG)
1% (w/v) yeast extract (Formedium)
2% (w/v) peptone (Formedium)
3% (v/v) glycerol (Sigma-Aldrich)

Synthetic Dextrose (SD)

0.145% (w/v) yeast nitrogen base without amino acids and ammonium sulphate (Formedium)
0.5% (w/v) ammonium sulfate (Ajax)
2% (w/v) glucose (Formedium) or 2% (w/v) galactose (Formedium)

Bacterial Media

Bacterial media were prepared as outlined in Green et al. (2012) (*68*).

Luria-Bertani (LB) Medium

1% (w/v) tryptone (Formedium)
0.5% (w/v) sodium chloride (NaCl) (Ajax)
0.5% (w/v) yeast extract (Formedium)
pH 7

2.4 Media Supplements

Table 2.3 Media supplements used in this study

	Solvent	**Final Concentration**
a) Antibiotics		
Ampicillin	Water	100 µg/ml
Kanamycin	Water	50 µg/ml
b) Starvation inducing drugs		
Sulfometuron methyl(SM)	DMSO	0.5 to 2 µg/ml
3-Amino-Tri azole (3-AT)	Water	15 to 160 mM
c) Amino acids		
Histidine	Water	20.9 mg/ml
Isoleucine	Water	6.6 mg/ml
Leucine	Water	13 mg/ml
Lysine	Water	7.3 mg/ml
Methionine	Water	7.5 mg/ml
Tryptophan	Water	8 mg/ml
Uracil	Water	2.2mg/ml
Valine	Water	2.9 mg/ml

2.5 Growth Conditions

Yeast growth conditions

All *Saccharomyces cerevisiae* cultures were grown at 30°C. Cultures were grown in liquid or on SD media supplemented with appropriate supplements (Table 2.3) or on/in YPD media or on YPG media. When grown in liquid media, cultures were shaken at 160 rpm. Solid cultures were maintained at 4°C.

Bacterial growth conditions

All *Escherichia coli* cultures were grown at 37°C in LB broth or on LB agar plates supplemented with appropriate antibiotics (Table 2.3). When grown in liquid media, the cultures were shaken at 150 rpm. Solid cultures were maintained at 4°C.

Storage of bacterial and yeast strains

Bacterial cultures were stored at -80°C in 30% (v/v) glycerol (Sigma-Aldrich)
Yeast cultures were stored at -80°C in 30% (v/v) glycerol (Sigma-Aldrich)

2.6 Plasmid DNA isolation and purification

Plasmid DNA purification by alkaline lyses

Bacterial plasmid DNA was isolated as outlined in Green et al. (2012). Bacterial cultures were grown overnight at 37°C. The cultures were pelleted by centrifugation at 12,000 rpm for 5 minutes and suspended on 100 µl of ice cold solution I. Cells were lyzed by addition of 200 µl of solution II followed by incubation at room temperature for 5 minutes. The suspension was neutralized by 150 µl of ice-cold solution III, followed by incubation on ice for 5 minutes. Cell debris and chromosomal DNA were pelleted by centrifugation at 12,000 rpm for 10 minutes at 4°C. The supernatant was extracted with an equal volume of phenol-chloroform-isoamyl alcohol and DNA was precipitated with an equal volume of isopropyl alcohol for 2 minutes and pelleted by centrifugation at 12,000 rpm for 10 minutes at room temperature. The DNA pellet was then washed

with 500 µl of 70% ethanol and dried under vacuum. The pellet was suspended in 20 µl of sterile water or TE.

Solution I	**Solution II**	**Solution III**
50 mM Tris-HCl (pH 8)	0.2 N NaOH	3M potassium acetate
10 mM Na_2EDTA (pH 8)	1% SDS	
100 µg/ml RNAse A		

Phenol-chloroform-isoamylalcohol	**TE**
Phenol 25 volumes	10 mM Tris-HCl (pH7.5)
Chloroform 24 volumes	1 mM Na2EDTA
Isoamyl alcohol 1 volume	

DNA purification

Extraction and purification of plasmid DNA from agarose gels was carried out using QIAquick Gel Extraction Kit (Qiagen). The desired DNA fragment was cut out of the agarose gel. The gel slice was solubilized in 3 volumes of buffer QG at 50°C for 10 min. The DNA fragment was then purified using QIAquick Gel Extraction Kit according to the manufacturer's protocol.

2.7 DNA digestions and ligations

The vector plasmids were cut by desired restriction enzymes at 37°C for 2 hours (*68*). To prevent re-ligation of the linearized plasmid 0.5 µl of Calf Intestinal Alkaline Phosphatase (CIP) (New England Biolabs) was added. To inactivate CIP, 2.5 µl of 200 mM EDTA was added and incubated for 10 minutes at 75°C.
Ligation reactions were performed at ratios of 1:3, 1:6 moles (vector to insert), using T4 DNA ligase (New England Biolabs) at 16°C. 3 µl of the ligation product was used for bacterial transformation.

2.8 Agarose gel electrophoresis

Agarose gels of desired concentrations (0.75-2% w/v) were prepared in 1X TAE buffer (*68*). 1 µl of ethidium bromide (10 mg/ml) was added to 100 ml of TAE agarose before pouring the gel. Samples were mixed with DNA loading dye and resolved on the agarose gel at a constant voltage of 80. After electrophoresis the DNA bands were visualized on a transilluminator and the images were captured using a Gel Doc imager (Bio Rad).

Tris Acetate EDTA (TAE) Buffer (50X)
2 M Tris
1 M Acetate
100 mM EDTA

DNA Loading Dye
0.25% Bromophenol Blue
0.25% Xylene Cyanol
50 % Glycerol

2.9 Transformation of yeast using lithium acetate method

Preparation of competent yeast

1 ml of an overnight yeast culture was added to 50 ml of YPD media and incubated at 30°C with shaking. After 3.5-4 hours the cells were pelleted by centrifugation at 4,200 rpm for 5 minutes and suspended in 5 ml of 0.1 M lithium acetate (LiOAc)(*69*). The suspension was subjected to centrifugation again at 4,200 rpm and the cells were pelleted. The pellets were suspended in 500 µl of solution 1. The cells were incubated at 30°C with gentle shaking for 30 minutes. The competent yeast cells were used immediately or stored at 4°C overnight and used the next day.

Solution 1
10 mM Tris-HCl
1 mM EDTA
100 mM LioAc (lithium acetate)

Transformation of yeast

Transformation of yeast was carried out as outlined in Evans et al. (1996) with some slight modifications in the procedure. Herring sperm single stranded DNA (10 mg/ml) was boiled at 100°C for 10 minutes. 5 µl of the carrier DNA, 5 µl of

plasmid DNA and 100 µl of yeast competent cells were incubated at 30°C for 30 minutes. 600 µl of solution 2 was added, mixed and incubated at 30°C for 45 minutes. The cells were incubated at 42°C for 15 minutes and immediately transferred onto ice for 2 minutes. The cells were centrifuged at 4,200 rpm for 3 min. The pellets were suspended in 50 µl of SD and plated on appropriate SD plates and incubated at 30°C for 2-3 days or until colonies were visible.

Solution 2
10 mM Tris-HCl
1 mM EDTA
100 mM LiOAc
40% PEG

2.10 *E-coli* transformation

Making *E.coli* competent

Competent *E.coli* cells were prepared as outlined in Green et al. (2012) (*68*). *E.coli* cultures (DH5α) grown overnight were inoculated into 200 ml of LB broth and grown to an optical density at OD_{600} of 0.4-0.5. The cells were then transferred to an ice-cold centrifuge bottle and centrifuged at 5,000 rpm for 10 min at 4°C. The cell pellet was suspended in 20 ml of ice-cold calcium chloride solution (*70*) and incubated on ice for 30 min. The cells were then pelleted, suspended in 4 ml of ice-cold glycerol calcium chloride solution and incubated on ice for minimum 6 hours. The suspension was aliquoted and frozen on dry ice and stored at -80°C.

Calcium chloride Solution
50 mM CaCl2
Filter sterilized

Glycerol-Calcium chloride solution
15% (v/v) Glycerol
50 mM CaCl2
Filter sterilized

E.coli transformation

The competent *E.coli* was thawn on ice and 1-5 µl of plasmid DNA or 3 µl of ligation products was added to 100 µl of competent *E.coli* and incubated on ice for 30 minutes. The cells were then incubated at 42°C for 1 min and immediately

cooled down on ice for 2 min. To recover the cells 500 µl of LB medium was added and incubated with shaking at 180 rpm at 37°C for an hour. The cells were then pelleted and plated on selective media.

2.11 Preparation of yeast cell extracts

Standard cell extracts preparation

Yeast cells were grown overnight and inoculated into appropriate media. The cells were grown in 50 ml of SD (synthetic dextrose) medium containing required amino acids. Cells were grown at 30°C to A_{600} = 1.5 and transferred to a clean falcon tube and spun down at 4,200 rpm for 3 minutes to pellet down the cells. The cell pellets were washed with ice-cold breaking buffer (without protease inhibitors) and transferred to a 2 ml Eppendorf tube and pelleted again to remove the buffer. These pellets were used right away to break open the cells.

For breaking cells 1 pellet volume of ice-cold breaking buffer (with protease inhibitors) and 1 pellet volume of acid washed glass beads (Sigma) were added to the cell pellet. The samples were subjected to vortexing at high speed for 30 seconds, alternating with 30 second intervals on ice-water mix for 10 times. The cell debris and glass beads were pelleted by centrifugation at 10,000 rpm for 10 min and at 4°C. The supernatant was collected in fresh tubes and protein concentration in the cell extract was determined by the Bradford protein estimation method (Section 2.12).

Subjecting yeast cells to formaldehyde cross-linking

Yeast cells grown overnight were inoculated into 300 ml of appropriate media. The cells were grown shaking at 150 rpm at 30°C to OD_{600} = 1-1.5. The cells were subjected to formaldehyde cross-linking at 4°C or at room temperature, as indicated in the specific experiments. For cross-linking at 4°C, the cells were transferred into a centrifuge bottle containing 75 g or ice chips and formaldehyde and kept on ice for 1 hour or 10 min (*71*). For cross-linking at room temperature, formaldehyde was added to the conical flasks containing cells and shaken for 10 min or 1 hour. To quench the cross-linking reaction, glycine (2.5 M) was added to

a final concentration of 0.1 M and incubated for 5 min. The cells were pelleted by centrifugation at 4,200 rpm for 5 min at 4°C, suspended in 5 ml of breaking buffer (without protease inhibitors), transferred to round bottom tubes and then re-pelleted by centrifugation at 4,200 rpm for 5 min at 4°C. The pellets were used right away for breaking.

Breaking buffer
30 mM HEPES –KOH
50 mM KCl
10% (v/v) Glycerol
1 mM PMSF
10 µg/ml Pesptatin
1 µg/ml Aprotinin
1 µg/ml Leupeptin
5 mM β-mercaptoethanol

Breaking Cells

The cell pellets were suspended in 200 µl of breaking buffer containing protease inhibitors. 700 µl of acid washed glass beads were added to the cell pellet (*72*). The cells were vortexed for 30 seconds with 30 second intervals on ice-water mix for 10 times. The cell debris and glass beads were pelleted by centrifugation at 4,200 rpm for 5 min at 4°C and the supernatant was transferred to 1.75 ml tubes. The supernatant was further clarified by centrifugation at 10,000 rpm for 10 min at 4°C. The supernatant containing the cell extract was transferred to 1.75 ml tubes and the protein concentration was measured by the Bradford method (Section 2.12).

2.12 Estimation of Protein Concentration

Bovine Serum Albumin (BSA) standards of increasing concentrations (2-14 µg) were made by diluting a stock of 10 mg/ml and 0.5 µl of unknown concentration were taken in duplicates in a 96 well microtitre plate. 150 µl of Bradford (*73*) was added to the samples in the plate and incubated for 5 min. Absorbance of the samples was read at 595 nm in a FLUOstar OPTIMA plate reader (BMG lab tech). A standard curve was plotted with the absorbance against the protein

concentration of the known standards. Protein concentration of the unknown sample was determined by comparison of its absorbance with the standard curve.

Bradford Solution
0.5 mg/ml Coomassies blue (G250)
25% Methanol
42.5% H3PO4
0.05N NaOH
Store in a dark bottle

2.13 Gradient Sodium Dodecyl Sulfate Polyacrylamide Gel Electrophoresis (SDS-PAGE)

A gradient sodium dodecyl sulfate polyacrylamide matrix was used to separate protein samples. 0.7% agarose (w/v) in 1.5 M Tris-HCl (pH 8.8) was used to seal the gaps between the spacers in between the two glass plates. A gradient chamber was used to make the gradient SDS-PAGE. 20 ml of 4% acrylamide and bis-acrylamide premix was taken in one chamber of the gradient mixer and 20 ml of 14 or 17% acrylamide bis-acrylamide mix in the other chamber. 20 µl of N,N,N',N'-TetraMethylEthyleneDiamine (TEMED) and 200 µl of 10% Ammonium Per-Sulfate (APS) was added to each chamber and mixed. The valves between the chambers were opened to facilitate mixing of the stocks in the chambers and a gradient acrylamide was poured between the glass plates, a comb was inserted and allowed to solidify for 45 min. After solidification of the gel the comb was removed and the wells were washed with protein running buffer to remove any unpolymerised acrylamide and the gel was assembled on the gel electrophoresis unit. The gel was covered with protein loading buffer and proteins samples that were mixed with protein loading dye and denatured at 95°C for 10 min were loaded on the gel along with a protein standard. The gel was run at 250 V and 100 mA until the dye front reached the end of the gel.

Premixes	4% Premix	17% Premix	Protein Loading Dye 2X
MilliQ water	75.3 ml	48.8 ml	0.1% (w/v) bromophenol blue
Acrylamide 40% (29:1)	12 ml	68 ml	4% (w/v) SDS
Tris-HCl (pH 8.8)	30 ml	40 ml	100 mM Tris-Cl (pH 6.8)
10% SDS	1.2 ml	1.6 ml	20% (v/v) glycerol
			10% beta-Mercaptoethanol

Protein Running Buffer
25 mM Tris
192 mM Glycine
1% SDS

40% Acrylamide Bisacrylamide mix
(29:1) Acrylamide:Bisacrylamide

2.14 Staining Proteins in acrylamide gels

After electrophoresis the gels were stained with colloidal Coomassie stain or Coomassie stain overnight and destained until protein bands were visible.

Coomassie brilliant blue stain
50% Methanol
10% Glacial acetic acid (v/v)
34% Methanol (v/v)
0.1% Commassie G-250

Colloidal Coomassie stain
10% Ammonium Sulfate (w/v)
3% Ortho-Phosphoric Acid
20% Ethanol
0.1% Commassie G-250

2.15 Western Blot and immune detection of proteins

Transferring proteins onto PVDF membrane

Proteins in the SDS-PAGE were transferred to immobilin-P PolyVinylidine DiFluoride (PVDF) membranes (Millipore) pore size 0.45 µm that was pre-treated with absolute methanol and then equilibrated in transfer buffer. The gel, membrane and Whatman filter paper were immersed between the two electrodes of the transfer units and the transfer was carried out for 3 hours at 24 V and 1 A.

Transfer Buffer
25 mM Tris base pH 8.3
192 M glycine
20% Methanol (v/v)

Table 2.4 List of primary antibodies used in this study

Primary antibody	Dilution	Source	Secondary antibody
Gcn1	1 in 1000	HL1405, Vazquez de Aldana et al, 1995	Anti-rabbit
Gcn2	1 in 1000	Beartiz A Catilho (Unpublished)	Anti-rabbit
Gcn20	1 in 1000	CV1317, Vazquez de Aldana et al, 1995	Anti-rabbit
c-Myc	1 in 500	Roche	Anti-mouse
eIF2α-P	1 in 1000	Invitrogen	Anti-rabbit
Pgk1	1 in 5000	Invirogen	Anti-mouse
GFP	1 in1000	Santa Cruz	Anti-rabbit

Table 2.5 List of secondary antibodies used in this study

Secondary antibody	Dilution	Source
Anti-rabbit	1 in 100,000	Pierce
Anti-mouse	1 in 50, 000	Pierce

Immunological detection of proteins

The membranes subjected to Western transfer were blocked by incubating with 5% non-fat milk (w/v) (Basics/Pams) in TBS-T for an hour with gentle agitation on a platform rocker to prevent non-specific protein antibody interactions. Membranes were then incubated with primary antibody (Table 2.4) diluted in 5% non-fat milk or 3% BSA for an hour. The membranes were washed with TBS-T sequentially for 5, 10 and 15 min. The membranes were then incubated with the appropriate secondary antibody (Table 2.5) for an hour. The membranes were washed with TBS-T sequentially for 5, 10 and 15 min. The membranes were then incubated with ECL substrate for 2-3 minutes and the chemiluminescence signal was detected in the Luminescent Image Analyser LAS-4000 (Fujifilm).

Tris Buffered Saline-Tween (TBS-T)
1M Tris-HCl pH 7.4
5 M NaCl
0.1% Tween 20

Densitometry analysis of the signals was done using the software Multi Gauge V3.1 (Fujifilm).

Calculation of relative levels of eIF2α –P from raw data

Sample	Signal intensity of bands		eIF2α-P/ Pgk1	Relative ratio to control	Normalised eIF2α-P levels	std err
	eIF2α-P	Pgk1				
WT +	20.66	9.2	2.2456521	1.0805358	1	0.0805358
WT +	20.16	10.55	1.9109004	0.9194641		
WT -	4.14	9.2	0.45	0.2165255	0.22746370	0.0109381
WT -	4.37	8.82	0.4954648	0.2384018		
*kem1*Δ +	9.31	7.69	1.2106631	0.5825323	0.56646656	0.0160657
*kem1*Δ +	9.54	8.34	1.1438848	0.5504007		
*kem1*Δ -	BDR	7.12	BDR	BDR	BDR	BDR
*kem1*Δ -	BDR	6.9	BDR	BDR	BDR	BDR

Note: BDR-Below Detection Range

2.16 Protein-Protein interaction assays

Anti-Myc antibody mediated Co-immunoprecipitation

To reduce background binding the cell extracts (0.5-1 mg) obtained from cells subjected to formaldehyde cross-linking and noncross-linked controls were pre-absorbed with 20 µl (100%) of protein A resin for 1 hour at 4°C. The tubes were then spun down at 1000 rpm and the supernatant was transferred into a fresh tube and 2.5 µl of anti-Myc antibody (5 mg/ml, Roche) was added and incubated for 2 hours at 4°C. The tubes were then spun down at 1000 rpm and the supernatant was transferred into a tube containing 20 µl (100%) of BSA coated protein A resin and incubated for 2 hours at 4°C. After centrifugation at 1000 rpm for 3 min at

4°C the supernatant was removed and the beads were washed six times using breaking buffer. The beads were suspended in 2X loading buffer, boiled at 95°C and 15 µl was separated via SDS-PAGE. In addition, an input control of 50-100 µg of protein was separated on the same gel.

The anti-Myc antibody mediated immunoprecipitation procedure and eluting the protein complexes were varied in some of the experiments and indicated under the individual results.

Anti-GFP immunoprecipitation

Cell extracts (0.5 – 1mg) were pre-adsorbed with 30 µl Sepharose beads for 60 minutes and the beads were pelleted. The extract were then incubated with 5% BSA coated anti-GFP antibody coated Sepharose beads (10 µl, 50%) for 2 hours at 4°C. Unbound proteins were washed off using breaking buffer and proteins associated with the beads were eluted by boiling in 2X protein loading dye at 95°C for 10 min. 15 µl of the eluates were loaded and separated via SDS-PAGE. In addition, an input control of 50-100 µg of protein was separated on the same gel.

The anti-GFP antibody mediated immunoprecipitation procedure was varied in some of the experiments and is indicated in the individual results.

Large scale anti-GFP immunoprecipitation of Gcn1 containing complexes and identification of the components via Mass Spectrometry.

The *gcn1*Δ (H2556) strain transformed with hc plasmid derived GCN1-Myc or vector alone were grwon in SD media with required amino acids to exponential phase (A600 = 1-1.5). At this point the cells were exposed to 0.3% formaldehdye for 10 minutes at room temperature and one set of sample was left untreated as a control. The cells were subjected to cell lysis and cell extract obtained. To reduce background binding the cell extract was preabsorbed with 20 µl (100%) of protein A resin for 1 hour at 4°C. The tubes were then spun down at 1000 rpm and the supernatant was transferred into a freah tube and 2.5 µl of anti-myc antibody (5 mg/ml, Roche) was added and incubated for 2 hours at 4°C. The tubes were then spun down at 1000 rpm and the supernatant was transferred into a tube

containing 20 µl (100%) of BSA coated protein A resin and incubated for 2 hours at 4°C. After centrifugation at 1000 rpm for 3 min at 4°C the supernatant was removed and the beads were washed six times using breaking buffer. Four independent anti-myc immunoprecipitation experiments were carried out with each 500 µg of protein. The final beads were pooled together and the bound proteins were eluted by boiling in 2X protein loading dye. A small fraction of the samples and an input control of 50 – 100 µg of protein were resolved by SDS-PAGE followed by western blotting with antibodies against Gcn1, Gcn2, Gcn20 and Pgk1. The other fraction of samples were subjected to LC-MS-MS.

2.17 Semi quantitative growth assay

Yeast were grown overnight in duplicate in 4 ml of appropriate liquid media at 30°C. The cultures were subjected to 10 fold serial dilutions and 5 µl of each dilution and undiluted cultures were spotted on appropriate plates. The plates were incubated at 30°C for several days. The growth was monitored every day by scanning the plates using a conventional document scanner.

2.18 Solubilization of the pellets after centrifugation steps

The pellets from the 4200 rpm and 10,000 rpm spins were suspended in breaking buffer by vortexing for 2 minutes. The suspended pellets were spun at 10,000 rpm for 5 minutes. The obtained pellet was suspended again with breaking buffer by vortexing again for 2 minutes. The suspended pellets were spun at 10,000 rpm for 5 minutes. To the pellet, 2X protein loading dye was added and boiled for 30 minutes at 65°C followed by boiling for 10 minutes at 75°C.

Chapter 3 Identification of potential Gcn1 binding proteins

In order to identify proteins that are binding to Gcn1 or are in complex with Gcn1 (Gcn1 BPs), two different approaches were employed. One was based on the available yeast protein–protein interaction data from the published large scale affinity purification studies (*74-77*) and the other was based on our *in house* experiments

3.1 Identification of potential Gcn1 binding proteins from published data

There are four protein-protein interaction studies that comprehensively identified components of protein complexes in yeast: Ho et al. (2002), Gavin et al.(2002), Gavin et al. (2006) and Krogan et al. (2006) (Table 3.1).

The basic principle behind all of the four affinity purification studies is that a piece of DNA encoding for a tag was inserted into the coding sequence of a protein (Figure 3.1). Cells expressing the tagged protein were grown to exponential phase and cell extracts obtained. The cell extracts were subjected to affinity purification and the proteins in the purified complexes were identified by Mass Spectrometry (MS). Despite the same basic principle, the affinity purification studies differ in many ways as outlined below.

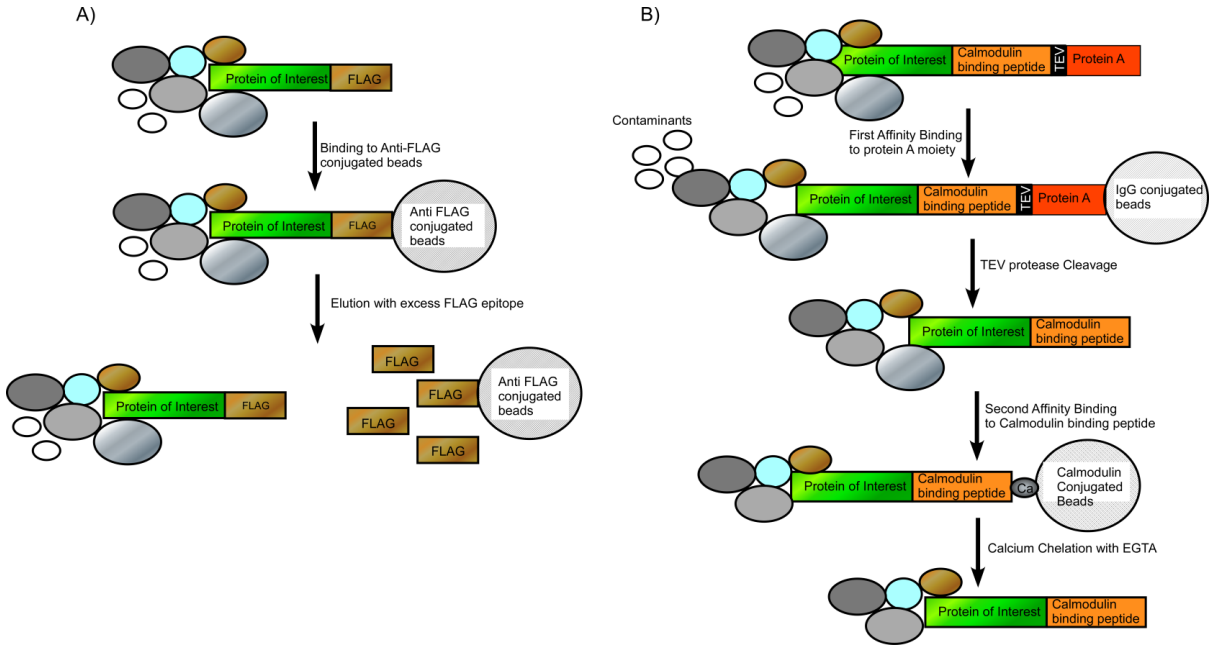

Figure 3. 1 Schematic representation of the TAP and FLAG affinity purification strategies.
A) In the TAP purification method the protein of interest is expressed in frame with a dual moiety. The calmodulin binding moiety is separated from the protein A moiety by a protease cleavage site (tobacco etch virus (TEV)). During TAP purification the protein A is immobilized on immunoglobulin G, the tag is then cleaved with TEV and the protein of interest that is fused to the calmodulin binding peptide is immobilized on calmodulin Sepharose in the presence of calcium. Chelating calcium with EGTA releases the protein of interest along with its interacting partners. B) In the FLAG purification, the protein of interest is expressed with a FLAG epitope and is purified on anti-FLAG Sepharose. Elution is effected by a large molar excess of the competing FLAG epitope.

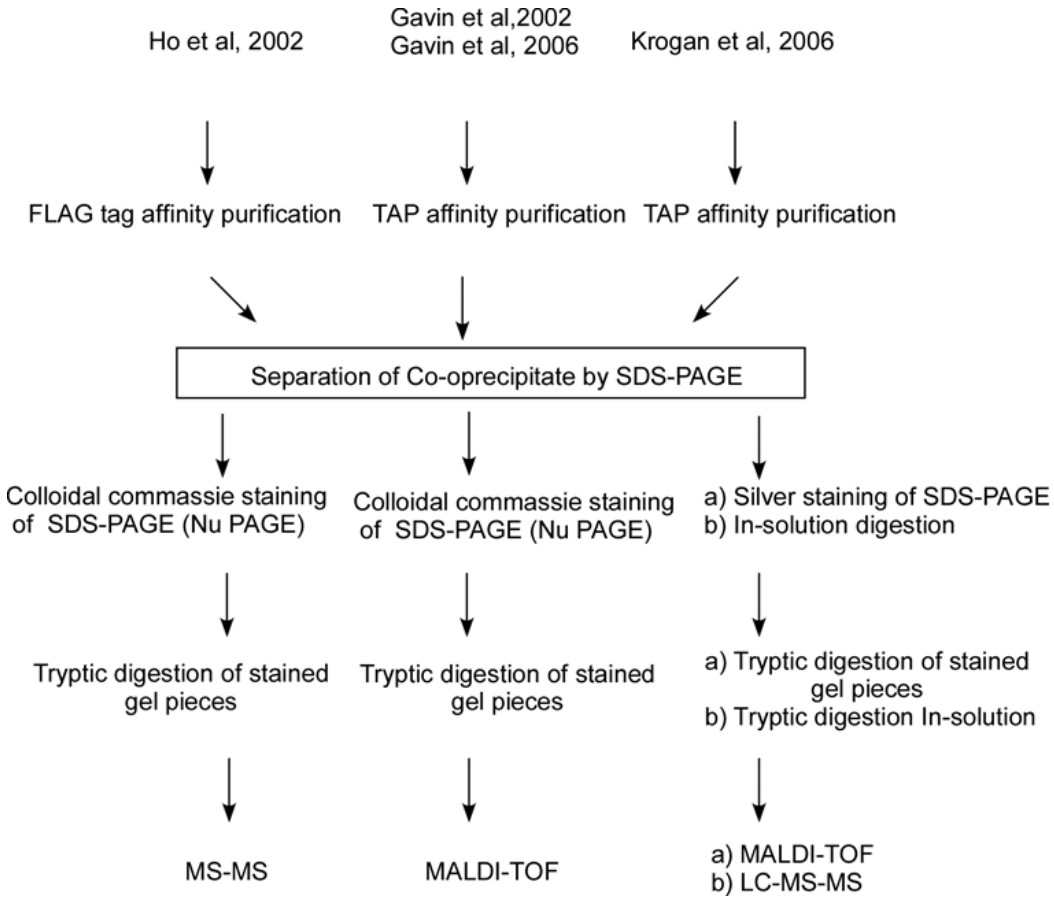

Figure 3.2. Overview of the different large-scale affinity purification studies carried out on yeast and the workflow.

Table 3.1 The general features of the previously published proteomic studies in the yeast *Saccharomyces cerevisiae*

	Ho Y et al. (2002)	Gavin et al. (2002)	Gavin et al. (2006)	Krogan et al. (2006)
Type of tag used	FLAG	TAP	TAP	TAP
Number of baits used	725	1739	1993	2357
Protein expression	Over-expression	Native level	Native level	Native level
Meidium used	Selective media	Rich media	Rich media	Rich media
Optical density	1.3 – 1.5	2 – 3	2 – 3	1 – 1.5

In the Ho et al. (2002) study proteins were tagged at the C-terminus with the FLAG epitope. Plasmids carrying the FLAG tagged genes under the galactose inducible promoter were introduced into the wild type. The plasmid-born genes were transiently over-expressed by adding galactose to exponentially growing cells. Cell extracts were obtained and subjected to FLAG-mediated affinity purification. Affinity-purified complexes were resolved by SDS-PAGE and the proteins were visualized using colloidal Coomassie stain, protein bands were cut out of the gel, digested with trypsin and analysed by Liquid Chromatography Tandem Mass Spectrometry (LC-MS/MS) (Figure 3.2).

Gavin et al. conducted two separate studies, one in 2002 and the other one in 2006. In these two studies and an additional study by Krogan et al. (2006), the genes encoding the proteins of interest were tagged at the C-terminus with the TAP (Tandem Affinity Purification) tag (*74, 76*). The TAP tag was fused to the ORFs (open reading frames) in frame via homologous recombination such that the epitope tagged proteins are expressed at native levels from their endogenous promoters. Cell extracts obtained from the cells expressing the TAP tagged proteins were obtained and subjected to tandem affinity purification (Figure 3.2). As the name indicates the TAP procedure involves two successive purifications. The first step is mediated via a protein A moiety and the second step is mediated via a calmodulin binding moiety (*78*) (Figure 3.1). Unlike the TAP purification procedure the FLAG tag mediated affinity purification involves a single step (Figure 3.2).

Though tagging and purification strategy remain the same in these studies (Gavin et al. (2002 and 2006) and Krogan et al. (2006) identification and analysis of protein complexes were slightly different. Gavin et al. (2002 and 2006) analyzed the protein complexes by separating them using NuPAGE® SDS-PAGE and staining the proteins with Commassie stain followed by in gel tryptic digestion of protein bands excised from the stained gel and subsequent MALDI-TOF MS (Matrix Assisted Laser Desorption Ionization-Time of Flight Mass Spectrometry) analysis. In order to increase interactome coverage and confidence Krogan et al. (2006) analyzed the complexes using two different methods and

combined the data. They stained the SDS-PAGE with silver stain to visualize proteins, the protein bands were cut out of the gel and subjected to MALDI-TOF. They also digested the samples *in-solution* with trypsin followed by LC-MS/MS. The proteins tagged and the proteins co-precipitated with the tagged proteins in the four affinity purification studies are available online as supplementary data for each study.

From these published protein-protein interaction studies, we extracted information on proteins that are presumably in a complex with Gcn1.

3.1.1 Minimal Gcn1 interactome

In principle, the minimal Gcn1 interactome was generated by identifying all tagged proteins (the baits) that co-precipitated Gcn1 (Figure 3.3B), and by identifying proteins that co-precipitated with tagged Gcn1 (Figure 3.3C). In addition to Gcn1, in many instances, additional proteins (preys) (Figure 3.3A) have co-precipitated with a tagged protein. However, since we cannot exclude the possibility that the tagged protein may form separate complexes with the bait; one containing Gcn1, the other containing other proteins, these other co-precipitating proteins were omitted in this analysis. Thus, in this analysis we only consider proteins that are presumably in the same complex with Gcn1, and therefore this shall be called the minimal Gcn1 interactome.

Gcn1 was used as bait only in the Gavin et al. (2006) study (Figure 3.3B). They have identified twenty-three proteins (Aha1, Gcn20, Gfa1, Kap123, Lys12, Sam1, Vma2, Tub1, Tub2, Vps1, YBR025C, Adh1, Idh2, Mir1, Pet9, Psa1, Rpl4b, Rpp0, Rps1b, Rps1, Sed51, Ssa2 and Tef2) co-precipitating with Gcn1 (Figure 3.3C). Gcn20 was found as a Gcn1 interaction partner, but surprisingly Gcn2 was not found. Since Gcn20 binds stronger to Gcn1 than Gcn2 (*2*), this suggests that this study was only able to identify strongly binding proteins.

If these proteins indeed form a complex then, when used as baits, they should pull down Gcn1. This was true for Gcn20 (*75, 76*), Gfa1, Vma2 (*74*),

Aha1, Kap123, Lys12, and Sam1 (*74, 76*), strongly supporting the idea that these proteins are in a complex containing Gcn1 (*24*) (Figure 3.3C).

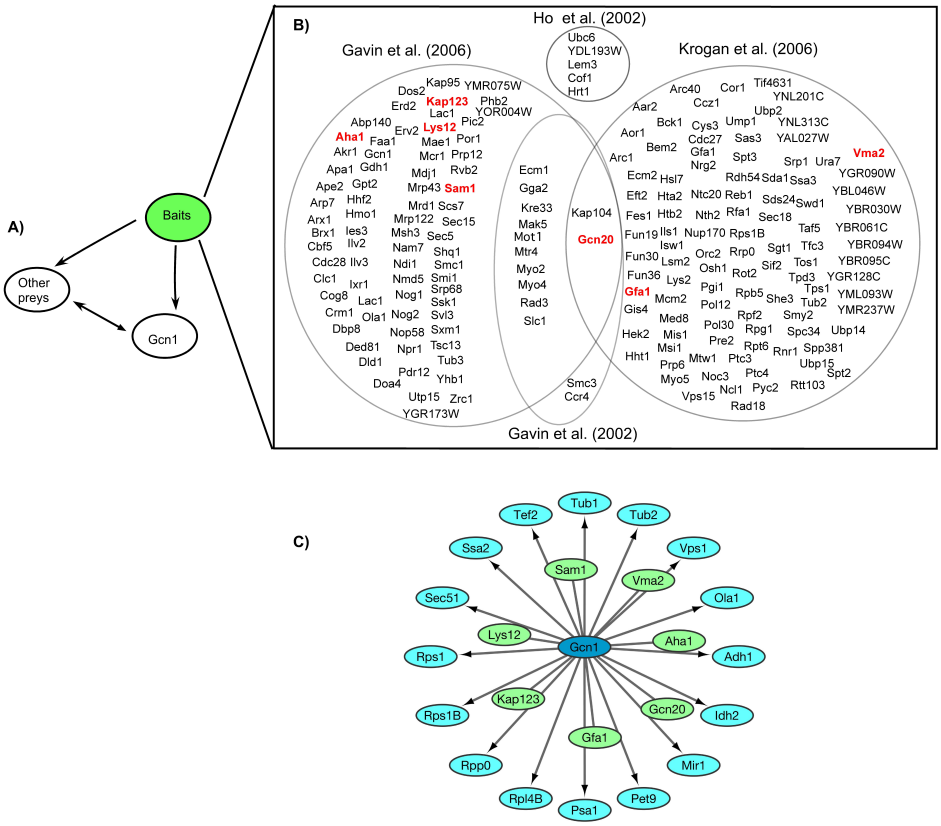

Figure 3.3. Minimal Gcn1 interactome. A) Different baits have co-precipitated Gcn1 in addition to several other prey proteins. B) Baits that co-precipitated Gcn1 in the four protein-protein interaction studies (*24-27*). Proteins that are co-precipitated by Gcn1 are highlighted in red. C) Proteins (preys) co-precipitated when Gcn1 was used as bait (green and cyan colored) (*24*). Gfa1 (*27*), Gcn20 (*24, 25, 27*), Aha1 (*24*), Vma2 (*27*), Sam1, Lys12 and Kap123 (*24*) each co-precipitated Gcn1, when used as bait (green colored).

In total, 195 proteins co-precipitated Gcn1: 74 proteins from the Gavin et al. (2006), 102 proteins from the Krogan et al. (2006), 10 proteins from the Gavin et al. (2002 and 2006), two proteins from the Gavin et al. (2002), two proteins from the Gavin et al. (2002 and 2006) and Krogan et al. (2006) and five proteins from the Ho et al. (2002) study.

There are two baits (Gcn20 and Kap104) common to all three TAP affinity purification studies and ten baits common to two TAP tagging studies (Figure 3.3B) which pulled down Gcn1. In addition to the identification of some common binding partners, different complexes were recovered even when the same tagged-protein was purified in different studies. For example the binding partners identified for Gcn20 were different in the three TAP tagged studies (*24, 25, 27*) (Figure 3.4).

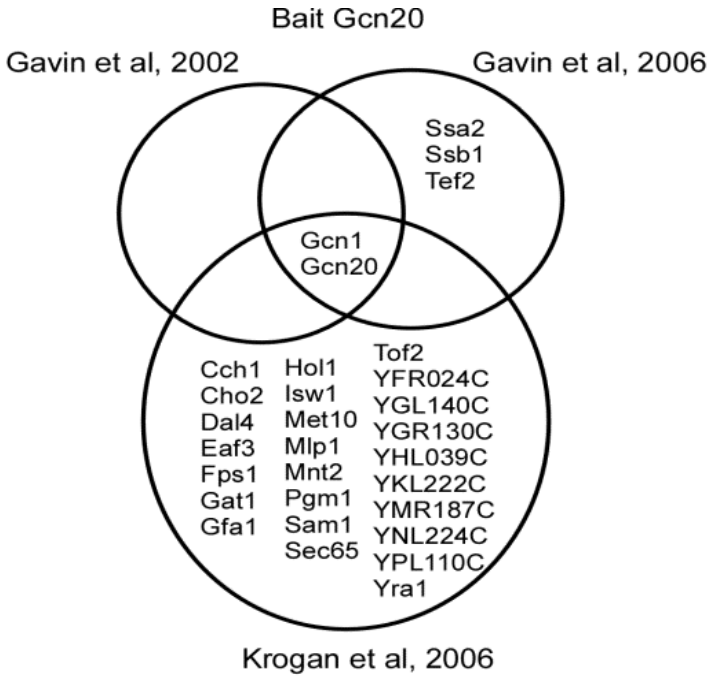

Figure 3.4. Proteins co-precipitated by Gcn20 in the indicated studies. Gcn20 was used as bait in Gavin et al. (2002 and 2006) and Krogan et al. (2006). The proteins co-precipitated by Gcn20 in each study are shown.

3.1.2 Extended Gcn1 interactome

As the same bait co-precipitated different binding partners in different studies, the decision was made to incorporate the preys co-precipitated by baits of the minimal Gcn1 interactome. Therefore, an extended Gcn1 interactome was generated from the preys co-precipitated along with Gcn1, by different baits in different affinity purification studies. The reasoning is that if the same interaction is found in different purification studies it is more likely to be a true interaction. If Gcn1 and

another protein (dubbed here X) were found to co-precipitate together by different baits and studies using different affinity purification procedures (TAP tag and FLAG tag), it is more likely that Gcn1 and protein X are interacting with each other.

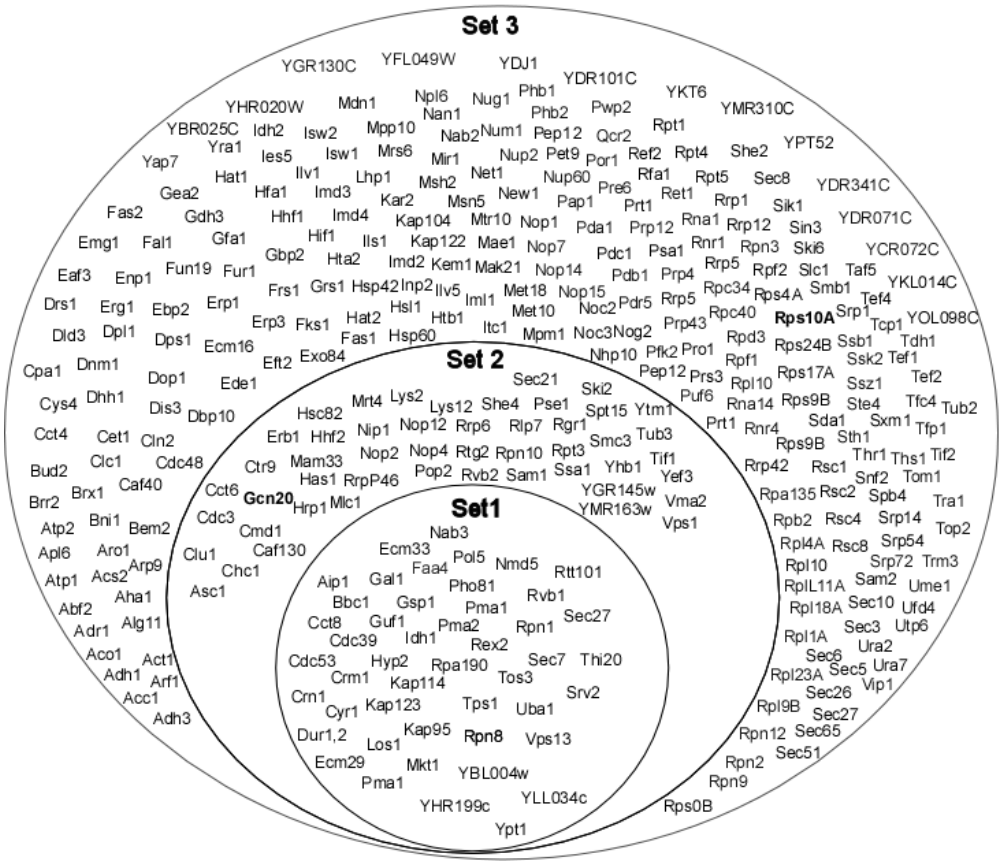

Figure 3.5. Extended Gcn1 interactome. Prey proteins that are found with Gcn1 in more than one study are included in this interactome. Preys found commonly in the Ho et al. (2002) (FLAG) study and at least in one of the three TAP tagged studies (Gavin, Bösche et al. 2002; Gavin, Aloy et al. 2006; Krogan, Cagney et al. 2006) are shown in set 1. Preys found in three different TAP tagging studies (Gavin, Bösche et al. 2002; Gavin, Aloy et al. 2006; Krogan, Cagney et al. 2006) are shown in set 2, and preys found in two TAP tagging studies (Gavin, Aloy et al. 2006; Krogan, Cagney et al. 2006) are shown in set 3.

There are 46 prey proteins that consistently co-precipitated with Gcn1 in the FLAG tagged interactome study and at least one of the three TAP tagged interactome study (Figure 3.5, Set 1). 48 prey proteins were found consistently in all three TAP tagged interactome study (Figure 3.5, Set 2), and 254 prey proteins

were found commonly in two of the three TAP tagged interactome study (Figure 3.5, Set 3).

The known binding partners of Gcn1, Gcn20 (*79, 80*) and Rps10A (Lee & Sattlegger, unpublished data) were identified in the extended interactome. Gcn20 was consistently found in all three different affinity purification studies (Figure 3.5, Set 2). Rps10A was identified in two of the three TAP tagged studies (Figure 3.5, Set 3). This suggests that the approach of this extended Gcn1 interactome identified potential interacting partners of Gcn1.

Interestingly the known regulators of Gcn2, eEF1A (TEF1/TEF2) (*81*), (Figure 3.5, Set 3) and Hsc82/Hsp90 (*82*) (Figure 3.5, Set 2) were found in the extended Gcn1 interactome.

Though we cannot exclude the possibility that protein X forms separate complexes, one containing Gcn1, protein X and the bait and the other one containing protein X, the bait and another protein (dubbed here Y). This incident cannot be identified in the previous approach. Therefore, in another approach, in order to identify proteins that are likely in a complex with Gcn1 we sought to determine whether protein X co-precipitates Gcn1 and the previously used bait when used as bait. If the interactions are observed in these two ways it is more likely that the proteins are in a same complex.

It was found that Kap123 (bait) was able to co-precipitate Kap95, Lys12 and Gcn1 (Figure 3.6, 1A). When Lys12 was used as bait, Gcn1 and Kap123 were co-precipitated but not kap95 (Figure 3.6, 1B). Similarly, Gcn1 and Kap123 were co-precipitated with Kap95 (Figure 3.6, 1.C) but not Lys12 (*24*). This may suggest that Kap123 and Gcn1 are members of two different complexes one containing Gcn1, Kap123 and Lys12 and the other one containing Gcn1, Kap123 and Kap95.

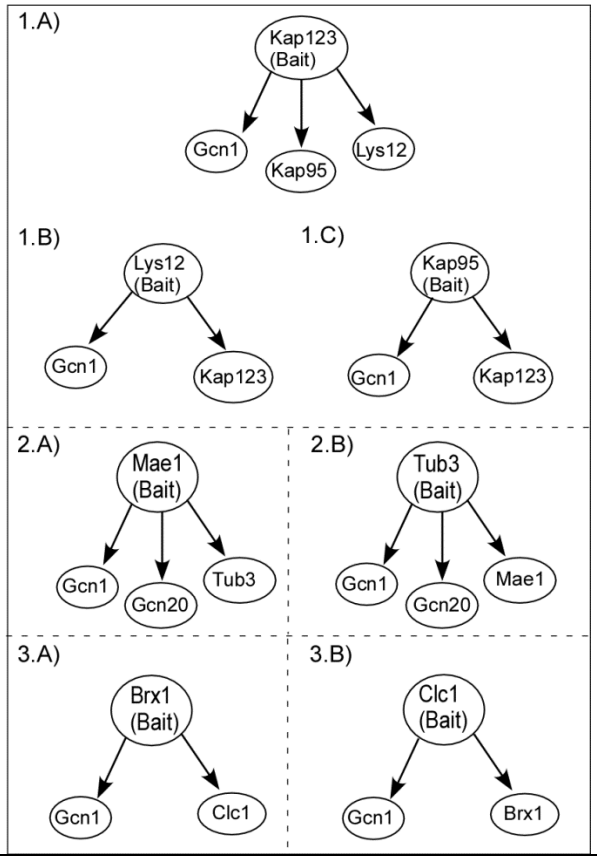

Figure 3.6. Identification of proteins potentially in the same complex with Gcn1. 1A) KAP123 (Bait) co-precipitated Gcn1, Kap95 and Lys12. 1B, C) Gcn1 and Kap123 were co-precipitated when Lys12 and Kap95 were used as baits. 2. A) Mae1 was able to co-precipitate Gcn1, Gcn20 and Tub3. 2. B) Tub3 co-precipitated Gcn1, Gcn20 and Mae1. 3.A) Brx1 co-precipitated Gcn1 and Clc1. 3.B) Clc1 co-precipitated Gcn1 and Brx1.

In another case, Gcn1, Gcn20 and Tub3 were co-precipitated by Mae1. Likewise, Gcn1, Gcn20 and Mae1 were co-precipitated by Tub3 (Figure 3.6, 2A, B) (*24*). These findings suggest that Gcn1, Gcn20, Mae1 and Tub3 are possibly in a same complex.

Brx1 was able to co-precipitate Gcn1 and Clc1. Gcn1 and Brx1 were co-precipitated by Clc1 (Figure 3.6, 3A, B), indicating that Gcn1, Clc1 and Brx1 are potentially in complexes containing Gcn1.

Taken together, these results suggest that Kap123, Kap95, Lys12, Mae1, Tub3, Brx1 and Clc1 are potentially in complexes containing Gcn1.

Of the four studies one used Kap123 as bait and interestingly Gcn20 was not found to be associated with Gcn1 (*24*). Similarly to Kap123, Brx1 co-precipitated Gcn1 but not Gcn20 (*24*). These findings suggest that Gcn1 is in a complex with many proteins that may not have Gcn20. It is possible that Gcn1 forms complexes that preclude Gcn2 and/or Gcn20. Or artificial expression systems could either push interactions in one way or force interactons that do not exist in the cell because of tags and overexpression.

3.1.3 Comprehensive affinity purification studies did not capture all the known interacting partners of Gcn1

Gcn1 was found to co-precipitate with 195 different bait proteins. As Gcn1, Gcn2 and Gcn20 are in the same complex, it was expected that Gcn2 and Gcn20 are present in all the co-precipitates that contain Gcn1. It was found that in the Gavin et al. (2006) study, seventeen out of the eighty-six co-precipitates contained Gcn20 along with Gcn1 but none of the co-precipitates contained Gcn2 (Figure 3.7). In the Gavin et al. (2002) pilot study there were two co-precipitates that contained Gcn1 along with Gcn20 but Gcn2 was not found in any of the fourteen Gcn1 containing co-precipitates.

In the Ho et al. (2002) study, either Gcn2 or Gcn20 was not found in the five co-precipitates that contained Gcn1.

Surprisingly, in the Krogan et al. (2006) study, there was only one co-precipitate that contained Gcn20 along with Gcn1 and 34 co-precipitates contained Gcn2 along with Gcn1 (which is known to be a weak interaction) out of the 104 co-precipitates that contained Gcn1 (Figure 3.7). It is possible that the interaction of Gcn2 with the 34 baits could have been stronger than its interaction with Gcn1. Unexpectedly among the 195 Gcn1 containing co-precipitates, Gcn1, Gcn2 and Gcn20 were not identified together in the same co-precipitate.

The known binding partners of Gcn1, Yih1 and Gir2 have not been identified either and this underscores that the Gcn1 interactome derived from the

published protein-protein interactions is not comprehensive. This also supports the idea that not all Gcn1-binding proteins have been identified.

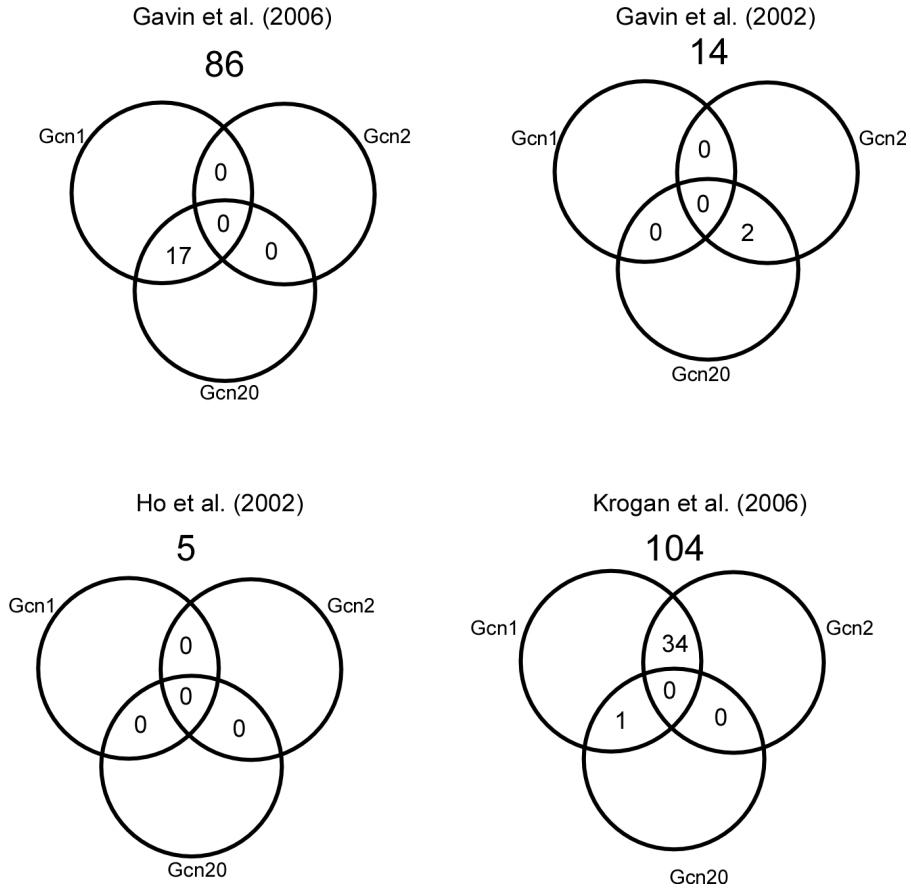

Figure 3.7. Occurrence of Gcn1-Gcn2, Gcn1-Gcn20 and Gcn1-Gcn2-Gcn20 interactions in the co-precipitates of indicated affinity purification studies.

3.1.4 Discussion

In order to create a Gcn1 interactome based on published data, the data on Gcn1 containing protein complexes from all published large scale affinity purification studies were accumulated. We reasoned that if a particular interaction is found in more than one study it is more likely that the interaction is true, in particular if these studies involved different purification procedures. The TAP tagging is a two-step affinity purification procedure involving natively expressed proteins, and

was proposed to effectively remove contaminants (*83*). Over-expression of proteins in the FLAG tagged study could drive weak interactions via mass action, therefore facilitating the identification of weak interactions. Such weakly interacting proteins are important because transient interactions are known to control many cellular processes (*84*).

The known Gcn1 binding proteins Gcn20 (*79, 80*) and Rps10A (Lee & Sattlegger, unpublished data) were identified in the extended Gcn1 interactome (Figure 3.5). In addition, the known Gcn2 regulating proteins, eEF1A (*TEF1*) (*81*) and Hsc82/Hsp90 (*82*) were identified in the extended Gcn1 interactome.

Aha1, Gfa1, Kap123, Lys12, Sam1 and Vma2 were identified as potential Gcn1 binding proteins as their interactions with Gcn1 were detected in both ways (Figure 3.3 C). Aha1 binds to Hsp90 and promotes its ATPase activity and is a co-chaperone of the Hsp90 family (*85, 86*). Aha1 is not required for cell growth under normal conditions, and is essential for cell growth under stress conditions. Expression of *AHA1* is regulated by heat shock and DNA replication stress (*87*). It is highly conserved and homologs of Aha1 are found in plants, flies, mice and humans (*86*). Similarly to Aha1, Gcn1 and Gcn2 are not required for cell growth under normal conditions and these proteins are required only under conditions of starvation and some other stress conditions (*10, 38*). This may suggest that Aha1 together with the Gcn1-Gcn2 complex is functional under conditions of DNA replication stress. Supporting this idea, strains lacking Gcn1 and Gcn2 are sensitive to methyl methane sulfonate, a DNA damaging agent (*9*).

Vma2 is another protein involved in DNA replication stress. It encodes for the beta subunit of the V-ATPase V1 domain. Vacuolar ATPases are ATP dependent proton pumps responsible for acidification of intracellular compartments. *VMA2* expression increases in response to DNA replication stress (*88, 89*).

Glutamine-fructose-6-phosphate amidotransferase, which converts fructose-6-phosphate to glucosamine-6-phosphate, is encoded by *GFA1* (*90, 91*). *GFA1* expression is induced by mating pheromones and perturbation of the cell

wall (*92*). It is possible that Gcn1, Gcn2 and Gfa1 function under conditions that disturb the cell wall. In accord with the idea a role of Gcn2 mediated regulation of translation initiation has been reported in cell wall integrity (*93*).

Kap123 (Karyopherin beta) is involved in the nuclear import of ribosomal proteins (*94*), histones H3 and H4 (*95*). Kap123 localizes to the cytoplasm, nuclear pore and nucleus (*96, 97*). It appears that Kap123 binds to Rpl25, Rps1a, Rpl8, Rpl18, Rpl12, Rpl32, Rpl11, and Rpl42, (*98*) and among these ribosomal proteins Rpl25 requires Kap123 to get imported into the nucleus efficiently (*99*). The interaction of Gcn1 with Kap123 and ribosomal proteins (refer to Section 3.2.7) may suggest a role for Gcn1 in the nuclear export/import of ribosomal proteins.

Lys12 is involved in the biosynthesis of lysine, and it is believed to be in the mitochondria where lysine biosynthesis takes place (*100*).

SAM1 encodes S-adenosyl methionine (Adomet) synthetases which catalyses transfer of the adenosyl group of ATP to the sulphur atom of methionine. It is involved in the methylation of RNAs, lipids and proteins (*101, 102*).

Interaction of Gcn1 with Lys12 and Sam1 indicates that Gcn1 may be involved in cellular processes, including but not limited to amino acid biosynthesis, nuclear import, methylation of RNAs and proteins.

However, as the functions of Gcn1 remain unknown the possible reasons for Gcn1 binding to proteins involved in several distinct functions in the cell could not be explained at this instant.

When the same protein was affinity purified different studies have identified different binding partners (*24, 25, 27*) (Figure 3.4). It is really hard to make conclusions out of different proteomic studies as there are uncontrolled variations between experiments. As mentioned before (Figure 3.2) the experimental procedures were different, thus it is not surprising that the resulting complexes looked very different. This may be due to contaminating proteins present in one study but not in the other, or due to a true binding partner being lost in one study but not in the other.

The weak interaction between Gcn1 and Gcn2 has been found under starved and unstarved conditions (*13*). However, Gcn2 was not identified in the minimal or in the extended Gcn1 interactome. This suggests that the nature of the purification procedures used in the large scale affinity purification studies has limited them to identify only stable complexes. Thus transient or weak interactions have likely escaped identification. We speculate that such transient or weak interactions are unable to withstand the stringent washing conditions (high salt or detergent) used in these large-scale affinity purifications to remove non-specifically bound proteins. In agreement with this idea, purification buffer used in the large-scale affinity purification studies contained non-ionic detergents (NP40 or triton X-100), which are known to change the conformation of proteins and dissociate some protein-protein interactions (*85*). In addition to the above-mentioned reasons, the inability to identify the known Gcn1 interacting partners may be due to; a) the size and location of the affinity tag. Considering that the TAP tag is ~20 kDa in size, tagging proteins with TAP could interfere with the function of these tagged proteins and obscure their binding to interacting partners (*78*), b) the particular interaction not occurring under the tested conditions, c) the affinity purification procedures were carried out in large scale and the purification procedure has not been optimized for each individual bait which is likely a contributing factor for not identifying all interaction partners of Gcn1.

3.2 Identification of Gcn1 binding proteins from *in house* data

As mentioned in the previous section (3.1.3) the comprehensive protein-protein interaction studies did not consistently detect the already known interacting partners of Gcn1. This suggested that very likely other Gcn1 binding proteins (Gcn1 BPs) remain unidentified. Therefore, we attempted to develop an experimental procedure to comprehensively identify novel proteins interacting with Gcn1. In this approach live cells are treated with formaldehyde which crosslinks protein-proein interactions. Proteins cross-linked to protein of interest are co-purified by affinity purification and subjected to a procedure which reverses the cross-links. After separation by SDS-PAGE proteins were visualized by colloidal Coomassie staining. Proteins were subjected to trypsin digestion, then peptides were extracted from the gel, follwed by Liquid Chromatography Tandem Mass Spectrometry (LC-MS-MS).

3.2.1 Stabilization of protein-protein interactions via formaldehyde mediated cross-linking

Identification of many novel protein-protein interactions using formaldehyde cross-linking followed by immunoprecipitation experiments has been reported. For example, novel proteins of the integrin beta-1 complex (*103*), 26S proteasome (*104*), M-Ras associated complex (*105*) and RNA polymerase II transcription complexes (*106*) have been identified using formaldehyde cross-linking.

Formaldehyde possesses two reactive groups that form covalent bonds with target molecules (proteins and DNA), thereby stabilizing weak interactions, (*107-110*). As a cross-linking agent formaldehyde has many advantages that make it suitable for protein-protein interaction studies. Formaldehyde is a homo-bifunctional cross-linker with a spacer arm (distance between the two reactive groups) of 2.3-2.7Å, meaning that only proteins that are in close proximity can be cross-linked (*111*) (Figure 3.8). Normally only truly interacting proteins will be in such close proximity, making it is less likely that it leads to non-specific cross-linking of proteins that just happen to reside next to each other in the cell. Due to

its small size, formaldehyde can permeate the cell wall and intracellular membranes very quickly (*103*), suggesting that it provides a snapshot of interactions that occur at the time of addition. Due to its small size formaldehyde can easily permeate cell walls and intracellular membranes resulting in inactivation of enzymes almost immediately upon addition to cells and therefore there will not be any enzymatic alterations of the proteins during harvesting and cell lyses (*111*). Furthermore, formaldehyde mediated cross-links are reversible by heat, making further downstream analysis more straight-forward such as Western blotting and Mass Spectrometry (*111*).

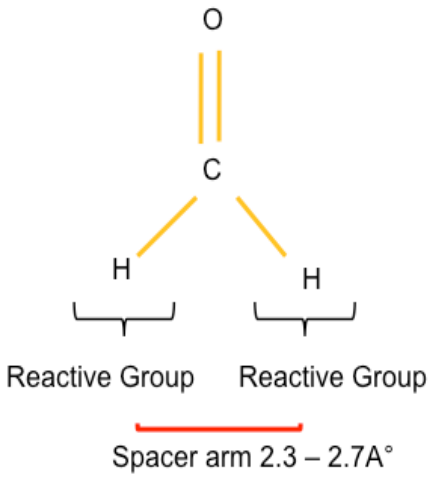

Figure 3.8. Structure of formaldehyde representing the two reactive groups and its spacer arm.

3.2.2 The TAP and Myc-tags do not affect Gcn1 function

It was reasoned that if the antibodies against Gcn1 interact with a protein-binding domain of Gcn1, it may disrupt the interaction of Gcn1 with its binding partners. Therefore, the decision was made to use an epitope tagged version of Gcn1 to affinity purify Gcn1 containing protein complexes from cell extracts. Gcn1 tagged at the C-terminus with TAP or Myc epitopes were available in the Sattlegger lab.

First it was investigated whether the tags affect the function of Gcn1. If tagging affects Gcn1 function, then Gcn2 activation would be impaired. Therefore, it is expected that strains with defective Gcn1 function will have a growth defect under amino acid starvation conditions.

To test this, plasmids carrying the Myc tagged *GCN1* from a low copy (lc) or high copy (hc) plasmid, untagged *GCN1* or vector alone (refer to Table 2.1) were introduced into the *gcn1*Δ strain. Wild type transformed with vector alone was used as a positive control. The resulting tranformants, strain containing chromosamally TAP tagged *GCN1* and *gcn1*Δ strain were subjected to semi quantitative growth assays in the presence of amino acid starvation inducing drugs, **3-Amino Triazole (3-AT)** or **Sulfometuron methyl (SM).** 3-AT causes starvation for histidine and it is a competitive inhibitor of the *HIS3* gene product, imidazole glycerolphosphate dehydratase, an enzyme involved in histidine biosynthesis (*112*). SM causes starvation for the branched amino acids by inhibiting the enzyme involved in the biosynthesis of these amino acids (*113*).

Saturated cultures of the indicated strains (Figure 3.9) were grown in liquid minimal media and the cultures were tenfold serially diluted. 5 µl of each dilution and undiluted cultures were spotted on plates containing 3-AT or SM, and no SM as a control. After spotting the cultures, the plates were incubated at 30°C and the growth was monitored for 7 to 10 days.

As expected, the wild type grew well on both the control and starvation plates and the strain lacking Gcn1 was unable to grow on either SM or 3-AT containing plates, suggesting the successful induction of starvation by 3-AT and SM (Figure 3.9).

Similar to the wild type, strains expressing the TAP tagged *GCN1* grew well on both the control and starvation plates. This result suggested that the TAP tagging has no effect on Gcn1 function, at least at the investigated SM concentration (Figure 3.9A).

As shown, (Figure 3.9B), similarly to the wild type, strains carrying the Myc tagged (lc or hc) and untagged Gcn1 were able to grow on both the control and starvation plates. But at higher concentrations of 3-AT, strain that expressed *GCN1* from the lc plasmid displayed a mild growth defect.

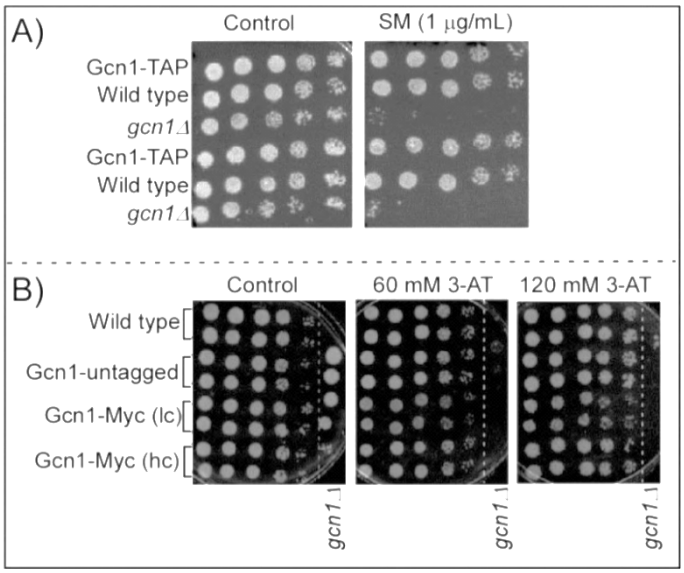

Figure 3.9. Semi quantitative growth assay of TAP tagged Gcn1 (A) and Myc tagged Gcn1 (B). Indicated strains were grown in liquid minimal media with appropriate amino acids. Saturated yeast cultures were 10 fold serially diluted, four different dilutions and undiluted cultures were spotted on plates containing SM, 3-AT and no drug as a control. Growth was monitored every day for 7 to 10 days. The experiment was performed with two independent biological replicates.

Though both the lc and hc plasmids expressed Myc-tagged *GCN1,* the growth defect was observed only in the strain that expressed *GCN1* from the lc plasmids. It is possible that *GCN1* from the lc plasmids was not expressed to the level that was expressed from its chromosomal gene. Therefore, the expression level of Gcn1 in these strains was investigated.

According to the western blot result, *GCN1* was expressed about 0.5 times more from the hc plasmid, and 0.5 times less from the lc plasmid, than endogenous *GCN1* (Figure 3.10). It is surprising to see that the lc plasmid expressed less Gcn1 than the endogenous gene. Considering that lc plasmids reside as 2-3 copies in the cell (*114*), one would expect that it leads to higher

Gcn1 levels than that in a wild type strain with chromosomal *GCN1*.

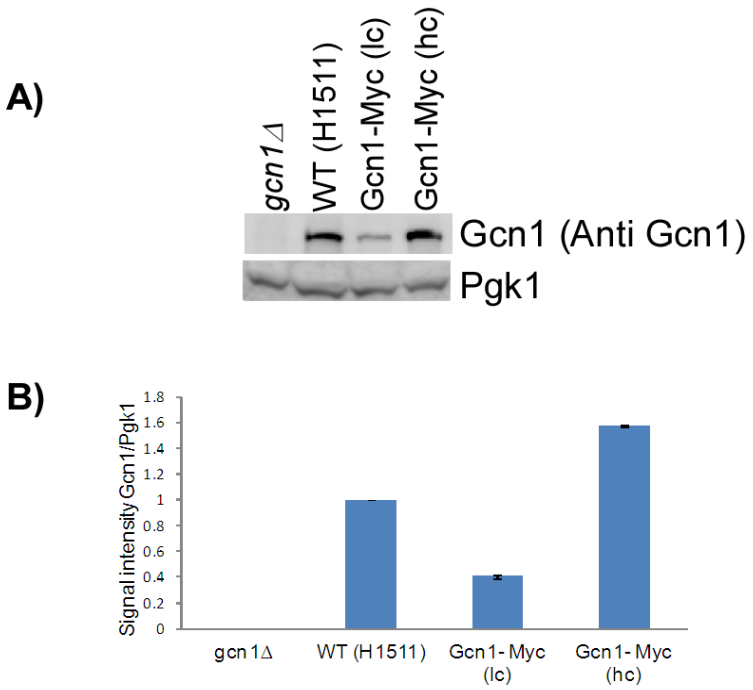

Figure 3.10. Expression levels of endogenous *GCN1*, and *GCN1* from a low copy and high copy plasmid. A) 50 µg of cell extracts from the *gcn1*Δ (H2556) strain transformed with low copy (lc) or high copy (hc) and the wild type (H1511) strains (refer to Table 2.1 and Table 2.2) were resolved by SDS-PAGE and the proteins were subjected to immunoblotting using antibodies against Gcn1 or Pgk1. B) The Gcn1 and Pgk1 signals were quantified using the Multi Gauge V3.1 software (Fujifilm) and the Gcn1/Pgk1 signal ratio was calculated and normalized to that of the wild type. The experiment was performed with two independent biological replicates and the standard error is indicated.

The fact that the hc plasmid, which is supposed to be maintained with 100 copies per cell (*114*) expressed only 0.5 times more than the endogenous *GCN1,* might indicate that the plasmid borne gene was not expressed efficiently, possibly because the promoter was truncated, or because the transcript was incomplete and prone to degradation. The low abundance of Gcn1 in the *gcn1*Δ strain harboring lc *GCN1* may explain why this strain showed slight 3-AT sensitivity.

Taken together, the results suggested that either Myc or TAP tagging does not have an effect on Gcn1 function.

3.2.3 Formaldehyde cross-linking does not affect anti-Myc antibody mediated immunoprecipitation of Gcn1-Myc

It was decided to subject the strains expressing tagged Gcn1 to formaldehyde cross-linking followed by affinity purification to isolate Gcn1 containing complexes. Formaldehyde is known to preferably react with the side chains of cysteine (C), tyrosine (Y), tryptophan (W), asparagine (N), glutamine (Q), arginine (R), histidine (H) and lysine (K) residues (*110*). It was reasoned that if these residues are involved in antigen-antibody binding, then their modification by formaldehyde may mask the epitope necessary for tag mediated affinity purification. Therefore, the sequence of the tags was investigated for the presence of potential residues that could be targeted by formaldehyde.

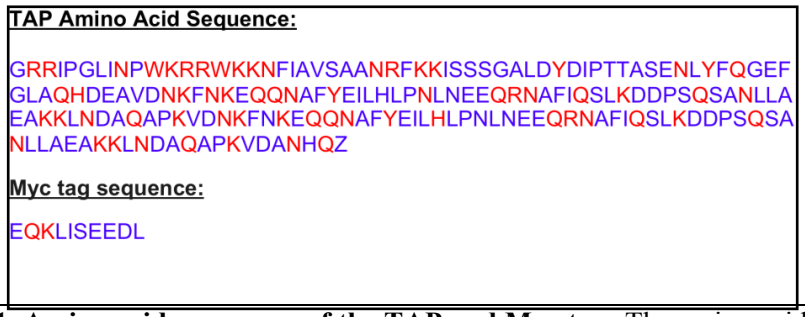

Figure 3.11. Amino acid sequences of the TAP and Myc tags. The amino acids that are highly reactive with formaldehyde are highlighted in red.

The Myc epitope is very small (~1.2 kDa) in size (*115*) and it contains two residues that are highly reactive with formaldehyde (Figure 3.11). The TAP tag is 20 kDa (*27*) in size and it contains many residues that could readily react with formaldehyde (Figure 3.11). Although our experimental results indicated that the TAP tag did not affect the function of Gcn1, we did not want to use the TAP tagged Gcn1 for our studies as it has more amino acids that can readily react with formaldehyde, which could result in antigen-epitope masking by formaldehyde. Therefore, we proceeded our studies with the Myc tagged Gcn1 only, expressed from a lc plasmid. Formaldehyde cross-linking followed by successful immunoprecipitation of the c-Myc tagged Ras has been reported by Vasilescu et

al. (2004), suggesting that this tag is suitable for our study.

Formaldehyde cross linking needs to be optimized for the protein being investigated, because it depends on the location, amount of amino acids, and their accessibility, for cross-linking. As it is a chemical reaction, the rate of cross-linking depends on the temperature, incubation time and the amount of formaldehyde used (*111*). Therefore, optimization experiments were required to find the best cross-linking conditions that stabilize Gcn1-containing complexes. Thus, the next approach was to optimize the conditions for effective cross-linking of Gcn1-containing complexes. For the optimization experiments, strain that expressed *GCN1*-Myc from a lc plasmid was used.

3.2.4 The effect of time and temperature on formaldehyde cross-linking of Myc-tagged Gcn1

To determine the effect of temperature on formaldehyde cross-linking, 1% formaldehyde (final concentration) was used to subject the cells to cross-linking at room temperature or at 4°C. In addition, it was investigated whether the antibodies against Myc would be able to immunoprecipitate the Myc-tagged Gcn1 from the cell extracts of formaldehyde treated cells.

Yeast cells expressing the *GCN1*-Myc, and the control strain (*gcn1*Δ) carrying the vector alone were grown to exponential phase and were then subjected to formaldehyde treatment (1%) for 10 or 60 minutes at room temperature or at 4ºC. Cell extract from the cells subjected to formaldehyde cross-linking and untreated control was obtained. 500 μg of cell extract was subjected to anti-Myc antibody mediated immunoprecipitation. The immunoprecipitates were resolved by SDS-PAGE and subjected to Western blotting with antibodies against Myc. The basic principle of the anti-Myc antibody mediated immunoprecipitation is given in Figure 3.12.

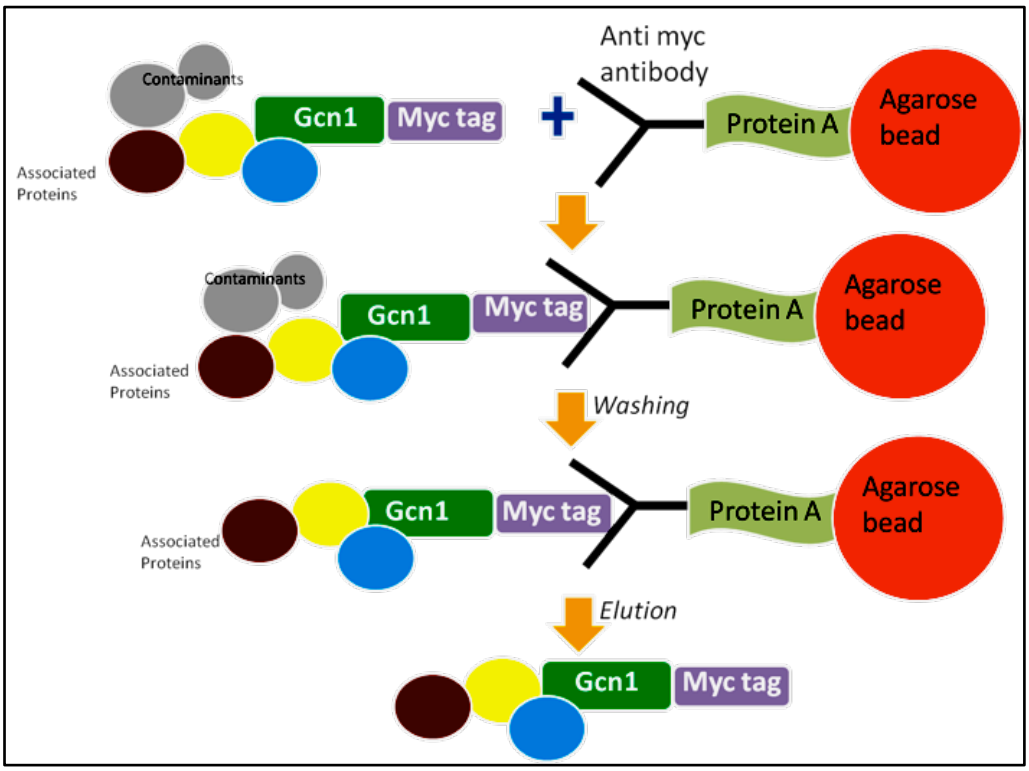

Figure 3.12. Basic principle of the anti-Myc antibody mediated immunoprecipitation. Gcn1 is expressed as a fusion protein carrying Myc tag at the C-terminus. Cell extract is prepared from these cells and then incubated with the antibody against the Myc-tag that is immobilized on a solid support (Agarose/Sepharose beads) via protein A. Unbound and non-specifically bound proteins are washed away from the solid support. Bound material is eluted from the beads by lowering the pH, competitive displacement or by boiling the beads with protein loading dye. For our optimization experiments the beads were boiled in protein loading dye.

A signal for Gcn1-Myc was detected in the imuunoprecipiates, obtained from the extracts of cells that were subjected to cross-linking at RT or at 4ºC and from the untreated control (Figure 3.13). This indicated that the anti-Myc antibody was able to immunoprecipitate Gcn1-Myc from the cell extracts.

The amount of Gcn1-Myc signal detected in the samples cross-linked at 4°C for 10 or 60 minutes did not show any difference when compared to the noncross-linked ones (Figure 3.13). This suggested that almost equal amount of Gcn1 was immunoprecipitated in these samples. But varying amounts of Gcn1 signal were

detected at different incubation times in the samples that were cross-linked at RT. The amount of Gcn1 signal detected in the samples cross-linked for 10 minutes was lower than that of the untreated control, indicating that less Gcn1 was immunoprecipitated in these samples (lanes 8 and 11). Almost no Gcn1 was detected in the samples cross-linked for 60 minutes (lanes 9 and 12). This indicated that less amount of Gcn1 was immunoprecipitated from cell extracts obtained from the cells subjected to formaldehyde cross-linking for increased incubation time. The result of this experiment suggested that the incubation time had no effect on formaldehyde cross-linking in the samples cross-linked at 4°C but the effect was obvious in the samples cross-linked at RT. Therefore, it was decided that cross-linking at RT for 10 minutes could be sufficient.

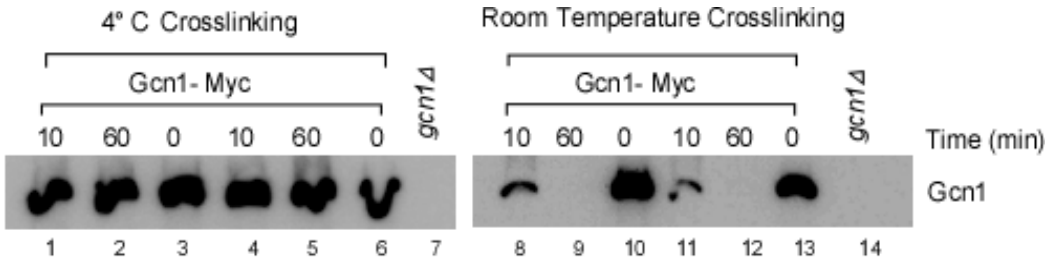

Figure 3.13. The effect of temperature and incubation time on formaldehyde cross-linking and anti-Myc antibody mediated immunoprecipitation. The *gcn1*Δ (H2556) strain transformed with lc plasmid carrying the c-Myc tagged *GCN1* or vector alone control (refer to Table 2.1) (lanes 7 and 14) were grown to exponential phase, cross-linked with 1% formaldehyde for 0, 10 or 60 minutes at room temperature or at 4°C. One set of sample was left untreated as a control (lanes 6 and 13). 500 µg of protein was subjected to anti-Myc immunoprecipitation. The immunoprecipitates were resolved by SDS-PAGE followed by Western blotting with antibodies against Myc. The experiment was performed with two independent biological replicates.

There could be two possible reasons why reduced amount of Gcn1 was immunoprecipitated from the cell extracts obtained from the cells subjected to formaldehyde cross-linking at room temperature; 1) if formaldehyde reaction with the Myc epitope destroys the binding sites for anti-Myc antibodies, this would lead to reduced Gcn1 immunoprecipitation from the cell extracts, 2) longer

incubation with formaldehyde could form unspecific protein cross-linking and protein aggregation which could be spun down in the process of generating the cell extracts (refer to Figure 3.15 for the procedure to make the cell extract).

To distinguish between these two possibilities, the effect of different formaldehyde concentrations on the protein yield in the whole cell extract was investigated. Gcn1-Myc containing cells were grown to exponential phase (A_{600}=1.5) and then exposed to different concentrations of formaldehyde (0.1%, 0.3%, 0.5% and 1%) for 10 minutes at RT. The cells were broken open, cell extracts obtained and protein concentrations in the cell extracts were estimated using the Bradford method. 50 µg of total protein from all of the four formaldehyde treated samples, including untreated control samples, were resolved by SDS-PAGE and subjected to Coomassie staining.

There was not much visible difference between the intensity of the banding patterns in the 0.1% formaldehyde treated samples and in the untreated control, indicating that the total amount of protein was almost the same in these two samples. This was not the case for cells treated with higher concentrations of formaldehyde. The 0.3, 0.5 and 1% formaldehyde treated samples have less protein as compared to the untreated samples (Figure 3.14). This suggested that cross-linking for 10 minutes with the increasing amount formaldehyde concentrations results in general protein loss. It has been reported that 1% formaldehyde for 30 minutes incubation results in 90% global protein loss (*103, 111*). In agreement with these studies (*103, 111*) this result also suggests that even 0.3 and 0.5% formaldehyde treatment for 10 minutes incubation time leads to a visible decrease in the total amount of protein in these samples.

As suggested previously (*103*) the protein loss due to formaldehyde cross-linking could be due to the formation of protein aggregates and cross-linking of nuclear proteins to DNA. In addition extensive cross-linking may result in cross-linked protein complexes to which cytoskeletons and other proteins can bind non-specifically resulting in big protein complexes. As the process of making the cell

extracts involves centrifugation at high-speed these bigger molecular complexes may have precipitated down in the pellets. It was evident from the previous experiment (Figure 3.14) that cross-linking leads to global protein loss, and Gcn1 is a big protein, it was reasoned that Gcn1 was cross-linked with other proteins and the big Gcn1 containing complexes may not be able to withstand the centrifugations used to prepare the cell extracts. Therefore, it was next investigated whether Gcn1 containing complexes were lost in the pellet.

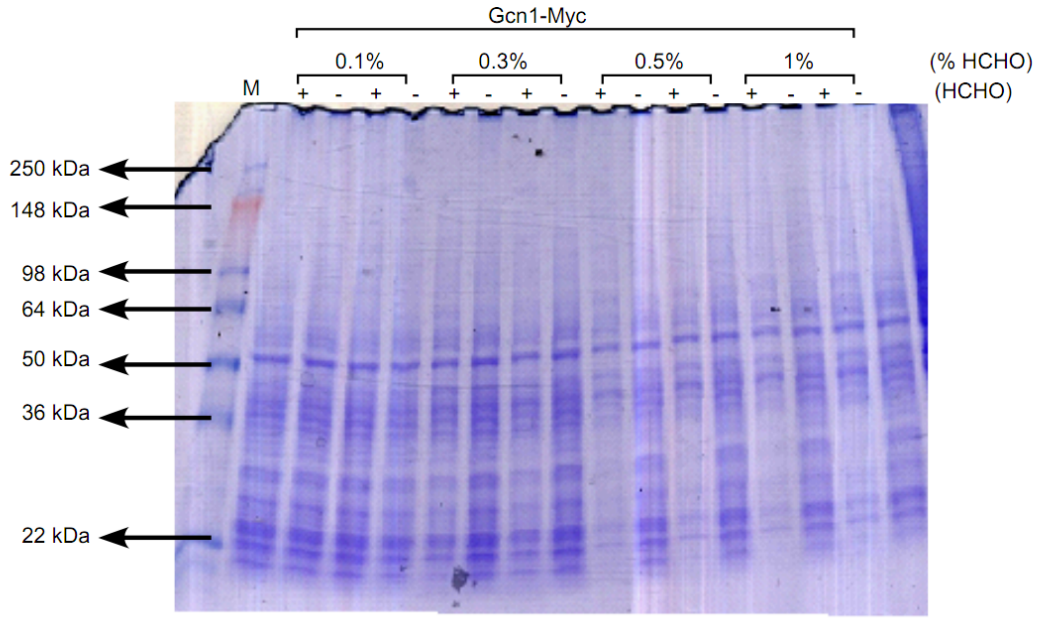

Figure 3.14. Comparison of the total protein concentration in cell extracts obtained from the cells subjected to formaldehyde cross-linking (+) or not (-), at room temperature. Strains expressing *GCN1*-Myc and the *gcn1*Δ strains (refer to Table 2.1) were grown to exponential phase and then treated with different concentrations of formaldehyde as indicated (+), and no formaldehyde as a control (-). 50 µg of protein was denatured at 95°C for 10 min and resolved by SDS-PAGE, and the proteins were visualized by the Coomassie brilliant blue stain. The experiment was performed with two independent biological replicates.

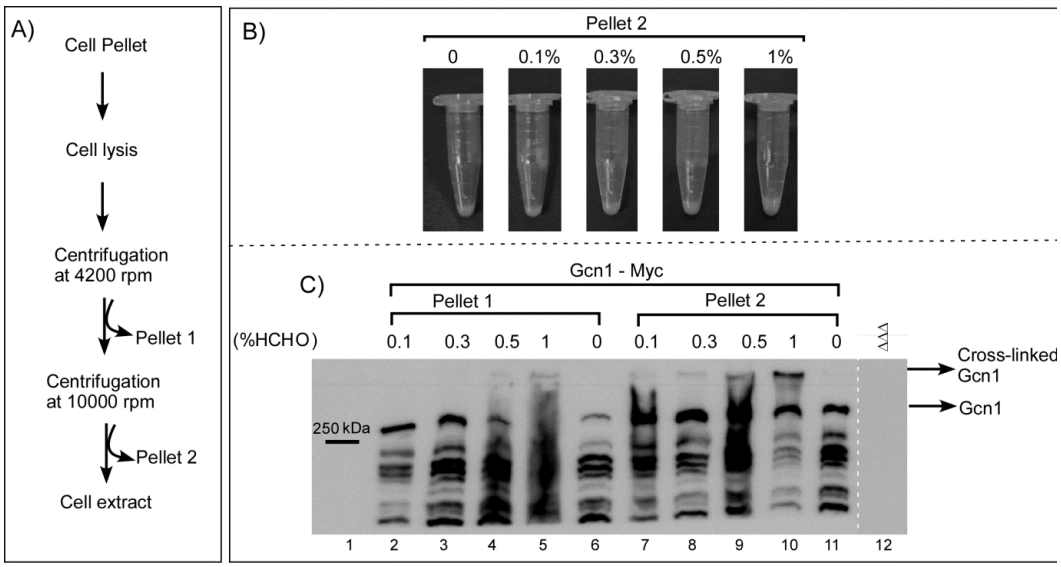

Figure 3.15. A) Overview of the steps involved in generating the cell extracts. B) Pellets of the 10,000 rpm spin from Figure 3.14. C) The pellets from the 4200 rpm and 10000 rpm centrifugations (pellets 1 and 2) were solubilized and subjected to SDS-PAGE followed by Western blotting with antibodies against Myc. Full length Gcn1 is supposed to run just above 250 kDa, the signal visible below 250 kDa is possibly due to degradation of Gcn1-Myc.

For generating cell extracts, the procedure was to vortex the tubes containing cells and 0.2 mm glass beads. The tubes were then subjected to centrifugation at 4200 rpm, and the supernatant was spun again at 10,000 rpm to remove the insoluble fraction. The final supernatant is the cell extract (Figure 3.15, A). If it is true that formaldehyde generates large molecular complexes and aggregates, then the protein aggregates should be found in the pellets formed during high-speed centrifugations conducted at 4200 rpm or 10000 rpm (Figure 3.15, B).

To test our prediction, the pellets from the 4,200 rpm and 10,000 rpm centrifugations were washed to remove traces of soluble protein, and then boiled in protein loading dye to bring the insoluble proteins into solution. The insoluble proteins were then denatured at 75°C before separating the sample using a 4-17% gradient SDS-PAGE. The separated proteins were subjected to Western blotting

with anti-Myc antibodies to investigate whether Gcn1 was present in the insoluble fractions. It was expected that denaturing the samples at 75°C will result in solubilization of the pellets and will not reverse all the formaldehyde mediated cross-links and the cross-linked Gcn1 containing complexes appear at a higher molecular weight than noncross-linked Gcn1.

A signal for Gcn1 was detected in the cell pellets, (Figure 3.15, lanes 6 and 11) that have not been subjected to formaldehyde cross-linking. This suggests that a certain amount of Gcn1 got lost even under non-cross linking procedures.
In pellet 1, a signal for Gcn1 at the higher molecular weight complexes was detected in the 0.5 and 1% formaldehyde treated cells. In pellet 2, the Gcn1 signal at the higher molecular weight complexes was detected from 0.3-1% formaldehyde concentrations. This indicated that the Gcn1 containing protein complexes in the pellets (Pellet 1 and 2) increased with increasing amount of formaldehyde concentrations. One possible reason for this would be that with increasing amount of formaldehyde treatment Gcn1 was possibly being cross-linked with proteins, DNA or RNA and the cross-linked complexes were unable to withstand the centrifugation speed thus precipitated down in the pellet.

The next step was to identify a formaldehyde concentration where Gcn1 loss was minimised and sufficient interactions of Gcn1 have been stabilized. For this, 50 μg of cell extracts from the cells treated with different concentrations of formaldehyde were denatured at 65°C or 95°C and the proteins were resolved by SDS-PAGE followed by Western blotting with anti-Myc antibodies. The idea behind this is that denaturing the samples at 65°C will predominantly not break the formaldehyde mediated cross-links, and in this case we should see cross-linked proteins migrating slower than expected in SDS-PAGE. On the other hand, denaturation of the samples at 95°C would reverse most of the cross-links and proteins should migrate in SDS-PAGE at the expected rate.

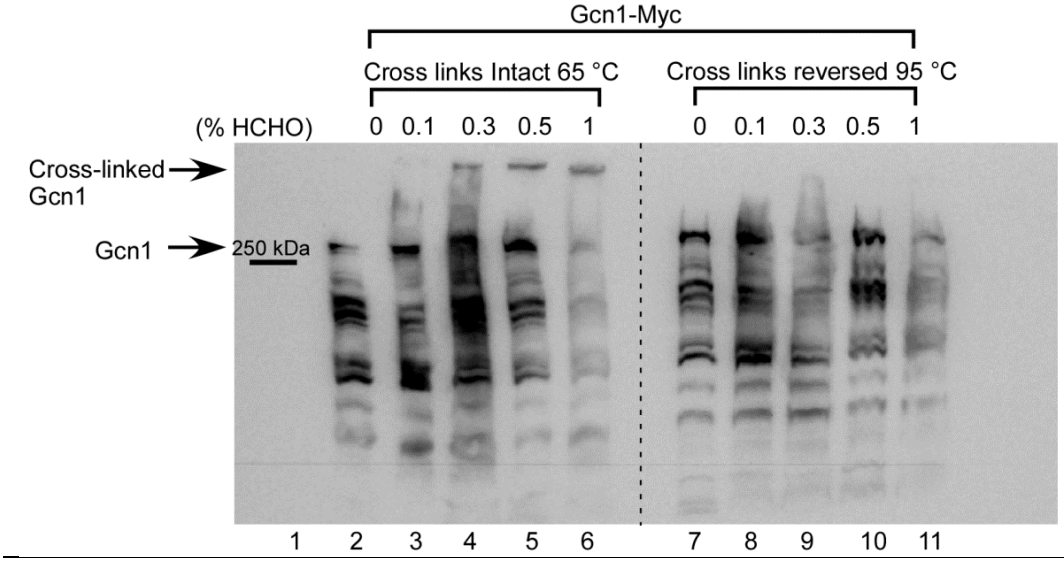

Figure 3.16. Stabilization of Gcn1 containing protein complexes by formaldehyde cross-linking. Formaldehyde mediated cross-links were preserved when samples were denatured at 65°C and formaldehyde mediated cross-links are reversed at 95°C. Samples were generated as in Figure 3.14, and then 50 µg of total protein were denatured at 65°C or at 95°C. These denatured samples were separated by SDS-PAGE followed by Western blotting with antibodies against Myc. Full length Gcn1 is supposed to run just above 250 kDa, the signal visible below 250 kDa is possibly due to degradation of Gcn1-Myc.

As expected, in the samples that were denatured at 95°C, the Myc antibodies detected Gcn1 at the expected molecular weight (just above 250 kDa) (Figure 3.16, lanes 7-11). In samples that were denatured at 65°C a signal was found at the expected molecular weight of 250 kDa (Figure 3.16, lanes 2-6) and also at a higher molecular weight. The higher molecular weight complexes were detectable in samples treated with 0.3 to 1% formaldehyde (Figure 3.16, lanes 4-6). The higher molecular weight band suggests that formaldehyde has successfully stabilized Gcn1 containing complexes. The proportion of Gcn1 migrating at this higher molecular weight increased with increasing amounts of formaldehyde, suggesting that with increasing amounts of formaldehyde concentrations more Gcn1 was cross-linked.

From our findings, we concluded that 0.1% formaldehyde is not sufficient to significantly stabilize Gcn1 containing complexes, and 0.5 and 1% formaldehyde results in significant protein loss (Figure 3.14 and 3.16). Therefore,

0.3% formaldehyde concentration appeared to be the best amount for sufficiently stabilizing Gcn1 containing complexes while not losing too much of these complexes during the cell extract preparation.

3.2.5 Optimization of Gcn1-Myc co-immunoprecipitation

In order to identify Gcn1 binding proteins (Gcn1-BPs), Gcn1 containing protein complexes needed to be affinity purified. Therefore, purification conditions needed to be optimized. We wanted to identify a condition where known Gcn1 binding partners (Gcn2 and Gcn20) are co-precipitated with Gcn1, but not with unrelated proteins, such as Phosphoglycerate kinase (Pgk1). Pgk1 is a key enzyme in glycolysis (*116*). Pgk1 is not known to associate with Gcn1, expressed at high levels in the cells and it was found as a contaminant in many affinity purification studies (*26*). As a control, Gcn2, Gcn20 should not co-precipitate when using a strain lacking Gcn1.

The cells that expressed Gcn1-Myc were subjected to formaldehyde cross-linking at room temperature with different concentrations of formaldehyde, cell extracts obtained and subjected to anti-Myc antibody mediated immunoprecipitation along with the noncross-linked control. The immunoprecipitation was carried out with a buffer composition that is regularly used in the Sattlegger lab (Section 2.11) that allows detection of the weak Gcn1-Gcn2 interaction.

As expected, the anti-Myc antibody successfully immunoprecipitated Gcn1 from cell extracts obtained from the cells that were subjected to formaldehyde cross-linking or not. As expected, the amount of proteins co-precipitated decreased with increasing formaldehyde concentrations (Figure 3.17). In order to test if the immunoprecipitation was specific to the Gcn1-Gcn2-Gcn20 complex the membrane was probed with antibodies against Gcn2, Gcn20 or Pgk1. The Western blot results revealed that Pgk1 and a considerate amount of Gcn2 and Gcn20 were present in the negative controls (Figure 3.17), indicating that the immunoprecipitation was not specific to the Gcn1-Gcn2-Gcn20 complex.

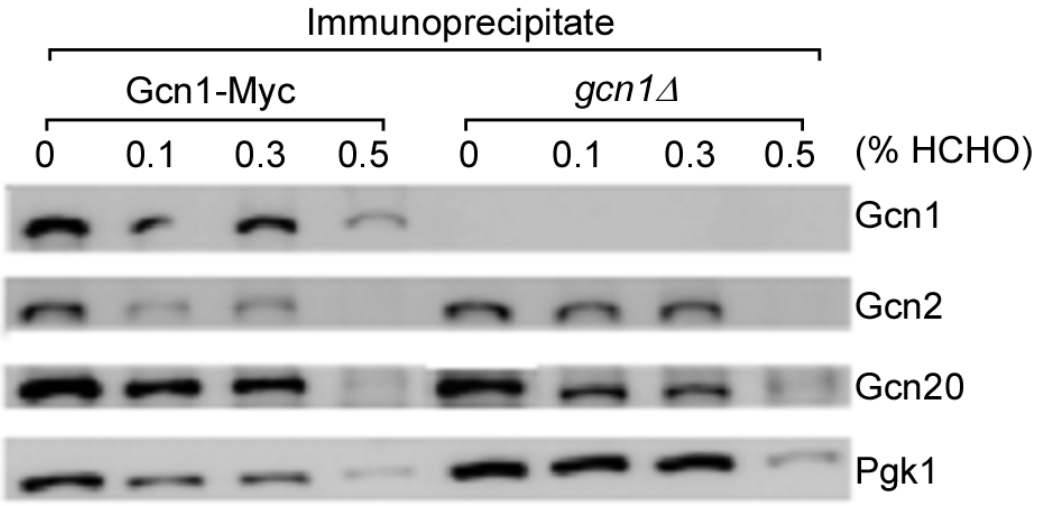

Figure 3.17. Anti-Myc antibody mediated immunoprecipitation of Gcn1-Myc from cell extracts obtained from cells that were subjected to formaldehyde cross-linking and not cross-linked. Indicated strains (refer to Table 2.1) were subjected to formaldehyde treatment as mentioned in Figure 3.14 and subjected to anti-Myc immunoprecipitation. The immunoprecipitates were separated by SDS-PAGE and subjected to Western blotting using antibodies against Myc, Gcn2, Gcn20 and Pgk1

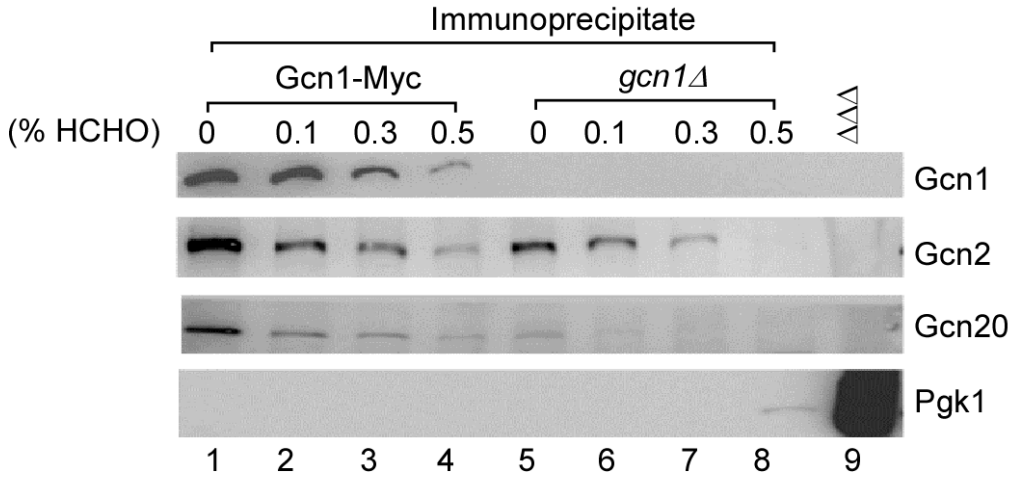

Figure 3.18. Anti-Myc antibody mediated immunoprecipitation of Gcn1-Myc from cell extracts obtained from cells that were subjected to formaldehyde cross-linking. Indicated strains (refer to Table 2.1) were subjected to formaldehyde treatment as mentioned in Figure 3.14 and subjected to anti-Myc immunoprecipitation. Cell extract from a strain deleted for *GCN1*, *GCN2* and *GCN20* (ΔΔΔ) was loaded along with the immunoprecipitates as a negative control. The samples were separated by SDS-PAGE and subjected to Western blotting with antibodies against Myc, Gcn2, Gcn20 or Pgk1

It was reasoned that the signal for Gcn2, Gcn20 and Pgk1 in the negative controls was possibly due to non-specific binding of these proteins to the agarose beads. Therefore, another set of experiments was performed where the beads were coated with BSA before subjecting them to immunoprecipitation.

As expected, the amount of Gcn1, Gcn2 and Gcn20 signal detected in the formaldehyde treated samples decreased with increasing formaldehyde concentrations (Figure 3.18). Gcn20 was detected in the co-precipitate of Gcn1-Myc and a weak signal for Gcn20 was detected in the co-precipitate of the *gcn1*Δ strain. In addition, a signal for Gcn2 was detected in the negative control (*gcn1*Δ). However no signal for Pgk1 was detected in any of the co-precipitates. This result suggested that pre-coating the beads with BSA removed the non-specifically bound Pgk1. However, a significant amount of non-specifically bound Gcn2 and Gcn20 was still present in the negative control (Figure 3.18, lanes 5-8).

In the previous experiments the immune complexes were dissociated from the agarose beads by boiling them in protein loading dye. It was expected that boiling the beads in protein loading dye would result in dissociation of proteins non-specifically bound to the Agarose beads in addition to dissociating the interactions between Myc and anti-Myc antibodies. Elution by changing the pH (low pH) involves reversing the antigen-antibody interactions possibly by affecting their binding sites and therefore, it was reasoned that the low pH elution will not result in elution of proteins that are non-specifically bound to Agarose beads. Thus, it was decided to investigate if lowering pH can elute the immune complexes and if that can help to reduce the non-specific background. In the low pH elution method the immune complex bound beads are incubated with low pH glycine (0.1M, pH 2.5) for 15 minutes (*117*) and the eluate is removed and then immediately being neutralized with Tris base (1M Tris-HCl, pH 8.5).

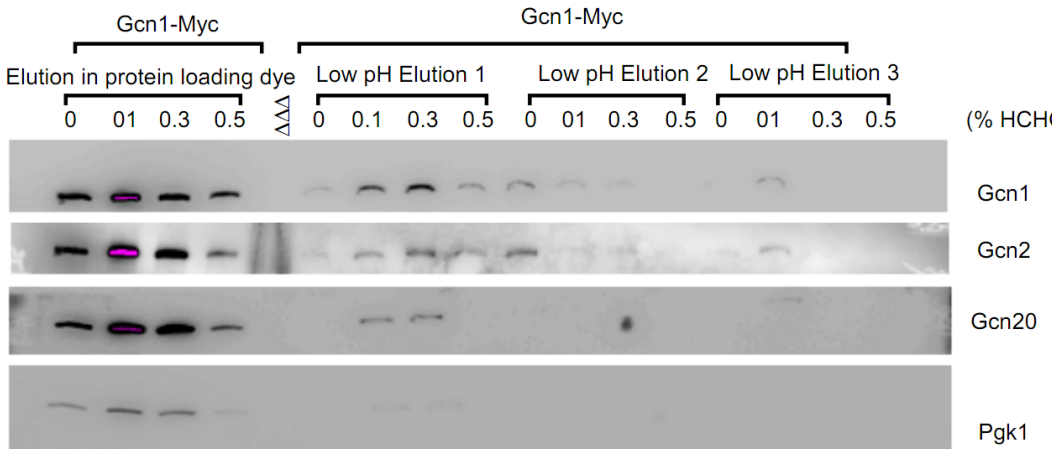

Figure 3.19. Comparison of low pH elution and elution by boiling in protein loading dye. The indicated strains (refer to Table 2.1) were subjected to formaldehyde treatment as described in Figure 3.14 and subjected to anti-Myc immunoprecipitation. The immune complexes were eluted by boiling in protein loading dye or low pH glycine (pH 2.5). Equal amounts of eluates were resolved by SDS-PAGE and subjected to Western blotting with antibodies against Myc, Gcn2, Gcn20 and Pgk1. Cell extract from a strain deleted for *GCN1*, *GCN2* and *GCN20* (ΔΔΔ) was loaded along with the immunoprecipitates as a negative control.

First it was investigated if low pH elution works in principle. The anti-Myc immunoprecipitation was performed as outlined before (Figure 3.18), but in duplicates. One set of samples was used for eluting the complexes by boiling the beads in protein loading dye, and with the other set of samples the immune complexes were eluted in low pH glycine (pH 2.5). Three sequential low pH eluates were collected and all samples were resolved by an SDS-PAGE along with the fractions eluted in protein loading dye.

The amount of Gcn1, Gcn2 and Gcn20 that were eluted by low pH glycine was a lot less than that eluted by protein loading dye, indicating that the low pH elution was very inefficient as compared to boiling in loading dye (Figure 3.19).

As the low pH elution was less efficient, eluates from four independent immunoprecipitations were pooled together and analyzed by SDS-PAGE followed by Western blotting. Only a weak signal for Pgk1 was detected in the Gcn1-Myc immunoprecipitate and a faint signal for Gcn2 was detected in the co-precipitate of *gcn1*Δ strain (Figure 3.20), meaning that low pH elution reduced the

amount of proteins un-specifically associated with the Gcn1 containing complexes. However, due to the low yield of immunoprecipitated proteins the low pH elution was not used further.

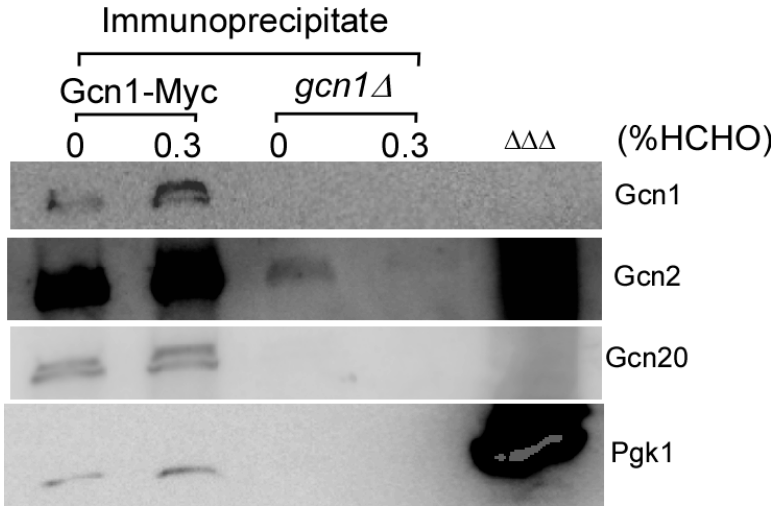

Figure 3.20. Eluting the immune complexes from the agarose beads by lowering pH reduced non-specifically bound proteins. Indicated strains were subjected to formaldehyde treatment as mentioned in Figure 3.14 and subjected to anti-Myc immunoprecipitation. The immune complexes were eluted by low pH glycine (pH 2.5). Cell extract from a strain deleted for *GCN1*, *GCN2* and *GCN20* (ΔΔΔ) was loaded along with the immunoprecipitates as a negative control. The samples were resolved by SDS-PAGE, subjected to Western blotting with antibodies against Myc, Gcn2, Gcn20 and Pgk1.

In another approach, to reduce the unspecific binding of proteins, the immunoprecipitation was performed in reverse-order. In this case the antibody was bound to Gcn1-Myc first and then the protein A conjugated agarose beads were added to immobilize the immune complexes (Figure 3.21).

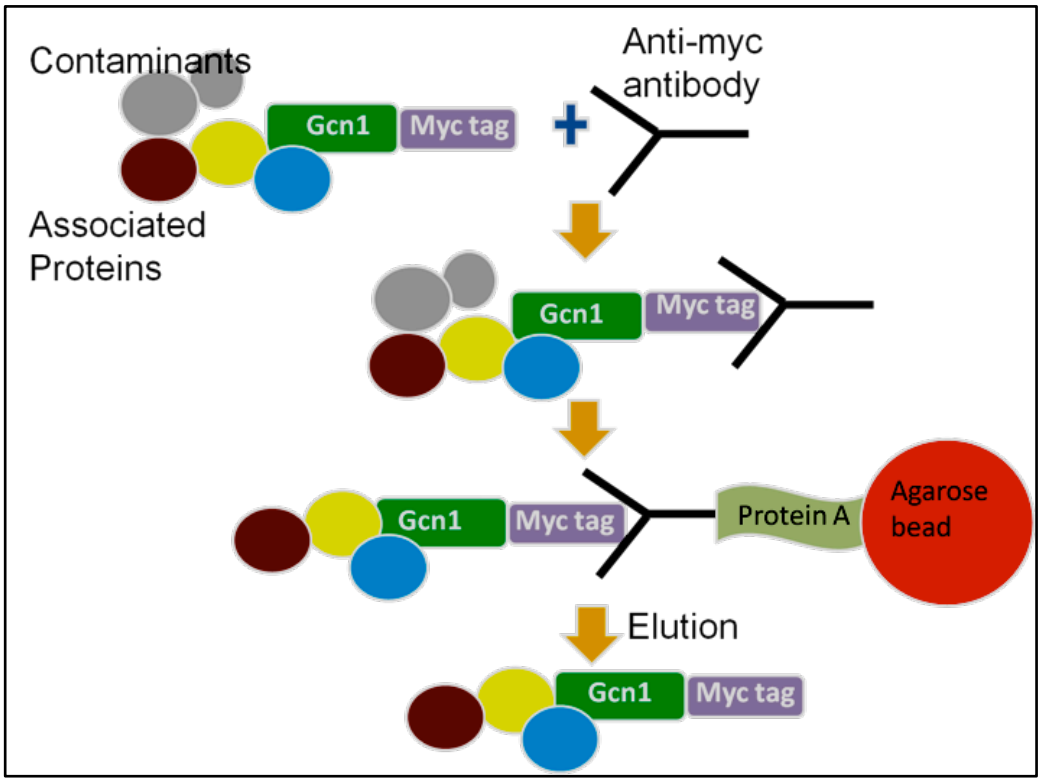

Figure 3.21. Basic principle of reverse-order anti-Myc immunoprecipitation. The protein of interest (Gcn1) is expressed as a fusion protein carrying the Myc tag at the C-terminus. Cell extracts are prepared from these cells and incubated with the anti-Myc antibody. The immune complexes are then bound to protein A coated agarose beads and eluted from the beads by low pH, competitive displacement, or boiling the beads with protein loading dye. For our optimization experiments, the beads were boiled in protein loading dye in order to elute the immune complexes.

The reverse-order immunoprecipitation was repeated with 0.1% formaldehyde treated cells or no formaldehyde treated samples as a control. 0.1% formaldehyde was used because the previous experiment (Figure 3.18) suggested that with less formaldehyde concentration, adequate amount of Gcn1 containing complexes can be precipitated and not much protein were lost. The immunoprecipitates were tested for the presence of Gcn1, Gcn2, Gcn20 and Pgk1.

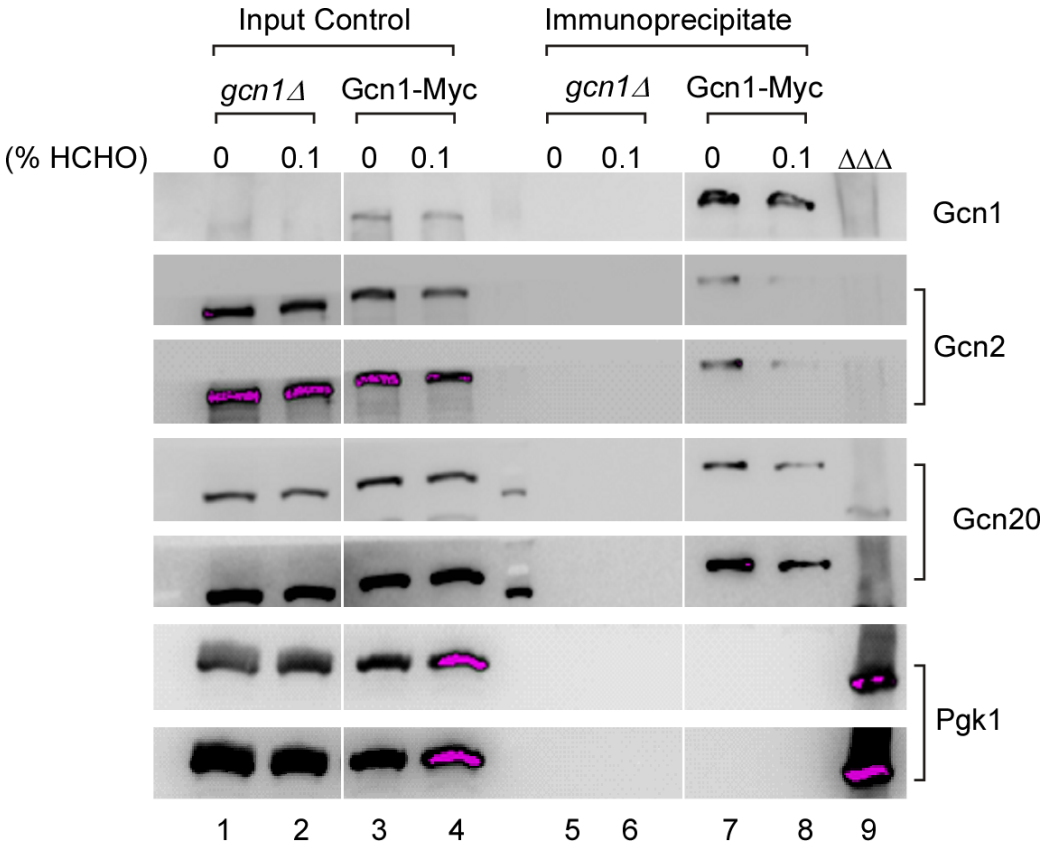

Figure 3.22. Performing the anti-Myc immunoprecipitation in reverse order removed the non-specifically bound proteins. Indicated strains (refer to Table 2.1) were subjected to formaldehyde treatment as mentioned in Figure 3.14 and subjected to anti-Myc immunoprecipitation as described Figure 3.21, and the immune complexes were eluted by boiling the beads in protein loading dye. Cell extract from a strain deleted for *GCN1*, *GCN2* and *GCN20* (ΔΔΔ) was loaded along with the immunoprecipitate samples as a negative control. The samples were separated by SDS-PAGE and subjected to Western blotting with antibodies against Myc, Gcn2, Gcn20 or Pgk1.

As shown in Figure 3.22, Gcn1, Gcn2 and Gcn20 were specifically immunoprecipitated in the Gcn1-Myc sample as compared to the negative control (*gcn1*Δ) and Pgk1 was not detected in the immunoprecipitate. In the *gcn1*Δ negative control, no Gcn2, Gcn20 and Pgk1 were detected, suggesting that the co-immunoprecipitation was specific to the Gcn1-Gcn2-Gcn20 complex.

Although a suitable experimental procedure has been identified, because lc plasmid derived *GCN1* expressed lower quantities of Gcn1 than the endogenous level and the amount of Gcn2 and Gcn20 co-precipitated were also less (refer to

Figure 3.22), the strain expressing *GCN1* to near physiological level (refer to Figure 3.10) from a hc plasmid was investigated. As carried out previously (Figure 3.16) with the strain expressing *GCN1*-Myc from a lc plasmid, it was investigated if Gcn1 got cross-linked and the cross-linked higher molecular weight complexes can be seen when the samples were denatured at 65°C.

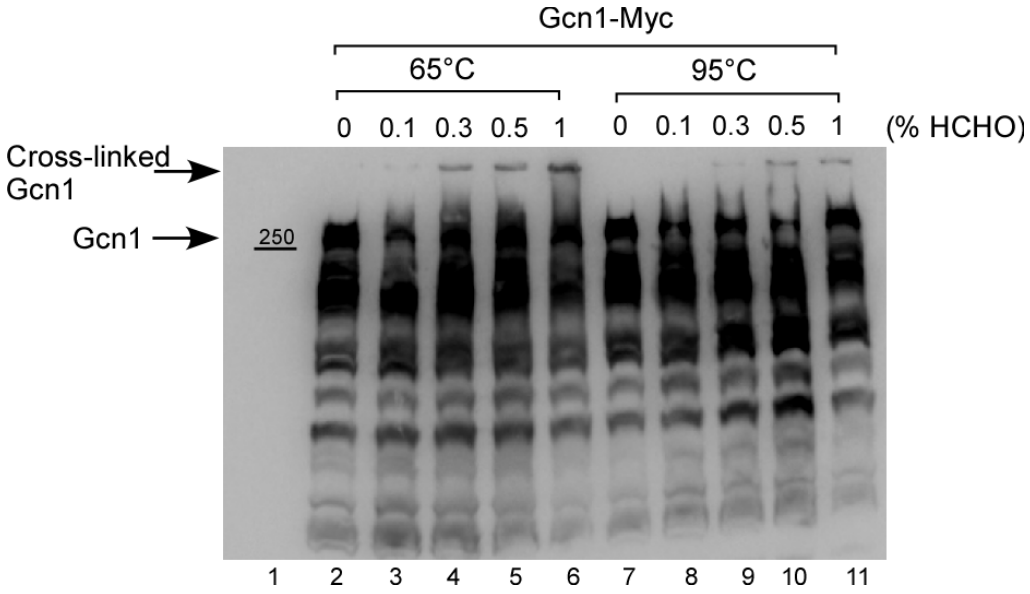

Figure 3.23. Stabilization of Gcn1 containing protein complexes by formaldehyde cross-linking. The *gcn1*Δ (H2556) strain transformed with high copy (hc) plasmid harboring *GCN1* (refer to Table 2.1) were subjected to formaldehyde cross-linking as indicated in Figure 3.14 and 50 µg of protein denatured at 65°C and 95°C (as mentioned in Fig 3.16) and resolved by SDS-PAGE, followed by Western blotting with anti-Myc antibody. Full length Gcn1 is supposed to run just above 250 kDa, the signal visible below 250 kDa is possibly due to degradation of Gcn1-Myc.

To test this the strain expressing *GCN1*-Myc from a hc plasmid was grown to exponential phase, subjected to formaldehyde cross-linking (0.1-1%) cell extracts obtained and 50 µg of cell extracts were denatured at 65°C or 95°C. The samples were resolved by SDS-PAGE followed by Western blotting as described in Figure 3.16.

As shown in Figure 3.23, formaldehyde untreated samples showed no signal for Gcn1 at a molecular weight that was far above 250 kDa. Such a signal

was only detected in formaldehyde treated cell extracts when denatured at 65°C, and the signal intensity increased with increasing concentrations of formaldehyde. Denaturing the samples at 95°C reversed most of the formaldehyde mediated cross-links, which is evident from the absence of the higher molecular weight complexes (Figure 3.23). This result was similar to that observed for samples expressing Gcn1-Myc from a low copy plasmid (Figure 3.16), suggesting that *GCN1*-Myc expressed from lc or hc resulted in similar findings.

Next it was investigated if the optimized conditions of anti-Myc antibody mediated immunoprecipitation co-purified sufficient amount of Gcn2 and Gcn20 in addition to immunoprecipitation of Gcn1-Myc from this strain. Cell extract from the above experiment was subjected to anti-Myc antibody mediated immunoprecipitation. The immunoprecipitation was carried out as outlined in Figure 3.21 and the immunoprecipitate was tested for the presence of Gcn1, Gcn2, Gcn20 and Pgk1.

As previously observed, the amounts of Gcn1, Gcn2 and Gcn20 in the immunoprecipitates were decreased with increasing concentrations of formaldehyde (Figure 3.24). In the *gcn1*Δ control no signals for Gcn2, Gcn20 and Pgk1 were detectable, demonstrating that the anti-Myc immunoprecipitation specifically immunoprecipitated the known binding partners of Gcn1, i.e. Gcn2 and Gcn20. Pgk1 was not seen in the immunoprecipitate, suggesting that un-specifically associating proteins were removed from the Gcn1 immunoprecipitate.

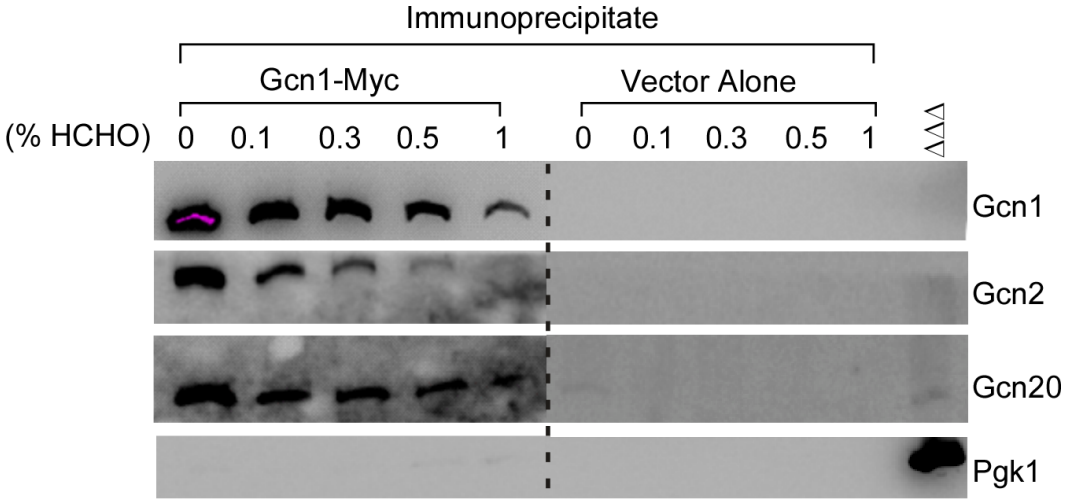

Figure 3.24. Anti-Myc antibody mediated immunoprecipitation of hc plasmid borne Gcn1-Myc. The *gcn1*Δ (H2556) strain transformed with hc plasmid derived *GCN1*-Myc (refer to Table 2.1) were subjected to formaldehyde cross-linking as indicated in Figure 3.14 and the cell extract obtained from the cells were subjected to anti-Myc immunoprecipitation as indicated in Figure 3.21. Cell extract from a strain deleted for *GCN1*, *GCN2* and *GCN20* (ΔΔΔ) was loaded along with the immunoprecipitate samples as a negative control. The samples were separated by SDS-PAGE and subjected to Western blotting with antibodies against Myc, Gcn2, Gcn20 and Pgk1.

Since the higher molecular weight complex formation was observed with 0.3% or more formaldehyde (Figure 3.23), and adequate amounts of Gcn2 and Gcn20 were co-immunoprecipitated with samples treated with 0.3% formaldehyde (Figure 3.24), it appeared that 0.3% formaldehyde was best suited for stabilizing Gcn1-containing complexes.

3.2.6 Large scale purification of Gcn1 containing complexes, and identification of the components via Mass Spectrometry

A large scale purification of Gcn1 containing complexes was necessary in order to have sufficient amount of samples for the subsequent identification of proteins in the Gcn1-containing complexes via Mass Spectrometry. Therefore, cells expressing Gcn1-Myc from a high copy plasmid, and the *gcn1*Δ strain containing empty vector, were grown to exponential phase. The cells were then subjected to formaldehyde (0.3%) cross-linking at room temperature for 10 minutes, cell

extracts obtained and subjected to anti-Myc antibody mediated immunoprecipitation with the optimised conditions. Four independent immunoprecipitations were performed, the beads were pooled together at the end of the experiment before elution by boiling in protein loading dye. An aliquot of the eluate was analyzed by SDS-PAGE followed by Western blotting using antibodies against Myc, Gcn2, Gcn20 or Pgk1.

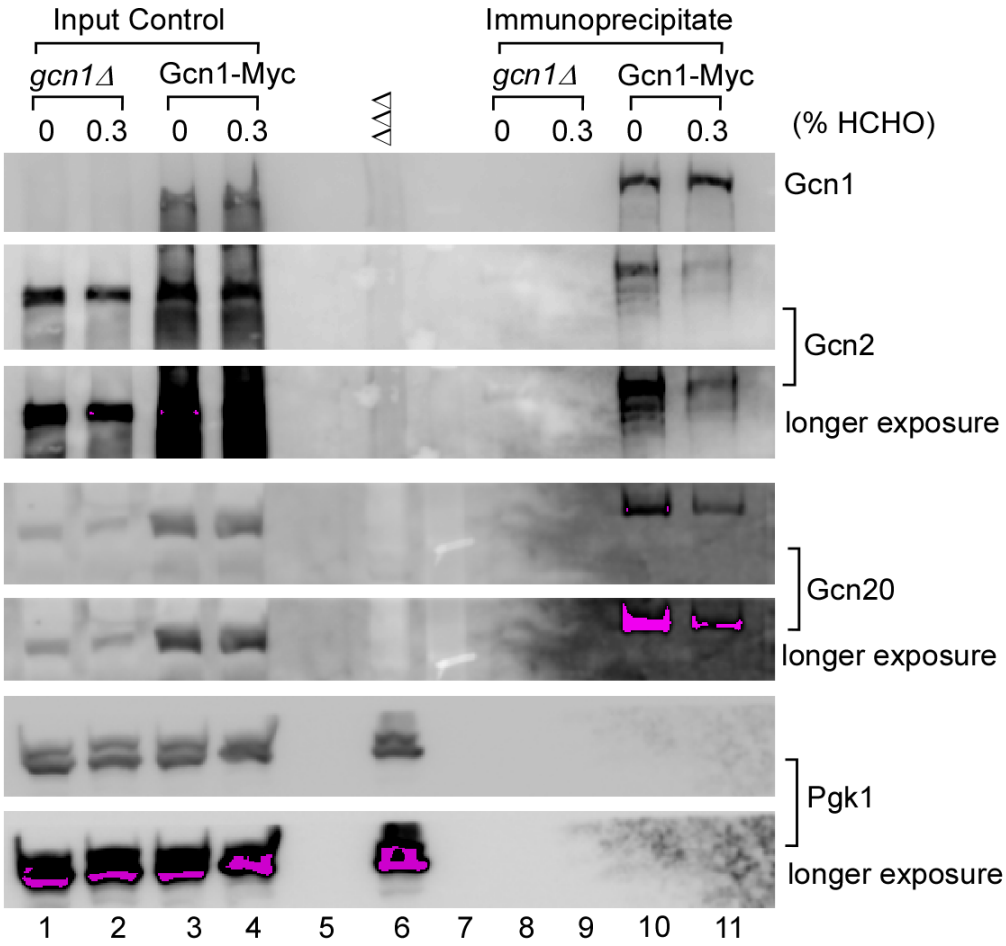

Figure 3.25. Gcn1 specific immunoprecipitation of Gcn1 binding proteins. The *gcn1*Δ (H2556) strain harbouring hc *GCN1*-Myc (refer to Table 2.1) was subjected to formaldehyde cross-linking as indicated in Figure 3.14, and the cell extract obtained from the cells were subjected to anti-Myc immunoprecipitation as indicated in Figure 3.21. Cell extract from a strain deleted for *GCN1*, *GCN2* and *GCN20* (ΔΔΔ) was loaded along with the immunoprecipitate as a negative control.

Gcn1, Gcn2 and Gcn20 were specifically immunoprecipitated in the Gcn1-Myc immunoprecipitate (Figure 3.25). A signal for Pgk1 was not detectable in the immunoprecipitates, suggesting that un-specifically bound proteins had been removed. As expected, compared to the non-cross linked samples, Gcn1, Gcn2 and Gcn20 were present in lower amounts in the 0.3% cross-linked samples. As expected, the amount of Gcn20 in the *gcn1Δ* sample was much less than in the Gcn1-Myc input sample, as observed and suggested previously, this is because Gcn20 is less stable in the absence of Gcn1 (*2*).

As the immune complexes were eluted from the beads by boiling the beads in protein loading dye, these samples cannot be subjected to Mass Spectrometry (MS). Therefore it was decided to separate the samples via SDS-PAGE, stain the gel to visualize proteins and then subject the gel lanes to MS analysis. As the co-precipitated proteins were likely to be lowly abundant, and to prevent diluting the samples too much when resolving them in the gel, it was aimed to run the samples in SDS-PAGE just far enough that all proteins entered the gel. To first test how far the sample has to enter the gel to have all proteins entered the gel even of very large, 50 µg of protein from the Gcn1-Myc sample was denatured at 95°C and resolved by SDS-PAGE for 6, 4, 2 or 1 cm from the slot followed by Western blotting with antibodies against Myc. The distance travelled by the samples was determined by measuring the distance between the dye front and slot.

A signal for Gcn1 was detected below the slot in samples that were run for 4 or 6 cm (Figure 3.26). In the samples ran for 2 and 1 cm the signal for Gcn1 was detected at the slot, raising the possibility that not all Gcn1 may fully entered the gel. These results indicated that Gcn1 can migrate below the slot if the samples are run for 4 or 6 cm below the well.

However, it was decided to run the samples on the gel for 5 cm, to be on the safe side that all Gcn1 would migrate below the slot and no Gcn1 will be lost in the subsequent staining procedure.

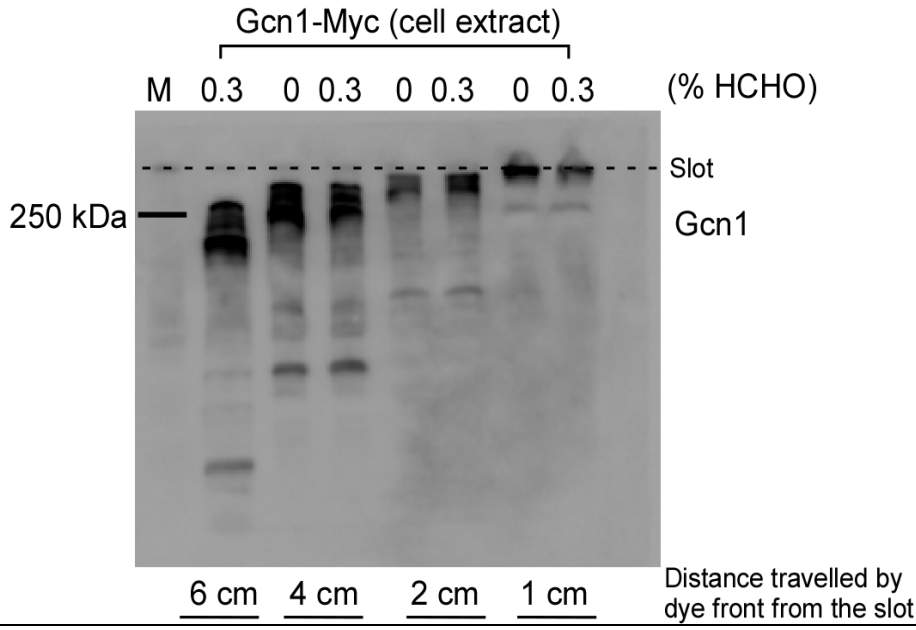

Figure 3.26. Western blot of samples that were resolved by SDS-PAGE for 6, 4, 2 or 1 cm. 50 µg of cell extract from the Gcn1-Myc strain indicated in Figure 3.25 was resolved by SDS-PAGE for indicated distances from the slot followed by Western blotting with an antibodies against Myc.

The gel was then stained with colloidal Coomassie stain to visualize the bands (Figure 3.27). In each lane only two bands were visible. This suggests that the proteins co-precipitated by Gcn1-Myc were not abundant to visualize by Colloidal Coomassie staining. The two visible bands around 64 kDa and 50 kDa may represent heavy and light chains of the anti-Myc antibodies. The high amounts of immunoglobulin can easily mask the identification of low abundance peptides. Therefore, these visible bands were cut out of the gel and analyzed separately from the rest of the lanes, via MS. The MS analysis was done at the Centre for Protein Research, University of Otago.

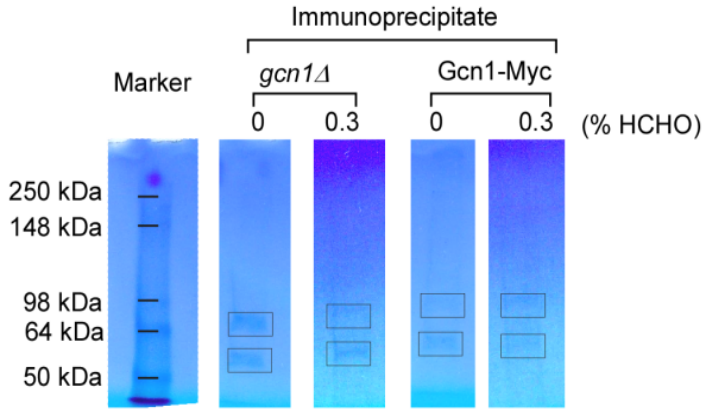

Figure 3.27. Colloidal Coomassie staining of SDS-PAGE. Immunoprecipitates from Figure 3.25 were resolved by SDS-PAGE for 5 cm and stained with colloidal Coomassie.

A summary of the work strategy employed for the identification of Gcn1 binding proteins is given in Figure 3.28.

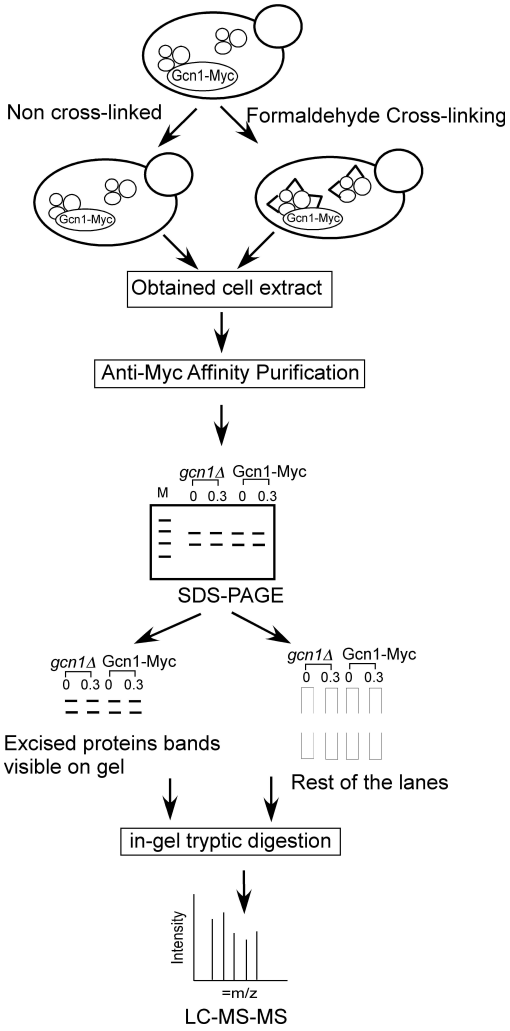

Figure 3.28. Work strategy of formaldehyde cross-linking followed by affinity purification and LC-MS-MS analysis. In order to create our *in house* Gcn1 interactome we have used an epitope tagged Gcn1 (Gcn1-Myc). The *gcn1*Δ cells carrying the hc plasmid borne Gcn1-Myc or vector alone were grown in minimal media to exponential phase and the cells were subjected to formaldehyde (0.3%) cross-linking *in vivo* at room temperature for 10 minutes. Extracts obtained from the cross-linked cells and untreated controls were subjected to anti-Myc antibody mediated co-immunoprecipitation in order to isolate proteins binding to the Gcn1-Myc. The co-precipitate was investigated for the presence of Gcn1 and known Gcn1 binding proteins (Gcn2 and Gcn20). After confirming that good amount of Gcn1 and the known Gcn1 binding proteins were detectable by Western blotting in the Gcn1-Myc co-precipitate, the samples were analyzed by MS. For MS analysis, the co-precipitates were subjected to SDS-PAGE electrophoresis and the gels were stained with colloidal Coomassie to visualize proteins. The stained gels were subjected to LC-MS-MS in order to identify proteins that were co-precipitated by the Gcn1-Myc.

3.2.7 Mass Spectrometry Identification of Proteins

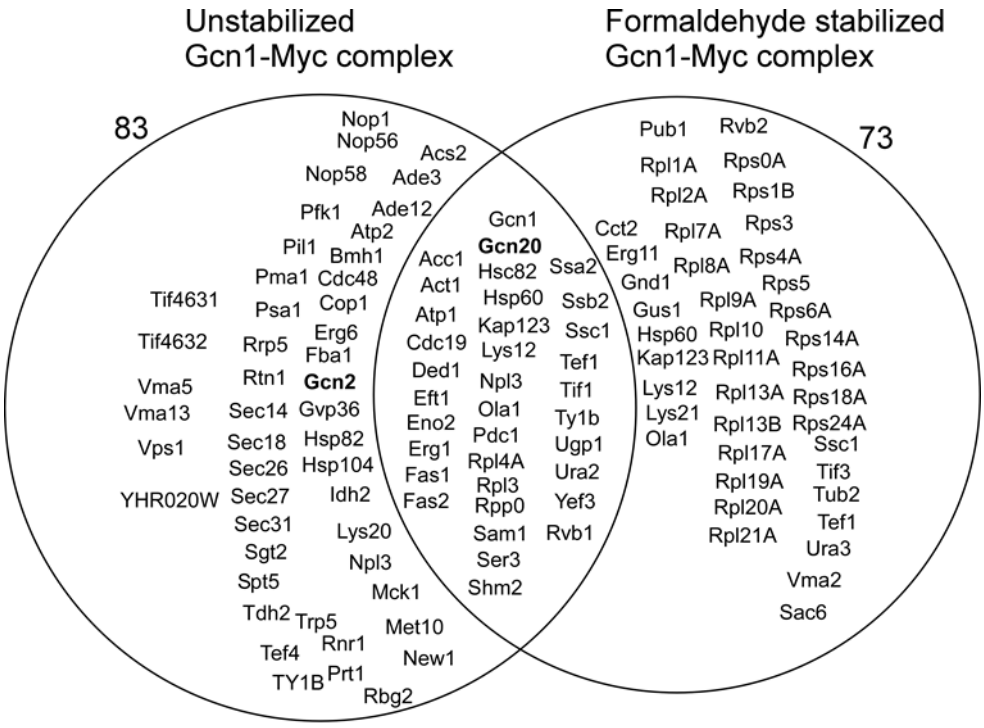

Figure 3.29. Proteins identified by Mass Spectrometry in the unstabilized and formaldehyde stabilized Gcn1-Myc complexes. Raw Mass Spectrometry data. Proteins identified in the unstabilized Gcn1-Myc complex (left circle), proteins identified in the formaldehyde stabilized Gcn1-Myc complex (right circle) and identified in both are in the middle. Proteins identified only in the negative control *(gcn1Δ)* were not included.

The sample obtained from 0.3% formaldehyde treated cells is referred as formaldehyde stabilized Gcn1-Myc complex and the untreated control is referred as unstabilized Gcn1-Myc complex in the following sections.

Mass Spectrometry identified 83 proteins in the un-stabilized Gcn1-Myc complex and 73 proteins in the formaldehyde stabilized Gcn1-Myc complex. There were 34 proteins commonly found between the formaldehyde stabilized and unstabilized Gcn1-Myc complexes. As expected, the known interacting partner of Gcn1, Gcn20, was found both in the formaldehyde stabilized and unstabilized Gcn1-Myc complexes. Unexpectedly, MS did not identify Gcn2 in the

formaldehyde stabilized Gcn1-Myc complex and it was found only in the unstabilized Gcn1-Myc complex. However, Western blot analysis revealed the presence of Gcn2 both in the un-stabilized and formaldehyde stabilized Gcn1-Myc complex (Figure 3.25). This suggests that the amount of Gcn2 that was present in the formaldehyde stabilized Gcn1-Myc complex could have been below the detection limit of Mass Spectrometry.

Mass Spectrometry results revealed that several proteins were present only in the formaldehyde stabilized or unstabilized Gcn1-Myc complex, but not in the *gcn1*Δ control. We reasoned that if a protein is not at all found in the control and present only in the Gcn1-Myc complex, then it is likely that the interaction is true. In accord with our reasoning, the known binding partner of Gcn1, Gcn20, was found only in the formaldehyde stabilized and unstabilized Gcn1-Myc complexes. Fas1, Fas2, Erg1 and Ura2 were found only in the formaldehyde stabilized and unstabilized Gcn1-Myc complex, but not at all in the negative control indicating the Gcn1 specific interactions of these proteins (Figure 3.29).

As like any other affinity purification study, we have also identified many proteins in the negative control. Several proteins co-precipitating with Gcn1 were also found in the negative control. It is possible that proteins that are abundant in the cell, or due to their biochemical nature, tend to bind to the resins used for affinity purifications (*118*). In order to preserve the weak interactions we have used a low stringency buffer (50mM KCl and no detergent) in addition to chemically cross-linking the interactions. As a result of the low stringency buffer, some contaminants may have not been fully removed during the purification procedure. It is also possible that the anti-Myc antibodies cross-reacted with one or more irrelevant proteins.

These unspecific proteins most likely can be identified based on the fact that each protein was given a score depend on how often it was identified using PSM (peptide search matches). PSM indicates the total number of identified peptide sequences. If a protein truly interacts with Gcn1, then it would be detected more

frequently in the Gcn1-Myc sample than in the negative control (*gcn1*Δ). So even if there was some unspecific binding, this quantitative measure allowed us to still identify putative interaction partners of Gcn1. Proteins found more than 2 times in the Gcn1-Myc sample than in the *gcn1*Δ control were considered as significant (Figure 3.30). Proteins identified only in the control and found below 2 times in the Gcn1-Myc complex than in the control (*gcn1*Δ) were not included in the analysis (Appendix, Table A.1).

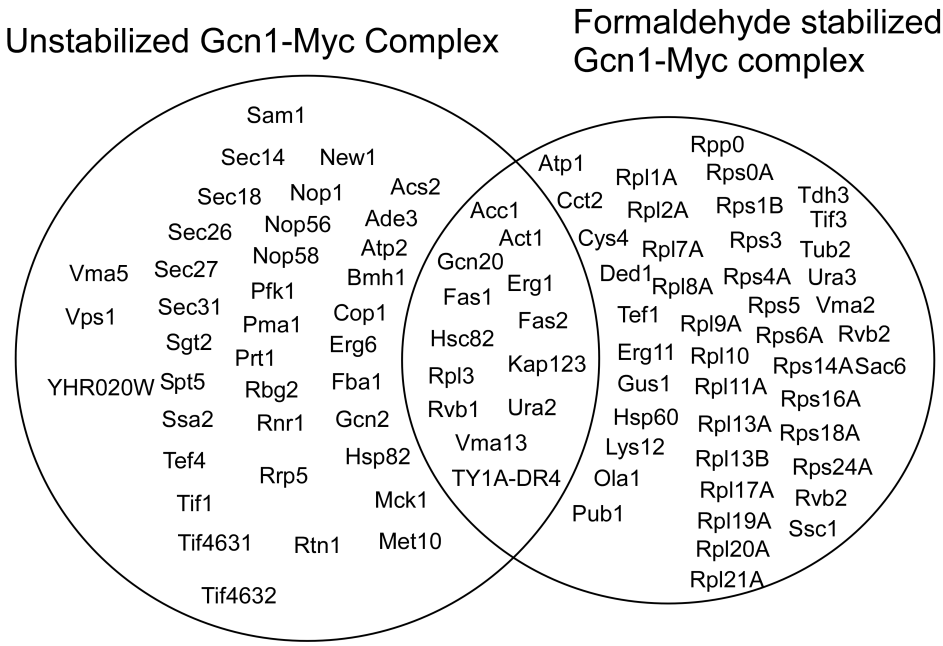

Figure 3.30. *in house* Gcn1 interactome. Proteins found in the unstabilized Gcn1-Myc complex, formaldehyde stabilized Gcn1-Myc complex and found in both. Proteins identified only in the Gcn1-Myc complexes (formaldehyde stabilized and unstabilized) and found more than 2 times in the Gcn1-Myc complexes than in the control (*gcn1*Δ) are shown.

The known interacting partners of Gcn1, Yih1 and Gir2 were not identified in the unstabilized and formaldehyde stabilized Gcn1-Myc complexes. A summary of the known Gcn1 and Gcn2 binding partners co-precipitated with Gcn1 that were found above the set limit of 2 is given in table 3.2.

Interestingly the known binding partners of Gcn2, eEF1A (TEF1/TEF2) (*81*) and Hsc82 (*82*) were identified both in the unstabilized and formaldehyde stabilized Gcn1-Myc complexes (Table 3.2).

Table 3.2 Identification of the known Gcn1 or Gcn2 binding proteins in the unstabilized and formaldehyde stabilized Gcn1-Myc complexes.

Known Gcn1 binding proteins	Unstabilized Gcn1-Myc Complex	Formaldehyde stabilized Gcn1-Myc Complex
Gcn2 (*13*) (*13*)	Yes	No
Gcn20 (*13*)	Yes	Yes
Yih1 (*53*)	No	No
Gir2 (*54*)	No	No
Known Gcn2 binding proteins	Unstabilized Gcn1-Myc Complex	Formaldehyde stabilized Gcn1-Myc Complex
eEF1A (*81*)	Yes	Yes
Hsp82/Hsc82 (*82*)	Yes	Yes

Ribosomal proteins were enriched in the formaldehyde stabilized Gcn1-Myc complex (Figure 3.30). There was only one ribosomal protein identified in the unstabilized Gcn1-Myc complex, but in the formaldehyde stabilized Gcn1-Myc complex, 24 ribosomal proteins were identified. This includes 10 proteins of the small subunit (Rps) (Rps0A, Rps1B, Rps3, Rps4A, Rps5, Rps6A, Rps14A, Rps16A, Rps18A and Rps24A) and 14 proteins of the large subunit (Rpl) (Rpl1A, Rpl2A, Rpl3, Rpl7A, Rpl8A, Rpl9A, Rpl10, Rpl11A, Rpl13A, Rpl13B, Rpl17A, Rpl19A, Rpl20A and Rpl21A) and one protein of the ribosomal stalk (Rpp0). The enrichment of ribosomal proteins in the formaldehyde stabilized Gcn1-Myc complex suggests that formaldehyde cross-linking stabilized the true interactions between Gcn1 and the ribosome.

Several groups of functionally related proteins have been identified in the *in house* Gcn1 interactome (Figure 3.30). These are proteins involved in fatty acid biosynthesis (Fas1, Fas2 and Acc1) and ergosterol biosynthesis (Erg1, Erg11 and Erg6), amino acid, nucleic acid biosynthesis (Lys12, Met10, Ade3, Ura2 and

Ura3) and transferring proteins from the endoplasmic reticulum to the Golgi (Sec18, Sec14, Sec27, Sec26 and Sec31). In addition, proteins involved in translation initiation, elongation (Tef1, Yef3, Tif1, Tif3, Tif4631 and Tif4632), rRNA processing (Nop1, Nop56 and Nop58), heat shock/chaperone proteins (Hsp60, Hsp82, Hsc82, Ssa2, Ssc1, and Sam1), cytoskeleton proteins (Tub2, Act1), vacuolar membrane ATPases (Vma2, Vma5 and Vma13) and vacuolar protein sorting (Vps1) were identified (Figure 3.30).

The molecular mass of the identified proteins ranged from 12 kDa to 300 kDa. This suggests that the experimental procedure used in this study resulted in the identification of small molecular weight proteins. Resolving the proteins for shorter distances by SDS-PAGE and subjecting the whole lanes for MS analysis rather than excising the visible protein bands may have culminated in the identification of proteins with less molecular mass. As one would expect fewer peptides were identified for these proteins in the MS.

Gcn1 was affinity purified in the study by Gavin et al. (2006). The purification buffer and purification procedure used in the study is not known to capture the weak interactions. In our study we used a low stringent buffer to preserve the weak interactions in the hope to more comprehensively identify more binding partners of Gcn1. As expected we have identified several proteins including Gcn2 co-precipitating with Gcn1, which have not been identified in the Gavin et al. (2006) study (Figure 3.31). This suggests that the experimental procedure and purification conditions used in our study resulted in the identification of more Gcn1 binding proteins, which could have escaped from identification in the study by Gavin et al. (2006). There were five proteins (Gcn20, Sam1, Vps1, Kap123 and Ssa2) commonly found in the co-precipitate of unstabilized Gcn1-Myc and co-precipitate of Gcn1 from the Gavin et al. (2006) study (Figure 3.31). Many proteins identified in their study have not been found in our study. This may indicate that apart from identification of the same Gcn1 binding proteins, different Gcn1 containing complexes have been identified in these two studies.

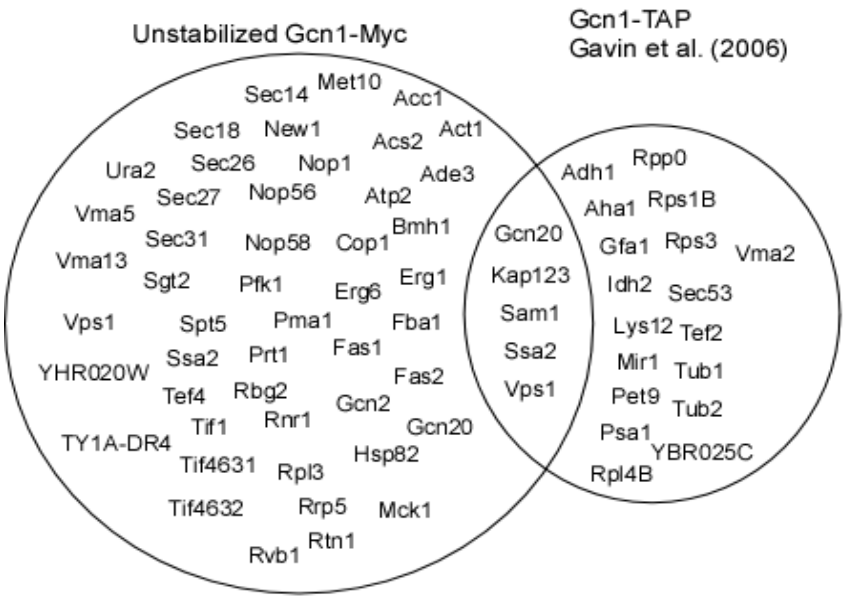

Figure 3.31. Comparison of proteins co-precipitated with Gcn1 in this study and proteins co-precipitated with Gcn1 in the Gavin et al. (2006) study. Proteins identified in the unstabilized Gcn1-Myc complex in our study (left circle). Proteins identified only in the Gcn1-Myc complexes and found more than 2 times in the Gcn1-Myc complexes than in the *gcn1*Δ control are shown. Proteins co-precipitated with Gcn1 in the study by Gavin et al. (2006) (right circle). Proteins common to both the studies are in the middle.

3.2.8 Gene Ontology (GO) of Gcn1 binding proteins

To gain insight on the localization (cellular compartment) and biological processes of Gcn1 binding proteins, identified in the *in house* Gcn1 interactome, we used the BiNGO (Biological Network Gene Ontology tool), plugin for Cytoscape (a network visualization tool). BiNGO annotates proteins with gene ontology (GO) terms and determines which GO categories are significantly overrepresented in a set of genes (*119*).

3.2.8.1 Cellular localization of Gcn1 binding proteins

To determine the localization of Gcn1 binding proteins and to investigate whether proteins localized in certain parts in the cell are overrepresented, enrichment analysis of their gene ontology terms was carried out. The enrichment analysis

was done using the "Hyper Geometric test" using the following parameters; GO_Cellular_component ontology, annotation for *Saccharomyces cerevisiae*. Hyper Geometric test identifies which sub populations are over or under represented in a sample. GO terms that were significant with *P*-Values of <0.05 were determined to be overrepresented.

Results of BiNGO revealed that proteins localized in the cytoplasm, cytosol, cytosolic ribosome, small and large ribosomal subunits, ribonucleoprotein complex, 90S pre-ribosome and intracellular non membrane bound organelle were overrepresented (Figure 3.32, colored circles), indicating that Gcn1 binding proteins are localized mainly in the cytoplasm and cytoplasmic organelles. The list of proteins is given in appendix (Table A.2).

3.2.8.2 Biological processes mediated by Gcn1 binding proteins

To further gain insight on the biological processes mediated by Gcn1 binding proteins, enrichment analysis of their gene ontology terms was performed. The enrichment analysis was done using the "Hyper Geometric test" using the following parameters; GO_Biological_process ontology, annotation for *Saccharomyces cerevisiae*. GO terms that were significant with *P*-Values of <0.05 were determined to be overrepresented.

The output from BiNGO revealed that proteins involved in the regulation of cellular biosynthetic process, regulation of translation, regulation of metabolic processes, and regulation of gene expression were overrepresented. Of these processes, Gcn1 mediated regulation of translation initiation is known. This result suggested that in addition to regulating translation initiation by regulating Gcn2, Gcn1 may be involved in regulating the gene expression, metabolic processes and biosynthetic processes of the cell (Figure 3.33). The list of the proteins is given in appendix (Table A.3).

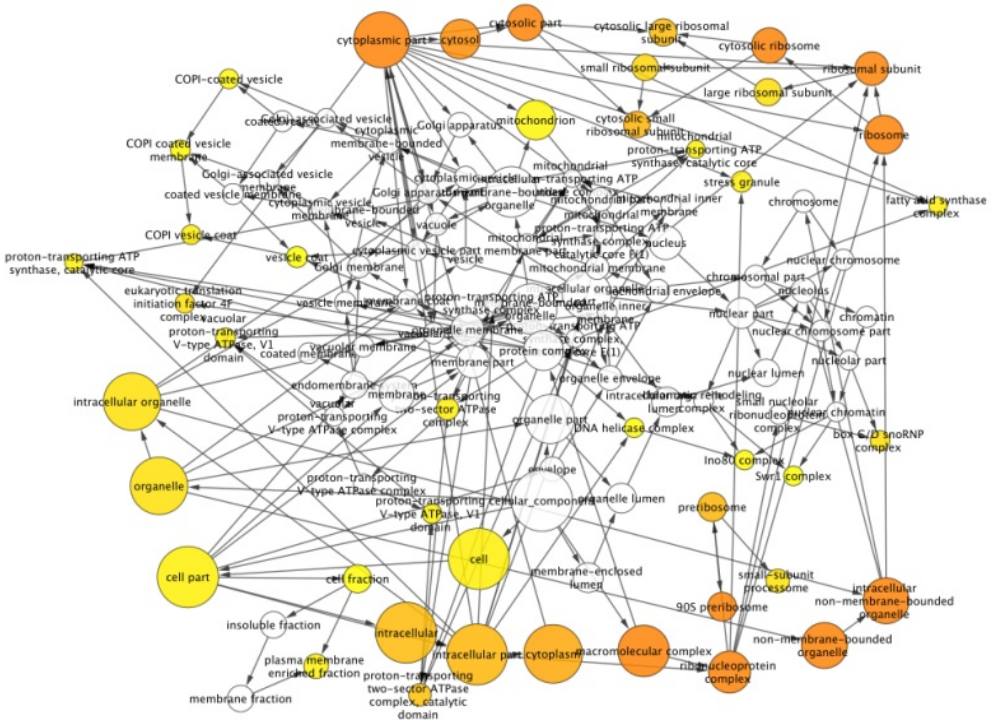

Figure 3.32. Localization of Gcn1 binding proteins predicted by BiNGO.Proteins of the *in house* Gcn1 interactome were subjected to BiNGO to annotate the localization of the proteins. Overrepresented categories are represented by colored circles. White circles are not significantly overrepresented. The area of circles is proportional to the number of genes in the test set annotated to the corresponding GO category.

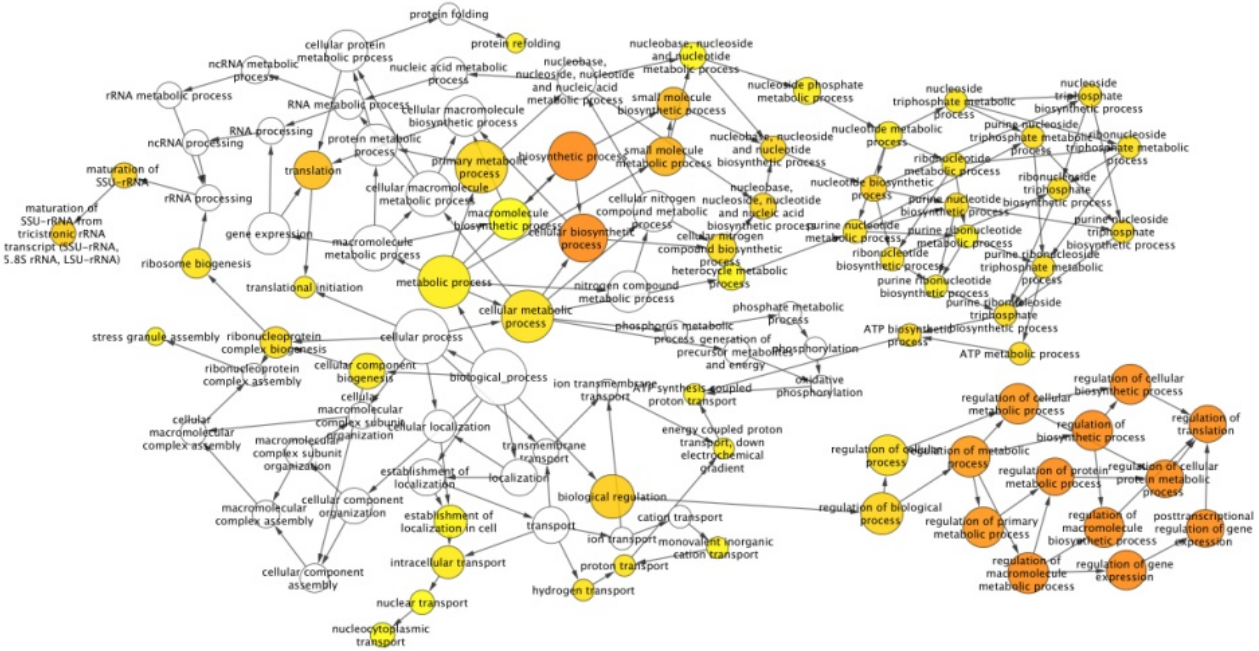

Figure 3.33. Pathway output from the BiNGO analysis. Biological processes mediated by Gcn1 binding proteins. Proteins of the *in house* Gcn1 interactome were subjected to BiNGO to annotate the biological processes mediated by the proteins. Overrepresented categories are represented by colored circles. White circles are not significantly overrepresented. The area of circles is proportional to the number of genes in the test set annotated to the corresponding GO category.

3.2.9 Comparative analysis of the three Gcn1 interactomes

As the minimal Gcn1 interactome majorly consists of proteins that co-precipitated Gcn1, it was expected that these proteins could be identified in the *in house* Gcn1 interactome. As outlined above, there are 7 proteins common to the *in house* Gcn1 interactome and minimal Gcn1 interactome (Figure 3.34).

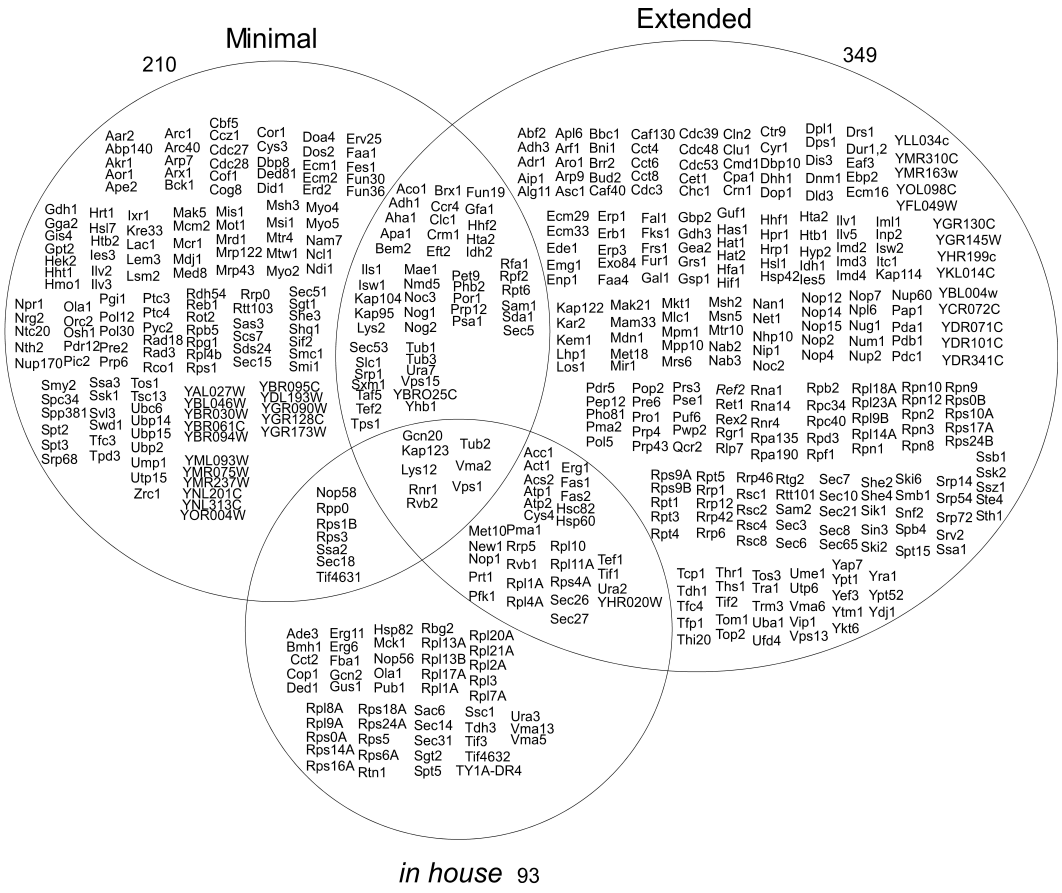

Figure 3.34. Comparison of the minimal, extended and *in-house* Gcn1 interactomes. Proteins found in each interactome, commonly in any two or all three Gcn1 interactomes are shown.

49 proteins are common to the extended and minimal interactome and 30 proteins common to the extended and *in house* interactome. 8 proteins (Gcn20, Kap123, Lys12, Rnr1, Rvb2, Tub2, Vma2 and Vps1) are found common to all the three interactomes.

However several Gcn1 binding proteins identified in the *in house* Gcn1 interactome have not been identified in the minimal or extended Gcn1 interactomes. This suggested that this study has identified many novel proteins that bind to Gcn1 and/or to its binding partners.

3.2.10 Discussion

In order to identify the strong and weak interacting partners of Gcn1, the decision was made to cross-link the protein-protein interactions *in vivo* in addition to using a less stringent purification conditions. We postulated that formaldehyde treatment of live cells would cross-link the epitope tagged Gcn1 to its interacting partners, and immunoprecipitation with an antibody against the epitope under less stringent conditions (50 mM KCl and no detergents), than that was used in the large scale affinity purification studies (*24-27*), will bring down the proteins associated with Gcn1, including the weak interacting partners of Gcn1.

Several factors that are known to affect formaldehyde cross-linking were investigated. It was found that the amount of total protein loss increased with increasing concentrations of formaldehyde. This finding is in agreement with the previous findings that cross-linking with 1% formaldehyde at room temperature for 30 minutes leads to significant protein loss (*111*). Protein loss due to formaldehyde cross-linking could be mainly because cross-linking of proteins to DNA, especially cross-linking of nuclear proteins to DNA and formation of higher molecular weight protein complexes. In conjunction with this idea, it was found that Gcn1 was lost in the pellets (4,200 rpm and 10,000) from the cross-linked cells and yet the amount of cross-linked Gcn1 containing complexes increased in a manner that is dependent on formaldehyde concentration. However, how formaldehyde leads to enrichment of cross-linked target complexes relative to noncross-linked material is poorly understood (*111*). One possible reason for the loss of Gcn1 with formaldehyde cross-linking would be that Gcn1 is in large protein complexes and cross-linking with formaldehyde stabilizes the Gcn1 interaction with other proteins, resulting in big molecular weight complexes

which may not withstand the centrifugation steps involved in making the cell extracts and therefore precipitate out. It has been reported that 0.3-0.5% formaldehyde for 10 min at room temperature results in a good balance between cross-linked material and overall protein loss (*103, 111*). However, it has been suggested that optimization will be required for any given bait (*111*). In accord with the previous findings, in this study, we have identified that 0.3% formaldehyde resulted in the best protein loss/cross-linking yield balance. Therefore, 0.3% formaldehyde was chosen to cross-link Gcn1 containing complexes.

Liquid Chromatography Tandem Mass Spectrometry (LC-MS/MS) was used to identify the proteins in the affinity purified Gcn1-Myc complexes.
The known binding partner of Gcn1, Gcn20, was identified consistently in the formaldehyde stabilized and unstabilized Gcn1-Myc complexes, while Gcn2 was not identified in the formaldehyde stabilized Gcn1-Myc complex. The fact that the known Gcn1 binding protein, Gcn20, was identified in both the formaldehyde stabilized and unstabilized Gcn1-Myc complexes suggested that only proteins strongly interacting with Gcn1 were identified in both the formaldehyde stabilized and unstabilized Gcn1-Myc complexes.

It has been shown that Yih1 and Gir2 interact with Gcn1 (*53, 56*), but the detected interactions involved over expression of these binding partners. In addition, it has been shown that the interaction of over expressed Gir2 with Gcn1 increased after inducing starvation with 3-AT in a dose dependent manner (*57*). Our *in-house* interactome did not detect Gir2 or Yih1 as Gcn1 binding partners, raising the possibility that these interactions may not happen under the given growth conditions, as suggested previously (*53, 56*). It is also possible that the endogenous levels of Yih1 and Gir2 were not sufficient to be detected via Mass Spectrometry.

Interestingly the known Gcn2 regulatory proteins, Hsc82 (Hsp90) (*82*) and eEF1A (*TEF1*) (*81*) were identified as Gcn1 binding proteins (Figure 3.30). The

fact that Hsc82 and eEF1A co-precipitated with Gcn1 in our study suggests that Gcn1 binds to Gcn2 which is in a complex with Hsc82 and eEF1A.

Several ribosomal proteins were identified as Gcn1 binding proteins in this study. The formaldehyde stabilized Gcn1-Myc complex contained 24 ribosomal proteins that were not present in the unstabilized Gcn1-Myc complex. However, only one ribosomal protein was identified in the unstabilized Gcn1-Myc complex. Ribosomal proteins were reported to be present frequently in affinity purifications, and they were considered as common contaminants in large-scale affinity purification studies (*24-27*). Therefore, it is possible that the ribosomal proteins identified in this study are due to nonspecific binding. If the identified ribosomal proteins are nonspecific contaminants, then it is expected that these proteins will be identified in the negative control (*gcn1*Δ) also. Contradicting this idea these ribosomal proteins were not at all detected in the negative control and identified only in the Gcn1-Myc complexes. The interactions between Gcn1 and ribosomal proteins can be further validated by purifying protein complexes associated with the ribosomal proteins and by investigating the presence of Gcn1 in the complexes.

Among the unstabilized and formaldehyde stabilized Gcn1-Myc complexes, the ribosomal proteins were enriched only in the formaldehyde stabilized Gcn1-Myc complex, suggesting that formaldehyde cross-linking has stabilized the true interactions between ribosomal proteins and Gcn1.

The first evidence that the Gcn1-Gcn20 complex binds to the ribosome was provided by Marton et al. (1997). The sequence similarity of Gcn1 and Gcn20 to that of eEF3 prompted these authors to investigate whether Gcn1 and Gcn20 associate with the ribosomes. Co-sedimentation assays revealed that Gcn1 and Gcn20 co-sediment with 80S ribosomes and polysomes. It has been shown that the ribosome binding by both Gcn1 and Gcn20 was increased in the presence of ATP suggesting that the energy level of ATP hydrolysis leads to a conformational change in the Gcn1-Gcn20 complex that promotes a strong and

stable interaction with translating ribosomes (*2*). Furthermore in the study by Sattlegger et al. (2005) it was shown that Gcn1 and Gcn20 were associated with polysomes in cell extracts prepared from formaldehyde treated cells that lacking exogenous ATP. In conclusion these findings suggested that the interaction of Gcn1-Gcn20 complex with polysomes is weak and that the interaction is detectable only when stabilized by ATP or by formaldehyde (*2, 30*). The fact that both small and large ribosomal proteins associated with Gcn1, only in the formaldehyde stabilized Gcn1-Myc complex support the previous finding that Gcn1 binds weakly to translating ribosomes.

All eukaryotic ribosomes consist of two subunits; small (40S) and large (60S) subunits which are built from RNA and proteins. The yeast cytoplasmic 80S ribosome consists of 79 proteins; 33 proteins in the 40S subunit and 46 proteins in the 60S subunit (*120*). 59 of the 79 ribosomal proteins retain 2 paralogous genomic copies which mostly differ in function and localization (*121*). The fact that overexpression of one ribosomal protein rescued the growth defect from deletion of its paralog led to the conclusion that proteins encoded by duplicated genes are functionally redundant (*122*). However, recent studies have shown paralogue specific differences in sporulation (*123*), actin organization (*124*) and bud site selection (*125*).

Although the ribosome is widely known as the protein synthesizing factory, several ribosomal proteins are bi-functional in other words, they not only constitute integral components of the ribosome but also carry out functions in the cell which are unrelated to protein synthesis (*126*). For example; Rps3, one of the small ribosomal subunit protein has been shown to induce apoptosis in some cell lines (*127*) and involved in DNA repair (*128*). It has been reported that constitutive expression of human Rpl7 arrests cell cycle and induces apoptosis (*129*). Overall, ribosomal proteins seem to be involved in other functions in addition to protein synthesis.

If Gcn1 binds to translating ribosomes then it is expected that all proteins of the 80S subunit will be co-precipitated with Gcn1. In contrast to our expectation not all the 80S ribosomal subunit proteins were co-precipitated with Gcn1. Of the 79, ribosomal proteins only 25 proteins were co-precipitated with Gcn1. These findings raise the possibility that Gcn1 may bind to extra-ribosomal proteins. Ribosomal proteins are synthesized in the cytoplasm and exported to the nucleus (*130*). The ribosomal proteins which are incorporated into the ribosomal subunit get exported to the cytoplasm and studies suggests that there is a pool of ribosomal proteins in the nucleus as well as in the cytoplasm not associated with ribosomes, to perform other functions (*130*). It is possible that Gcn1 binds to these extra-ribosomal proteins to carry out a yet to be identified function. Or Gcn1 is involved in the export of ribosomal proteins from the nucleus to the cytoplasm or in the import of ribosomal proteins from the cytoplasm to the nucleus. Whether Gcn1 is involved in the nuclear import of ribosomal proteins can be tested by investigating whether the ribosomal proteins interacting with Gcn1 have nuclear localization signals.

It is possible that Gcn1 binds to a small region on the 80S ribosome. This idea is reasonable as the ribosome is far larger (3.3 MDa) than Gcn1 (300 kDa).

It has been demonstrated that the region (1-2052) of Gcn1 (almost three-quarters of Gcn1) interacts with translating ribosomes (*4*) and mutations in two distinct regions of *GCN1* (M1 and M7) resulted in impaired polyribosome binding by Gcn1, suggesting that Gcn1 has several contact points on the ribosome (*30*). In this study it was found that Rps0A, Rps1B, Rps3, Rps4A, Rps5, Rps6A, Rps14, Rps16A, Rps18A, Rps24A, Rpp0, Rpl1A, Rpl2A, Rpl3, Rpl7A, Rpl8a, Rpl9A, Rpl10, Rpl11A, Rpl13A, Rpl13B, Rpl17A, Rpl19A, Rpl20A and Rpl21A bind to Gcn1. These findings are in agreement with the previous findings that Gcn1 has several contact points on the ribosome (*30*) including the small and large subunits.

The results from this study and the results of the yeast two-hybrid screening (Sattlegger research group, unpublished) conducted by the Sattlegger

group may help to determine the contact points of Gcn1 on the ribosome (Table 3.3).

Previously the Sattlegger group conducted yeast two-hybrid (Y2H) screening to find interactions between Gcn1 and small ribosomal proteins (Rps) (Sattlegger group, unpublished). In this screening two fragments of Gcn1 encompassing amino acids (1-900) and (1060-1777) and the small ribosomal proteins were used as prey and bait. The Y2H screening for the large ribosomal subunit proteins has not been carried out yet.

Rps10A, Rps13, Rps15, Rps17A, Rps19A, Rps23A, Rps25A, Rps28A, Rps29A, Rps31A and Rps31B have been found to interact with Gcn1 in the Y2H screening and these proteins were not co-precipitated with Gcn1 in our study. It is possible that the interacting proteins were less abundant, therefore Mass Spectrometry failed to identify them. Supporting this idea, the true interacting partner of Gcn1, Gcn2 was not identified in the formaldehyde stabilized Gcn1-Myc complex. Additionally, it has been demonstrated that formaldehyde cross-linking leads to global protein loss (*111*) and we have found that a significant amount of Gcn1 was lost in the pellets in a manner that is dependent on formaldehyde concentration. For stabilization of Gcn1 containing complexes 0.3% formaldehyde was used. At this concentration there was a considerate amount of total protein loss and no cross-linked Gcn1 containing complexes were observed below the concentration of 0.3% (Figure 3.23), therefore it is possible that there was some amount of proteins lost during the sample preparation step. Alternatively, it is possible that these interactions identified in the Y2H are due to false positives and Y2H has an estimated false positive rate of 70% (*131*).

Further insight on the ribosomal proteins required for Gcn2 activation was gained by comparing the data from this study and the Y2H screening (Sattlegger group, unpublished) with the ribosomal-gene knockout screening (Jochmann and Sattlegger, unpublished) carried out in the Sattlegger lab. This screening was based on the idea that if ribosomal proteins are necessary for a functional Gcn1-

ribosome interaction, then the absence of the ribosomal proteins would impair Gcn2 activation. In this study the small and large ribosomal proteins were knocked out one at a time and the Gcn2 function in these strains was investigated by an eIF2α phosphorylation assay. The ribosomal gene knockout screening required deletion of the respective genes, therefore only the non-essential proteins were investigated.

Comparing the results from our study with the Y2H screening (Sattlegger group, unpublished) and ribosomal gene knock out screening (Jochmann and Sattlegger, unpublished) resulted in the identification of Rps18A and Rpl21A as potential Gcn1 binding proteins required for promoting Gcn2 function. In our study it was found that Rps18A co-precipitated with Gcn1, supporting the previous findings. Rps18A was found to interact with Gcn1 in the Y2H screening and a strain lacking Rps18A showed a SM^s phenotype and reduction in eIF2α-P levels (Jochmann and Sattlegger, unpublished). Similarly to Rps18A, Rpl21A was co-precipitated with Gcn1, and a strain lacking Rpl21A showed a SM^s phenotype in addition to reduced eIF2α-P levels. These findings strongly support the previous idea that Rps18A and Rpl21A are crucial binding partners of Gcn1 and are necessary for Gcn2 activation under amino acid starvation condition.

Strains lacking Rps25B, Rps26A or Rps28B showed sensitivity to SM and reduced eIF2α -P levels. However, these proteins did not show interactions with Gcn1 either in the Y2H screening or in the co-immunoprecipitation assay. Additionally, a strain lacking Rpl34B, one of the 60S subunit proteins, showed a SM^s sensitive phenotype and reduced eIF2α-P level and it had not been immunoprecipitated by Gcn1 in our study. Y2H screening for Rpl34B has not been carried out. The fact that deletion of Rps25B, Rps26A, Rps28B or Rpl34B resulted in reduced Gcn2 mediated eIF2α-P level, would support the idea that these proteins are necessary for efficient Gcn2 function. It is possible that these proteins bind directly to Gcn2 instead of Gcn1. It is known that Gcn2 associates with the ribosome (*132*) and the ribosome association of Gcn2 is required for its *in vivo* activation under amino acid limiting conditions (*133, 134*).

Gcn1-bound to translating ribosomes was proposed to be required to sense the occurrence of starvation signal (*2, 135*). It has been proposed that in the Gcn1-ribosome complex, uncharged tRNAs entering the ribosomal A-site are transferred to Gcn2 *via* Gcn1 which in turn results in Gcn2 activation and this indicates that Gcn1 must bind close to the A-site in order to carry out its function (*4*). Furthermore, it has been shown that overexpression of Gcn1 confers sensitivity to paromomycin, a drug that affects the fidelity of translation by binding to the ribosomal A-site, supporting the idea that Gcn1 may bind close to the ribosomal A-site (*4*). In order to visualize the ribosomal proteins co-precipitated with Gcn1 on the ribosome and to determine if these proteins are localized close to the ribosomal A-site, a P-site bound Met-tRNAi^{Met}-80S ribosome was reconstructed from the data obtained from Fernandez et al. (2013) (Figure 3.35). Of the proteins co-precipitated by Gcn1, Rps5 is located in the head domain (*136*) of the 40S subunit and Rps18A is located at the top of the head of the 40S subunit (Gene data obtained from nextprot (http://www.nextprot.org/db/entry/NX_P62269)). Studies suggest that Rpl3 may function as sensor of the tRNA occupancy status of the A-site (*137*). Rps18A, Rps5 and Rpl3 have been co-precipitated with Gcn1 in our study; additionally Rps5 and Rps18A have shown interactions with Gcn1 in the Y2H screening. Furthermore, it has been shown that reduced levels of Rps18A leads to paramomycin sensitivity (*138*) suggesting that Rps18A may bind close to the A-site.

Rps3, Rps16A, Rps0A and Rps14A are located around the head region where Rps18A and Rps5 are located (Figure 3.35). Furthermore Rps3 appears to be directly involved in ribosome-aminoacyl-tRNAs interactions during translation (*139*), forms part of the domain on the ribosome where the initiation of translation takes place and found cross-linked to the translation initiation factors eIF2 (*140*) and eIF3 (*140*). Taken together, these results support the idea that Gcn1 binds proximal to the A-site.

With the approach used in the ribosomal gene knockout screening it was not possible to study the effects of Rps5 and Rpl3 on Gcn2 function as they are essential for cell growth and knockout of these proteins would render cells unviable. Therefore, their role in facilitation of Gcn2 activation could not be determined.

Among the ribosomal proteins co-precipitated by Gcn1, deletion of Rps6A and Rps24A did not show a significant reduction in the eIF2α-P level (Jochmann and Sattlegger, unpublished).

It has been speculated that the regulatory function of the ribosome can occur by incorporating different paralogues proteins (*141*). Thus, it would be possible that the parologous protein compensated for the deletion of these proteins. Among the 79 ribosomal proteins, 59 proteins are encoded by two paralogous genes (*121, 142*).

In our study several ribosomal proteins that are not localized close to the A-site have also been co-precipitated with Gcn1 and among them deletion of Rpl21A resulted in reduced Gcn2 mediated eIF2 phosphorylation, suggesting that Gcn1 has several contact points on the ribosome in addition to the A-site that are required for efficient Gcn2 function.

For some of the ribosomal proteins that were co-precipitated with Gcn1 in this study, the Y2H and the ribosomal gene knockout screenings were not carried out (Table 3.3).

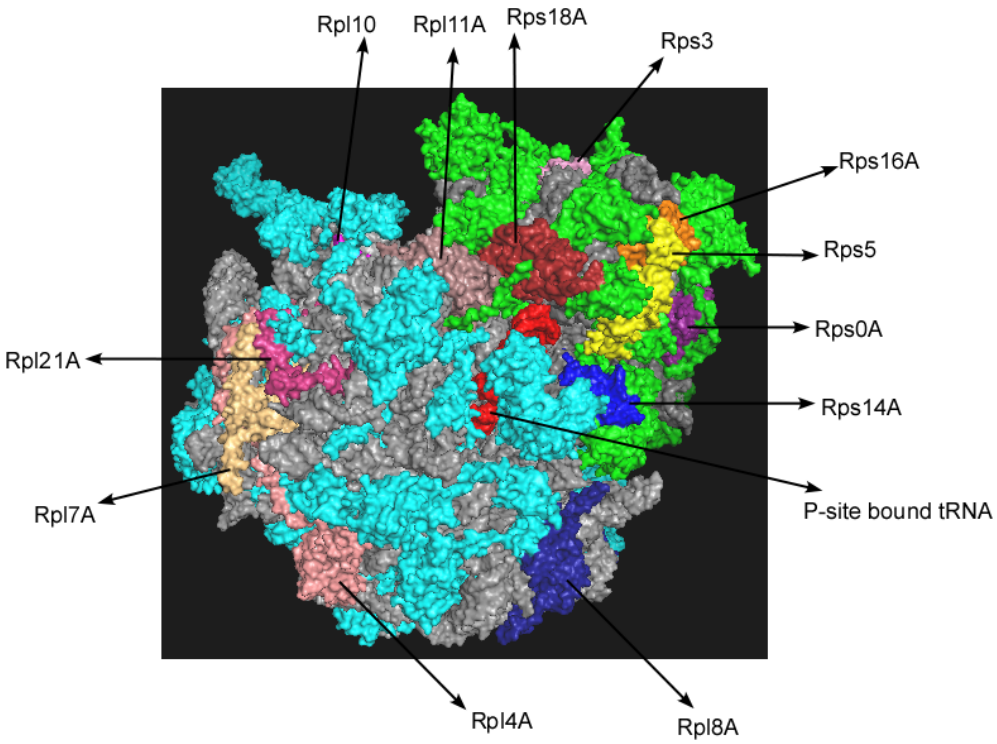

Figure 3.35. Surface representation of the 80S ribosome of *Saccharomyces cerevisiae* in a P-site Met-tRNAi^{Met} bound state. Small and large ribosomal proteins are represented in green and cyan respectively. rRNA is represented in grey and Met-tRNAi^{Met} is represented in red. The ribosomal proteins co-precipitated by Gcn1 are colored distinctly and labeled. The ribosome was reconstructed from the Met-tRNAi^{Met}-eIF5B bound 80S ribosomal data (4BYL, 4BYN, 4BYO, 4BYP and 4BYS) of Fernandez et al. (2013) by using PyMOL 1.1 (DeLano Scientific LLC). In this picture eIF5B was not included. Not all the ribosomal proteins co-precipitated by Gcn1 are shown, as it was not possible to visualize all of them in one orientation.

Gcn1 co-precipitating ribosomal proteins under replete conditions suggest that the ribosome-Gcn1 interaction is happening under replete conditions. This is in agreement with the previous findings that Gcn1 is located on the ribosomes under replete conditions (*2, 4, 143*).

Of the identified Gcn1 binding proteins (Figure 3.30), Act1, Fas1, Kap123, Hsc82, Rvb1, Tef1 and Ura2 were listed as common contaminants in affinity purifications as they were found frequently in all purifications or identified non-specifically in control affinity purifications of the large scale affinity purification

studies (*25-27*). Therefore, it is possible that these proteins were identified in the Gcn1-Myc complexes due to nonspecific binding. Arguing against this idea, the true interacting partners of Gcn2, Hsc82 (Hsp90) (*82*) and Tef1 (*81*) were identified indicating that the identified proteins may not be due to nonspecific binding. However, it should be kept in mind that false positives cannot be completely ruled out in affinity purifications.

The *in house* Gcn1 interactome identified proteins putatively in a complex with Gcn1. However, it is unable to reveal the stoichiometry and localization of the protein complexes. It is possible that more than one Gcn1 containing complex has been immunoprecipitated and different Gcn1 containing complexes contain different binding partners.

Several proteins localized in the mitochondria were identified as Gcn1 binding proteins. Of the identified Gcn1 binding proteins, Acc1, Atp1, Cys4, Erg6, Fas1, Fas2, Hsc82, Hsp60, Lys12, New1, Rps18A, Rps24A, Ssc1, Tif4631 and Ura2 are localized in the mitochondria (*144*). Additionally, Gcn1 was found in the mitochondrial fraction (*144*). The fact that Gcn1 was identified in the mitochondrial fraction and several Gcn1 binding proteins identified in our study are localized in the mitochondria suggests that Gcn1 is probably associated with the mitochondria or these proteins are localized both in the mitochondria and cytoplasm. As supporting evidence for the later, 6 (Atp1, Cys4, Hsp60, Rps18, New1 and Ssc1) out of the 20 proteins are localized in both the mitochondria and cytoplasm (gene data obtained from the SGD).

Several proteins involved in the endoplasmic reticulum to Golgi protein trafficking (Se14, Sec18, Sec26, Sec27 and Sec28) and rRNA processing (Nop1, Nop56, and Nop58) were identified as Gcn1 binding proteins, indicating that Gcn1 may have a role in rRNA processing and trafficking of proteins from the endoplasmic reticulum to the Golgi.

We used BiNGO (Biological Network Gene Ontology tool), to determine which gene ontology (GO) categories are statistically overrepresented in the

identified Gcn1 binding proteins. As expected, proteins localised in the cytosolic ribosomal subunits were overrepresented (Figure 3.32). Additionally, proteins localised in the mitochondria, stress granules, vacuolar ATPase complex, were overrepresented. Additionally, proteins involved in the regulation of cellular biosynthetic process, regulation of translation, regulation of metabolic processes, and regulation of gene expression were overrepresented (Figure 3.33). These findings indicate that Gcn1 may be localized in different places in the cell and regulate several other cellular processes in addition to regulating the translation initiation.

Table 3.3 Comparison of the results obtained from the Y2H (Sattlegger group, unpublished) and ribosomal gene knockout screening (Jochmann and Sattlegger, unpublished) with the results obtained from this study.

The list of cytoplasmic ribosomal proteins of *Saccharomyces cerevisiae* was obtained from Ben-Shem et al. (2011).

All ribosomal proteins	Yeast two hybrid		SMs	Reduction in eIF2-P level	Co-precipitating with Gcn1
	Interaction with Gcn1 fragment (1-900)	Interaction with Gcn1 fragment (1060 - 1777)			
Rps0A	Yes	Yes	ND	No	Yes
Rps1B	-	-	ND	ND	Yes
Rps2	-	-	ND	ND	No
Rps3	-	-	ND	ND	Yes
Rps4A	-	-	SM[s]	ND	Yes
Rps5	Yes		ND	ND	Yes
Rps6A	-	-	ND	No	Yes
Rps7A	-	-	ND	ND	No
Rps8A	-	-	ND	ND	No
Rps9A		Yes	ND	ND	No
Rps9B	-	-	SMs	No	No
Rps10A	Yes	Yes	SM[s]	Yes	No
Rps11A	-	-	ND	ND	No
Rps12	-	-	ND	ND	No
Rps13	-	Yes	ND	ND	No
Rps14A	-	-	SM[s]	ND	Yes
Rps15	Yes	Yes	ND	ND	No

Rps16A	-	-	SMs	ND	Yes
Rps17A	-	Yes	SMs	No	No
Rps18A		Yes	SM^s	Yes	Yes
Rps19A		Yes	ND	ND	No
Rps20	-	-	ND	ND	No
Rps21A	-	-	ND	ND	No
Rps22A	-	-	ND	ND	No
Rps23A	-	Yes	ND	ND	No
Rps24A	-	-	SMs	No	Yes
Rps25A	Yes	Yes	ND	ND	No
Rps25B	-	-	SM^s	Yes	No
Rps26A	-	-	SM^s	Yes	No
Rps27A,B	-	-			No
Rps28A	-	Yes	ND	ND	No
Rps28B	-	-	SM^s	Yes	No
Rps29A	-	Yes	ND	ND	No
Rps30A	-	-	SM^s	No	No
Rps31A	-	Yes	ND	ND	No
Asc1					No
Rpp0					Yes
Rpl1A					Yes
Rpl2A					Yes
Rpl3					Yes
Rpl4B					Yes
Rpl5					No
Rpl6A			SM^s	No	No
Rpl7A					Yes
Rpl8A					Yes
Rpl9A					Yes
Rpl10					Yes
Rpl11A					Yes
Rpl12A					No
Rpl13A, B					Yes
Rpl14A			SM^s	No	No
Rpl15A					No
Rpl16A					No
Rpl17A					No
Rpl18B			SM^s	No	No
Rpl19A					Yes
Rpl20A					Yes
Rpl21A	ND	ND	SM^s	Yes	Yes
Rpl22A					No
Rpl23A					No
Rpl24A					No

Rpl25					No
Rpl26A					No
Rpl27A					No
Rpl28A					No
Rpl29					No
Rpl30					No
Rpl31A					No
Rpl32					No
Rpl33A					No
Rpl34B			SM^s	Yes	No
Rpl35A			SM^s	No	No
Rpl36A					No
Rpl37A					No
Rpl38					No
Rpl39					No
Rpl40A					No
Rpl41A					No
Rpl42A					No
Rpl43A					No
Rpl43B					No
P1/P2					No

Note: - No interaction, Empty cell - Interaction was not tested

Chapter 4 Identification of Gcn1 binding proteins that are positive regulators of Gcn2

As outlined in the previous chapter new potential Gcn1 binding proteins were identified. It was next investigated which of these proteins are required for promoting Gcn2 function.

4.1 Screening of gene knockout mutants-encoding for Gcn1 binding proteins for impaired GAAC response

It was expected that if a protein is required to promote the GAAC, then cells lacking this protein would have an impaired GAAC response. Therefore, in order to identify which of the putative Gcn1 binding proteins are required for promoting the GAAC, strains were used that lacked one of these proteins at a time, to score for impaired growth under starvation conditions. As this procedure required the deletion of the respective genes, only the non-essential proteins could be investigated.

The principle behind this growth assay is that only induction of the GAAC allows cells to grow under amino acid limiting conditions. Amino acid starvation was induced by a drug that interferes with the biosynthesis of amino acids, and the ability of the strains to induce the GAAC was scored by comparing the growth rate of the wild type to that of the gene deletion mutants.

As the wild type has all proteins required to induce the GAAC, in our assay, we expected that these strains would grow under replete as well as under amino acid starvation conditions. Strains unable to activate GAAC were expected to have an impaired growth on starvation medium as compared to control medium. Deletion of genes that are not required for GAAC would not lead to a growth deficit on starvation plates; they were expected to grow well on both control and starvation plates. The *gcn2*Δ strain was expected to grow on control plates but not on starvation plates, as Gcn2 is essential to induce the GAAC response.

A drug known as Sulfometuron methyl (SM) was used to induce amino acid starvation. SM inhibits acetohydroxy acid synthase II, an enzyme involved in the biosynthesis of branched amino acids (Leucine, Isoleucine and Valine) (*113*).

Saturated cultures of gene deletion mutants, wild type (BY4741) and *gcn2*Δ strain, were subjected to tenfold serial dilutions and 5 µl of each dilution and 5 µl of diluted cultures were spotted on plates containing solid minimal medium (SD) with different concentrations (0.5-2 µg/ml) of SM and a plate without SM as a control. Additionally, the cultures were spotted on Yeast-Peptone-Glycerol (YPG) media containing plates. SD media enables to monitor the growth rate of the investigated strains under replete conditions. YPG is a nutrient rich media which contains glycerol instead of glucose. YPG media enables the identification of colonies with defective mitochondria known as petites. Due to defect in the respiratory chain petites are unable to grow on media containing non-fermentable carbon sources such as glycerol and form small colonies in the presence of fermentable carbon sources such as glucose (*145*).
The cells were grown at 30°C, growth was monitored every day for 7 to 8 days and documented using a document scanner.

A growth defect of strains in the presence of SM is being referred as SM sensitive (SM^S) and a growth rate similar to that of the wild type as wild type phenotype. Petites identified in this screening were not included in the subsequent screening (Appendix A.4). Additionally several strains were unable to grow or had a severe growth defect on SD media and these strains were also not included in the subsequent screening. Some of the gene knockout mutants encoding for ribosomal proteins, which showed sensitivity to SM, were not included either, because they have already been investigated by others (Jochmann and Sattlegger).

As there were several Gcn1 binding proteins identified in the three different Gcn1 interactomes it was not possible to screen all of them for their effect on Gcn2 function. We have managed to screen 66 gene deletion strains encoding for proteins found in the extended Gcn1 intreactome, common to the minimal and extended, common to the *in house* and extended or identified in all

three Gcn1 intreactomes. The strains were grown in minimal media and subjected to semi quantitative growth assays. The gene deletion mutants that were sensitive to SM and subjected to further screening are shown in Figure 4.1. The results of all the strains investigated are shown in appendix (A.5).

In all SM^S screening experiments it was validated that the *gcn2*Δ strain was able to grow on the control plates, but not on the starvation plates, ensuring that SM has successfully induced amino acid starvation. The wild type was validated to be able to grow on all plates, including the ones containing SM. The gene knockout-mutants were tested for their growth behaviour on replete medium, and their growth rate was compared to that on SM plates. Reduced growth of the gene deletion mutants on the starvation plates as compared to those on replete plates and to that of the wild type suggests that the deletion mutants are sensitive to SM.

Among the 66 strains tested, it was found that strains lacking Prs3 (*prs3*Δ) (Figure 4.1, Set 1), Vps1 (*vps1*Δ) (Figure 4.1, Set 2), Vps13 (*vps13*Δ) (Figure 4.1, Set 3), Kem1 (*kem1*Δ) (Figure 4.1, Set 4), Dhh1 (*dhh1*Δ), Ilv1 (*ilv1*Δ) (Figure 4.1, Set 5), Rnr1 (*rnr1*Δ), Msn5 (*msn5*Δ) (Figure 4.1, Set 7), Sin3 (*sin3*Δ) (Figure 4.1, Set 8), and Tps1 (*tps1*Δ) (Figure 4.1, Set 9) were sensitive to SM.

As expected, mutants lacking Vps1 (*vps1*Δ) (Figure 4.1, Set 2), Rnr1 (*rnr1*Δ) (Figure 4.1, Set 7), and Sin3 (*sin3*Δ) (Figure 4.1, Set 8) were growing slowly on the control plates as compared to the wild type. This suggests that the absence of these proteins conferred a slow growing phenotype (gene data obtained from the yeast genome database (SGD)) and the growth defect was exacerbated on the starvation plates, indicating that these strains were sensitive to SM and that this is possibly due to the gene deletions.

As an example for deletion strains that had a wild type phenotype, strains lacking Dnm1 (*dnm1*Δ) and Pho81 (*pho81*Δ) are illustrated (Figure 4.1, Set 6 and 8). Mutants lacking Dnm1 and Pho81 grew similar to the wild type both in the control and starvation plates. This suggested that the absence of these proteins did not affect the strain's growth under replete or starvation conditions and that these

proteins are not required for promoting the GAAC.

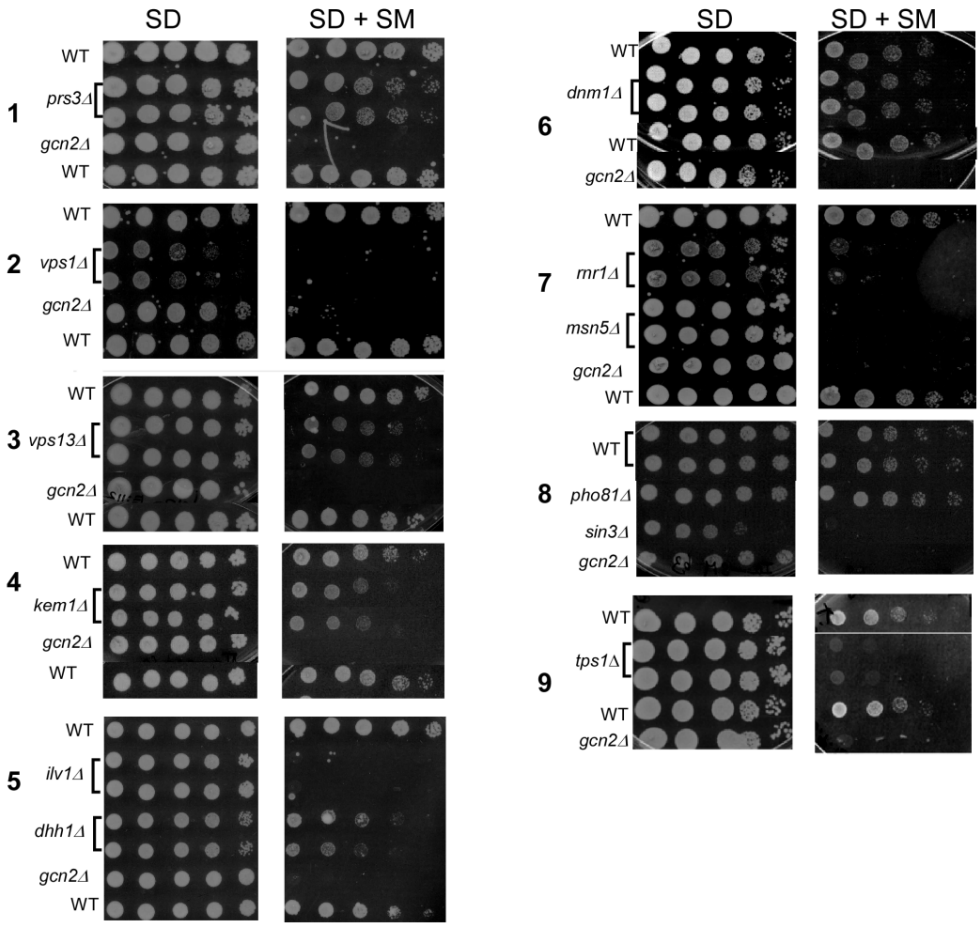

Figure 4.1. Comparison of growth rates of the wild type with gene deletion mutants. Semi quantitative growth assay of gene deletion mutants, wild type and *gcn2*Δ strains (refer to Table 2.2). Indicated strains were grown to saturation and the saturated cultures were subjected to tenfold serial dilution and 5 µl of each dilution, and 5 µl of undiluted culture, were spotted on solid media containing SM and no SM as a control and incubated at 30°C. Growth was monitored every day for 7 to 10 days.

4.2 Screening of the SM sensitive strains for impaired Gcn2 function

The SM sensitivity observed in our screening is a first indication that the GAAC was impaired in those strains. As described earlier the GAAC response consists of several steps, such as sensing the starvation signal, activation of Gcn2,

phosphorylation of eIF2α, derepression of Gcn4 expression and expression of Gcn4 target genes. A defect in any of the steps could result in impaired GAAC. However, a SM^S phenotype could also be due to mechanisms unrelated to the GAAC.

In order to test which of the potential new Gcn1 binding proteins truly affected Gcn2 activation, we measured the amount of eIF2α in the respective gene knockout mutants. Eukaryotic initiation factor 2-alpha (eIF2α) is the substrate of Gcn2, hence reduced levels of phosphorylated eIF2α (eIF2α-P) would be indicative of impaired Gcn2 activation. If eIF2α-P levels of the SM^S strains are equal to that of the wild type under starvation conditions, this would mean that the gene deletions do not have any effect on Gcn2 activation.

If the eIF2α-P levels of the SM^S strains are less than that of the wild type under starvation conditions, this will indicate that the proteins missing in these strains are required for Gcn2 activation.

Wild type, strains that showed a SM^S phenotype and *gcn2*Δ strains were grown in liquid minimal media overnight and the cultures were inoculated in duplicate into fresh liquid medium. Cells were grown to exponential phase and starvation was induced by the addition of SM. After starving for an hour the cells were cross-linked with formaldehyde to prevent any enzymatic changes happening to the phospho-protein (eIF2α-P) during cell breakage. The cells were pelleted, cell extracts prepared and subjected to SDS-PAGE followed by Western blotting with antibodies against eIF2α-P and Pgk1. Pgk1 was used as a reference for equal loading, to take into account the differences in eIF2α-P level that could have caused by gel loading errors. Pgk1 is phosphoglycerate kinase 1, a housekeeping gene involved in glycolysis (*146*).

The outcome of the screening is shown in Figure 4.2. As expected, eIF2α-P levels of the wild type under starved conditions (+) were increased as compared to the eIF2α-P levels in replete conditions (-), assuring that the SM induced starvation resulted in increased eIF2α-P levels (Figure 4.2). A signal for eIF2α-P in the *gcn2*Δ strain was not detected, as Gcn2 is essential to phosphorylate eIF2α under

amino acid starvation conditions.

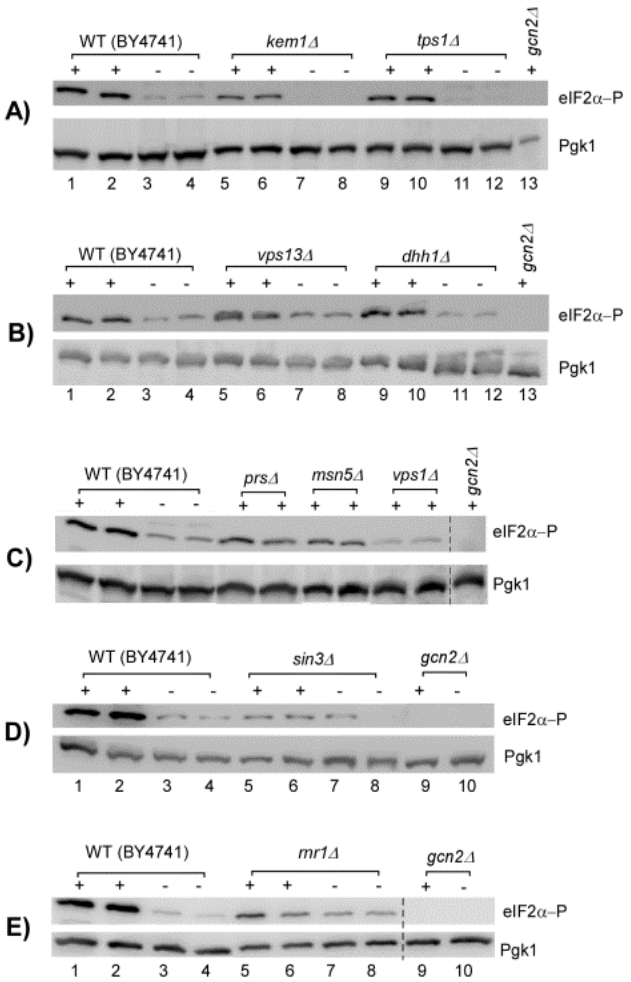

Figure 4.2. Comparison of eIF2α-P levels of the gene deletion mutants to that of the wild type under starvation (+) and replete conditions (-). The wild type, gene deletion mutants and *gcn2*Δ strains (refer to Table 2.2) were grown to exponential phase in minimal media and then starvation was induced by the addition of SM to a final concentration of 1 µg/ml. After an hour cells were cross-linked, pelleted and cell extracts obtained. For each cell extract 10 µg of total protein was subjected SDS-PAGE followed by Western blotting with antibodies against eIF2α-P or Pgk1. For *prs3*Δ, *msn5*Δ and *vps1*Δ strains the eIF2α-P levels under starved conditions only have been shown (panel C).

To investigate if the reduction in eIF2α-P levels as compared to that of the wild type was significant a one tailed student t-test was performed. *P* values less than 5% were considered likely to have 95% true difference. The student t-test revealed that strains lacking Msn5 (*msn5*Δ), Vps1 (*vps1*Δ), Sin3 (*sin3*Δ), Kem1 (*kem1*Δ)

and Rnr1 (*rnr1*Δ) had significant reductions in the eIF2α-P levels under starved conditions as compared to that of the wild type (Figure 4.3). Absence of Dhh1 (*dhh1*Δ), Prs3 (*prs3*Δ) and Vps13 (*vps13*Δ) did not result in a significant reduction in eIF2α-P level compared to that of the isogenic wild type.

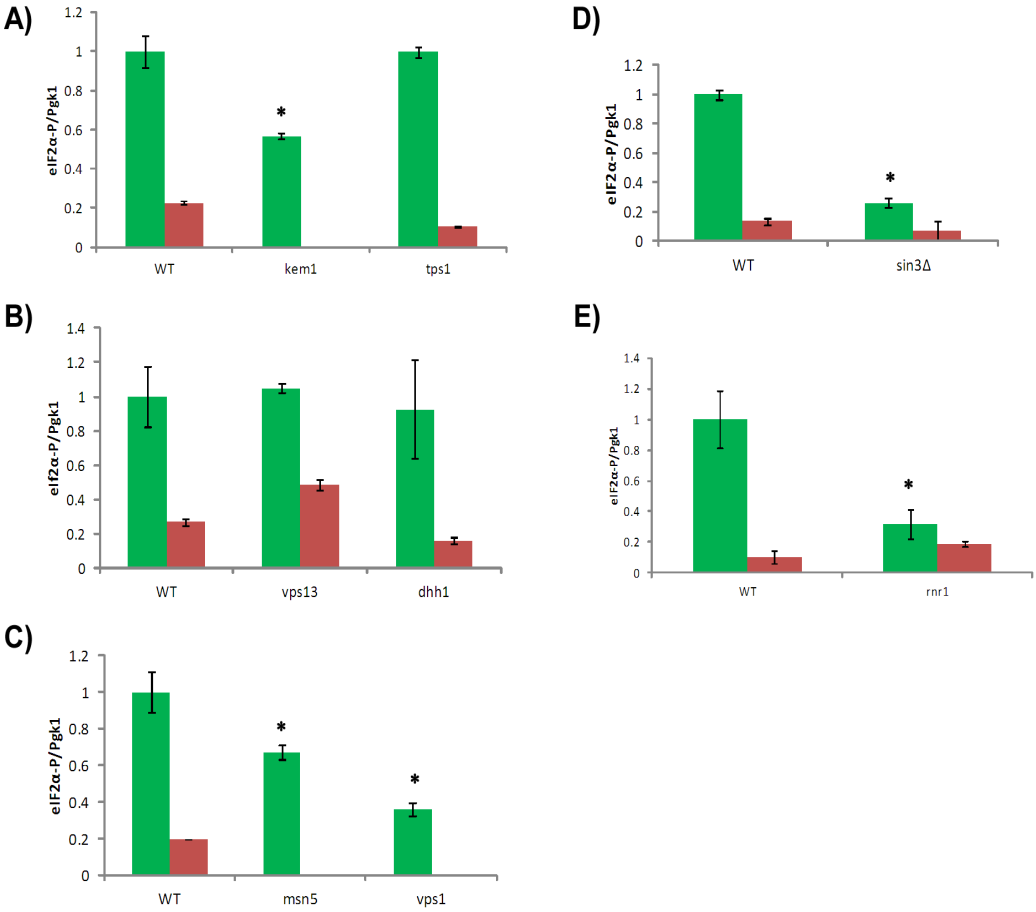

Figure 4.3. Comparison of eIF2α phosphorylation levels of gene knockout strains relative to wild type. The signal intensity of the eIF2α-P and Pgk1 from Figure 4.2 was quantified using the Multi Gauge software. The ratio of eIF2α-P/Pgk1 was calculated and normalized to that of the wild type. The error bars of two independent colonies are indicated. The star indicates the strains that showed a statistically significant difference in eIF2α-P levels as compared to that of the wild type.

Reduced eIF2α-P in these deletion mutants was in agreement with the idea that Gcn2 function was affected and the lacking proteins may be important to promote Gcn2 function under amino acid starvation conditions.

4.3 Complementation assays

Five gene deletion mutants had reduced eIF2α-P levels, suggesting that Gcn2 function was impaired in these mutants. If the observed SM^S phenotype and reduced eIF2α-P levels were due to removal of the proteins, then reintroducing the genes encoding the missing proteins must reverse the SM^S phenotype. Plasmids carrying yeast chromosomal fragments were available from a yeast tiling collection in the Sattlegger lab. Initial complementation was accomplished using tiling collection plasmids carrying yeast 2 micron sequence necessary for maintaining a high copy number in yeast, yeast *LEU2* marker and a 10 kb insert of a chromosomal fragment encoding the gene of interest amongst others.

To investigate whether the SM^S phenotype was due to deletion of the respective genes, gene deletion mutants were transformed with the tiling collection plasmid carrying the missing gene or vector alone. The wild type was transformed with the vector alone and *gcn1*Δ or *gcn2*Δ strain was transformed with the vector alone or tiling plasmids as negative controls.

The resulting transformants were subjected to semi-quantitative growth assays as outlined in Figure 4.1. For *SIN3, MSN5* and *KEM1* two different tiling collection plasmids were available. The two different plasmids carried overlapping chromosomal fragments where the overlapping part carried the complementing gene. If one of the plasmid complements the SM^S phenotype but not the other then this may indicate that the genes common in both the plasmids are not responsible for rescuing the SM^S phenotype (Figure 4.4). If the tiling plasmids resulted in successful complementation then the next step was to clone the gene of interest and conduct a true complementation assay using a plasmid carrying only the gene of interest.

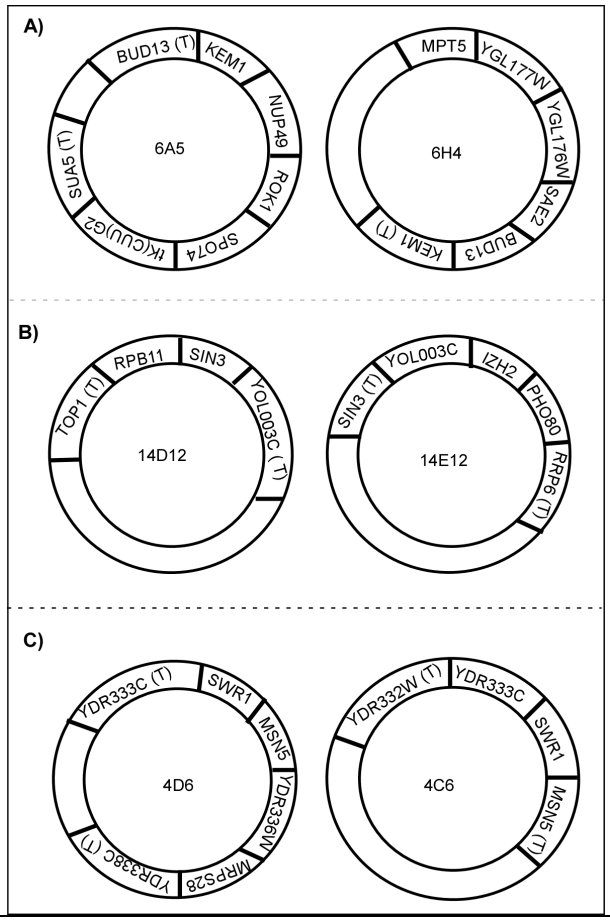

Figure 4.4. The tilling collection plasmids containing full length or truncated *KEM1*, *SIN3* and *MSN5*. The genes present in each plasmid are shown. (T) Indicates truncated genes either at N-terminus or C-terminus.

As expected, the wild type transformed with the vector control grew well on both the control and starvation plates (Figure 4.5). The *gcn2*Δ and *gcn1*Δ strains transformed with the vector control or tiling plasmid were able to grow on the control plates, but not on starvation plates indicating successful induction of starvation by SM.

The *kem1*Δ strain transformed with the plasmid 6H4 carrying N-terminally truncated *KEM1* or vector alone were able to grow equally well on the control plates, but both were unable to grow on starvation plates. But strains carrying the plasmid 6A5 that contains full length *KEM1* were able to grow almost similar to the wild type on starvation plates, supporting the idea that introducing *KEM1* back

into the *kem1*Δ mutants restored the SM^S phenotype. *KEM1* and *BUD13* are common to these two plasmids (6A5 and 6H4). As the SM^S phenotype was rescued only by the strain carrying 6A5 plasmid, suggesting that *BUD13* was not responsible for reversing the SM^S phenotype.

Likewise *sin3*Δ mutants transformed with the plasmid 14E12 carrying a C-terminally truncated *SIN3* did not complement the SM^S phenotype of the *sin3*Δ mutant. But transformants carrying the plasmid 14D12 with full length *SIN3* partially complemented the growth defect of the *sin3*Δ mutant. The gene that is commonly present in both the plasmid is YOL003C. The fact that the plasmid carrying the full length YOL003C did not complement the SM^S suggests that the effect was not due to YOL003C.

Similarly *msn5*Δ mutants transformed with the plasmid 4C6 harbouring a C-terminally truncated *MSN5* did not complement the SM^S phenotype but the plasmid 4D6 carrying full length *MSN5* gene partially complemented the SM^S phenotype of the *msn5*Δ mutants. YDR333C is commonly found in both the plasmids. As the SM^S phenotype was complemented only by the 4D6 plasmid suggests that it was not due to YDR333C.

The finding that the SM^S phenotype of the *sin3*Δ and *msn5*Δ mutants was partially complemented by the 14D12 and 4D6 plasmids supported the idea that the SM^S of these mutant was possibly due to the absence of the proteins. However it needs to be investigated whether plasmid borne *MSN5* or *SIN3* alone complements the SM^S phenotype.

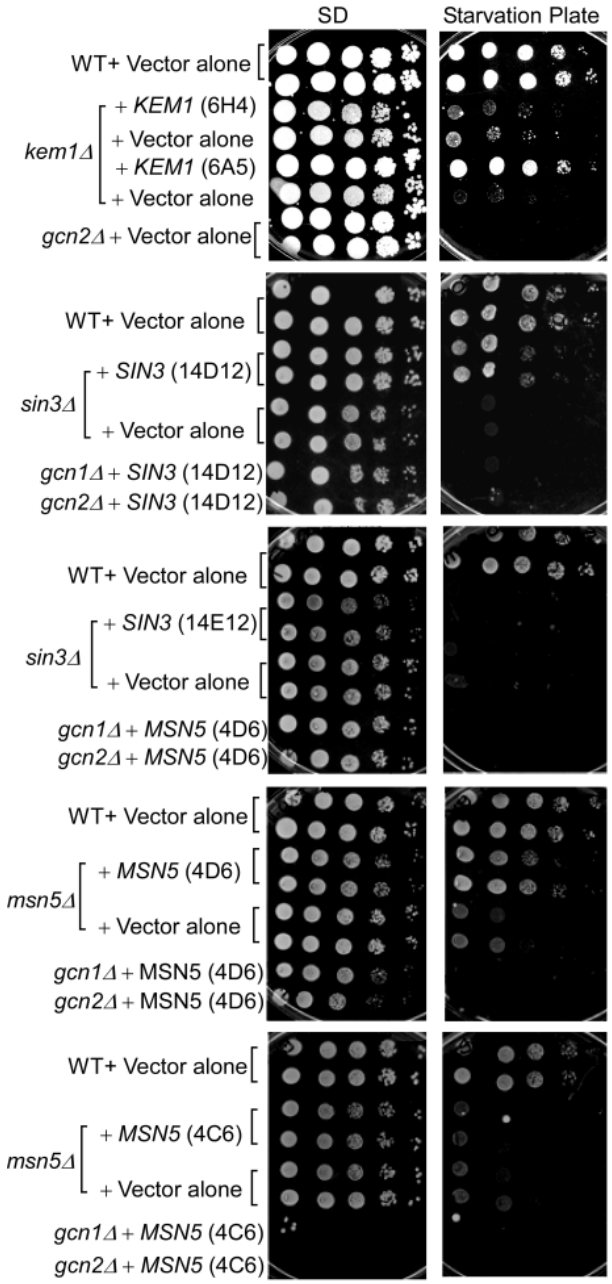

Figure 4.5. Gene complementation assay of *kem1*Δ, *sin3*Δ and *msn5*Δ strains. Plasmids containing *KEM1*, *SIN3, MSN5* and vector alone (refer to Table 2.1) were transformed into *kem1*Δ, *sin3*Δ, *msn5*Δ and wild type respectively and subjected to semi quantitative growth assay. As a control either vector alone or vector containing the deleted gene were transformed into respective gene deletion mutants.

The fact that the tilling plasmid that carries full length *KEM1* in addition to other genes has fully complemented the SM^S phenotype of the *kem1*Δ strain supports the idea that the SM^S phenotype of the *kem1*Δ strain was due to the absence of *KEM1* and that reintroducing *KEM1* into the *kem1*Δstrainrestored the SM^S phenotype. But it is possible that other genes in the plasmid 6A5 have caused the effect. Therefore, it was necessary to carry out a complementation assay with a plasmid carrying *KEM1* alone.

To perform this, *KEM1* was cut out of the tilling plasmid 6A5 by *Xho1* and *Xba1* (restriction enzymes) such that it has its endogenous promoter and introduced into a low copy vector (pRS316).
The plasmid carrying *KEM1* or vector alone was introduced into *kem1*Δ strain and wild type. As a negative control the plasmid containing *KEM1* was introduced into *gcn1*Δ strain. The resulting transformants were subjected to a semi quantitative growth assay along with the positive and negative controls as outlined in Figure 4.1.

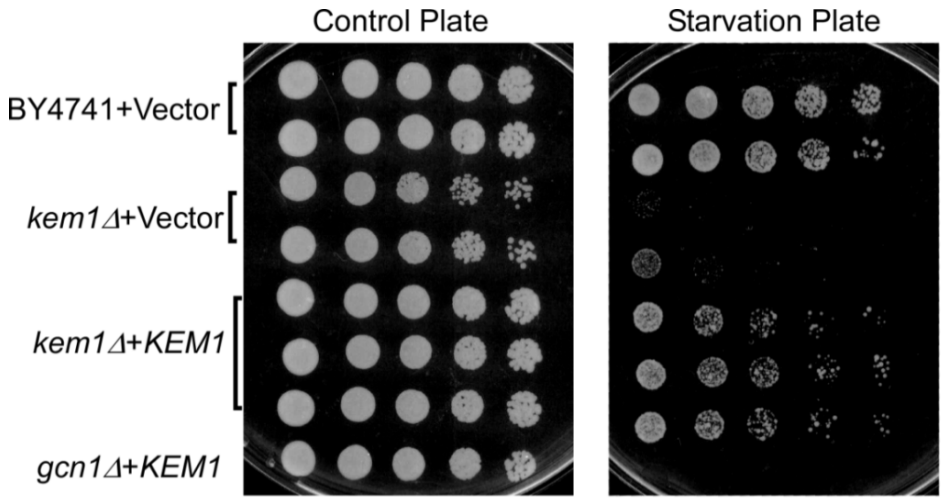

Figure 4.6. **Complementation assay of *kem1*Δ strain with low copy plasmid derived Kem1.** Wild type, *kem1*Δ and *gcn1*Δstrains were transformed with vector alone or vector containing *KEM1* and the resulting transformants were subjected to semi quantitative growth assay.

As expected, the wild type transformed with the vector alone was able to grow on both the control and starvation plates. The *gcn1*Δ strain carrying the plasmid containing *KEM1* grew on the control plate but did not grow on starvation plate suggesting that SM had induced starvation (Figure 4.6). The *kem1*Δ strain harbouring a plasmid borne *KEM1* grew better than the ones that carry vector alone. The *kem1*Δ *s*train carrying plasmid borne *KEM1* grew similar to the wild type on the control plate and on starvation plate, it showed growth impairment. This suggested that the SM^S phenotype of *kem1*Δ strain was rescued by expressing *KEM1* from a plasmid but it was only partial.

Due to time constraints, single gene complementation assay for *MSN5, SIN3* was not carried out.

4.4 Discussion

In this study gene deletion mutants lacking potential Gcn1 binding proteins have been investigated for their impaired GAAC stress response and Gcn2 function. 66 gene knockout mutants were screened for sensitivity to SM; a drug that causes starvation for branched amino acids. These strains were deleted for genes encoding for the proteins found in the extended Gcn1 interactome, common to the minimal and extended Gcn1 interactome, common to the *in house* and extended Gcn1 interactome or identified in all three Gcn1 intreactomes. Sensitivity to SM is a primary indication of impaired GAAC response. Of the 66 strains investigated, 10 were sensitive to SM (SM^S).

One limitation of the semi quantitative assay is the determination of SM^S phenotype of strains that have a very slow growth rate. In this case, these slow growing strains (*vps1*Δ*, rnr1*Δ and *sin3*Δ*)* were considered as SM sensitive and further subjected to a phospho eIF2α western blot analysis in order to investigate if Gcn2 function in these mutants has been impaired. *prs3*Δ, *vps1*Δ*, vps13*Δ*, kem1*Δ*, tps1*Δ*, dhh1*Δ, *ilv1*Δ *,rnr1*Δ*, msn5*Δ and *sin3*Δ strains were sensitive to SM. The severity of the SM sensitivity of the investigated strains varied from very

mild to very severe. Gene deletion mutants that are involved in amino acid biosynthetic pathways had a very severe SM^S phenotype. As an example the strain lacking Ilv1 (*ilv1*Δ) is illustrated (Figure 4.1, Set 5). Ilv1 is involved in the biosynthesis of isoleucine (*147*) and its expression is under the GAAC control (*9*). As most of the amino acid biosynthetic genes are under the GAAC control, therefore, it is expected that the deletion of the genes will confer SM^S phenotype. Therefore, amino acid biosynthetic genes that we have found in our studies were not included in our phospho eIF2α western blot analysis.

It is possible that the observed SM^s phenotype is due to mechanisms unrelated to the GAAC for example; 1) if these proteins are involved in membrane permeability then deletion of the genes encoding for these proteins may result in entry of more drug into these cells making them sensitive to SM, 2) absence of proteins involved in drug efflux pumps may lead to increased intracellular accumulation of the drug due to impaired efflux, 3) proteins functioning downstream of Gcn2 activation such as Gcn4; (Gcn4 is the downstream effector of the GAAC pathway, is imported into the nucleus and transcribes the genes involved in stress response, therefore deletion of these proteins could make the strains sensitive to SM), 4) deletion of proteins functioning in nuclear import of Gcn4 (Gcn4 needs to be transported into the nucleus to be able to transcribe stress response genes) may also lead to SM^S phenotype, 5) deletion of genes targeted by Gcn4 (e.g. amino acid biosynthetic genes) could also cause SM^S phenotype. We are interested in the proteins that facilitate Gcn2 activation; therefore, the eIF2α-P level of the SM^S strains was investigated under amino acid starvation condition to check whether the SM^S phenotype was due to impaired Gcn2 function.

Among the 9 strains investigated five of them (*kem1*Δ, *vps1*Δ, *sin3*Δ, *msn5*Δ, *and rnr1*Δ) had significant reduction of eIF2α-P level as compared to the isogenic wild type.

Strains lacking Tps1 (*tps1*Δ), Vps13 (*vps13*Δ) or Dhh1 (*dhh1*Δ) were sensitive to SM (Figure 4.1) but they did not show a reduction in eIF2α-P level (Figure 4.2 and 4.3) suggesting that downstream signalling of the GAAC or some other mechanisms unrelated to the GAAC could have caused the SM^S phenotype in these strains.

A study carried out with the gene knockout mutants for their sensitivity to chemicals in yeast has identified several strains as multidrug sensitive (*148*). In the study Parsons et al. (2004), twelve inhibitory compounds (camptothecin, hydroxyurea, benomyl, caffeine, cycloheximide, cyclosporine, FK506, fluconazole, rapamycin, sulfometuron methyl, tunicamycin, and wortmanin) were used to screen 4700 *Saccharomyces cerevisiae* gene knockout mutants. Absence of genes encoding for proteins involved in vacuolar proteins sorting ((Vps), Vps16, Vps25, Vps36, Vps67, Vam7, Vam6, Stp22, Snf7, Did4, Ies6) proteins involved in vacuolar membrane H^+-ATPase complex ((Vma), (Vma2, Vma4, Vma5, Vma6, Vma7, Vma8, Vma10, Vma13, Vma22, Ppa1, Vma11 and Vph2) a proton pump that maintains the low vacuolar pH were reported to be sensitive to many drugs (multidrug sensitivity). Therefore, the SM^S phenotype of *vma2*Δ and *vma6*Δ strains was most likely due to multidrug sensitivity and therefore these strains were not included in the eIF2α-P screening.

It has been reported that the vacuolar H^+-ATPases are also localized on the plasma membranes (*149*). It is possible that the absence of plasma membrane associated vacuolar H^+-ATPases could result in increased intracellular accumulation of drugs, which could result in sensitivity to the drugs. In conjunction with this idea, *vps13*Δ strain was sensitive to SM but it did not show a reduction in eIF2α-P level, suggesting that the SM^S phenotype of the *vps13*Δ strain was due to multi drug sensitivity.

The strain lacking Prs3 (*prs3*Δ) has been reported to be sensitive to tunicamycin and wortmanin (*148*). In our screening the *prs3*Δ strain did not show a significant reduction of eIF2α-P level despite having a SM^S phenotype.

Therefore the SM^S sensitive phenotype of the *prs3*Δ strain in our screening was considered to be due to general drug sensitivity.

Although the *dhh1*Δ and *tps1*Δ strains were sensitive to SM, eIF2α-P level was not reduced in these strains. This suggested that a mechanism unrelated to the GAAC was responsible for the SM^S phenotype of the *dhh1*Δ and *tps1*Δ strains.

Strain lacking Rnr1 (*rnr1*Δ) had significant reduction of eIF2α-P level compared to that of the wild type indicating that Gcn2 function was impaired.

The *vps1*Δ *s*train was sensitive to caffeine, cyclosporine A, FK506, fluconazole, and rapamycin (*148*). Therefore, it was expected that the SM^S phenotype of the *vps1*Δ strain would be possibly due to multi drug sensitivity. Interestingly, in contrast to our expectation, the *vps1*Δ strain showed a reduction in eIF2α-P level compared to that of the wild type, suggesting that Gcn2 function in the *vps1*Δ strain was impaired. This idea is further supported by the fact that Vps1 was consistently co-precipitated by Gcn1 in our study and the study by Gavin et al. (2006). These findings indicate that Vps1 is potentially in a complex with Gcn1 and Gcn2 and that it promotes Gcn2 activation. However, it has to be verified whether complementing the *vps1*Δ strain for the loss of Vps1 restores the SM^S phenotype and eIF2α-P level of the *vps1*Δ strain.

Strains lacking Sin3 (*sin3*Δ), Msn5 (*msn5*Δ) and Kem1 (*kem1*Δ) were not reported to be sensitive to any drugs including SM in the study by Parson et al. (2004). However, in our study it was found that *sin3*Δ*, msn5*Δ and *kem1*Δ were sensitive to SM. In addition to showing a SM^S phenotype these strains also showed a reduced eIF2α-P level indicative of impaired Gcn2 function. It is possible that the deletion strains used in the study by Parson et al. (2004) had some secondary mutations to revert the defect.

However, introducing *SIN3* from a tilling plasmid has only partially rescued the SM^S phenotype of *sin3*Δstrain. In addition to *SIN3* the tiling plasmid contains *TOP1*, *RPB11* and YOL003C. YOL003C encodes for

palmitoyltransferase and is required for palmitoylation of amino acid permeases (*150*). Over-expression of YOL003C is known to decrease the growth of the strain (gene data obtained from the yeast genome database). This indicates that the partial complementation of SM^S phenotype of *sin3*Δ strain was due to the presence of YOL003C. However, this needs to be investigated by complementing the *sin3*Δ strain with a plasmid containing *SIN3* alone.

Expression of *KEM1* from the tiling plasmid (high copy) that also carries some other genes had fully complemented the SM^S phenotype of *kem1*Δ strain (Figure 4.5). But a low copy plasmid borne *KEM1* only partially rescued the SM^S phenotype of the *kem1*Δ strain (Figure 4.6). One possible reason for this could be that the low copy plasmid was not producing enough of Kem1 as compared to the endogenous level or *KEM1* expressed from the tiling plasmid. Thus, it is possible that different expression levels of Kem1 from the low and high copy plasmids contribute to the observed difference in rescuing the SM^S phenotype of *kem1*Δ mutants. This can be tested by cloning *KEM1* into a high copy plasmid and by investigating if the high copy plasmid derived *KEM1* could fully complement the SM^S of the *kem1*Δ strain. It is also possible that the promoter of *KEM1* was truncated or the upstream sequences required for efficient transcription of *KEM1* was truncated.

Due to time constraint we were unable to investigate the single gene complementation for *msn5*Δ and *sin3*Δ mutants.

A summary of the results are given in Table 4.1 and in Figure 4.7.

Table 4.1 Overview of the screenings of gene knockout mutants-encoding for Gcn1 binding proteins for their sensitivity to SM, and reduced eIF2α-P level.

Strains name	SM^S	↓ eIF2-P	Single gene Complementation
*kem1*Δ	SM^S	Yes	Yes
*vps1*Δ	SM^S	Yes	Not investigated
*vps13*Δ	SM^S	No	Not investigated
*prs3*Δ	SM^S	No	Not investigated
*dhh1*Δ	SM^S	No	Not investigated
*rnr1*Δ	SM^S	Yes	Not investigated
*msn5*Δ	SM^S	Yes	Not investigated
*sin3*Δ	SM^S	Yes	Not investigated
*tps1*Δ	SM^S	No	Not investigated

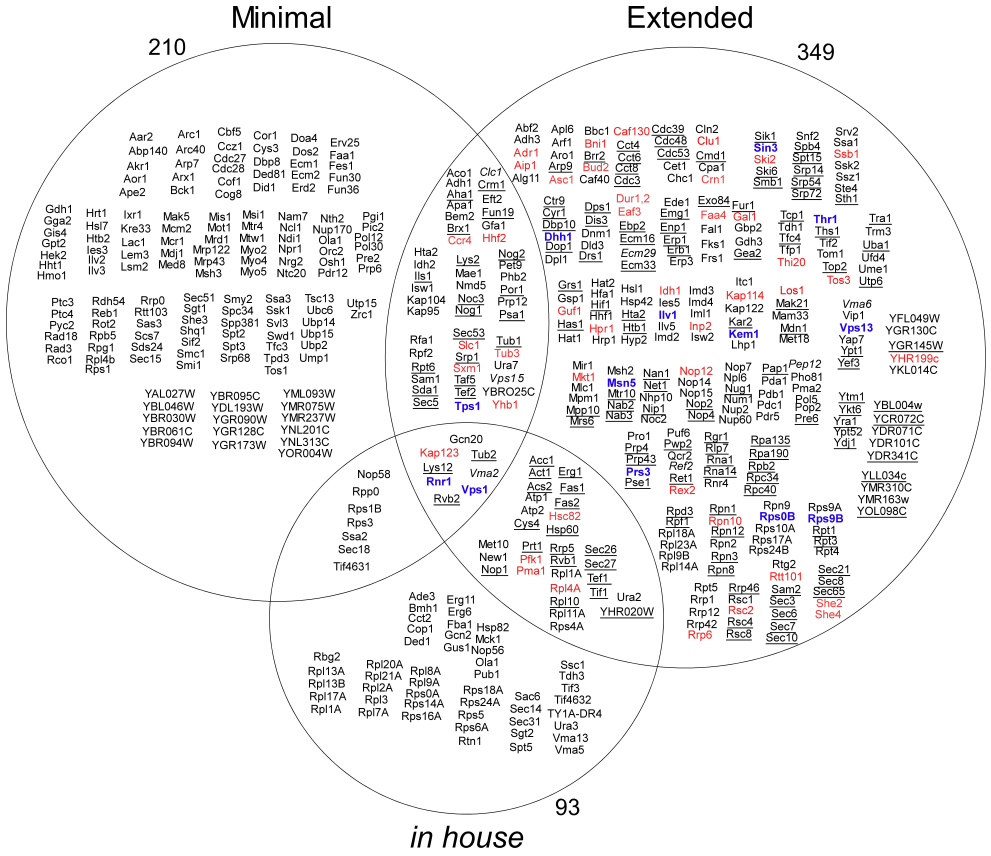

Figure 4.7. Summary of the SM^{s} and eIF2α-P screenings. Red - strains that did not show a SM^{S} phenotype. Blue - strains that showed a SM^{S} phenotype. Underlined- proteins essential for cell viability. Italics-petites, showed severe growth impairment or no growth on minimal media.

Chapter 5 Reciprocal immunoprecipitation of Gcn1 binding proteins

Potential Gcn1 binding proteins were identified from the published large scale affinity purification studies and by affinity purification of Gcn1 under less stringent conditions from the cell extract obtained from the cells subjected to cross-linking *in vivo*.

Next we wanted to verify whether these proteins are truly in a complex with Gcn1. It was reasoned that if the proteins are in a complex with Gcn1 and if the interactions are strong enough, then, they would co-precipitate Gcn1 when used as baits.

To test this, we have employed an *in vivo* co-immunoprecipitation assay using proteins that were expressed at native levels. Since antibodies against all Gcn1 binding proteins were not available, epitope tagged proteins were used. The Sattlegger lab has a collection of yeast strains (Life Technologies) where a single ORF at a time is GFP tagged and expressed from its endogenous promoter.

Strains carrying the GFP tagged Gcn1-binding proteins were subjected to anti-GFP antibody mediated immunoprecipitation and the immunoprecipitates were investigated for the presence of Gcn1 and the respective GFP tagged proteins. In addition, the presence of Gcn2 and Gcn20 was also investigated, as Gcn1 is known to be in a complex with Gcn2 and Gcn20.

Before performing the co-immunoprecipitation experiments the experimental conditions for the anti-GFP antibody mediated immunoprecipitation needed to be optimized.

5.1 Optimization of anti-GFP antibody mediated co- immunoprecipitation

For optimizing the anti-GFP antibody mediated co-immunoprecipitation, the well-characterized protein-protein interactions of the GAAC pathway (i.e.) the interactions between Gcn1, Gcn2 and Gcn20 were used as a reference. Gcn1-Gcn2 interaction was used as a positive control for weak interactions, and Gcn1-Gcn20 interaction as a positive control for strong interactions. As done previously (Section 3.2.5) Pgk1 was used as a control for non-specific binding.

Our aim was to identify a condition where Gcn1, Gcn2 and Gcn20 can be immunoprecipitated but not Pgk1, from the cell extracts of strains expressing *GCN1*-GFP, *GCN2*-GFP or *GCN20*-GFP. Strains expressing *PGK1*-GFP and wild type (BY4741) were used as negative controls. It was expected that anti-GFP antibody mediated immunoprecipitation of Pgk1 from the strain expressing *PGK1*-GFP would only immunoprecipitate Pgk1 and it would not co-precipitate Gcn1, Gcn2 and Gcn20, as Pgk1 is not known to bind to any of these proteins. As the wild type (BY4741), does not express any GFP tagged proteins, the anti-GFP antibody was not expected to co-precipitate Gcn1, Gcn2 and Gcn20 from the cell extracts of the wild type. In addition, the immunoprecipitate from the wild type could indicate the level of non-specific binding of proteins to the Sepharose beads.

We were aware of the fact that GFP tagging may affect the function of proteins or their interactions with Gcn1, however, this approach was still considered worthwhile to verify the interaction of proteins with Gcn1. The functionality of the GFP tagged Gcn1, Gcn2 and Gcn20 have already been investigated (Ramesh and Sattlegger, unpublished) and except of Gcn2 the function of Gcn1 and Gcn20 were not affected by GFP tagging.

First the amount of anti-GFP antibody was determined that was necessary to coat the protein A Sepharose beads. In order to test this, varying amounts of anti-GFP antibody (0.05-1 µg, Santa Cruz) were incubated with equal amounts of protein A beads. Unbound antibodies were washed off and the bound antibodies were boiled off the beads in protein loading dye. Samples were then separated by SDS-PAGE and immunoblotted using antibodies against GFP.

As expected, the sample that contained only the Sepharose beads did not have any signal for GFP (Figure 5.1). A linear increase of GFP signal was detected with increasing amounts of antibodies from 0.05-1 µg. This suggested that increasing the amount of anti-GFP antibody resulted in increased binding of the antibody to protein A beads. The signal detected for 1 µg of antibody was very strong and the signal may not be saturated indicating that the concentration of the antibody could have been high.

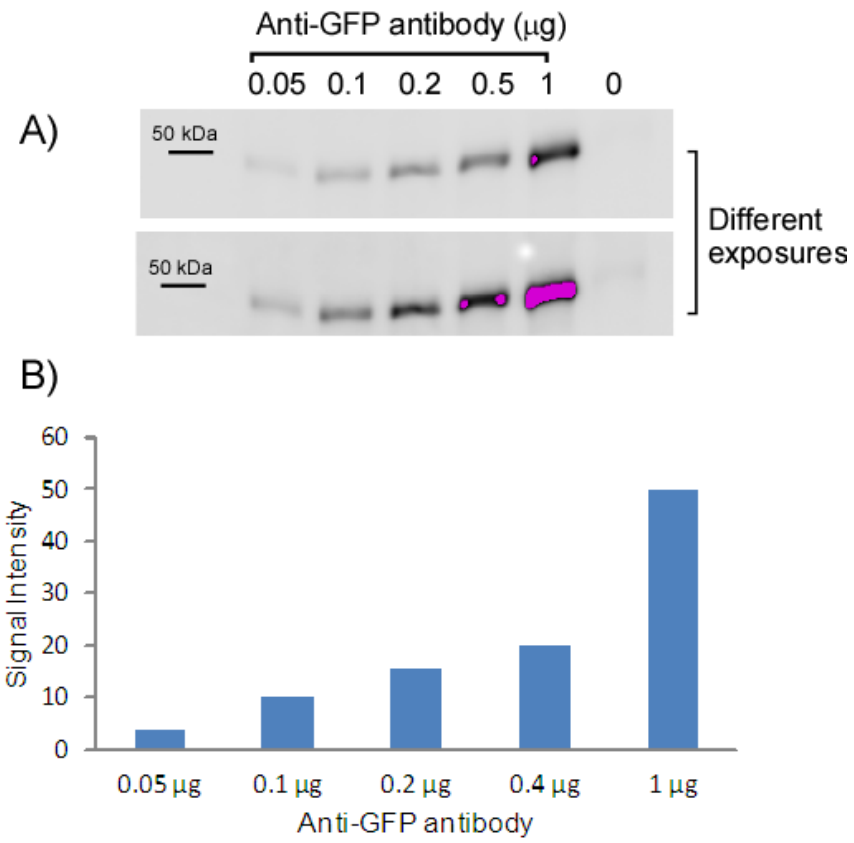

Figure 5.1. Determination of the anti-GFP antibodies required to coat the protein A Sepharose beads. A) Varying amounts of anti-GFP antibody (0.05-1 µg) was incubated with 20 µl of protein A Sepharose beads (100%) for 2 hours at 4°C. Unbound antibodies were washed off and the beads were boiled in protein loading dye. The denatured samples were separated by SDS-PAGE, followed by Western blotting with antibodies against GFP. B). The GFP signal was quantified using the Multi Gauge V3.1 software (Fujifilm).

Denaturation of antibodies would result in dissociation of the heavy chains (55 kDa) and light chains (25 kDa). As the gel was run for longer the light chains of the antibodies were run off the gel, so only the heavy chains of anti-GFP antibody was detected (Figure 5.1).

It was reasoned that a concentration of more than 0.5 µg of antibody may result in more background binding of proteins; therefore, it was decided to use 0.5 µg of the anti-GFP antibody for our anti-GFP antibody mediated immunoprecipitation.

Next it was investigated if the anti-GFP antibody was able to immunoprecipitate GFP tagged proteins from the cell extracts of strains that expressed GFP tagged proteins. 500 and 1000 µg of proteins from the strains that expressed *GCN1*-GFP, *GCN2-GFP*, *GCN20*-GFP or *PGK1*-GFP and wild type were subjected to anti-GFP antibody mediated immunoprecipitation with protein A beads coated with 0.5 µg of the anti-GFP antibody. The immunoprecipitates were resolved by SDS-PAGE and subjected to immunoblotting with antibodies against GFP, Gcn1, Gcn2 or Gcn20.

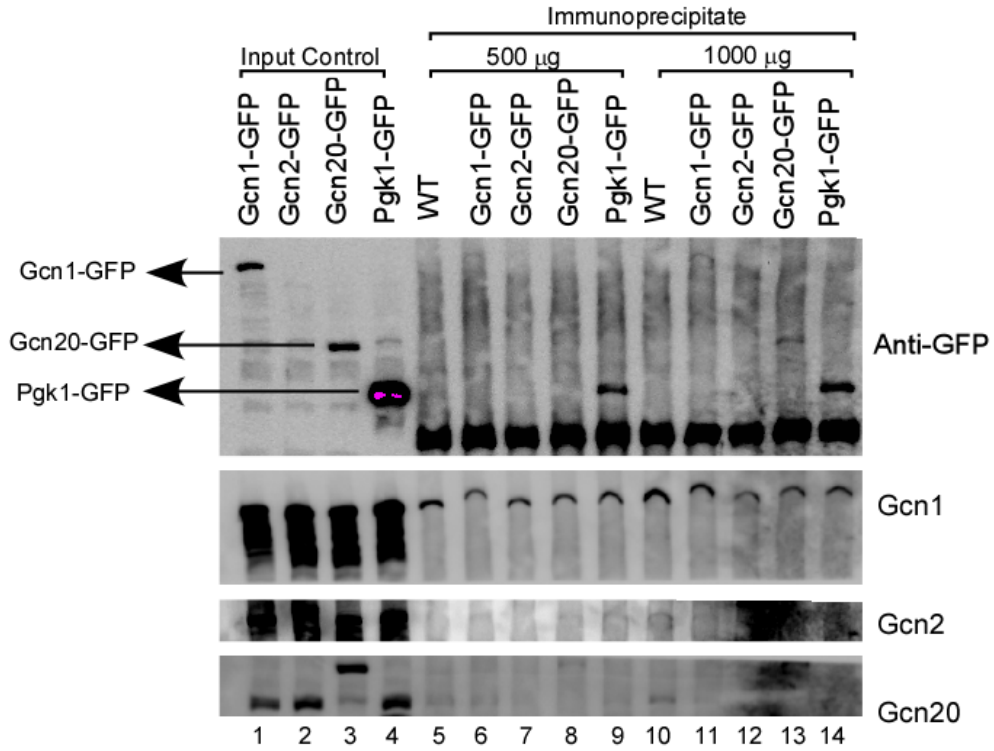

Figure 5.2. Anti-GFP antibody mediated immunoprecipitation. Indicated strains (refer to Table 2.2) were grown to exponential phase (A_{600} = 1.2-1.5) in minimal media with appropriate amino acids. 500 or 1000 µg of cell extracts were subjected to anti-GFP antibody mediated immunoprecipitation. The immunoprecipitates and 50 µg of input controls were resolved by SDS-PAGE and subjected to Western blotting with antibodies against GFP, Gcn1, Gcn2 or Gcn20.

As indicated in Figure 5.2, signals for GFP tagged Gcn1, Gcn20 and Pgk1 were detected in the input control and a signal for GFP tagged Gcn2 was not detected in the input control. This suggested that the GFP tagging may interfere with the expression of Gcn2.

In the immunoprecipitates from the 500 µg of cell extracts no signal was detected for GFP tagged Gcn1, Gcn2 and Gcn20. However a signal for GFP tagged Pgk1 was detected in the immunoprecipitate obtained from the 500 µg of cell extract of the Pgk1-GFP tagged strain. GFP tagged Gcn1, Gcn20 and Pgk1 were detected in the immunoprecipitates from the 1000 µg of cell extracts obtained from the strains that expressed *GCN1*-GFP, *GCN20*-GFP or *PGK1*-GFP. As one would expect this suggested that the increasing amount of cell extracts resulted in more amounts of the proteins to be immunoprecipitated. However a clear signal for Gcn2-GFP was not detected in the input control or in the immunoprecipitates obtained from both the 500 µg and 1000 µg of cell extracts, likely because insufficient amount of this protein was expressed.

Next the specificity of the anti-GFP immunoprecipitation was investigated by probing the membrane with antibodies against Gcn1, Gcn2 or Gcn20 (Figure 5.2). A clear signal for Gcn1 was detected in the Gcn1-GFP, Gcn2-GFP and Gcn20-GFP immunoprecipitates. However a signal for Gcn1 was also detected in the negative controls (Pgk1-GFP and wild type). Additionally, the signal intensity detected for Gcn1 in the negative controls was almost the same as detected in the Gcn1-GFP, Gcn2-GFP and Gcn20-GFP immunoprecipitates. This suggested that the immunoprecipitation was not specific to the Gcn1-Gcn2-Gcn20 complex. However a clear signal for Gcn2 and Gcn20 was not detected in the immunoprecipitates, suggesting that the amounts of these proteins co-precipitated was not sufficient to detect via Western blotting. In order to have adequate amount of proteins in the immunoprecipitates, to be able to detect via Western blotting, it was decided to use more amounts of cell extracts for the immunoprecipitation. The cell extracts' concentration was increased from 1 mg to 2 or 4 mg and subjected to anti-GFP antibody mediated immunoprecipitation

followed by Western blotting as outlined before (Figure 5.2).

In contrast to the last experiment a clear signal for Gcn2 and Gcn20 was detected in the immunoprecipitates (Figure 5.3, lanes 1-10). This suggested that increasing the amount of cell extracts improved the signal intensity detected for Gcn2 and Gcn20 in the immunoprecipitates (lanes 1-10). Signals for Gcn1, Gcn2 and Gcn20 were detected in Gcn1-GFP, Gcn2-GFP and Gcn20-GFP immunoprecipitates (lanes 1-3 and 6-8). Again signals for Gcn1 and Gcn2 were detected in the negative controls (Pgk1-GFP and WT). This suggested that the anti-GFP immunoprecipitation was not yet specific to the Gcn1-Gcn2-Gcn20 complex.

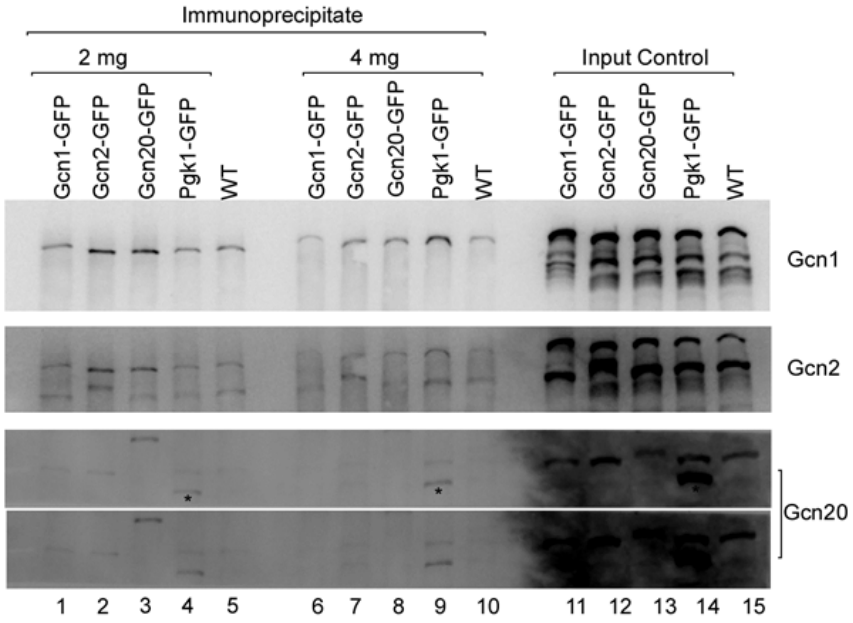

Figure 5.3. Anti-GFP antibody mediated immunoprecipitation. Indicated strains (refer to Table 2.2) were grown to exponential phase (A_{600} = 1.2-1.5) in minimal media with appropriate amino acids. Two different concentrations of cell extracts (2mg and 4mg) from the strains that were subjected to anti-GFP immunoprecipitation as mentioned in Figure 5.2. * Indicates the signal of Pgk1-GFP.

However, there was no significant difference in the signal intensity detected for Gcn1, Gcn2 and Gcn20 in the immunoprecipitates obtained from 2 mg or 4 mg of cell extracts suggesting that the GFP tagged proteins present in the

2 mg of cell extracts was enough to bind the entire GFP antibodies used.

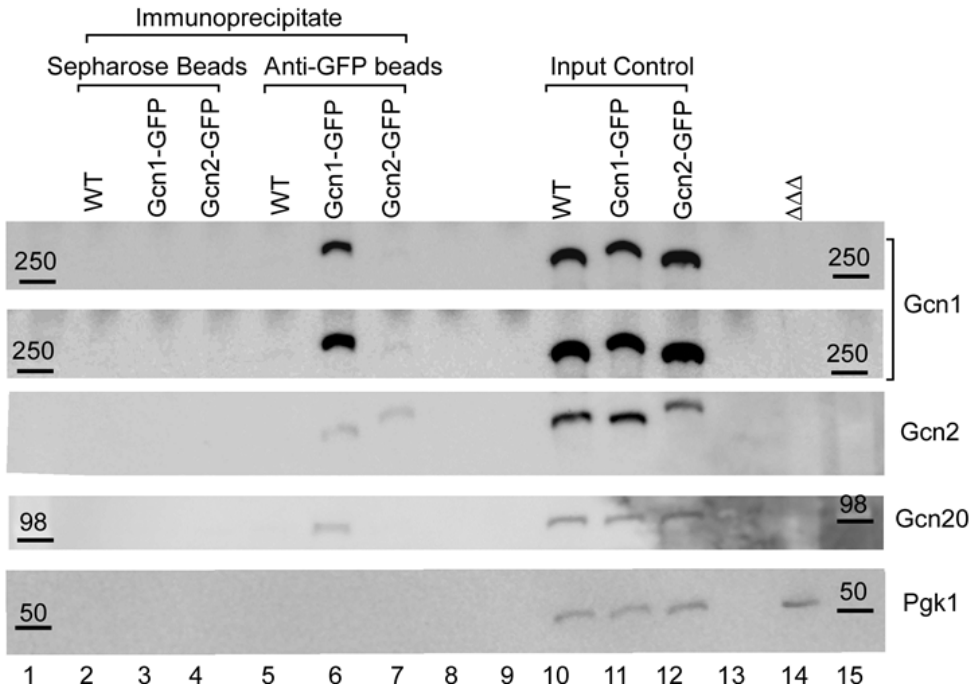

Figure 5.4. Anti-GFP antibody mediated immunoprecipitation with a commercially available anti-GFP antibody coated Sepharose. Indicated strains (refer to Table 2.2) were grown to exponential phase (A_{600} = 1.2-1.5) in minimal media with appropriate amino acids. 1 mg of cell extracts from the strain that expressed *GCN1*-GFP or *GCN2*-GFP and wild type were subjected to anti-GFP immunoprecipitation with 10 µl of (50%) anti-GFP coated Sepharose beads for 2 hours at 4°C and the immunoprecipitates were boiled in loading dye and resolved by SDS-PAGE. Cell extracts from a strain deleted for *GCN1*, *GCN2* and *GCN20* (ΔΔΔ) was loaded along with the immunoprecipitate as a negative control. The SDS-PAGE was subjected to Western blotting with antibodies against Gcn1, Gcn2, Gcn20 or Pgk1.

In the next trial a commercially available anti-GFP antibody coated Sepharose (Abcam) was used to immunoprecipitate the GFP tagged proteins. The immunoprecipitation was carried out with 1 mg of cell extracts and with the commercially available anti-GFP antibody coated Sepharose beads. In addition to the wild type control, Sepharose beads that were not conjugated with anti-GFP antibody were used as negative control.

Gcn1 was not detected in the negative controls (Figure 5.4, lanes 2-5) and a signal for Gcn1 was detected in the input control and in the Gcn1-GFP immunoprecipitate. Similarly to Gcn1, signals for Gcn2 and Gcn20 were not detected in the negative control (lanes 2-5) and detected in the Gcn1-GFP immunoprecipitate and in the input controls. Pgk1 was not detectable in any of the immunoprecipitates, indicating that the anti-GFP antibody mediated immunoprecipitation was specific to the Gcn1-Gcn2-Gcn20 complex.

However, only a faint signal for Gcn1, Gcn2 and no Gcn20 was detected in the Gcn2-GFP immunoprecipitate. The fact that the Gcn2-GFP immunoprecipitate had less Gcn1 and no Gcn20 supports the idea that the GFP tagging of Gcn2 interferes with Gcn2-Gcn1 binding. In accord with this idea, the strain expressing *GCN2*-GFP was unable to grow under starvation conditions (Ramesh and Sattlegger, unpublished).

5.2 Validation of the interactions between Gcn1 and Gcn2 binding proteins

As the conditions for specifically immunoprecipitating the GFP tagged proteins were optimized, the interactions of Gcn1 with Gcn1 binding proteins were validated with the optimised conditions. As there were several hundred Gcn1 binding proteins identified, it was not possible to test all of them. Therefore, only some of the potential Gcn1 binding proteins were chosen. It was reasoned that proteins identified in the unstabilized and formaldehyde stabilized Gcn1-Myc complexes would be interesting as these are more likely to be true interactions. Of the several proteins common to the unstabilized and formaldehyde stabilized Gcn1-Myc complexes Acc1, Fas1, Fas2, Ura2 and Kap123 were chosen. Proteins identified from the extended Gcn1 interactome whose removal from the cells resulted in impaired Gcn2-mediated eIF2α phosphorylation were also considered to be interesting: these are Kem1, Sin3, Vps1, Msn5 and Rnr1.

All experiments described below involve different strains that expressed the GFP tagged Gcn1 binding proteins mentioned above. In all the experiments described below the strains were grown to exponential phase (A_{600} = 1.2-1.5) in minimal media with appropriate amino acids. 1 mg of cell extracts was subjected

to anti-GFP antibody mediated immunoprecipitation as outlined in Figure 5.4. The immunoprecipitates were resolved by SDS-PAGE followed by Western blotting. The membrane was investigated for the presence of Gcn1, Gcn2, Gcn20 and the respective GFP tagged proteins.

An immunoprecipitation experiment was carried out to validate whether Kem1 interacts with Gcn1, and whether it also forms a complex with the Gcn1 binding partners Gcn2 and Gcn20. Cell extract obtained from the strain that expressed *KEM1*-GFP was subjected to anti-GFP antibody mediated immunoprecipitation along with the positive (*GCN20*-GFP) and negative (WT, *PGK1*-GFP) controls.

The membrane was first probed with anti-GFP antibody to check whether the antibody successfully immunoprecipitated the GFP tagged proteins.
Signals for GFP tagged Gcn20, Kem1 and Pgk1 were detected in the input controls and immunoprecipitates (Figure 5.5). This finding suggested that Gcn20, Kem1 and Pgk1 were immunoprecipitated from the cell extracts of strains that expressed *GCN20*-GFP, *KEM1*-GFP or *PGK1*-GFP respectively.

Next it was investigated whether Gcn20 and Kem1 co-purified Gcn1, Gcn2, and Gcn20. For this the membrane was probed consecutively with antibodies against Gcn1, Gcn2, Gcn20 and Pgk1. As expected, signals for Gcn1, Gcn2 and Gcn20 were detected in the Gcn20-GFP immunoprecipitate. This suggested that Gcn20 was able to co-precipitate Gcn1 and Gcn2, as expected (Figure 5.5). Additionally, signals for Gcn1, Gcn2 and Gcn20 were detected in the Kem1-GFP immunoprecipitate, indicating that similarly to Gcn20, Kem1 was able to co-precipitate Gcn1, Gcn2 and Gcn20.

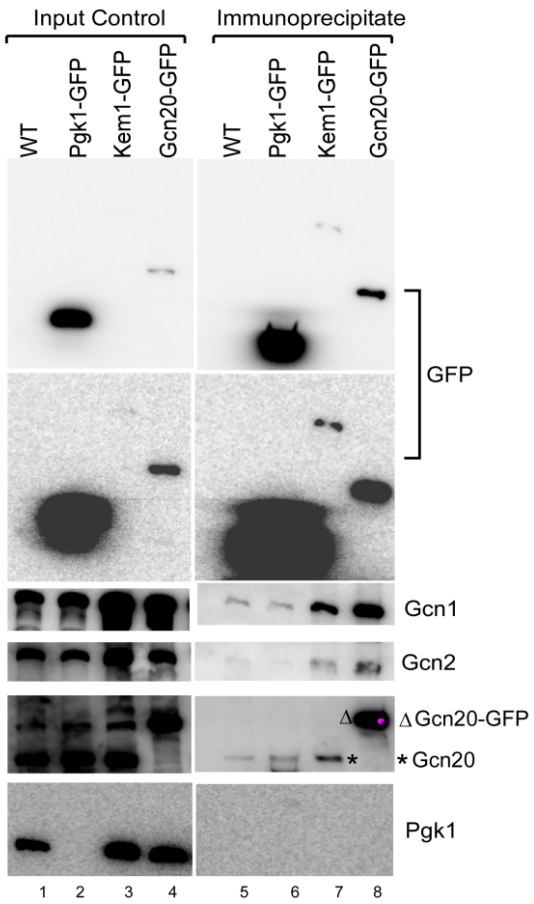

Figure 5.5. Anti-GFP antibody mediated immunoprecipitation of Gcn20-GFP, Kem1-GFP and Pgk1-GFP. Indicated strains (refer to Table 2.2) were grown to exponential phase (A_{600} = 1.2-1.5) in minimal media with appropriate amino acids. 1 mg of cell extracts from the indicated strains was subjected to anti-GFP immunoprecipitation and the immunoprecipitates were processed as outlined in figure 5.4. A signal for Pgk1 was not detectable in the input control and in the Pgk1-GFP immunoprecipitate. The membrane was probed with anti-GFP antibodies first and then probed with antibodies against Pgk1. Therefore, it is possible that the anti-Pgk1 antibodies were not able to bind to Pgk1 and that a signal for Pgk1 was not detected

However, weak signals for Gcn1, Gcn2 and Gcn20 were detected in the negative controls (lanes 5 and 6). The wild type did not have any GFP tagged proteins and signals for Gcn1, Gcn2 and Gcn20 were detected with the anti-GFP coated Sepharose beads incubated with the cell extract obtained from the wild type. This indicated that some amount of Gcn1, Gcn2 and Gcn20 were non-specifically bound to the resin used for immunoprecipitation. Though more amount of Pgk1 was immunoprecipitated from the strain that expressed *PGK*1-GFP, the signal

intensity of Gcn1, Gcn2 and Gcn20 appeared to be the same as that of the wild type (lanes 5 and 6). This indicated that these proteins were non-specifically bound to the resin regardless of what proteins were immunoprecipitated. However the signal intensity of Gcn1, Gcn2 and Gcn20 detected in the negative controls was much lower than that detected in the Kem1-GFP or Gcn20-GFP immunoprecipitates, indicating that Gcn1, Gcn2 and Gcn20 were specifically immunoprecipitated with Kem1 or Gcn20.

In another experiment the interactions of Acc1, Fas1, Fas2 and Ura2 with Gcn1 and their interactions with the Gcn1 binding partners Gcn2 and Gcn20 were tested.

Cell extracts obtained from the strains that expressed GFP tagged *ACC1*, *FAS1*, *FAS2* or *URA2* were subjected to anti-GFP antibody mediated immunoprecipitation along with the positive (*GCN1*-GFP, *GCN2*-GFP and *GCN20*-GFP) and negative (WT) controls.

It was reasoned that co-purified proteins will be less abundant than the proteins primarily immunoprecipitated, therefore the presence co-purified proteins (Gcn1, Gcn2 and Gcn20) was investigated first and then the presence of GFP tagged proteins was investigated.

A signal for Gcn1 was detected in the input controls and in the Gcn1-GFP, Gcn2-GFP, Gcn20-GFP, Fas1-GFP, Fas2-GFP, Acc1-GFP or Ura2-GFP immunoprecipitates (Fig 5.6). This indicated that Gcn1 was immunoprecipitated by Gcn1-GFP, Gcn2-GFP, Gcn20-GFP, Fas1-GFP, Fas2-GFP, Acc1-GFP or Ura2-GFP. The membrane was sequentially probed with antibodies against Gcn2, Gcn20 and Pgk1. Signals for Gcn2 and Gcn20 were detected in the input controls (lanes 1-8) and immunoprecipitates (lanes 9-15) indicating that Gcn2 and Gcn20 were also co-precipitated.

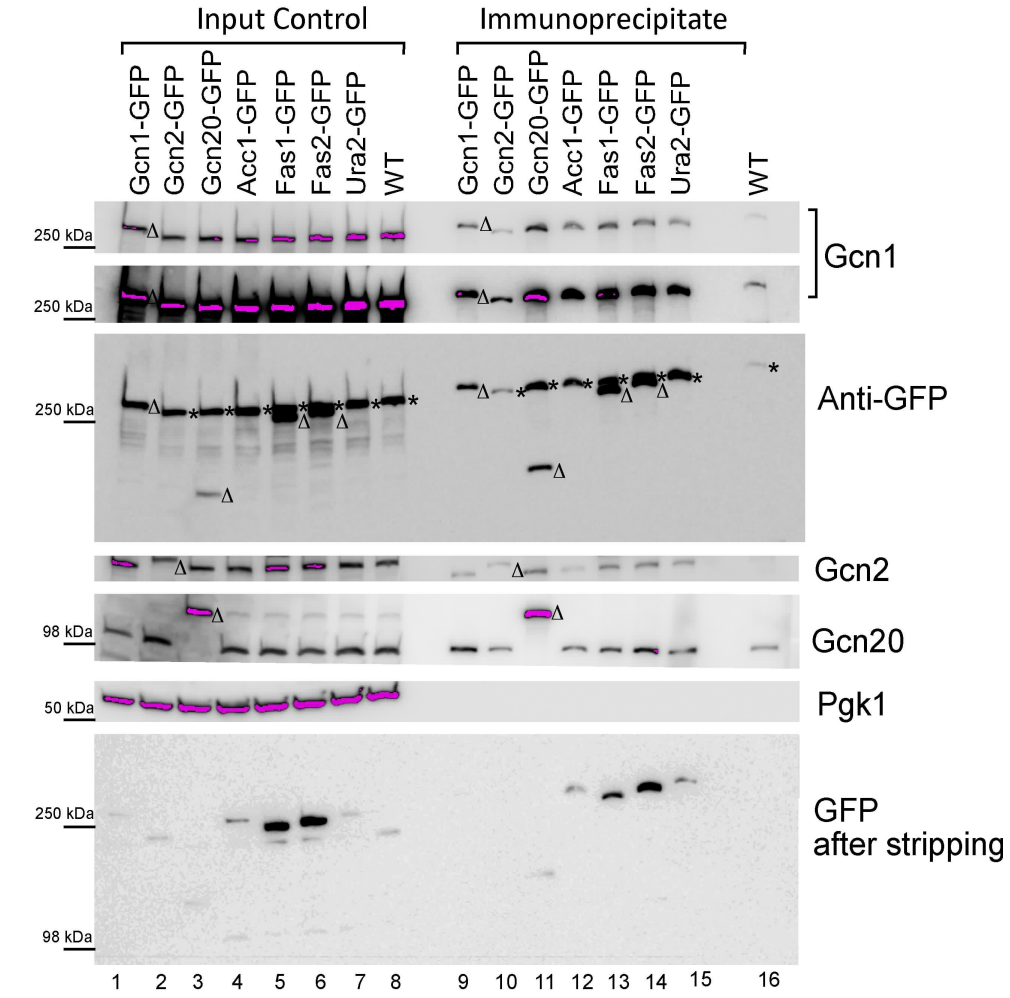

Figure 5.6. Anti-GFP immunoprecipitation of Gcn1-GFP, Gcn2-GFP, Gcn20-GFP, Acc1-GFP, Fas1-GFP, Fas2-GFP and Ura2-GFP. Indicated strains (refer to Table 2.2) were grown to exponential phase (A_{600} =1.2-1.5) in minimal media with appropriate amino acids. 1 mg of cell extracts from the indicated strains was subjected to anti-GFP immunoprecipitation and the immunoprecipitates were processed as outlined in Figure 5.4. * and Δ represent the location of the respective full length protein.

As shown earlier (Figure 5.4 and 5.5), Gcn1-GFP, Gcn2 and Gcn20 were co-immunoprecipitated with Gcn1-GFP (Figure 5.6, lane 9). Likewise Gcn1 and Gcn20 were co-immunoprecipitated with Gcn2-GFP. These findings indicated that all the positive controls have worked as expected. In contrast to the previous experiment (Fig 5.4), a clear signal for Gcn1 and Gcn20 were detected in the

immunoprecipitate of *GCN2-GFP*. However the amounts of Gcn1 and Gcn20 immunoprecipitated by Gcn2 were less than that of Gcn1-GFP. There was some amount of Gcn1, Gcn2 and Gcn20 detected in the negative control (lane 16) in addition to a very faint signal for Pgk1 in the Gcn1-GFP, Gcn2-GFP or Fas1-GFP immunoprecipitates, indicating the background binding of the proteins to Sepharose beads. However the signal intensities of Gcn1, Gcn2 and Gcn20 in the negative control were far lower than that of the other immunoprecipitates (compare lanes 9-15 to lane 16), suggesting that the co-immunoprecipitations were specific.

To investigate whether Gcn1, Gcn2 and Gcn20 were co-precipitated with Fas1, Fas2, Acc1 and Ura2 next the membrane was probed with anti-GFP antibody. GFP signals for Fas1-GFP, Fas2-GFP and Gcn20-GFP were detected, indicating that the proteins were detected in the immunoprecipitates and input controls just below the signal of Gcn1 (Figure 5.6).

The fact that Gcn1, Gcn2 and Gcn20 co-precipitated with Fas1 and Fas2 suggests that Fas1 and Fas2 are interacting with Gcn1 presumably in the Gcn1-Gcn2-Gcn20 complex.

However, it was not possible to conclude whether Acc1 and Ura2 were co-precipitated or not, as GFP signals for Acc1-GFP and Ura2-GFP were not detected (Figure 5.6, row 3). It is possible that these proteins were run exactly at the same place, where Gcn1 was on the membrane, as the molecular weights of Acc1 and Ura2 are close to that of Gcn1. It was reasoned that if Acc1 and Ura2 were exactly at the place where Gcn1 was on the membrane, then the anti-Gcn1 antibody could have hindered the binding of anti-GFP antibody to Acc1-GFP and Ura2-GFP. Therefore, the bound antibodies were stripped off the membrane and then the membrane was again probed with antibodies against GFP.

As expected, GFP signals for Acc1 and Ura2 were detected exactly at the size of Gcn1 (lanes 12 and 15), indicating that Acc1 and Ura2 were immunoprecipitated. In conclusion, the results of this experiment suggested that Acc1, Fas1, Fas2 and Ura2 interact with Gcn1 presumably in the Gcn1-Gcn2-Gcn20 complex.

However, signals for Gcn1-GFP and Gcn2-GFP were not detected, indicating that subjecting the membrane to stripping has reduced the strong signal detected for Gcn20-GFP and abolished the signal for Gcn1, possibly by removing the proteins from the membrane.

Another anti-GFP antibody mediated immunoprecipitation experiment was carried out with the cell extracts obtained from the strains that expressed *SIN3*-GFP, *MSN5*-GFP, *VPS1*-GFP, *RNR1*-GFP or *KAP123*-GFP along with the positive (*GCN20*-GFP) and negative controls (*PGK*1-GFP and wild type).

The membrane was probed sequentially with antibodies against Gcn1, Gcn2, Gcn20, Pgk1 and GFP.

Signals for Gcn1, Gcn2 and Gcn20 were detected in the input controls and in the Gcn20-GFP and Msn5-GFP immunoprecipitates and not detected in the Sin3-GFP, Vps1-GFP, Rnr1-GFP and Kap123-GFP immunoprecipitates (Figure 5.7).

Signals for Gcn1, Gcn2 and Gcn20 were not detected in the negative controls, suggesting that these proteins were not bound non-specifically to the anti-GFP antibody coated Sepharose used for immunoprecipitation.

Signals for GFP tagged Gcn20, Rnr1, Kap123 and Msn5 were detected in the immunoprecipitates (lanes 9, 12, 13 and 14) in addition to the input controls (lanes 1, 4, 5 and 6). This suggested that Rnr1, Kap123 and Msn5 were immunoprecipitated with the anti-GFP antibody. Signals for Pgk1 or Pgk1-GFP was detected in the input controls and in the Pgk1-GFP immunoprecipitate (lanes 1-8 and 15) and not detected in the other immunoprecipitates (lanes 9-14 and 16).

The fact that Pgk1 was only immunoprecipitated in the Pgk1-GFP immunoprecipitate and that it was not present in the other immunoprecipitates indicated that the immunoprecipitates were more likely free from non-specifically bound proteins. Signals for GFP tagged Sin3 and Vps1 were not detected either in the input controls or in the immunoprecipitates. This suggested that the GFP tagged Sin3 and Vps1 were not expressed and that these proteins were not immunoprecipitated with the anti-GFP antibody. It is possible that the GFP

tagging interferes with the expression of these proteins or the tag was not present or not expressed.

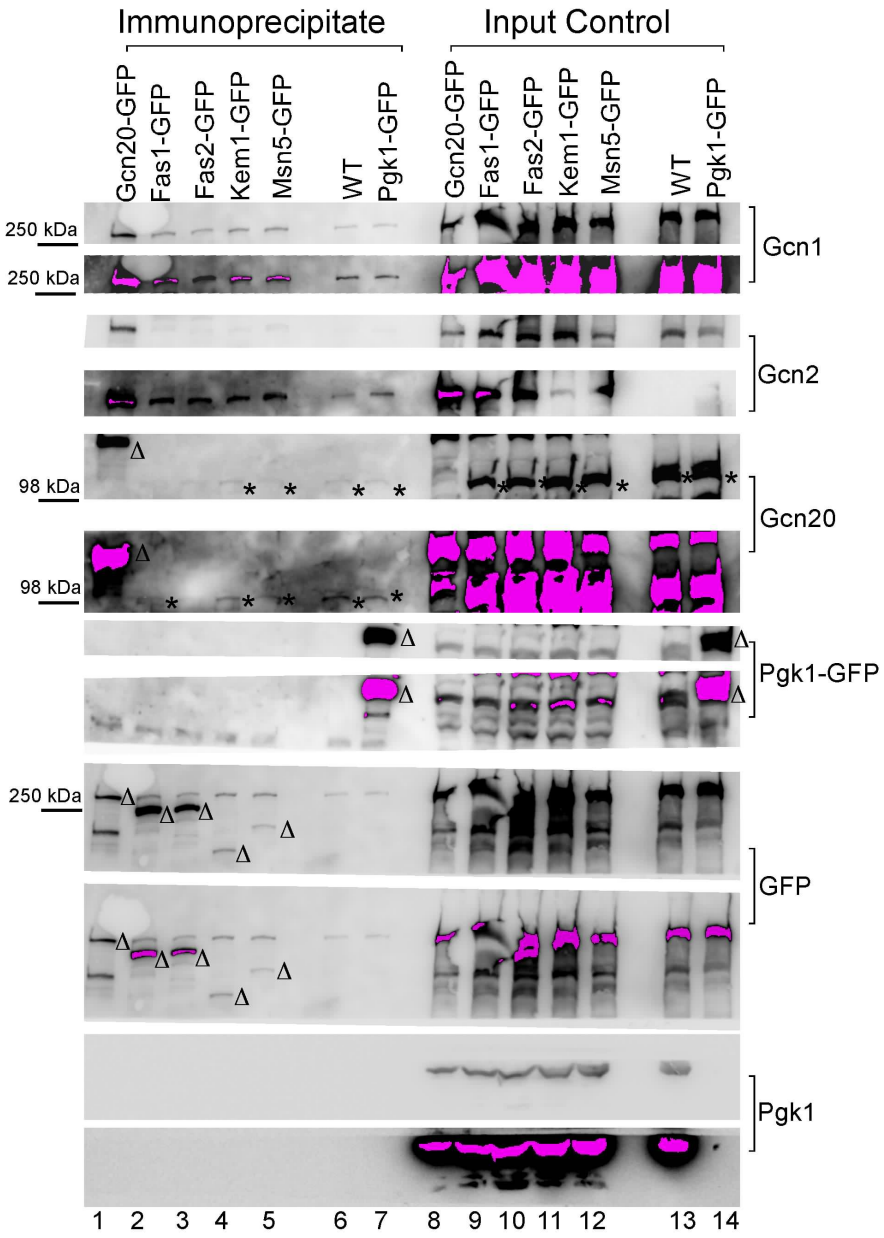

Figure 5.7. Anti-GFP immunoprecipitation of Gcn20-GFP, Sin3-GFP, Vps1-GFP, Rnr1-GFP, Kap123-GFP, Msn5-GFP and Pgk1-GFP. Indicated strains (refer to Table 2.2) were grown to exponential phase (A_{600} = 1.2-1.5) in minimal media with appropriate amino acids. 1 mg of cell extracts from the indicated strains was subjected to anti-GFP immunoprecipitation and the immunoprecipitates were processed as outlined in Figure 5.4. * and Δ represent the location of the respective full length protein.

Taken together, the Western blot results revealed that Gcn1, Gcn2 and Gcn20 were co-purified with Msn5-GFP but not with Rnr1-GFP or Kap123-GFP. The fact that Gcn1, Gcn2 and Gcn20 co-precipitated with Msn5 suggested that Msn5 interacts with Gcn1 presumably in the Gcn1-Gcn2-Gcn20 complex.

Since Msn5, Fas1, Fas2 and Kem1 resulted in co-immunoprecipitation of Gcn1, Gcn2 and Gcn20 in another independent experiment the reproducibility of Fas1, Fas2, Msn5 and Kem1 co-immunoprecipitating Gcn1, Gcn2 and Gcn20 were investigated. As the previous experiment (Figure 5.6) revealed that Fas1 and Fas2 ran very close to Gcn1 on the membrane, in this experiment a lower percentage SDS-PAGE (4-12%) was used to enable Fas1 and Fas2 to migrate below Gcn1.

As performed previously the membrane was probed sequentially with antibodies against Gcn1, Gcn2, Gcn20, Pgk1 and GFP. Signals for Gcn1 and Gcn2 were detected in the input controls and in the Gcn20-GFP, Fas1-GFP, Fas2-GFP, Kem1-GFP and Msn5-GFP immunoprecipitates (Figure 5.8). Signals for Gcn1 and Gcn2 were also detected in the negative controls. The signal intensities of Gcn1 and Gcn2 detected in the negative controls were much less than that of the Gcn20-GFP, Fas1-GFP, Fas2-GFP, Kem1-GFP and Msn5-GFP immunoprecipitates, indicating that the background binding of these proteins despite their specific interactions with Fas1, Fas2, Kem1 and Msn5.

Signals for Pgk1 or Pgk1-GFP were detected in the input controls and in the Pgk1-GFP immunoprecipitate. A signal for Pgk1 was not detected in the Gcn20-GFP, Fas1-GFP, Fas2-GFP, Kem1-GFP or Msn5-GFP immunoprecipitates, indicating that the immunoprecipitates did not contain any non-specifically bound proteins.

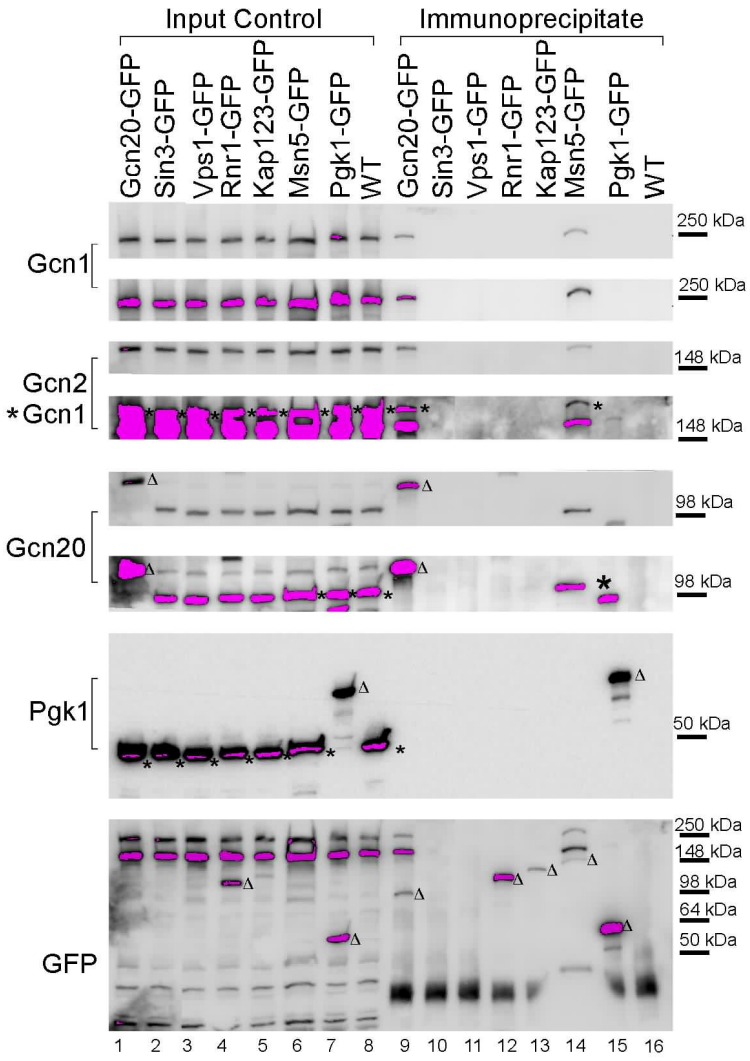

Figure 5.8. Anti-GFP immunoprecipitation of Gcn20-GFP, Fas1-GFP, Fas2-GFP, Kem1-GFP, Msn5-GFP and Pgk1-GFP. Indicated strains (refer to Table 2.2) were grown to exponential phase (A_{600} = 1.2-1.5) in minimal media with appropriate amino acids. 1 mg of cell extracts from the indicated strains was subjected to anti-GFP immunoprecipitation and the immunoprecipitates were processed as outlined in Figure 5.4. * and Δ indicate the location of the respective full length protein.

Unexpectedly, the signal intensity for Gcn20 detected in the Fas1-GFP, Fas2-GFP, Kem1-GFP and Msn5-GFP were similar or lower than that of the negative controls. This indicated that Gcn20 did not show an interaction with Fas1, Fas2, Kem1 or Msn5 in this experiment. It would be possible that Fas1, Fas2, Kem1 and Msn5 interact with Gcn1 that is not in complex with Gcn20.

5.3 Discussion

The aim was to verify the interactions of new Gcn1-binding proteins with Gcn1. It was reasoned that if the identified Gcn1 binding proteins are interacting with Gcn1 via stable interactions, then immunoprecipitation of the proteins would result in co-immunoprecipitation of Gcn1. Furthermore, the immunoprecipitation experiments would also reveal whether the Gcn1 binding proteins bind to Gcn1 alone or to Gcn1 in complex with Gcn2 and/or Gcn20.
Of the more than one hundred identified proteins a list of potential Gcn1 binding proteins was chosen to investigate whether immunoprecipitating the proteins results in co-immunoprecipitation of Gcn1. It was reasoned that proteins identified in the extended interactome and resulted in reduced Gcn2-mediated eIF2α phosphorylation (Kem1, Sin3, Vps1, Msn5 and Rnr1) would be more interesting. Furthermore, proteins identified consistently in the unstabilized Gcn1-Myc complex, formaldehyde stabilized Gcn1-Myc complex and extended Gcn1 interactome were still considered as interesting (Acc1, Fas1, Fas2, Kap123 and Ura2).

To investigate this, cell extracts obtained from the strains containing chromosomally GFP tagged genes encoding for the above mentioned proteins were subjected to anti-GFP antibody mediated immunoprecipitation. The immunoprecipitates were investigated for the presence of the proteins immunoprecipitated and the proteins co-immunoprecipitated (Gcn1, Gcn2 and Gcn20).
Our experimental results revealed that Kem1, Fas1, Fas2 or Msn5 interact with Gcn1. The interactions of these proteins with Gcn1 were found in two independent experiments. The fact that Gcn1 and Gcn2 were co-precipitated with Kem1, Fas1, Fas2 or Msn5 suggests that these proteins interact with Gcn1 which is complexed with Gcn2.

Although Gcn20 was co-precipitated specifically once with Kem1 (Figure 5.5), Fas1, Fas2 (Figure 5.6) or Msn5 (Figure 5.7), this scenario was not found in the

next experiment (Figure 5.8). This would indicate that the interactions of Gcn20 with Fas1, Fas2, Kem1 or Msn5 are weak or the experimental procedure was not able to preserve the interactions of Gcn20 with Fas1, Fas2, Kem1, and Msn5 and that Gcn20 was dissociated from the complex. Considering the fact that in the Gcn1-Gcn2-Gcn20 complex the interaction between Gcn1-Gcn20 is more stable than that of Gcn1-Gcn2, is not supporting the idea that Gcn20 was dissociated from the complex. The fact that Fas1, Fas2, Kem1 or Msn5 consistently co-precipitated with Gcn1-Gcn2 and not with Gcn20 indicates that the interactions of Fas1, Fas2, Kem1 or Msn5 with Gcn1-Gcn2 are stronger than their interactions with Gcn1-Gcn20.

It cannot be ruled out that different Gcn1 containing complexes were immunoprecipitated by Fas1, Fas2, Kem1 and Msn5 in these experiments (Fig 5.5, 5.6, 5.7 and 5.8) and different Gcn1 containing complexes contained different binding partners with some core interactions; such as Gcn1-Gcn2. In line with this idea, several Gcn1 containing complexes have been identified that contained Gcn2 but not Gcn20 (refer to Section 3.1.2).

It is also possible that the detected interactions of Gcn20 with Fas1, Fas2, kem1 or Msn5 were not true interactions. However, it needs to be investigated further whether Fas1, Fas2, Msn5 or Kem1 interact with Gcn1 in the Gcn1-Gcn2-Gcn20 complex or in a Gcn1-Gcn2 complex. Due to time constraints this was not done.

Though Rnr1 and Kap123 were identified to be in a complex with Gcn1 (refer to Figure 3.34) they did not show interactions with Gcn1 in the anti-GFP antibody mediated immunoprecipitation assay. It is possible that the GFP tag interferes with the binding of these proteins to Gcn1. It has been shown that the GFP tagging can alter the localization of proteins (*151*). Therefore, it would also be possible that the GFP tagging affects the localization of Kap123 and Rnr1, and that these proteins are mislocalized, thus not able to bind to their interacting partners. Additionally, the GFP tagging can also affect the functions of tagged proteins, resulting in the expression of non-functional proteins in the cell. It is sensible to tag the proteins with a different tag such as Myc, which is of small size

and carry out the immunoprecipitation experiments. However, further co-immunoprecipitation experiments are required to validate the interactions.

Chapter 6 Is Kem1 involved in Gcn1 mediated activation of Gcn2?

Having found that Kem1 may be required for promoting Gcn2 function, we wished to gain more understanding about the mechanism or relevance of Kem1 dependent Gcn2 activation.

First, we wanted to test whether Kem1 truly promotes Gcn1-mediated Gcn2 activation, or whether the Kem1 effect does not involve Gcn1. For this we took advantage of two different mutant forms of Gcn2 that render the protein constitutively active (Gcn2^{c}-E803V, abbreviated as Gcn2^{c}) and constitutively hyperactive (Gcn2^{c}-R794G-F842L, abbreviated as Gcn2^{Hyper}). The constitutively active mutant weakens association between the protein kinase and C-terminal regions which in turn enhances tRNA binding by Gcn2. Its constitutive activity is still dependent on Gcn1 (*152*), possibly because it requires binding of tRNAs to the His-RS domain adjacent to the kinase domain and Gcn1 delivers tRNAs to Gcn2.

In contrast to Gcn2^{c}, the Gcn2^{Hyper} bypasses the requirement of all regions flanking the protein kinase domain for kinase activity, and as expected, it is active even in the absence of Gcn1 or in the absence of tRNA binding (*66*). Constitutive Gcn2 hyperphosphorylate eIF2α, thereby leading to reduced protein synthesis even under replete conditions. This has a dramatic impact on the protein production rate, and therefore Gcn2^{c} results in a slow growth phenotype while Gcn2^{Hyper} stops growth almost completely. Thus, the growth defect is indicative of Gcn2 hyperactivity.

We reasoned that if Kem1 is involved in Gcn1 mediated activation of Gcn2, then in the *kem1*Δ strain Gcn1 would have an impaired or lost its ability to deliver tRNAs to Gcn2. This would mean that constitutive activation of Gcn2^{c} would be impaired or it cannot become constitutively active in a *kem1*Δ strain. In contrast, because Gcn2^{Hyper} does not require Gcn1 to become constitutively active, its activity would not be reduced or abolished in a *kem1*Δ strain. If Kem1 is functioning via some other mechanisms and not via that is mediated by Gcn1 then both Gcn2^{c} and Gcn2^{Hyper} would remain constitutively active in the *kem1*Δ strain.
To investigate this, we introduced plasmids carrying *GCN2^{c}* or *GCN2^{Hyper}* under a

galactose inducible promoter, or a vector alone, into strains lacking Gcn1 (*gcn1*Δ), Gcn2 (*gcn2*Δ), Gcn3 (*gcn3*Δ), Kem1 (*kem1*Δ) and wild type. The resulting transformants were subjected to a semi quantitative growth assay as outlined in Figure 4.1. As the mutant forms of *GCN2* were cloned under the galactose inducible promoter, expression of the proteins was achieved by growing them on a galactose containing plate. As control a plate containing glucose was used.

As expected on glucose containing plates the wild type, *gcn1*Δ, *gcn2*Δ, *gcn3*Δ and *kem1*Δ grew almost equally regardless of whether they carried vector alone, *GCN2*^{c} or *GCN2*^{Hyper} (Figure 6.1). However, on galactose containing plates the wild type over expressing Gcn2^{c} or Gcn2^{Hyper} grew slower than the one that carried vector alone, suggesting that Gcn2^{c} and Gcn2^{Hyper} are constitutively active. The *gcn1Δ* strain carrying vector alone or GCN2^{c} grew equally and the one carrying *GCN2*^{Hyper} showed a growth effect. This suggested that in the *gcn1Δ* strain Gcn2^{c} is not constitutively active as its activation is dependent on tRNA binding or Gcn1, whilst Gcn2^{Hyper} is still constitutively active as it does not require Gcn1 for activation. The *gcn2Δ* strain carrying vector alone grew well on galactose containing plates however the *gcn2Δ* strain over expressing Gcn2^{c} or Gcn2^{Hyper} showed an impaired growth, and the one over expressing Gcn2^{Hyper} exhibited a severe growth defect. These findings indicated that both the Gcn2^{c} and Gcn2^{Hyper} are constitutively active in the *gcn2Δ* strain

Gcn3 encodes for alpha subunit of translation initiation factor eIF2B. eIF2B consists of five subunits (α, β, λ, δ and ε) and is the guanine nucleotide exchange factor for eIF2 (*8*). Gcn3 mediates the inhibitory effect of eIF2α phosphorylation on translation initiation therefore in the absence of Gcn3 eIF2α-P does not lead to reduced protein synthesis (*153, 154*) and therefore, the constitutive active Gcn2^{c} or Gcn2^{Hyper} in the *gcn3Δ* strain will not lead to a growth defect and the same was found. These findings suggest that all the controls behaved as expected.

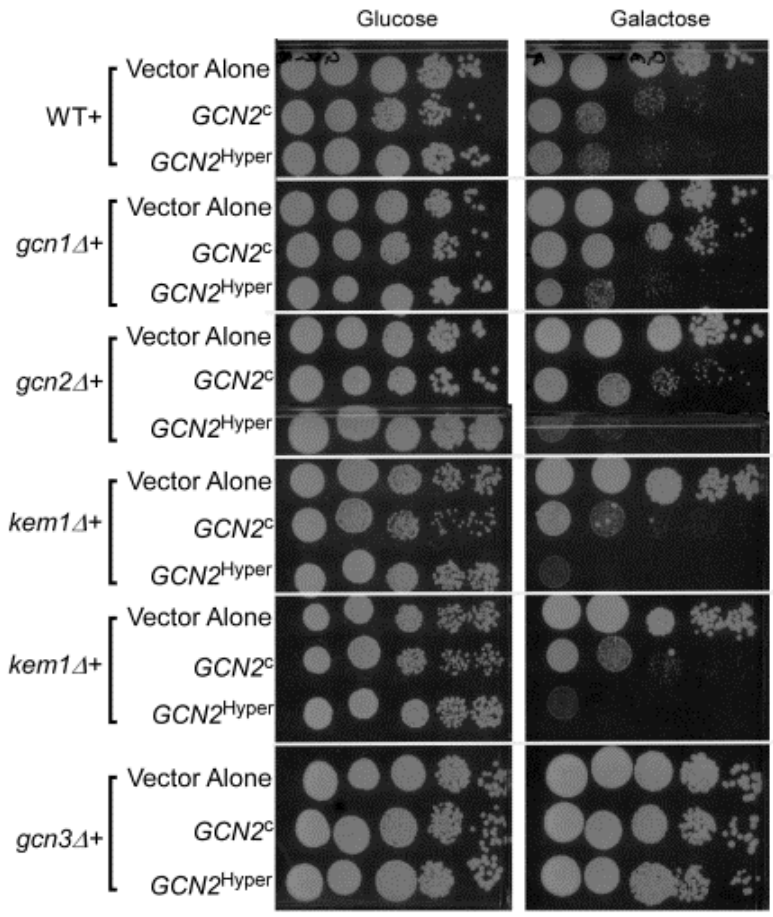

Figure 6.1. Semi quantitative growth assay. Comparison of growth rates of the wild type, *gcn1Δ, gcn2Δ, gcn3Δ* and *kem1Δ*strain each carrying vector alone,or plasmid borne $GCN2^{c}$ or $GCN2^{Hyper}$ under a galactose inducible promoter. Saturated cultures of the indicated strains were subjected to 10 fold serial dilutions and 5 µl of each dilution and 5 µl of undiluted culture were spotted on solid media containing glucose or galactose as a carbon source and incubated at 30°C. Growth was monitored every day for several days.

The *kem1*Δ strain that over expressed $GCN2^{c}$ or $GCN2^{Hyper}$ grew slower than the one carrying vector alone and the strain that over expressed $GCN2^{Hyper}$ grew worse than the one that over expressed $GCN2^{c}$. This suggests that the $Gcn2^{c}$ and $Gcn2^{Hyper}$ are constitutively active in the *kem1*Δ strain. However, in contrast to the wild type control, $Gcn2^{c}$ did not impair growth of a *kem1Δ* strain as severely as $Gcn2^{Hyper}$. In an alternative explanation, $Gcn2^{Hyper}$ is more active in the *kem1*Δ strain than in the wild type. In the *kem1*Δ strain the constitutive activation of $Gcn2^{Hyper}$ that does not require Gcn1 was not impaired. However, in the *kem1*Δ

strain the constitutive activation of Gcn2^{c} that is dependent on Gcn1 was impaired indicating that tRNA binding or transfer of tRNAs to Gcn2 was impaired.

Discussion

Having found that Kem1 may be required for promoting Gcn2 function, it was investigated whether Kem1 is required for Gcn1-mediated uncharged tRNA transfer to Gcn2.

It was predicted that if Kem1 is involved in Gcn1 mediated activation of Gcn2 then the constitutive activation of Gcn2^{c} which is dependent on Gcn1 would be impaired as compared to Gcn2^{Hyper} that does not require Gcn1.

The results revealed that the wild type that overexpressed *GCN2*^{c} or *GCN2*^{Hyper} grew equally, but slower than the ones that carried vector alone, indicating that constitutive and hyper active Gcn2 resulted in slow growth phenotype and that the constitutive activation of either Gcn2^{c} or Gcn2^{Hyper} was not affected in the wild type (Figure 6.1). As expected, these findings indicated that the starvation signal to Gcn2^{c} was not affected in the wild type.

Similar to the wild type the *kem1*Δ strain that overexpressed *GCN2*^{c} or *GCN2*^{Hyper} grew much slower than the ones that carried vector alone. This suggested that similar to the wild type *GCN2*^{c} and *GCN2*^{Hyper} were constitutively active in the *kem1*Δ strain. However, in contrast to the wild type the *kem1*Δ strain that overexpressed *GCN2*^{c} grew better than the ones that overexpressed *GCN2*^{Hyper} but still did not grow as well as the *gcn1*Δ strain. These findings indicated that the constitutive activation of Gcn2^{c} was impaired in the *kem1*Δ strain, at least in part. This suggests that Kem1 may be required at least in part for Gcn1 mediated delivery of uncharged tRNAs to Gcn2.

We cannot exclude the possibility that in a *kem1*Δ strain Gcn2^{Hyper} caused a clearly stronger growth defect than Gcn2^{c} in a *kem1*Δ strain, because of the lower abundance of Gcn2^{c} as compared to its abundance in the wild-type. This would

imply that Kem1 is required for the efficient expression of $Gcn2^c$, or for its stability. This could be tested by scoring for Gcn2 protein levels in Western blots.

Alternatively, there may be another mechanism that could have resulted in impaired growth of the *kem1*Δ strain that overexpressed $GCN2^c$ than the wild type that overexpressed $GCN2^c$. This mechanism is based on the fact that Kem1 is involved in maintaining the mRNA levels. The level of an mRNA is determined by its synthesis and degradation rate. mRNA degradation usually commences with a shortening of the 3' poly A tail (*155*) followed by removal of the 5' capping (de-capping) (*156*). The de-capped mRNAs are then degraded in 5'- 3' direction by the Kem1 exonuclease (*157*). Additionally, it has been demonstrated that Kem1 is required for buffering of transcript level and reduced levels of Kem1 leads to global mRNA stabilization (*158*). These stabilized mRNAs can be used to synthesise proteins which in turn would decrease the uncharged tRNA pool as these uncharged tRNAs can be charged and used to translate the stabilized mRNAs. Thus it is possible that in a *kem1*Δ strain the uncharged tRNA pool is decreased and therefore not much uncharged tRNAs around to bind to Gcn2. Therefore, in the *kem1*Δ strain the activation of $Gcn2^c$ that is dependent on tRNA binding was affected and the activation of $Gcn2^{Hyper}$ that does not require tRNA binding was not impaired. Arguing against this idea an interaction between Kem1 and Gcn1 was identified in this study.

Kem1 was reported to function in degradation of decapped mRNAs (*157*) and mRNAs with premature stop codon and thus prevents accumulation of potentially harmful truncated proteins (*159*). Kem1's function does not show a clear functional connection to the GAAC, making it not straight forward to establish a model of how Kem1 promotes Gcn2 activity. We cannot exclude the possibility that the effect of Kem1 on Gcn2 activity is indirect. Arguing against this scenario would be the fact that Kem1 physically interacts with Gcn1. It is possible that the Gcn2 activating function is an additional function of Kem1 that has not been discovered before.

Nevertheless, our results support the idea that Kem1 may be required for efficient Gcn1 function, and/or for efficient delivery of uncharged tRNAs to Gcn2. However, it needs to be investigated further whether Kem1 deletion truly impairs Gcn2 activation by impairing the Gcn1 mediated tRNAs delivery to Gcn2.

In order to shed more light on how Kem1 promotes Gcn2 function, it would be advisable to map which domain of Kem1 is required to promote the Gcn2 promoting function, or whether a specific characterized Kem1 function is also required to promote Gcn2 function. It would be important to test whether specific Kem1 functions can be dissected from the Gcn2 promoting function. Kem1 domains, their functions and Kem1 mutations have been generated and characterized. Studies suggest that deletion of Kem1 leads to loss of cell viability upon prolonged incubation in medium lacking nitrogen (*160*) and hypersensitivity to benomyl; a microtubule destabilizing agent. Overexpression of the region 1-255 of Kem1 alleviated the benomyl sensitivity caused by deletion of Kem1, indicating that this region of Kem1 is sufficient for its function (*161*).

Similar to *KEM1* deletion, strain lacking Gcn1 or Gcn2 has shown hypersensitivity to benomyl, indicating that Gcn1 and Kem1 may be involved in activating Gcn2 upon exposure to benomyl (*162*).

Conclusions

Under most stress conditions the cell regulates global protein synthesis in order to survive. This regulation involves slowing down the general protein synthesis, increasing the synthesis of stress response proteins which is mediated via a cascade of events in the GAAC signalling, one of which is the activation of Gcn2 which is dependent on Gcn1. As Gcn1 contains almost 20 HEAT repeats, and it has been proposed to function in protein-protein interactions, it was expected that Gcn1 binds to other proteins in addition to Gcn2 and Gcn20.

The scope of this thesis was to identify novel potential Gcn1 binding proteins that promote Gcn2 function.

In this study a comprehensive Gcn1 interactome was generated and the interactions of Gcn1 with a few Gcn1 binding proteins were investigated. As expected, Gcn1 is interacting with several proteins and this is in agreement with our hypothesis that Gcn1 is interacting with far more proteins than it was thought.

It was identified that Gcn1 is binding to proteins involved in a wide variety of functions in the cell. Proteins involved in cellular processes, including but not limited to amino acid biosynthesis, fatty acid biosynthesis, ergosterol biosynthesis and cytoskeleton, are binding to Gcn1.

In this study it was shown that the small ribosomal proteins (Rps0A, Rps1B, Rps3, Rps4A, Rps5, Rps6A, Rps14, Rps16A, Rps18A, Rps24A) and large ribosomal subunit proteins (Rpl1A, Rpl2A, Rpl3, Rpl4A, Rpl7A, Rpl8a, Rpl9A, Rpl10, Rpl11A, Rpl13, Rpl19A, Rpl20A and Rpl21A) and a protein of the ribosomal stalk (Rpp0) bind to Gcn1 or to Gcn1 binding proteins. Of the ribosomal proteins interacting with Gcn1, Rps18A and Rpl21A have been shown to have a role in Gcn2 activation under amino acid starvation conditions (Viviane unpublished data).

In this study it was shown that Fas1, Fas2, Kem1 and Msn5 interact with Gcn1 which is complexed with Gcn2.

Fas1 and Fas2 are α and β subunits of the fatty acid synthetase (FAS) complex that catalyses the synthesis of the fatty acid palmitate from acetyl coA, malonyl CoA and NADPH (*163*). It appears that feeding increases FAS expression (*164*). The intake of high carbohydrate diets following periods of fasting increases FAS mRNA levels and enzyme concentration (*165*). It has been demonstrated that depriving HepG2 cells of any essential amino acid dampens the induction of FAS expression normally associated with feeding (*166*). This suggests that FAS expression is regulated according to nutrition availability.

A potential co-ordinate regulation of amino acid and fatty acid biosynthesis during the starvation for essential amino acid was shown by Guo et al. (2007). They have reported that the phosphorylated state of eIF2α in the livers was significantly increased in wild-type mice consuming a leucine-deficient diet compared to mice fed a complete diet, whereas $Gcn2^{-/-}$ mice lacked this induction. Consistent with the changes in the eIF2 phosphorylation FAS enzyme activity was suppressed significantly by leucine deprivation in the livers of $Gcn2^{+/+}$ mice, but was increased in $Gcn2^{-/-}$mice (*44*).

Considering that the expression level of FAS is regulated by Gcn2 under feeding and amino acid starvation conditions it could not have been anticipated that Fas1 and Fas2 bind to Gcn1-Gcn2 complex. Yet we found that Fas1 and Fas2 interact with Gcn1 that is complexed with Gcn2. Fas1 and Fas2 are essential genes, therefore with the approach employed in our study to identify the proteins promoting Gcn2 function, we were unable to study the effect of these proteins on Gcn2 function.

Msn5 is a multi-functional protein, involved in catabolite repression, calcium signalling and cell proliferation (*167*). Msn5 is involved in the bidirectional movement of cargoes between the nucleus and the cytoplasm (*168*). Mutants lacking Msn5 show defects in the shuttling of tRNAs between the nucleus and the cytoplasm (*169*). Nuclear accumulation of $tRNA^{His}$ and $tRNA^{Tyr}$ was found in *msn5*Δ cells (*170*). Strains lacking Msn5 are sensitive to high temperatures, high

sodium, lithium and manganese concentrations and alkaline pH (*167*). Subcellular distribution of eEF1A between the nucleus and the cytoplasm is dependent on Msn5.(*170*). It is possible that in *msn5*Δ cells, either defect in tRNA transport or impaired distribution of eEF1A between the nucleus and the cytoplasm have resulted in impaired Gcn2 activity. Or Msn5 is involved directly in facilitating Gcn2 activation, by a mechanism that is not known yet.

This study provided the evidence for Kem1's function in delivering Gcn1-mediated tRNA delivery to Gcn2. However, there are still a few questions that remain unanswered; for example, how exactly the absence of Msn5 and Kem1 lead to impaired Gcn2 activation.

The results from this study are beginning to reveal novel Gcn1 binding proteins and their role in the general amino acid control pathway. As expected, Gcn1 interacting with several proteins suggests that a complex network exists between the GAAC and other signalling pathways.

Future directions

In this study, several Gcn1 binding proteins were identified, but their interactions with Gcn1 have not been verified for all of them. The interactions of Gcn1 binding proteins with Gcn1 can be investigated using the anti-GFP antibody mediated immunoprecipitation as performed in chapter 5.

Some of the ribosomal proteins co-precipitated with Gcn1 and several Gcn1 binding proteins identified in this study are essential for cell viability, therefore, with the approach used in this study we were unable to study their effect on Gcn2 function. The overexpression of these proteins is an alternative method to study their effect on Gcn2 function.

The SM^S and eIF2α –P screenings were not carried out for all the identified Gcn1 binding proteins. The SM^S and eIF2α –P screenings can be carried out for the rest of the Gcn1 binding proteins identified in this study.

Single gene complementation for *sin3*Δ, *rnr1*Δ, *vps1*Δ and *msn5*Δ strains needs to be carried out to confirm whether the observed SM^S phenotype and impaired Gcn2 mediated eIF2-P levels are due to removal of the genes from the cells.

Further experiments to map the binding site of Kem1 and Gcn1 need to be carried out. Homologues of Kem1 are found in higher eukaryotes (*171*). Homologs of Kem1 can be expressed in yeast to check whether the higher eukaryotic homologs can do the same function in yeast.

To understand the biological roles of these interactions, *in vivo* interaction assays using the Bimolecular Fluorescense Complementation (BiFC) technique can be carried out. This technique can provide the cellular localization of the interactions.

The Gcn1 interactome generated in this study is obtained from cells grown under replete conditions. Purification of Gcn1 containing complexes can be done from the cells subjected to amino acid starvation or other stresses where Gcn1/Gcn2 function is implicated. Comparison of the Gcn1 interactomes obtained under different stress conditions would shed some light on the interactions of Gcn1 that are necessary to overcome the stresses.

Getting the complete list of proteins promoting Gcn2 function is fundamental for understanding Gcn1 activation. As Gcn2 is involved in several key functions and implicated in several diseases, it is important to understand the mechanism of Gcn2 regulation. Understanding the molecular mechanism of Gcn2 regulation may lead to the identification of novel signalling pathways and novel drug targets for Gcn2 associated diseases.

Appendix

A.1 Verification of pRS1

The plasmid constructed for experiments in chapter 4 pRS1 was verified by restriction digestion. *Xho1* and *Xba1* sites were used as diagnostic sites to check for insertion of KEM1. Digestion of pRS1 with Xho1 and Xba1 released an insert of 6.5 kb as expected, (Figure A.1 lanes 4 and 8).

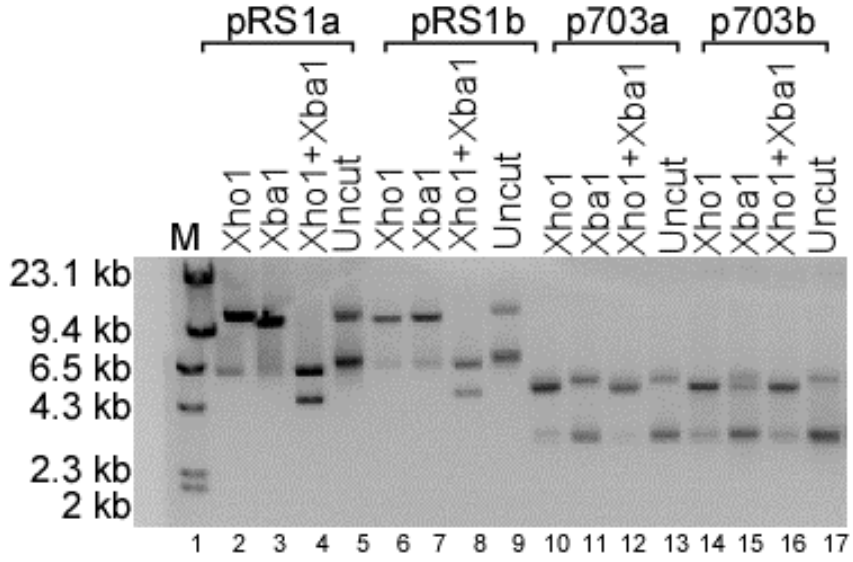

Figure A.0.1. Verification of pRS1 by restriction digestion.Plasmids pRS1 and p703 were digested with *Xho1* and *Xba1*. After digestion the samples were resolved on 0.75% agarose gel, stained with ethidium bromide and visualized in a transilluminator

Table A.1 Proteins removed from the LC-MS-MS raw purification list

Protein removed from the LC-MS-MS raw purification list
Proteins found only in negative control
SAH1
SSB1
LYS20
RPS19A
RPS25B
Proteins found below 2 times in the Gcn1-Myc sample than in the negative control
TIF1
SSA2
SER3
SSB2
ARG5,6
YEF3
EFT1
ENO2
ADH1
SHM2

PDC1
NPL3
UGP1
YEF3
CDC19
EFT1
ADE12
PIL1
YHB1
HSP104
SER3
OLA1
SSC1
DED1
ENO2
TDH2
GCS1
GVP36
SHM2
TRP5
ATP1
SSE1
NPL3
HSP60
CDC48
VMA1

Table A.2 Categorization of overrepresented proteins under the major GO localization identified by BiNGO analysis.

GO-ID	Description	Localization	corr p-val	p-val	cluster freq	total freq	genes
5840	Ribosome		9.15E-15	4.49E-17	28/90	31.1% 275/6198 4.4%	RPL20A RPS1B RPS3 RPL9A TEF4 TEF1 RPL17A RPL3 RPL7A GCN2 RPL21A RPL4A RPL2A RPS0A RPP0 RPS14A RPS5 GCN1 RPS6A TIF4631 TIF4632 RPL13A RPS4A TIF1 TIF3 RPS24A GCN20 RPS18A
22626	Cytosolic ribosome		1.08E-13	1.06E-15	22/90	24.4% 169/6198 2.7%	RPL21A RPL4A RPL20A RPL2A RPP0 RPS0A RPS14A GCN1 RPS5 RPS3 RPS1B RPS6A RPL9A RPL13A RPS4A RPL17A RPL3 RPL7A RPS24A GCN2 GCN20 RPS18A
30529	Ribonucleoprotein complex		5.61E-13	8.25E-15	35/90	38.8% 556/6198 8.9%	RPL20A PUB1 RPS3 RPS1B RPL9A TEF4 TEF1 RPL17A RPL3 RPL7A GCN2 RPL21A RPL4A RRP5 RPL2A RPS0A RPP0 RPS14A RPS5 GCN1 PRT1 RPS6A TIF4631 TIF4632 NOP1 NEW1 RPL13A RPS4A TIF1
							NOP58 TIF3 NOP56 RPS24A GCN20 RPS18A
44445	Cytosolic part		1.29E-12	2.52E-14	23/90	25.5% 219/6198 3.5%	RPL21A RPL4A RPL20A RPL2A RPP0 RPS0A PFK1 RPS14A CCT2 RPS5 RPS3 RPS1B RPS6A RPL9A FAS1 FAS2 RPL13A RPS4A RPL17A RPL3 RPL7A RPS24A RPS18A
32991	macromolecular complex		4.70E-11	1.15E-12	59/90	65.5% 1829/6198 29.5%	RVB2 CCT2 PUB1 RPS3 RVB1 COP1 RPL9A ATP1 ATP2 GCN2 SEC31 RPL21A RNR1 RPL4A RRP5 VPS1 RPS0A TUB2 KAP123 PRT1 FAS1 VMA2 FAS2 NOP1 VMA5 RPS4A ACT1 TIF1 TIF3 SSC1 VMA13
							SPT5 RPL20A PFK1 RPS1B TEF4 TEF1 RPL17A RPL3 RPL7A SEC26 SEC27 RPL2A RPP0 RPS14A RPS5 GCN1 RPS6A TIF4631 TIF4632 NEW1 RPL13A GUS1 NOP58 MET10 NOP56 RPS24A GCN20 RPS18A
43228	non membrane bounded organelle		1.37E-10	4.72E-12	44/90	48.8% 1078/6198 17.3%	RPL20A RVB2 RVB1 RPS3 RPS1B RPL9A ATP1 TEF4 TEF1 RPL17A RPL3 RPL7A GCN2 RPL21A RPL4A RPL2A RRP5 VPS1 RPP0 ACS2 HSP60 RPS0A RPS14A TUB2 GCN1 RPS5 KAP123 RPS6A TIF4631
							TIF4632 NOP1 NEW1 RPL13A SAC6 RPS4A ACT1 TIF1 NOP58 TIF3 NOP56 RPS24A GCN20 RPS18A SSC1
43232	intracellular non membrane bound organelle		1.37E-10	4.72E-12	44/90	48.8% 1078/6198 17.3%	RPL20A RVB2 RVB1 RPS3 RPS1B RPL9A ATP1 TEF4 TEF1 RPL17A RPL3 RPL7A GCN2 RPL21A RPL4A RPL2A RRP5 VPS1 RPP0 ACS2 HSP60 RPS0A RPS14A TUB2 GCN1 RPS5 KAP123 RPS6A TIF4631 TIF4632
							NOP1 NEW1 RPL13A SAC6 RPS4A ACT1 TIF1 NOP58 TIF3 NOP56 RPS24A GCN20 RPS18A SSC1
44444	Cytosolic part		9.29E-10	3.64E-11	72/90	80.0% 2864/6198 46.2%	ERG6 CCT2 PUB1 RTN1 RPS3 ERG1 COP1 RPL9A TDH3 ATP1 ATP2 LYS12 GCN2 CYS4 SEC31 RPL21A RNR1 RPL4A VPS1 ACS2 HSP60 RPS0A TUB2 PRT1 VMA2 FAS1 VMA5 FAS2 LYS21 RPS4A HSC82 ACT1
							TIF1 TIF3 SSC1 VMA13 SPT5 RPL20A PFK1 RPS1B ERG11 TEF4 TEF1 RPL17A PMA1 FBA1 RPL3 RPL7A SEC26 SEC27 ACC1 RPL2A RPP0 RPS14A SSA2 GCN1 RPS5 RPS6A TIF4631 TIF4632 SEC18 NEW1 RPL13A
							GUS1 SAC6 URA2 GND1 URA3 RPS24A GCN20 RPS18A SEC14
33279	ribosomal subunit		1.32E-08	5.84E-10	19/90	21.1% 234/6198 3.7%	RPL21A RPL4A RPL20A RPL2A RPS0A RPP0 RPS14A RPS5 RPS3 RPS1B RPS6A RPL9A RPL13A RPS4A RPL17A RPL3 RPL7A RPS24A RPS18A
30686	90 S preribosome		3.54E-08	1.74E-09	12/90	13.3% 83/6198 1.3%	RPS6A NOP1 RPS4A RRP5 NOP58 RPP0 RPS0A RPS14A NOP56 RPS5 RPS1B RPS3
5829	cytosol		1.44E-07	7.74E-09	30/90	33.3% 674/6198 10.8%	RPL20A PFK1 CCT2 RPS1B RPS3 RPL9A RPL17A FBA1 RPL3 RPL7A RPL21A RPL4A RPL2A ACS2 RPS0A RPP0 RPS14A RPS5 GCN1 SSA2 RPS6A FAS1 FAS2 RPL13A RPS4A URA3 RPS24A GCN20 RPS18A SEC14
5737	cytoplasm		1.41E-06	8.31E-08	81/90	90.0% 4073/6198 65.7%	ERG6 CCT2 PUB1 RTN1 RPS3 ERG1 COP1 RPL9A TDH3 ATP1 ATP2 LYS12 SGT2 ADE3 GCN2 CYS4 SEC31 RPL21A RNR1 RPL4A VPS1 ACS2 HSP60 OLA1 RPS0A TUB2 KAP123 PRT1 VMA2 FAS1 VMA5 FAS2 LYS21
							RPS4A YHR020W HSC82 ACT1 TIF1 UGP1 TIF3 SSC1 VMA13 SPT5 RPL20A PFK1 RPS1B ERG11 TEF4 TEF1 PMA1 RPL17A RPL3 FBA1 RPL7A SEC26 RBG2 SEC27 ACC1 RPL2A RPP0 RPS14A SSA2 GCN1 HSP82 RPS5
							GCN20 RPS18A SEC14 DED1 RPS6A TIF4631 TIF4632 SEC18 NEW1 RPL13A GUS1 SAC6 URA2 GND1 URA3 RPS24A
22627	cytosolic small ribosomal subunit		4.30E-06	2.74E-07	9/90	10.0% 64/6198 1.0%	RPS6A RPS4A RPS0A RPS14A RPS24A RPS18A RPS5 RPS1B RPS3
30684	preribosome		5.56E-06	3.81E-07	12/90	13.3% 133/6198 2.1%	RPS6A NOP1 RPS4A RRP5 NOP58 RPP0 RPS0A RPS14A NOP56 RPS5 RPS1B RPS3
44424	intracellular part		6.16E-06	4.53E-07	89/90	98.8% 5103/6198 82.3%	ERG6 RVB2 CCT2 PUB1 RTN1 RPS3 ERG1 RVB1 COP1 RPL9A TDH3 ATP1 ATP2 LYS12 SGT2 ADE3 GCN2 CYS4 SEC31 RPL21A RNR1 RPL4A RRP5 VPS1 RPS0A OLA1 HSP60 ACS2 TUB2 KAP123 PRT1 VMA2 FAS1
							VMA5 NOP1 FAS2 LYS21 RPS4A YHR020W HSC82 ACT1 TIF1 UGP1 TIF3 SSC1 VMA13 SPT5 RPL20A PFK1 RPS1B ERG11 TEF4 TEF1 PMA1 RPL17A RPL3 FBA1 RPL7A SEC26 RBG2 SEC27 ACC1 RPL2A BMH1 RPP0
							RPS14A SSA2 GCN1 HSP82 RPS5 DED1 RPS6A TIF4631 TIF4632 SEC18 NEW1 RPL13A GUS1 SAC6 NOP58 URA2 GND1 MET10 NOP56 URA3 RPS24A GCN20 RPS18A SEC14
5622	intracellular		9.07E-06	7.34E-07	89/90	98.8% 5132/6198 82.8%	ERG6 RVB2 CCT2 PUB1 RTN1 RPS3 ERG1 RVB1 COP1 RPL9A TDH3 ATP1 ATP2 LYS12 SGT2 ADE3 GCN2 CYS4 SEC31 RPL21A RNR1 RPL4A RRP5 VPS1 RPS0A OLA1 HSP60 ACS2 TUB2 KAP123 PRT1 VMA2 FAS1
							VMA5 NOP1 FAS2 LYS21 RPS4A YHR020W HSC82 ACT1 TIF1 UGP1 TIF3 SSC1 VMA13 SPT5 RPL20A PFK1 RPS1B ERG11 TEF4 TEF1 PMA1 RPL17A RPL3 FBA1 RPL7A SEC26 RBG2 SEC27 ACC1
							RPL2A BMH1 RPP0 RPS14A SSA2 GCN1 HSP82 RPS5 DED1 RPS6A TIF4631 TIF4632 SEC18 NEW1 RPL13A GUS1 SAC6 NOP58 URA2 GND1 MET10 NOP56 URA3 RPS24A GCN20 RPS18A SEC14
22625	cytosolic large ribosomal subunit		9.07E-06	7.56E-07	10/90	11.1% 93/6198 1.5%	RPL21A RPL9A RPL13A RPL4A RPL20A RPL2A RPL17A RPL3 RPP0 RPL7A
33178	proton transporting two sector ATPase comple		1.75E-05	1.55E-06	5/90	5.5% 15/6198 0.2%	VMA2 VMA5 ATP1 ATP2 VMA13
15935	small ribosomal subunit		1.03E-04	9.61E-06	9/90	10.0% 97/6198 1.5%	RPS6A RPS4A RPS0A RPS14A RPS24A RPS18A RPS5 RPS1B RPS3
15934	large ribosomal subunit		2.59E-04	2.54E-05	10/90	11.1% 137/6198 2.2%	RPL21A RPL9A RPL13A RPL4A RPL20A RPL2A RPL17A RPL3 RPP0 RPL7A
16281	eukaryotic translation initiation factor 4F comp		2.69E-04	2.90E-05	3/90	3.3% 5/6198 0.0%	TIF4631 TIF4632 TIF1
31428	box C/D snoRP		2.69E-04	2.90E-05	3/90	3.3% 5/6198 0.0%	NOP1 NOP58 NOP56
43229	intracellular organelle		3.00E-04	3.53E-05	77/90	85.5% 4127/6198 66.5%	ERG6 RVB2 PUB1 RTN1 RPS3 ERG1 RVB1 COP1 RPL9A TDH3 ATP1 ATP2 LYS12 ADE3 GCN2 CYS4 SEC31 RPL21A RPL4A RRP5 VPS1 ACS2 HSP60 RPS0A TUB2 KAP123 VMA2 FAS1 VMA5 NOP1 FAS2 LYS21 RPS4A
							HSC82 ACT1 TIF1 TIF3 SSC1 VMA13 SPT5 RPL20A PFK1 RPS1B ERG11 TEF4 TEF1 RPL17A PMA1 RPL3 FBA1 RPL7A SEC26 SEC27 ACC1 RPL2A BMH1 RPP0 RPS14A SSA2
							GCN1 RPS5 RPS6A TIF4631 TIF4632 SEC18 NEW1 RPL13A GUS1 SAC6 NOP58 URA2 GND1 NOP56 RPS24A GCN20 RPS18A SEC14
43226	organelle		3.00E-04	3.53E-05	77/90	85.5% 4127/6198 66.5%	ERG6 RVB2 PUB1 RTN1 RPS3 ERG1 RVB1 COP1 RPL9A TDH3 ATP1 ATP2 LYS12 ADE3 GCN2 CYS4 SEC31 RPL21A RPL4A RRP5 VPS1 ACS2 HSP60 RPS0A TUB2 KAP123 VMA2 FAS1 VMA5 NOP1 FAS2 LYS21 RPS4A
							HSC82 ACT1 TIF1 TIF3 SSC1 VMA13 SPT5 RPL20A PFK1 RPS1B ERG11 TEF4 TEF1 RPL17A PMA1 RPL3 FBA1 RPL7A SEC26 SEC27 ACC1 RPL2
							BMH1 RPP0 RPS14A SSA2 GCN1 RPS5 RPS6A TIF4631 TIF4632 SEC18 NEW1 RPL13A GUS1 SAC6 NOP58 URA2 GND1 NOP56 RPS24A GCN20 RPS18A SEC14
32040	small subunit processome		3.80E-04	4.66E-05	6/90	6.6% 46/6198 0.7%	RPS6A NOP1 RRP5 NOP58 RPS14A NOP56
10494	stress granule		1.07E-03	1.36E-04	4/90	4.4% 19/6198 0.3%	TIF4631 TIF4632 PUB1 PRT1
16469	proton transporting two-sector ATPase complex		1.15E-03	1.53E-04	5/90	5.5% 36/6198 0.5%	VMA2 VMA5 ATP1 ATP2 VMA13
30126	COPI vesicle coat		1.15E-03	1.57E-04	3/90	3.3% 8/6198 0.1%	COP1 SEC26 SEC27
44464	cell part		1.29E-03	1.89E-04	90/90	100.0 5639/6198 90.9%	ERG6 RVB2 CCT2 PUB1 RTN1 RPS3 ERG1 RVB1 COP1 RPL9A TDH3 ATP1 ATP2 LYS12 SGT2 ADE3 GCN2 CYS4 SEC31 RPL21A RNR1 RPL4A RRP5 VPS1 RPS0A OLA1 HSP60 ACS2 TUB2 KAP123 PRT1 VMA2 FAS1 VM
							NOP1 FAS2 LYS21 RPS4A YHR020W HSC82 ACT1 TIF1 UGP1 TIF3 SSC1 VMA13 SPT5 RPL20A PFK1 RPS1B ERG11 TEF4 TEF1 PMA1 RPL17A RPL3 FBA1 RPL7A SEC26 RBG2 SEC27 MCK1 ACC1 RPL2A BMH1 RPP0
							SSA2 GCN1 HSP82 RPS5 DED1 RPS6A TIF4631 TIF4632 SEC18 NEW1 RPL13A GUS1 SAC6 NOP58 URA2 GND1 MET10 NOP56 URA3 RPS24A GCN20 RPS18A SEC14
5623	cell		1.29E-03	1.93E-04	90/90	100.0 5640/6198 90.9%	ERG6 RVB2 CCT2 PUB1 RTN1 RPS3 ERG1 RVB1 COP1 RPL9A TDH3 ATP1 ATP2 LYS12 SGT2 ADE3 GCN2 CYS4 SEC31 RPL21A RNR1 RPL4A RRP5 VPS1 RPS0A OLA1 HSP60 ACS2 TUB2 KAP123 PRT1 VMA2 FAS1 VM
							FAS2 LYS21 RPS4A YHR020W HSC82 ACT1 TIF1 UGP1 TIF3 SSC1 VMA13 SPT5 RPL20A PFK1 RPS1B ERG11 TEF4 TEF1 PMA1 RPL17A RPL3 FBA1 RPL7A SEC26 RBG2 SEC27 MCK1
							ACC1 RPL2A BMH1 RPP0 RPS14A SSA2 GCN1 HSP82 RPS5 DED1 RPS6A TIF4631 TIF4632 SEC18 NEW1 RPL13A GUS1 SAC6 NOP58 URA2 GND1 MET10 NOP56 URA3 RPS24A GCN20 RPS18A SEC14
45267	proton transport ATP synthase, catalytic core		1.29E-03	2.09E-04	2/90	2.2% 2/6198 0.0%	ATP1 ATP2
5754	mitochondrial proton-transporting V-type ATPa		1.29E-03	2.09E-04	2/90	2.2% 2/6198 0.0%	ATP1 ATP2
5835	COPI coated vesicle membrane		1.29E-03	2.09E-04	2/90	2.2% 2/6198 0.0%	FAS1 FAS2
33180	fatty acid synthase complex		1.36E-03	2.34E-04	3/90	3.3% 9/6198 0.1%	VMA2 VMA5 VMA13
221	vacuolar proton transporting V-type, V1 domain		1.36E-03	2.34E-04	3/90	3.3% 9/6198 0.1%	VMA2 VMA5 VMA13
1950	plasma membrane enriched fraction		1.60E-03	2.82E-04	7/90	7.7% 89/6198 1.4%	TDH3 HSC82 PMA1 BMH1 UGP1 SSA2 HSP82
5739	mitochondrion		2.03E-03	3.67E-04	30/90	33.3% 1125/6198 18.1%	ERG6 SPT5 PFK1 RTN1 ATP1 TDH3 ATP2 LYS12 TEF4 TEF1 PMA1 FBA1 CYS4 ACC1 VPS1 HSP60 GCN1 SSA2 FAS1 TIF4631 FAS2 LYS21 NEW1 GUS1 HSC82 URA2 GND1 RPS24A RPS18A SSC1
30663	proton transportin ATP synthase complex, cata		2.41E-03	4.49E-04	3/90	3.3% 11/6198 0.1%	COP1 SEC26 SEC27
30137	COPI coated vesicle		3.02E-03	5.93E-04	3/90	3.3% 12/6198 0.1%	COP1 SEC26 SEC27
31011	Ino80 complex		3.02E-03	5.93E-04	3/90	3.3% 12/6198 0.1%	ACT1 RVB2 RVB1
267	cell fraction		3.70E-03	7.44E-04	11/90	12.2% 244/6198 3.9%	MCK1 TDH3 HSC82 PMA1 BMH1 VPS1 UGP1 URA3 SSA2 HSP82 ERG1
33202	DNA helicase complex		3.70E-03	7.62E-04	3/90	3.3% 13/6198 0.2%	ACT1 RVB2 RVB1
812	Swr1 complex		4.49E-03	9.60E-04	3/90	3.3% 14/6198 0.2%	ACT1 RVB2 RVB1
30120	vesicle coat		4.49E-03	9.69E-04	4/90	4.4% 31/6198 0.5%	SEC31 COP1 SEC26 SEC27

Table A.3 Categorization of overrepresented proteins under the major GO processes identified by BiNGO analysis

GO-ID	Biological processes	corr p-val	p-val	cluster freq	total freq	genes
10606	post transcriptional regulation of transcription	1.92E-25	1.45E-22	32/90	35.5%	206/6207 3. RPL20A PFK1 PUB1 RPS1B TEF4 TEF1 RPL17A FBA1 RPL3 RPL7A ADE3 GCN2 RPL4A RPL2A HSP60 OLA1 RPS0A KAP123 RPS5 GCN1 PRT1 FAS1 TIF4631 TIF4632 NEW1 RPL13A GUS1 RPS4A TIF1 URA2 RPS24A GCN20
6417	regulation of translation	3.80E-25	1.45E-22	31/90	34.4%	192/6207 3. RPL20A PFK1 PUB1 RPS1B TEF4 TEF1 RPL17A FBA1 RPL3 RPL7A ADE3 GCN2 RPL4A RPL2A OLA1 RPS0A KAP123 RPS5 GCN1 PRT1 FAS1 TIF4631 TIF4632 NEW1 RPL13A GUS1 RPS4A TIF1 URA2 RPS24A GCN20
32268	regulation of cellular protein metabolic process	7.75E-25	1.97E-22	32/90	35.5%	215/6207 3. RPL20A PFK1 PUB1 RPS1B TEF4 TEF1 RPL17A FBA1 RPL3 RPL7A ADE3 GCN2 RPL4A RPL2A BMH1 OLA1 RPS0A KAP123 RPS5 GCN1 PRT1 FAS1 TIF4631 TIF4632 NEW1 RPL13A GUS1 RPS4A TIF1 URA2 RPS24A GCN20
51246	regulation of protein metabolic process	3.16E-21	6.02E-19	32/90	35.5%	279/6207 4. RPL20A PFK1 PUB1 RPS1B TEF4 TEF1 RPL17A FBA1 RPL3 RPL7A ADE3 GCN2 RPL4A RPL2A BMH1 OLA1 RPS0A KAP123 RPS5 GCN1 PRT1 FAS1 TIF4631 TIF4632 NEW1 RPL13A GUS1 RPS4A TIF1 URA2 RPS24A GCN20
10556	regulation of macromolecule biosynthetic process	7.91E-11	1.21E-08	38/90	42.2%	888/6207 14 SPT5 RPL20A RVB2 PFK1 PUB1 RVB1 RPS1B TEF4 TEF1 RPL17A FBA1 RPL3 RPL7A ADE3 GCN2 RPL4A RPL2A VPS1 OLA1 RPS0A GCN1 HSP82 RPS5 KAP123 PRT1 TIF4631 FAS1 TIF4632 NEW1 RPL13A GUS1 RPS4A HSC82 ACT1 TIF1 URA2 RPS24A GCN20
31326	regulation of cellular biosynthetic process	1.41E-10	1.63E-08	38/90	42.2%	905/6207 14 SPT5 RPL20A RVB2 PFK1 PUB1 RVB1 RPS1B TEF4 TEF1 RPL17A FBA1 RPL3 RPL7A ADE3 GCN2 RPL4A RPL2A VPS1 OLA1 RPS0A GCN1 HSP82 RPS5 KAP123 PRT1 TIF4631 FAS1 TIF4632 NEW1 RPL13A GUS1 RPS4A HSC82 ACT1 TIF1 URA2 RPS24A GCN20
9889	regulation of biosynthetic process	1.66E-10	1.63E-08	38/90	42.2%	910/6207 14 SPT5 RPL20A RVB2 PFK1 PUB1 RVB1 RPS1B TEF4 TEF1 RPL17A FBA1 RPL3 RPL7A ADE3 GCN2 RPL4A RPL2A VPS1 OLA1 RPS0A GCN1 HSP82 RPS5 KAP123 PRT1 TIF4631 FAS1 TIF4632 NEW1 RPL13A GUS1 RPS4A HSC82 ACT1 TIF1 URA2 RPS24A GCN20
60255	regulation of macromolecule metabolic process	1.71E-10	1.63E-08	40/90	44.4%	1003/6207 1 SPT5 RPL20A RVB2 PFK1 PUB1 RVB1 RPS1B TEF4 TEF1 RPL17A RPL3 FBA1 RPL7A ADE3 GCN2 RPL4A RPL2A BMH1 VPS1 HSP60 OLA1 RPS0A GCN1 HSP82 RPS5 KAP123 PRT1 TIF4631 FAS1 TIF4632 NEW1 RPL13A GUS1 RPS4A HSC82 ACT1 TIF1 URA2 RPS24A GCN2
9058	biosynthetic process	2.18E-10	1.70E-08	62/90	68.8%	2245/6207 3 ERG6 RVB2 RPS3 ERG11 RVB1 RPL9A TDH3 ATP1 ATP2 LYS12 GCN2 ADE3 CYS4 RPL21A RNR1 RPL4A ACS2 RPS0A PRT1 FAS1 VMA2 FAS2 VMA5 LYS21 RPS4A YHR020W HSC82 TIF1 UGP1 TIF3 SSC1 VMA13 SPT5 RPL20A RPS1B ERG11 TEF4 TEF1 RPL17A PMA1 FBA
						RPL3 RPL7A ACC1 RPL2A BMH1 RPP0 RPS14A SSA2 RPS5 DED1 RPS6A TIF4631 TIF4632 RPL13A GUS1 URA2 GND1 MET10 URA3 RPS24A RPS18A
10468	regulation of gene expression	2.23E-10	1.70E-08	37/90	41.1%	874/6207 14 SPT5 RPL20A RVB2 PFK1 PUB1 RVB1 RPS1B TEF4 TEF1 RPL17A FBA1 RPL3 RPL7A ADE3 GCN2 RPL4A RPL2A VPS1 HSP60 OLA1 RPS0A GCN1 RPS5 KAP123 PRT1 TIF4631 FAS1 TIF4632 NEW1 RPL13A GUS1 RPS4A ACT1 TIF1 URA2 RPS24A GCN20
44249	cellular biosynthetic process	4.32E-10	2.99E-08	61/90	67.7%	2212/6207 3 ERG6 RVB2 RPS3 RVB1 RPL9A TDH3 ATP1 ATP2 LYS12 GCN2 ADE3 CYS4 RPL21A RNR1 RPL4A ACS2 RPS0A PRT1 FAS1 VMA2 FAS2 VMA5 LYS21 YHR020W RPS4A HSC82 TIF1 UGP1 TIF3 SSC1 VMA13 SPT5 RPL20A RPS1B ERG11 TEF4 TEF1 RPL17A PMA1 FBA1 RPI
						RPL7A ACC1 RPL2A BMH1 RPP0 RPS14A RPS5 SSA2 DED1 RPS6A TIF4631 TIF4632 RPL13A GUS1 URA2 GND1 MET10 URA3 RPS24A RPS18A
31323	regulation of cellular metabolic process	2.50E-09	1.46E-07	39/90	43.3%	1045/6207 1 SPT5 RPL20A RVB2 PFK1 PUB1 RVB1 RPS1B TEF4 TEF1 RPL17A FBA1 RPL3 RPL7A ADE3 GCN2 RPL4A RPL2A BMH1 VPS1 OLA1 RPS0A GCN1 HSP82 RPS5 KAP123 PRT1 TIF4631 FAS1 TIF4632 NEW1 RPL13A GUS1 RPS4A HSC82 ACT1 TIF1 URA2 RPS24A GCN20
80090	regulation of primary metabolic process	2.50E-09	1.46E-07	39/90	43.3%	1045/6207 1 SPT5 RPL20A RVB2 PFK1 PUB1 RVB1 RPS1B TEF4 TEF1 RPL17A FBA1 RPL3 RPL7A ADE3 GCN2 RPL4A RPL2A BMH1 VPS1 OLA1 RPS0A GCN1 HSP82 RPS5 KAP123 PRT1 TIF4631 FAS1 TIF4632 NEW1 RPL13A GUS1 RPS4A HSC82 ACT1 TIF1 URA2 RPS24A GCN20
19222	regulation of metabolic process	4.48E-09	2.44E-07	40/90	44.4%	1115/6207 1 SPT5 RPL20A RVB2 PFK1 PUB1 RVB1 RPS1B TEF4 TEF1 RPL17A RPL3 FBA1 RPL7A ADE3 GCN2 RPL4A RPL2A BMH1 VPS1 HSP60 OLA1 RPS0A GCN1 HSP82 RPS5 KAP123 PRT1 TIF4631 FAS1 TIF4632 NEW1 RPL13A GUS1 RPS4A HSC82 ACT1 TIF1 URA2 RPS24A GCN2
44281	small molecule metabolic process	4.83E-08	2.46E-06	34/90	37.7%	912/6207 14 ERG6 PFK1 ERG1 ATP1 TDH3 ATP2 ERG11 LYS12 PMA1 FBA1 ADE3 GCN2 CYS4 RNR1 ACC1 BMH1 ACS2 HSP60 VMA2 FAS1 VMA5 NOP1 FAS2 LYS21 GUS1 YHR020W UGP1 URA2 GND1 MET10 URA3 SEC14 SSC1 VMA13
44283	small molecule biosynthetic process	1.03E-07	4.89E-06	21/90	23.3%	390/6207 6. RNR1 ACC1 VMA2 FAS1 TDH3 ATP1 VMA5 FAS2 ATP2 LYS12 LYS21 PMA1 FBA1 URA2 MET10 URA3 GCN2 ADE3 SSC1 VMA13 CYS4
6412	translation	1.70E-07	7.64E-06	34/90	37.7%	959/6207 15 RPL20A RPS3 RPS1B RPL9A TDH3 TEF4 TEF1 RPL17A RPL3 RPL7A GCN2 RPL21A RPL4A RPL2A RPS0A RPP0 RPS14A RPS5 SSA2 DED1 PRT1 RPS6A TIF4631 TIF4632 RPL13A GUS1 HSC82 YHR020W RPS4A TIF1 GND1 TIF3 RPS24A RPS18A
462	maturation of SSU-rRNA from tricistronic rRNA transcript (SSU-rRNA, 5.8S rRNA, LSU-rRNA)	7.46E-07	3.16E-05	10/90	11.1%	93/6207 1.4 RPS6A NOP1 RRP5 NOP58 RPS0A RPS14A NOP56 RPS24A RPS18A RPS1B
65007	biological regulation	8.24E-07	3.31E-05	48/90	53.3%	1792/6207 2 SPT5 RPL20A RVB2 PFK1 CCT2 PUB1 RPS1B RVB1 TEF4 TEF1 PMA1 RPL17A RPL3 FBA1 RPL7A ADE3 GCN2 RPL4A RPL2A BMH1 VPS1 HSP60 OLA1 RPS0A GCN1 HSP82 RPS5 KAP123 DED1 PRT1 TIF4631 VMA2 FAS1 TIF4632 VMA5 NEW1 RPL13A GUS1 SAC6 RPS4A
						HSC82 ACT1 TIF1 URA2 RPS24A GCN20 SSC1 VMA13
9165	nucleotide biosynthetic process	9.38E-07	3.57E-05	11/90	12.2%	119/6207 1.9 VMA2 VMA5 ATP1 RNR1 ATP2 PMA1 URA2 URA3 ADE3 SSC1 VMA13
30490	maturation of SSU-rRNA	1.34E-06	4.86E-05	10/90	11.1%	99/6207 1.5 RPS6A NOP1 RRP5 NOP58 RPS0A RPS14A NOP56 RPS24A RPS18A RPS1B
50789	regulation of nucleobase, nucleoside, nucleotide and nucleic acid biosynthetic process	1.86E-06	6.46E-05	43/90	47.7%	1545/6207 2 SPT5 RPL20A RVB2 PFK1 CCT2 PUB1 RVB1 RPS1B TEF4 TEF1 RPL17A RPL3 FBA1 RPL7A ADE3 GCN2 RPL4A RPL2A BMH1 VPS1 HSP60 OLA1 RPS0A GCN1 HSP82 RPS5 KAP123 DED1 PRT1 TIF4631 FAS1 TIF4632 NEW1 RPL13A GUS1 SAC6 RPS4A HSC82 ACT1 TIF1
						URA2 RPS24A GCN20
34654	nucleobase, nucleoside and nucleotide biosynthetic process	2.27E-06	7.21E-05	11/90	12.2%	130/6207 2. VMA2 VMA5 ATP1 RNR1 ATP2 PMA1 URA2 URA3 ADE3 SSC1 VMA13
34404	primary metabolic process	2.27E-06	7.21E-05	11/90	12.2%	130/6207 2. VMA2 VMA5 ATP1 RNR1 ATP2 PMA1 URA2 URA3 ADE3 SSC1 VMA13
44238	primary metabolic process	3.05E-06	9.30E-05	74/90	82.2%	3697/6207 5 ERG6 RVB2 CCT2 PUB1 RPS3 ERG1 RVB1 RPL9A TDH3 ATP1 ATP2 LYS12 ADE3 GCN2 CYS4 RPL21A RNR1 RPL4A RRP5 ACS2 HSP60 RPS0A PRT1 FAS1 VMA2 VMA5 NOP1 FAS2 LYS21 RPS4A YHR020W HSC82 ACT1 TIF1 UGP1 TIF3 SSC1 VMA13 SPT5 RPL20A PFK1
						RPS1B ERG11 TEF4 TEF1 RPL17A PMA1 FBA1 RPL3 RPL7A MCK1 ACC1 RPL2A BMH1 RPP0 RPS14A SSA2 HSP82 RPS5 DED1 RPS6A TIF4631 TIF4632 RPL13A GUS1 NOP58 URA2 GND1 MET10 NOP56 URA3 RPS24A RPS18A SEC14
6754	ATP biosynthetic process	3.60E-06	1.06E-04	7/90	7.7%	46/6207 0.7 VMA2 VMA5 ATP1 ATP2 PMA1 SSC1 VMA13
46034	ATP metabolic process	4.18E-06	1.18E-04	7/90	7.7%	47/6207 0.7 VMA2 VMA5 ATP1 ATP2 PMA1 SSC1 VMA13
9206	purine nucleoside triphosphate biosynthetic process	5.58E-06	1.47E-04	7/90	7.7%	49/6207 0.7 VMA2 VMA5 ATP1 ATP2 PMA1 SSC1 VMA13
9145	purine nucleoside triphosphate biosynthetic process	5.58E-06	1.47E-04	7/90	7.7%	49/6207 0.7 VMA2 VMA5 ATP1 ATP2 PMA1 SSC1 VMA13
22613	ribonucleoprotein complex biogenesis	7.16E-06	1.79E-04	19/90	21.1%	423/6207 6. RRP5 RVB2 RPS0A RPP0 RPS14A PUB1 RPS5 RPS3 RPS1B RPS6A TIF4631 TIF4632 NOP1 NEW1 RPL3 NOP58 NOP56 RPS24A RPS18A
9201	nucleoside triphosphate biosynthetic process	7.34E-06	1.79E-04	7/90	7.7%	51/6207 0.8 VMA2 VMA5 ATP1 ATP2 PMA1 SSC1 VMA13
44271	cellular nitrogen compound biosynthetic process	7.54E-06	1.79E-04	16/90	17.7%	310/6207 4. RNR1 VMA2 ATP1 VMA5 ATP2 LYS12 LYS21 PMA1 URA2 MET10 URA3 GCN2 ADE3 SSC1 CYS4 VMA13
50794	regulation of cellular process	8.17E-06	1.89E-04	39/90	43.3%	1400/6207 2 SPT5 RPL20A RVB2 PFK1 PUB1 RVB1 RPS1B TEF4 TEF1 RPL17A FBA1 RPL3 RPL7A ADE3 GCN2 RPL4A RPL2A BMH1 VPS1 OLA1 RPS0A GCN1 HSP82 RPS5 KAP123 PRT1 TIF4631 FAS1 TIF4632 NEW1 RPL13A GUS1 RPS4A HSC82 ACT1 TIF1 URA2 RPS24A GCN20
9205	purine ribonucleoside triphosphate metabolic process	9.55E-06	2.02E-04	7/90	7.7%	53/6207 0.8 VMA2 VMA5 ATP1 ATP2 PMA1 SSC1 VMA13
9144	purine nucleoside triphosphate metabolic process	9.55E-06	2.02E-04	7/90	7.7%	53/6207 0.8 VMA2 VMA5 ATP1 ATP2 PMA1 SSC1 VMA13
9142	nucleoside triphosphate biosynthetic process	9.55E-06	2.02E-04	7/90	7.7%	53/6207 0.8 VMA2 VMA5 ATP1 ATP2 PMA1 SSC1 VMA13
6164	purine nucleoside biosynthetic process	9.84E-06	2.03E-04	8/90	8.8%	74/6207 1.1 VMA2 VMA5 ATP1 ATP2 PMA1 ADE3 SSC1 VMA13
9196	ribonucleoside triphosphate metabolic process	1.23E-05	2.46E-04	7/90	7.7%	55/6207 0.8 VMA2 VMA5 ATP1 ATP2 PMA1 SSC1 VMA13
9260	ribonucleotide biosynthetic process	1.46E-05	2.85E-04	8/90	8.8%	78/6207 1.2 VMA2 VMA5 ATP1 ATP2 PMA1 URA3 SSC1 VMA13
15992	proton transport	1.75E-05	3.20E-04	6/90	6.6%	39/6207 0.6 VMA2 VMA5 ATP1 ATP2 PMA1 VMA13
6163	purine nucleotide metabolic process	1.76E-05	3.20E-04	8/90	8.8%	80/6207 1.2 VMA2 VMA5 ATP1 ATP2 PMA1 ADE3 SSC1 VMA13
44237	cellular metabolic process	1.76E-05	3.20E-04	74/90	82.2%	3826/6207 6 ERG6 RVB2 CCT2 PUB1 RPS3 RVB1 RPL9A TDH3 ATP1 ATP2 LYS12 GCN2 ADE3 CYS4 RPL21A RNR1 RPL4A RRP5 ACS2 HSP60 RPS0A PRT1 FAS1 VMA2 VMA5 NOP1 FAS2 LYS21 RPS4A YHR020W HSC82 ACT1 TIF1 UGP1 TIF3 SSC1 VMA13 SPT5 RPL20A PFK1 RPS1B
						ERG11 TEF4 TEF1 RPL17A PMA1 FBA1 RPL3 RPL7A MCK1 ACC1 RPL2A BMH1 RPP0 RPS14A SSA2 HSP82 RPS5 DED1 RPS6A TIF4631 TIF4632 SEC18 RPL13A GUS1 NOP58 URA2 GND1 MET10 NOP56 URA3 RPS24A RPS18A SEC14
42254	ribosome biogenesis	1.89E-05	3.36E-04	17/90	18.8%	372/6207 5 RRP5 RVB2 RPS0A RPP0 RPS14A RPS5 RPS3 RPS1B RPS6A TIF4631 NOP1 NEW1 RPL3 NOP58 NOP56 RPS24A RPS18A
6818	hydrogen transport	2.03E-05	3.51E-04	6/90	6.6%	40/6207 0.6 VMA2 VMA5 ATP1 ATP2 PMA1 VMA13
9259	ribonucleotide metabolic process	2.32E-05	3.92E-04	8/90	8.8%	83/6207 1.3 VMA2 VMA5 ATP1 ATP2 PMA1 URA3 SSC1 VMA13
9141	nucleoside triphosphate metabolic process	2.74E-05	4.54E-04	7/90	7.7%	62/6207 0.9 VMA2 VMA5 ATP1 ATP2 PMA1 SSC1 VMA13
46907	intracellular transport	4.00E-05	6.45E-04	22/90	24.4%	610/6207 9. SEC31 ACC1 VPS1 RPS0A HSP60 TUB2 SSA2 HSP82 RPS5 RTN1 KAP123 RPS3 COP1 SEC18 NEW1 ACT1 TEF1 RPS18A SEC26 SEC14 SEC27 SSC1
6413	translation initiation	4.06E-05	6.45E-04	6/90	6.6%	45/6207 0.7 TIF4631 TIF4632 TIF1 TIF3 DED1 PRT1
44085	cellular component biogenesis	4.40E-05	6.84E-04	28/90	31.1%	903/6207 14 RVB2 PUB1 RPS1B RPS3 ATP1 ATP2 RPL3 RRP5 BMH1 HSP60 RPS0A RPP0 RPS14A TUB2 RPS5 HSP82 RPS6A TIF4631 NOP1 SEC18 TIF4632 NEW1 ACT1 HSC82 NOP58 NOP56 RPS24A RPS18A
9152	purine ribonucleotide biosynthetic process	5.04E-05	7.67E-04	7/90	7.7%	68/6207 1.0 VMA2 VMA5 ATP1 ATP2 PMA1 SSC1 VMA13
9117	nucleotide metabolic process	5.29E-05	7.75E-04	12/90	13.3%	214/6207 3. VMA2 VMA5 ATP1 RNR1 ATP2 PMA1 URA2 GND1 URA3 ADE3 SSC1 VMA13
6753	nucleoside phosphate metabolic process	5.29E-05	7.75E-04	12/90	13.3%	214/6207 3. VMA2 VMA5 ATP1 RNR1 ATP2 PMA1 URA2 GND1 URA3 ADE3 SSC1 VMA13
15985	energy coupled proton transport, down electrochemical gradient	6.14E-05	8.62E-04	5/90	5.5%	30/6207 0.4 VMA2 VMA5 ATP1 ATP2 VMA13
15986	ATP synthesis coupled proton transport	6.14E-05	8.62E-04	5/90	5.5%	30/6207 0.4 VMA2 VMA5 ATP1 ATP2 VMA13
8152	metabolic process	6.22E-05	8.62E-04	75/90	83.3%	4008/6207 (ERG6 RVB2 CCT2 PUB1 RPS3 ERG1 RVB1 RPL9A TDH3 ATP1 ATP2 LYS12 ADE3 GCN2 CYS4 RPL21A RNR1 RPL4A RRP5 ACS2 HSP60 RPS0A PRT1 FAS1 VMA2 VMA5 NOP1 FAS2 LYS21 RPS4A YHR020W HSC82 ACT1 TIF1 UGP1 TIF3 SSC1 VMA13 SPT5 RPL20A
						PFK1 RPS1B ERG11 TEF4 TEF1 RPL17A PMA1 FBA1 RPL3 RPL7A MCK1 ACC1 RPL2A BMH1 RPP0 RPS14A SSA2 HSP82 RPS5 DED1 RPS6A TIF4631 TIF4632 SEC18 RPL13A GUS1 NOP58 URA2 GND1 MET10 NOP56 URA3 RPS24A RPS18A SEC14
9150	purine ribonucleotide metabolic process	7.98E-05	1.09E-03	7/90	7.7%	73/6207 1.1 VMA2 VMA5 ATP1 ATP2 PMA1 SSC1 VMA13
42026	protein refolding	8.52E-05	1.14E-03	4/90	4.4%	17/6207 0.2 HSC82 HSP60 HSP82 SSC1
34063	stress granule assembly	9.89E-05	1.30E-03	3/90	3.3%	7/6207 0.1 TIF4631 TIF4632 PUB1
51649	establishment of localization in cell	1.26E-04	1.63E-03	22/90	24.4%	658/6207 10 SEC31 ACC1 VPS1 RPS0A HSP60 TUB2 SSA2 HSP82 RPS5 RTN1 KAP123 RPS3 COP1 SEC18 NEW1 ACT1 TEF1 RPS18A SEC26 SEC14 SEC27 SSC1
15672	monovalent inorganic cation transport	1.29E-04	1.64E-03	6/90	6.6%	55/6207 0.8 VMA2 VMA5 ATP1 ATP2 PMA1 VMA13
46483	heterocycle metabolic process	1.41E-04	1.77E-03	12/90	13.3%	237/6207 3.8 VMA2 VMA5 ATP1 ATP2 PMA1 URA2 MET10 URA3 ADE3 SSC1 VMA13 CYS4
55086	nucleobase, nucleoside and nucleotide metabolic process	1.93E-04	2.38E-03	12/90	13.3%	245/6207 3.9 VMA2 VMA5 ATP1 RNR1 ATP2 PMA1 URA2 GND1 URA3 ADE3 SSC1 VMA13
51169	nuclear transport	2.66E-04	3.17E-03	9/90	10.0%	148/6207 2.3 ACC1 NEW1 TEF1 RPS0A RPS18A RPS5 KAP123 RTN1 RPS3
6913	nucleocytoplasmic transport	2.66E-04	3.17E-03	9/90	10.0%	148/6207 2.3 ACC1 NEW1 TEF1 RPS0A RPS18A RPS5 KAP123 RTN1 RPS3
9059	macromolecule biosynthetic process	3.00E-04	3.52E-03	41/90	45.5%	1749/6207 2 SPT5 RPL20A RVB2 RVB1 RPS3 RPS1B RPL9A TDH3 TEF4 TEF1 RPL17A RPL3 RPL7A GCN2 RPL21A RNR1 RPL4A RPL2A BMH1 RPP0 RPS0A RPS14A SSA2 RPS5 DED1 PRT1 RPS6A TIF4631 TIF4632 FAS2 RPL13A GUS1 RPS4A YHR020W HSC82 TIF1 UGP1 GND1 TIF3 RI

A.2. Results of the SM^{S}screening

Strains deleted for genes encoding Gcn1binding proteins, wild type and *gcn2*Δ were grown to saturation. Saturated cultures were subjected to 10 fold serial dilutions and 5 µl of each dilution and 5 µl of undiluted culture were transferred to solid medium (SD) containing amino acid starvation inducing drug (SM) and SD media not containing any starvation drug. Plates were incubated at 30°C until colonies were visible.

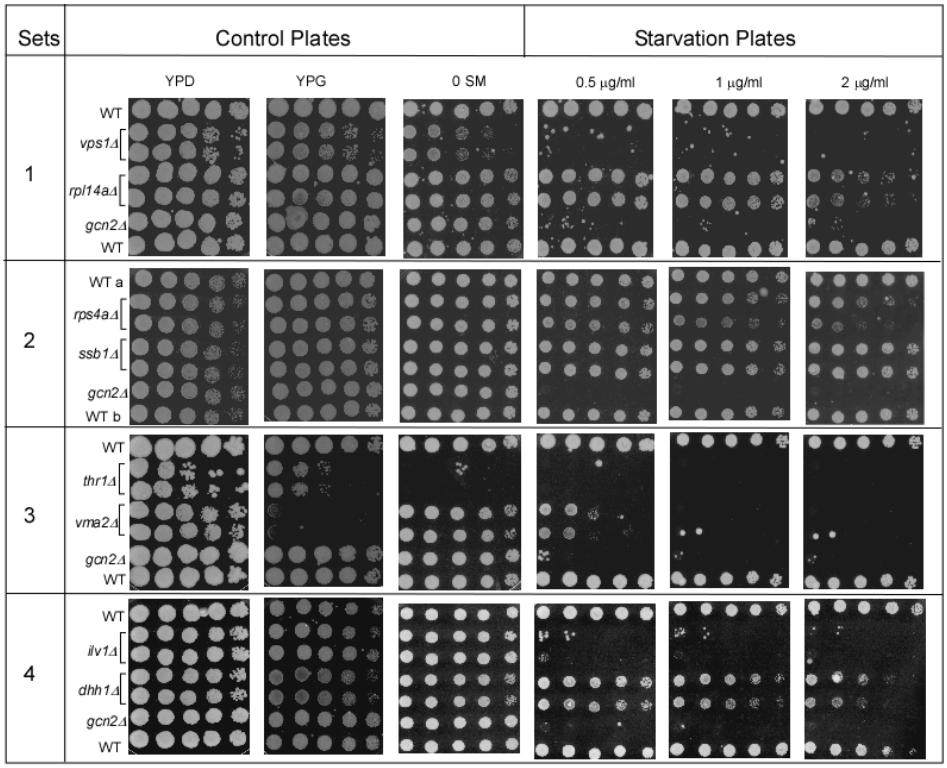

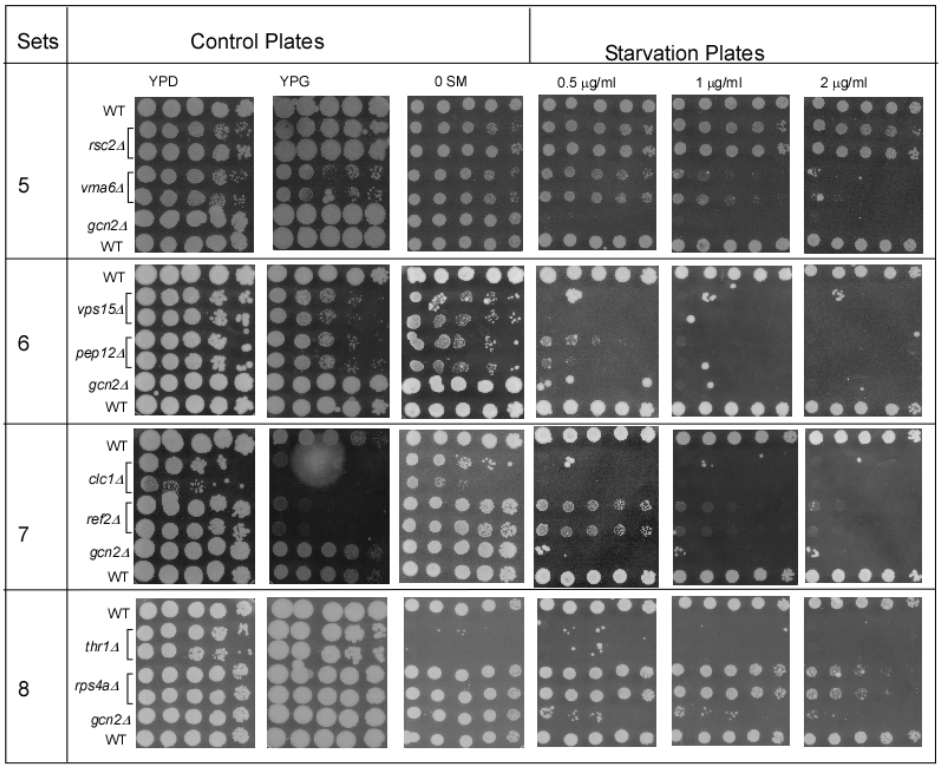
Sets
Control Plates
Starvation Plates
YPD
YPG
0 SM
0.5 μg/ml
1 μg/ml
2 μg/ml
5
WT
rsc2Δ
vma6Δ
gcn2Δ
WT
6
WT
vps15Δ
pep12Δ
gcn2Δ
WT
7
WT
clc1Δ
ref2Δ
gcn2Δ
WT
8
WT
thr1Δ
rps4aΔ
gcn2Δ
WT

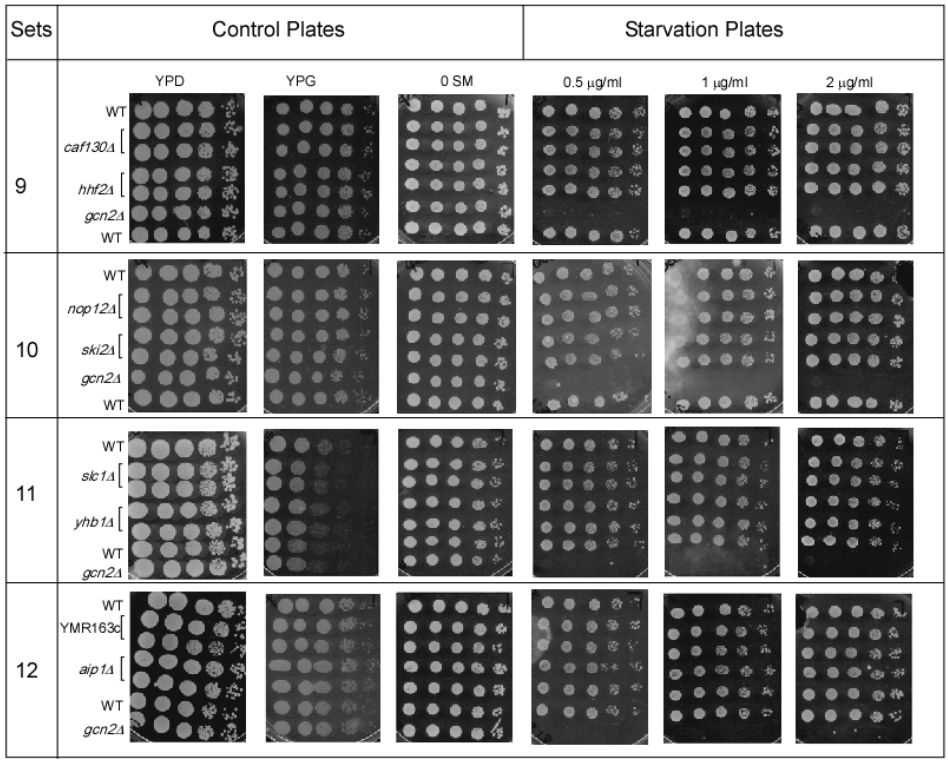
Sets
Control Plates
Starvation Plates
YPD
YPG
0 SM
0.5 μg/ml
1 μg/ml
2 μg/ml
9
WT
caf130Δ
hhf2Δ
gcn2Δ
WT
10
WT
nop12Δ
ski2Δ
gcn2Δ
WT
11
WT
slc1Δ
yhb1Δ
WT
gcn2Δ
12
WT
YMR163c
aip1Δ
WT
gcn2Δ

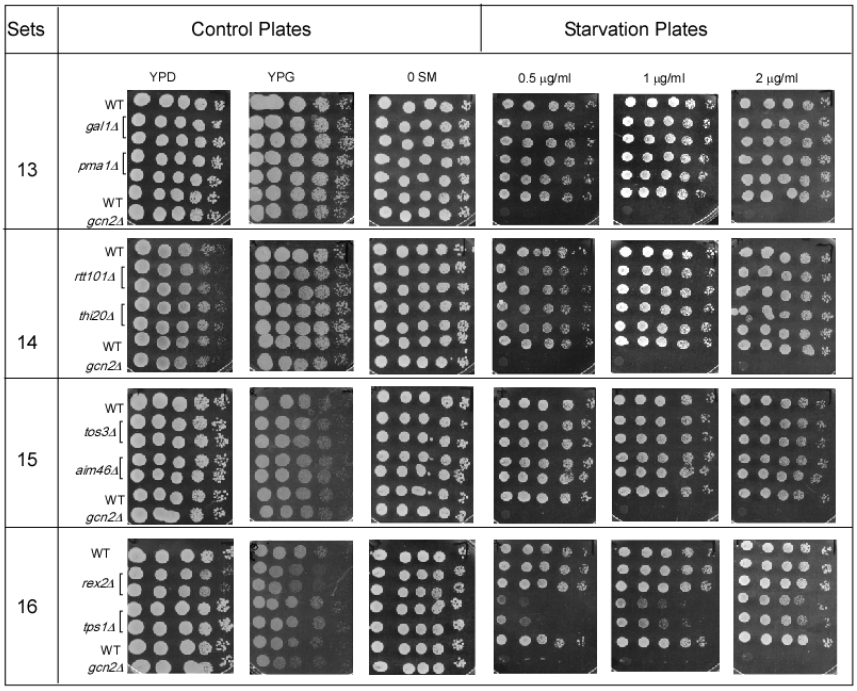
Sets
Control Plates
Starvation Plates
YPD
YPG
0 SM
0.5 μg/ml
1 μg/ml
2 μg/ml
13
WT
gal1Δ
pma1Δ
WT
gcn2Δ
14
WT
rtt101Δ
thi20Δ
WT
gcn2Δ
15
WT
tos3Δ
aim46Δ
WT
gcn2Δ
16
WT
rex2Δ
tps1Δ
WT
gcn2Δ

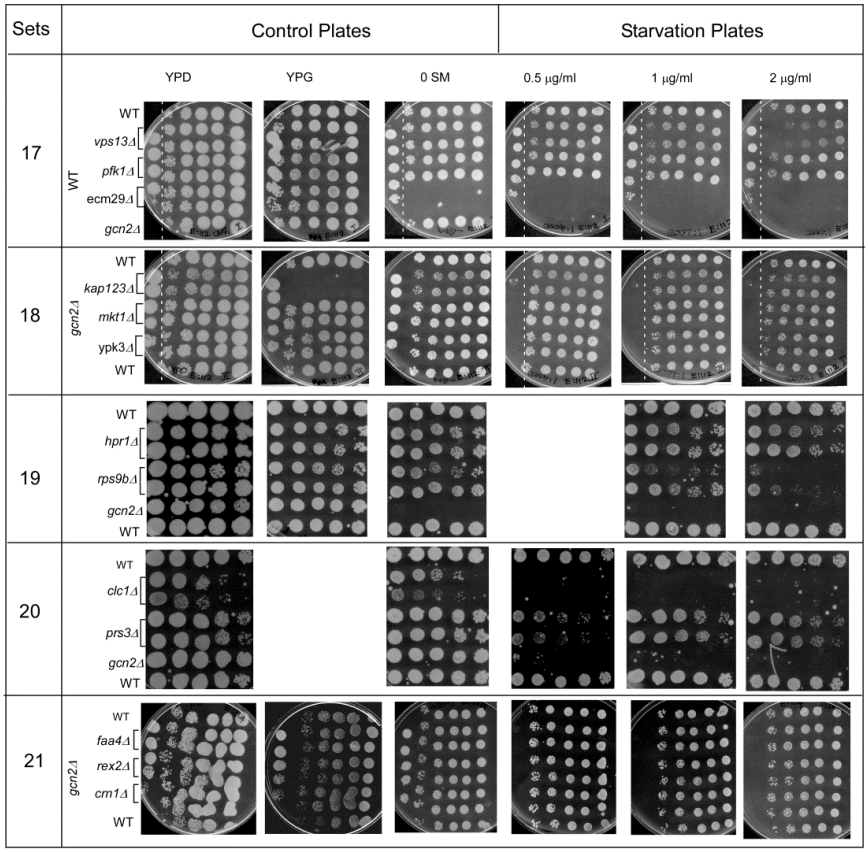
Sets
Control Plates
Starvation Plates
YPD
YPG
0 SM
0.5 μg/ml
1 μg/ml
2 μg/ml
17
WT
vps13Δ
pfk1Δ
ecm29Δ
gcn2Δ
18
gcn2Δ
WT
kap123Δ
mkt1Δ
ypk3Δ
WT
19
WT
hpr1Δ
rps9bΔ
gcn2Δ
WT
20
WT
clc1Δ
prs3Δ
gcn2Δ
WT
21
gcn2Δ
WT
faa4Δ
rex2Δ
crn1Δ
WT

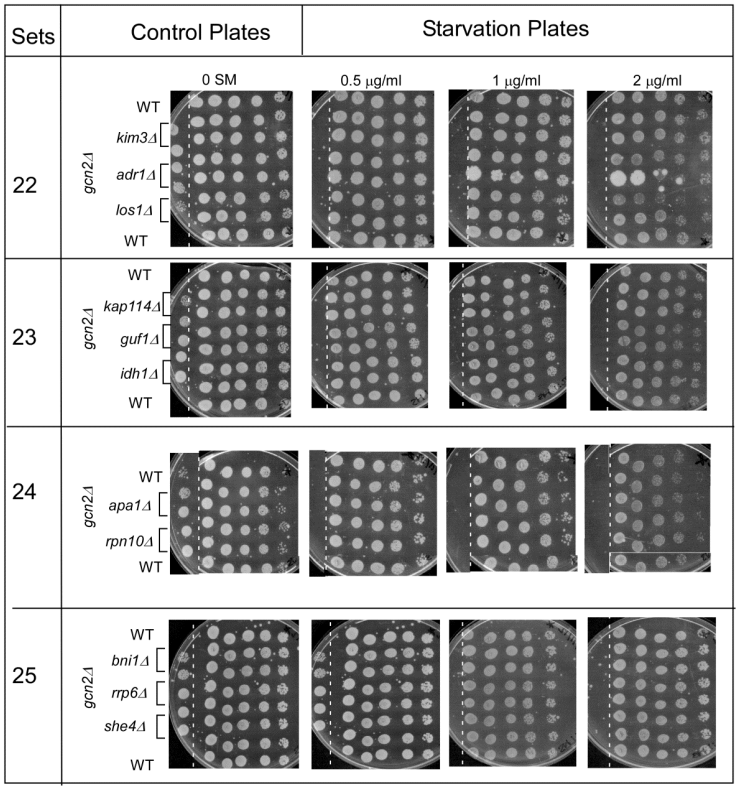
Sets
Control Plates
Starvation Plates
0 SM
0.5 μg/ml
1 μg/ml
2 μg/ml
22
WT
kim3Δ
adr1Δ
los1Δ
WT
gcn2Δ
23
WT
kap114Δ
guf1Δ
idh1Δ
WT
gcn2Δ
24
WT
apa1Δ
rpn10Δ
WT
gcn2Δ
25
WT
bni1Δ
rrp6Δ
she4Δ
WT
gcn2Δ

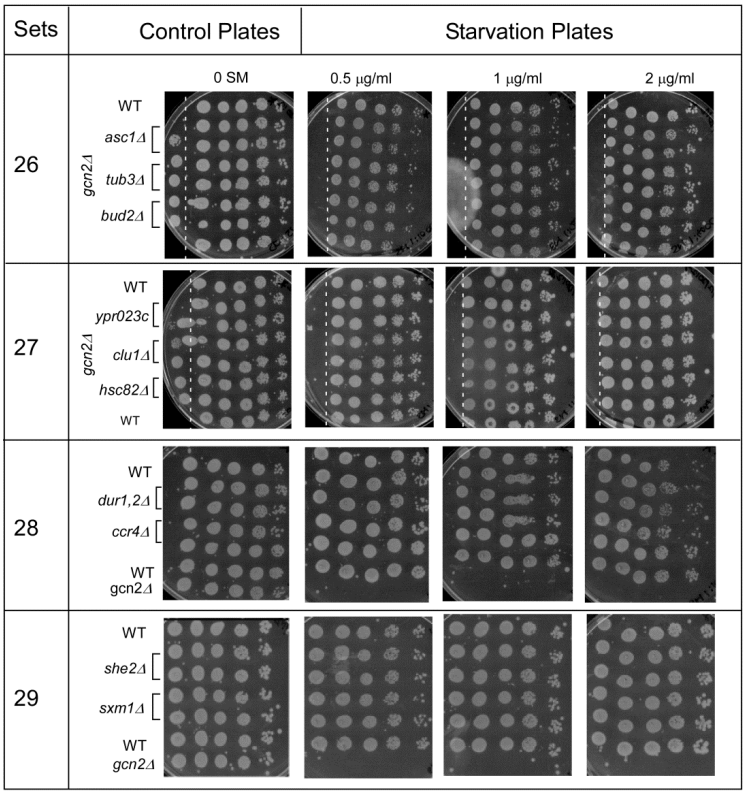
Sets
Control Plates
Starvation Plates
0 SM
0.5 μg/ml
1 μg/ml
2 μg/ml
26
WT
asc1Δ
tub3Δ
bud2Δ
gcn2Δ
27
WT
ypr023c
clu1Δ
hsc82Δ
WT
gcn2Δ
28
WT
dur1,2Δ
ccr4Δ
WT
gcn2Δ
29
WT
she2Δ
sxm1Δ
WT
gcn2Δ

Table A.4 Summary of the SM sensitivity screening

	Strains name	ORF name	General characteristics	SMs	↓ eIF2-P	Gene Complementation
1	*Kem1*Δ	YGL173C		SM^S	Yes	
2	*rnr1*Δ	YER070W		SM^S	Yes	
3	*msn5*Δ	YDR335W		SM^S	Yes	
4	*sin3*Δ	YOL004W		SM^S	Yes	
5	*vps1*Δ	YKR001C		SM^S	Yes	
6	*rpl14a*Δ	YKL006W		SM^S		
7	*rps4*aΔ	YJR145C		SM^S		
8	*ssb1*Δ	YDL229W		Not SM^S		
9	*thr1*Δ	YHR025W		SM^S		
10	*vma2*Δ	YBR127C	petite			
11	*ilv1*Δ	YER086W		SM^S		
12	*dhh1*Δ	YDL160C		SM^S		
13	*rsc2*Δ	YLR357W		Not SM^S		
14	*vma6*Δ	YLR447C	petite			
15	*vps15*Δ	YBR097W	Impaired growth on SD			
16	*pep12*Δ	YOR036W	Impaired growth on SD			
17	*clc1*Δ	YGR167W	Impaired growth on SD			
18	*ref2*Δ	YDR195W	petite			
19	*caf130*Δ	YGR134W		Not SM^S		
20	*hhf2*Δ	YNL030W		Not SM^S		
21	*nop12*Δ	YOL041C		Not SM^S		
22	*ski2*Δ	YLR398C		Not SM^S		
23	*slc1*Δ	YDL052C		Not SM^S		
24	*yhb1*Δ	YGR234W		Not SM^S		
25	*inp2*Δ	YMR163C		Not SM^S		
26	*aip1*Δ	YMR092C		Not SM^S		
27	*gal1*Δ	YBR020W		Not SM^S		
28	*pma1*Δ	YGL008C		Not SM^S		
29	*rtt101*Δ	YJL047C		Not SM^S		
30	*thi20*Δ	YOL055C		Not SM^S		
31	*tos3*Δ	YGL179C		Not SM^S		

32	*aim46*Δ	YHR199C		Not SM^S		
33	*rex2*Δ	YLR059C		Not SM^S		
34	*tps1*Δ	YBR126C		Not SM^S		
35	*vps13*Δ	YLL040C		SM^S		
36	*pfk1*Δ	YGR240C		Not SM^S		
37	*ecm29*Δ	YHL030W	No growth on SD			
38	*kap123*Δ	YER110C		Not SM^S		
39	*mkt1*Δ	YNL085W		Not SM^S		
40	*ypk3*Δ	YBR028C		Not SM^S		
41	*hpr1*Δ	YDR138W		Not SM^S		
42	*rps9b*Δ	YBR189W	SM^s	SM^S		
43	*prs3*Δ	YHL011C		SM^S		
44	*kim3*Δ	YPR164W		Not SM^S		
45	*adr1*Δ	YDR216W		Not SM^S		
46	*los1*Δ	YKL205W		Not SM^S		
47	*kap114*Δ	YGL241W		Not SM^S		
48	*guf1*Δ	YLR289W		Not SM^S		
49	*idh1*Δ	YNL037C		Not SM^S		
50	*apa1*Δ	YCL050C		Not SM^S		
51	*rpn10*	YHR200W		Not SM^S		
52	*bni1*Δ	YNL271C		Not SM^S		
53	*rrp6*Δ	YOR001W		Not SM^S		
54	*she4*Δ	YOR035C		Not SM^S		
55	*asc1*Δ	YMR116C		Not SM^S		
56	*tub3*Δ	YML124C		Not SM^S		
57	*bud2*Δ	YKL092C		Not SM^S		
58	*eaf3*Δ	YOR035C		Not SM^S		
59	*clu1*Δ	YMR012W		Not SM^S		
60	*hsc82*Δ	YMR186W		Not SM^S		
61	*dur1,2*Δ	YBR208C		Not SM^S		
62	*ccr4*Δ	YAL021C		Not SM^S		
63	*she2*Δ	YKL130C		Not SM^S		
64	*sxm1*Δ	YDR395W		Not SM^S		
65	*faa4*Δ	YMR246W		Not SM^S		
66	*rex2*Δ	YLR059C		Not SM^S		

References

1. Hinnebusch, A. G. (1988) Mechanisms of gene regulation in the general control of amino acid biosynthesis in Saccharomyces cerevisiae, *Microbiological reviews 52*, 248.
2. Marton, M. J., de Aldana, C. V., Qiu, H., Chakraburtty, K., and Hinnebusch, A. G. (1997) Evidence that GCN1 and GCN20, translational regulators of GCN4, function on elongating ribosomes in activation of eIF2alpha kinase GCN2, *Molecular and cellular biology 17*, 4474-4489.
3. Ramirez, M., Wek, R. C., Vazquez de Aldana, C. R., Jackson, B. M., Freeman, B., and Hinnebusch, A. G. (1992) Mutations activating the yeast eIF-2 alpha kinase GCN2: isolation of alleles altering the domain related to histidyl-tRNA synthetases, *Molecular and cellular biology 12*, 5801-5815.
4. Sattlegger, E., and Hinnebusch, A. G. (2000) Separate domains in GCN1 for binding protein kinase GCN2 and ribosomes are required for GCN2 activation in amino acid-starved cells, *Embo Journal 19*, 6622-6633.
5. Dong, J., Qiu, H., Garcia-Barrio, M., Anderson, J., and Hinnebusch, A. G. (2000) Uncharged tRNA activates GCN2 by displacing the protein kinase moiety from a bipartite tRNA-binding domain, *Molecular Cell 6*, 269-279.
6. Padyana, A. K., Qiu, H., Roll-Mecak, A., Hinnebusch, A. G., and Burley, S. K. (2005) Structural basis for autoinhibition and mutational activation of eukaryotic initiation factor 2α protein kinase GCN2, *Journal of Biological Chemistry 280*, 29289-29299.
7. Dever, T. E., Feng, L., Wek, R. C., Cigan, A. M., Donahue, T. F., and Hinnebusch, A. G. (1992) Phosphorylation of initiation factor 2α by protein kinase GCN2 mediates gene-specific translational control of< i> GCN4</i> in yeast, *Cell 68*, 585-596.
8. Pavitt, G. D., Ramaiah, K. V., Kimball, S. R., and Hinnebusch, A. G. (1998) eIF2 independently binds two distinct eIF2B subcomplexes that catalyze and regulate guanine–nucleotide exchange, *Genes & development 12*, 514-526.
9. Natarajan, K., Meyer, M. R., Jackson, B. M., Slade, D., Roberts, C., Hinnebusch, A. G., and Marton, M. J. (2001) Transcriptional profiling shows that Gcn4p is a master regulator of gene expression during amino acid starvation in yeast, *Molecular and cellular biology 21*, 4347-4368.
10. Hinnebusch, A. G. (2005) Translational regulation of gcn4 and the general amino acid control of yeast*, *Annu. Rev. Microbiol. 59*, 407-450.
11. Kubota, H., Sakaki, Y., and Ito, T. (2000) GI domain-mediated association of the eukaryotic initiation factor 2α kinase GCN2 with its activator GCN1 is required for general amino acid control in budding yeast, *Journal of Biological Chemistry 275*, 20243-20246.
12. Doerks, T., Copley, R. R., Schultz, J., Ponting, C. P., and Bork, P. (2002) Systematic identification of novel protein domain families associated with nuclear functions, *Genome research 12*, 47-56.
13. Garcia-Barrio, M., Jinsheng, D., Ufano, S., and Hinnebusch, A. G. (2000) Association of GCN1-GCN20 regulatory complex with the N-terminus of eIF2a kinase GCN2 is required for GCN2 activation, *Embo Journal 19*, 1887-1899.
14. Wek, S. A., Zhu, S., and Wek, R. C. (1995) The histidyl-tRNA synthetase-related sequence in the eIF-2 alpha protein kinase GCN2 interacts with

tRNA and is required for activation in response to starvation for different amino acids, *Molecular and cellular biology 15*, 4497-4506.
15. Diallinas, G., and Thireos, G. (1994) Genetic and biochemical evidence for yeast GCN2 protein kinase polymerization, *Gene 143*, 21-27.
16. Qiu, H., Dong, J., Hu, C., Francklyn, C. S., and Hinnebusch, A. G. (2001) The tRNA-binding moiety in GCN2 contains a dimerization domain that interacts with the kinase domain and is required for tRNA binding and kinase activation, *The EMBO Journal 20*, 1425-1438.
17. Qiu, H., Garcia-Barrio, M. T., and Hinnebusch, A. G. (1998) Dimerization by translation initiation factor 2 kinase GCN2 is mediated by interactions in the C-terminal ribosome-binding region and the protein kinase domain, *Molecular and cellular biology 18*, 2697-2711.
18. Narasimhan, J., Staschke, K. A., and Wek, R. C. (2004) Dimerization is required for activation of eIF2 kinase Gcn2 in response to diverse environmental stress conditions, *Journal of Biological Chemistry 279*, 22820-22832.
19. Marton, M., Crouch, D., and Hinnebusch, A. (1993) GCN1, a translational activator of GCN4 in Saccharomyces cerevisiae, is required for phosphorylation of eukaryotic translation initiation factor 2 by protein kinase GCN2, *Molecular and cellular biology 13*, 3541-3556.
20. Dealdana, C. R. V., Marton, M. J., and Hinnebusch, A. G. (1995) GCN20, A NOVEL ATP BINDING CASSETTE PROTEIN, AND GCN1 RESIDE IN A COMPLEX THAT MEDIATES ACTIVATION OF THE EIF-2-ALPHA KINASE GCN2 IN AMINO ACID-STARVED CELLS, *Embo Journal 14*, 3184-3199.
21. Andrade, M. A., and Bork, P. (1995) HEAT repeats in the Huntington's disease protein, *Nature genetics 11*, 115-116.
22. Andrade, M. A., Petosa, C., O'Donoghue, S. I., Müller, C. W., and Bork, P. (2001) Comparison of ARM and HEAT protein repeats, *Journal of molecular biology 309*, 1-18.
23. Good, M. C., Zalatan, J. G., and Lim, W. A. (2011) Scaffold proteins: hubs for controlling the flow of cellular information, *Science 332*, 680-686.
24. Gavin, A.-C., Aloy, P., Grandi, P., Krause, R., Boesche, M., Marzioch, M., Rau, C., Jensen, L. J., Bastuck, S., and Dümpelfeld, B. (2006) Proteome survey reveals modularity of the yeast cell machinery, *Nature 440*, 631-636.
25. Gavin, A.-C., Bösche, M., Krause, R., Grandi, P., Marzioch, M., Bauer, A., Schultz, J., Rick, J. M., Michon, A.-M., and Cruciat, C.-M. (2002) Functional organization of the yeast proteome by systematic analysis of protein complexes, *Nature 415*, 141-147.
26. Ho, Y., Gruhler, A., Heilbut, A., Bader, G. D., Moore, L., Adams, S.-L., Millar, A., Taylor, P., Bennett, K., and Boutilier, K. (2002) Systematic identification of protein complexes in Saccharomyces cerevisiae by mass spectrometry, *Nature 415*, 180-183.
27. Krogan, N. J., Cagney, G., Yu, H., Zhong, G., Guo, X., Ignatchenko, A., Li, J., Pu, S., Datta, N., and Tikuisis, A. P. (2006) Global landscape of protein complexes in the yeast Saccharomyces cerevisiae, *Nature 440*, 637-643.

28. Dean, M., Hamon, Y., and Chimini, G. (2001) The human ATP-binding cassette (ABC) transporter superfamily, *Journal of lipid research 42*, 1007-1017.
29. Triana-Alonso, F. J., Chakraburtty, K., and Nierhaus, K. H. (1995) The elongation factor 3 unique in higher fungi and essential for protein biosynthesis is an E site factor, *Journal of Biological Chemistry 270*, 20473-20478.
30. Sattlegger, E., and Hinnebusch, A. G. (2005) Polyribosome Binding by GCN1 Is Required for Full Activation of Eukaryotic Translation Initiation Factor 2&alpha Kinase GCN2 during Amino Acid Starvation, *Journal of Biological Chemistry 280*, 16514-16521.
31. Hinnebusch, A. G. (1993) Gene-specific translational control of the yeast GCN4 gene by phosphorylation of eukaryotic initiation factor 2, *Molecular microbiology 10*, 215-223.
32. Berlanga, J. J., Santoyo, J., and de Haro, C. (1999) Characterization of a mammalian homolog of the GCN2 eukaryotic initiation factor 2α kinase, *European Journal of Biochemistry 265*, 754-762.
33. Chen, J.-J. (2000) Heme-regulated eIF2alpha kinase, *COLD SPRING HARBOR MONOGRAPH SERIES 39*, 529-546.
34. Clemens, M. J. (1997) PKR—a protein kinase regulated by double-stranded RNA, *The international journal of biochemistry & cell biology 29*, 945-949.
35. Harding, H. P., Zhang, Y., Bertolotti, A., Zeng, H., and Ron, D. (2000) < i> Perk</i> Is Essential for Translational Regulation and Cell Survival during the Unfolded Protein Response, *Molecular Cell 5*, 897-904.
36. Dever, T. E., and Hinnebusch, A. G. (2005) GCN2 whets the appetite for amino acids, *Molecular Cell 18*, 141-142.
37. Towle, H. C. (2007) The metabolic sensor GCN2 branches out, *Cell metabolism 5*, 85-87.
38. Castilho, B. A., Shanmugam, R., Silva, R. C., Ramesh, R., Himme, B. M., and Sattlegger, E. (2014) Keeping the eIF2 alpha kinase Gcn2 in check, *Biochimica et Biophysica Acta (BBA)-Molecular Cell Research*.
39. Baird, T. D., and Wek, R. C. (2012) Eukaryotic initiation factor 2 phosphorylation and translational control in metabolism, *Advances in Nutrition: An International Review Journal 3*, 307-321.
40. Yang, R., Wek, S. A., and Wek, R. C. (2000) Glucose Limitation Induces GCN4Translation by Activation of Gcn2 Protein Kinase, *Molecular and cellular biology 20*, 2706-2717.
41. Rolfes, R. J., and Hinnebusch, A. G. (1993) Translation of the yeast transcriptional activator GCN4 is stimulated by purine limitation: implications for activation of the protein kinase GCN2, *Molecular and cellular biology 13*, 5099-5111.
42. Hao, S., Ross-Inta, C., and Gietzen, D. (2010) The sensing of essential amino acid deficiency in the anterior piriform cortex, that requires the uncharged tRNA/GCN2 pathway, is sensitive to wortmannin but not rapamycin, *Pharmacology Biochemistry and Behavior 94*, 333-340.
43. Hao, S., Sharp, J. W., Ross-Inta, C. M., McDaniel, B. J., Anthony, T. G., Wek, R. C., Cavener, D. R., McGrath, B. C., Rudell, J. B., and Koehnle, T. J. (2005) Uncharged tRNA and sensing of amino acid deficiency in mammalian piriform cortex, *Science 307*, 1776-1778.

44. Guo, F., and Cavener, D. R. (2007) The GCN2 eIF2α kinase regulates fatty-acid homeostasis in the liver during deprivation of an essential amino acid, *Cell metabolism 5*, 103-114.
45. Goossens, A., Dever, T. E., Pascual-Ahuir, A., and Serrano, R. (2001) The Protein Kinase Gcn2p Mediates Sodium Toxicity in Yeast, *Journal of Biological Chemistry 276*, 30753-30760.
46. Guillem, H., Rafael, A.-S., Consuelo, M., Silvia, L., Jose, R. M., and Ramon, S. (2012) A novel role for protein kinase Gcn2 in yeast tolerance to intracellular acid stress, *Biochemical Journal 441*, 255-264.
47. Nomura, W., Maeta, K., Kita, K., Izawa, S., and Inoue, Y. (2008) Role of Gcn4 for adaptation to methylglyoxal in< i> Saccharomyces cerevisiae</i>: Methylglyoxal attenuates protein synthesis through phosphorylation of eIF2α, *Biochemical and Biophysical Research Communications 376*, 738-742.
48. Nomura, W., Maeta, K., Kita, K., Izawa, S., and Inoue, Y. (2010) Methylglyoxal activates Gcn2 to phosphorylate eIF2α independently of the TOR pathway in Saccharomyces cerevisiae, *Applied microbiology and biotechnology 86*, 1887-1894.
49. Uluisik, I., Kaya, A., Fomenko, D. E., Karakaya, H. C., Carlson, B. A., Gladyshev, V. N., and Koc, A. (2011) Boron stress activates the general amino acid control mechanism and inhibits protein synthesis, *PLoS ONE 6*, e27772.
50. Cherkasova, V. A., and Hinnebusch, A. G. (2003) Translational control by TOR and TAP42 through dephosphorylation of eIF2α kinase GCN2, *Genes & development 17*, 859-872.
51. Mascarenhas, C., Edwards-Ingram, L. C., Zeef, L., Shenton, D., Ashe, M. P., and Grant, C. M. (2008) Gcn4 is required for the response to peroxide stress in the yeast Saccharomyces cerevisiae, *Molecular Biology of the Cell 19*, 2995-3007.
52. Steffensen, L., and Pedersen, P. A. (2006) Heterologous expression of membrane and soluble proteins derepresses GCN4 mRNA translation in the yeast Saccharomyces cerevisiae, *Eukaryotic cell 5*, 248-261.
53. Sattlegger, E., Swanson, M. J., Ashcraft, E. A., Jennings, J. L., Fekete, R. A., Link, A. J., and Hinnebusch, A. G. (2004) YIH1 is an actin-binding protein that inhibits protein kinase GCN2 and impairs general amino acid control when overexpressed, *Journal of Biological Chemistry 279*, 29952-29962.
54. Wout, P. K., Sattlegger, E., Sullivan, S. M., and Maddock, J. R. (2009) Saccharomyces cerevisiae Rbg1 protein and its binding partner gir2 interact on polyribosomes with Gcn1, *Eukaryotic cell 8*, 1061-1071.
55. Sattlegger, E., Barbosa, J. A. R. G., Moraes, M. C. S., Martins, R. M., Hinnebusch, A. G., and Castilho, B. A. (2011) Gcn1 and Actin Binding to Yih1, *Journal of Biological Chemistry 286*, 10341-10355.
56. Wout, P., Sattlegger, E., Sullivan, S., and Maddock, J. (2009) Saccharomyces cerevisiae Rbg1 protein and its binding partner Gir2 interact on Polyribosomes with Gcn1, *Eukaryotic cell 8*, 1061-1071.
57. Ishikawa, K., Ito, K., Inoue, J. i., and Semba, K. (2013) Cell growth control by stable Rbg2/Gir2 complex formation under amino acid starvation, *Genes to Cells 18*, 859-872.

58. Costa-Mattioli, M., Gobert, D., Harding, H., Herdy, B., Azzi, M., Bruno, M., Bidinosti, M., Mamou, C. B., Marcinkiewicz, E., and Yoshida, M. (2005) Translational control of hippocampal synaptic plasticity and memory by the eIF2α kinase GCN2, *Nature 436*, 1166-1173.
59. Maurin, A.-C., Jousse, C., Averous, J., Parry, L., Bruhat, A., Cherasse, Y., Zeng, H., Zhang, Y., Harding, H. P., and Ron, D. (2005) The GCN2 kinase biases feeding behavior to maintain amino acid homeostasis in omnivores, *Cell metabolism 1*, 273-277.
60. Wang, Y., Ning, Y., Alam, G. N., Jankowski, B. M., Dong, Z., Nör, J. E., and Polverini, P. J. (2013) Amino acid deprivation promotes tumor angiogenesis through the GCN2/ATF4 pathway, *Neoplasia 15*, 989-997.
61. Ye, J. (2010) The role of the transcription factor ATF4 in tumor progression under nutrient deprivation and hypoxia.
62. Deng, J., Harding, H. P., Raught, B., Gingras, A.-C., Berlanga, J. J., Scheuner, D., Kaufman, R. J., Ron, D., and Sonenberg, N. (2002) Activation of GCN2 in UV-irradiated cells inhibits translation, *Current biology 12*, 1279-1286.
63. Berlanga, J. J., Ventoso, I., Harding, H. P., Deng, J., Ron, D., Sonenberg, N., Carrasco, L., and de Haro, C. (2006) Antiviral effect of the mammalian translation initiation factor 2 alpha kinase GCN2 against RNA viruses, *Embo Journal 25*, 1730-1740.
64. del Pino, J., Jiménez, J. L., Ventoso, I., Castelló, A., Muñoz-Fernández, M. Á., de Haro, C., and Berlanga, J. J. (2012) GCN2 has inhibitory effect on human immunodeficiency virus-1 protein synthesis and is cleaved upon viral infection, *PLoS ONE 7*, e47272.
65. Sikorski, R. S., and Hieter, P. (1989) A system of shuttle vectors and yeast host strains designed for efficient manipulation of DNA in Saccharomyces cerevisiae, *Genetics 122*, 19-27.
66. Qiu, H., Hu, C., Dong, J., and Hinnebusch, A. G. (2002) Mutations that bypass tRNA binding activate the intrinsically defective kinase domain in GCN2, *Genes & development 16*, 1271-1280.
67. Foiani, M., Cigan, A., Paddon, C., Harashima, S., and Hinnebusch, A. (1991) GCD2, a translational repressor of the GCN4 gene, has a general function in the initiation of protein synthesis in Saccharomyces cerevisiae, *Molecular and cellular biology 11*, 3203-3216.
68. Green, M. R., and Sambrook, J. (2012) *Molecular cloning: a laboratory manual*, Cold Spring Harbor Laboratory Press New York.
69. Ito, H., Fukuda, Y., Murata, K., and Kimura, A. (1983) Transformation of intact yeast cells treated with alkali cations, *Journal of Bacteriology 153*, 163-168.
70. Mandel, M., and Higa, A. (1970) Calcium-dependent bacteriophage DNA infection, *Journal of molecular biology 53*, 159-162.
71. Valášek, L., Szamecz, B., Hinnebusch, A. G., and Nielsen, K. H. (2007) < i> In Vivo</i> Stabilization of Preinitiation Complexes by Formaldehyde Cross-Linking, *Methods in enzymology 429*, 163-183.
72. Visweswaraiah, J., Dautel, M., and Sattlegger, E. (2011) Generating highly concentrated yeast whole cell extract using low-cost equipment, *Nat. Prot. Exchange*.

73. Bradford, M. M. (1976) A rapid and sensitive method for the quantitation of microgram quantities of protein utilizing the principle of protein-dye binding, *Analytical biochemistry 72*, 248-254.
74. Krogan, N., Cagney, G., Yu, H., Zhong, G., Guo, X., Ignatchenko, A., Li, J., Pu, S., Datta, N., and Tikuisis, A. (2006) Global landscape of protein complexes in the yeast Saccharomyces cerevisiae, *Nature 440*, 637-643.
75. Gavin, A., Bösche, M., Krause, R., Grandi, P., Marzioch, M., Bauer, A., Schultz, J., Rick, J., Michon, A., and Cruciat, C. (2002) Functional organization of the yeast proteome by systematic analysis of protein complexes, *Nature 415*, 141-147.
76. Gavin, A., Aloy, P., Grandi, P., Krause, R., Boesche, M., Marzioch, M., Rau, C., Jensen, L., Bastuck, S., and Dümpelfeld, B. (2006) Proteome survey reveals modularity of the yeast cell machinery, *Nature 440*, 631-636.
77. Ho, Y., Gruhler, A., Heilbut, A., Bader, G., Moore, L., Adams, S., Millar, A., Taylor, P., Bennett, K., and Boutilier, K. (2002) Systematic identification of protein complexes in Saccharomyces cerevisiae by mass spectrometry, *Nature 415*, 180-183.
78. Puig, O., Caspary, F., Rigaut, G., Rutz, B., Bouveret, E., Bragado-Nilsson, E., Wilm, M., and Seraphin, B. (2001) The tandem affinity purification (TAP) method: a general procedure of protein complex purification, *Methods 24*, 218-229.
79. de Aldana, C., Marton, M., and Hinnebusch, A. (1995) GCN20, a novel ATP binding cassette protein, and GCN1 reside in a complex that mediates activation of the eIF-2 alpha kinase GCN2 in amino acid-starved cells, *The EMBO Journal 14*, 3184.
80. Garcia-Barrio, M., Dong, J., Ufano, S., and Hinnebusch, A. (2000) Association of GCN1–GCN20 regulatory complex with the N-terminus of eIF2 kinase GCN2 is required for GCN2 activation, *The EMBO Journal 19*, 1887-1899.
81. Visweswaraiah, J., Lageix, S., Castilho, B. A., Izotova, L., Kinzy, T. G., Hinnebusch, A. G., and Sattlegger, E. (2011) Evidence that eukaryotic translation elongation factor 1A (eEF1A) binds the Gcn2 protein C terminus and inhibits Gcn2 activity, *Journal of Biological Chemistry 286*, 36568-36579.
82. Donzé, O., and Picard, D. (1999) Hsp90 binds and regulates the ligand-inducible α subunit of eukaryotic translation initiation factor kinase Gcn2, *Molecular and cellular biology 19*, 8422-8432.
83. Puig, O., Caspary, F., Rigaut, G., Rutz, B., Bouveret, E., Bragado-Nilsson, E., Wilm, M., and Séraphin, B. (2001) The tandem affinity purification (TAP) method: a general procedure of protein complex purification, *Methods 24*, 218-229.
84. Ozbabacan, S. E. A., Engin, H. B., Gursoy, A., and Keskin, O. (2011) Transient protein–protein interactions, *Protein Engineering Design and Selection 24*, 635-648.
85. Tan, Y.-J., and Ting, A. E. (2000) Non-ionic detergent affects the conformation of a functionally active mutant of Bcl-XL, *Protein engineering 13*, 887-892.
86. Lotz, G. P., Lin, H., Harst, A., and Obermann, W. M. (2003) Aha1 binds to the middle domain of Hsp90, contributes to client protein activation, and

stimulates the ATPase activity of the molecular chaperone, *J Biol Chem 278*, 17228-17235.
87. Tkach, J. M., Yimit, A., Lee, A. Y., Riffle, M., Costanzo, M., Jaschob, D., Hendry, J. A., Ou, J., Moffat, J., Boone, C., Davis, T. N., Nislow, C., and Brown, G. W. (2012) Dissecting DNA damage response pathways by analysing protein localization and abundance changes during DNA replication stress, *Nat Cell Biol 14*, 966-976.
88. Forgac, M. (1999) Structure and properties of the vacuolar (H+)-ATPases, *Journal of Biological Chemistry 274*, 12951-12954.
89. Tkach, J. M., Yimit, A., Lee, A. Y., Riffle, M., Costanzo, M., Jaschob, D., Hendry, J. A., Ou, J., Moffat, J., and Boone, C. (2012) Dissecting DNA damage response pathways by analysing protein localization and abundance changes during DNA replication stress, *Nature cell biology 14*, 966-976.
90. Mengin-Lecreulx, D., and van Heijenoort, J. (1993) Identification of the glmU gene encoding N-acetylglucosamine-1-phosphate uridyltransferase in Escherichia coli, *Journal of Bacteriology 175*, 6150-6157.
91. Mengin-Lecreulx, D., and Van Heijenoort, J. (1994) Copurification of glucosamine-1-phosphate acetyltransferase and N-acetylglucosamine-1-phosphate uridyltransferase activities of Escherichia coli: characterization of the glmU gene product as a bifunctional enzyme catalyzing two subsequent steps in the pathway for UDP-N-acetylglucosamine synthesis, *Journal of Bacteriology 176*, 5788-5795.
92. Watzele, G., and Tanner, W. (1989) Cloning of the glutamine:fructose-6-phosphate amidotransferase gene from yeast. Pheromonal regulation of its transcription, *J Biol Chem 264*, 8753-8758.
93. Rivera-Ruiz, M. E., Rodríguez-Quiñones, J. F., Akamine, P., and Rodríguez-Medina, J. R. (2010) Post-transcriptional regulation in the myo1Δ mutant of Saccharomyces cerevisiae, *BMC genomics 11*, 690.
94. Sydorskyy, Y., Dilworth, D. J., Yi, E. C., Goodlett, D. R., Wozniak, R. W., and Aitchison, J. D. (2003) Intersection of the Kap123p-mediated nuclear import and ribosome export pathways, *Mol Cell Biol 23*, 2042-2054.
95. Mosammaparast, N., Guo, Y., Shabanowitz, J., Hunt, D. F., and Pemberton, L. F. (2002) Pathways mediating the nuclear import of histones H3 and H4 in yeast, *Journal of Biological Chemistry 277*, 862-868.
96. Mosammaparast, N., Guo, Y., Shabanowitz, J., Hunt, D. F., and Pemberton, L. F. (2002) Pathways mediating the nuclear import of histones H3 and H4 in yeast, *J Biol Chem 277*, 862-868.
97. Sydorskyy, Y., Dilworth, D., Yi, E., Goodlett, D., Wozniak, R., and Aitchison, J. (2003) Intersection of the Kap123p-mediated nuclear import and ribosome export pathways, *Molecular and cellular biology 23*, 2042-2054.
98. Rout, M. P., Blobel, G., and Aitchison, J. D. (1997) A distinct nuclear import pathway used by ribosomal proteins, *Cell 89*, 715-725.
99. Schlenstedt, G., Smirnova, E., Deane, R., Solsbacher, J., Kutay, U., Görlich, D., Ponstingl, H., and Bischoff, F. R. (1997) Yrb4p, a yeast Ran–GTP-binding protein involved in import of ribosomal protein L25 into the nucleus, *The EMBO Journal 16*, 6237-6249.

100. Jonker, J., Wiegant, W., van der Spek, J., and Grivell, L. (1998) Identification of YIL094C as the gene for homo-isocitrate dehydrogenase (LYS12) in Saccharomyces cerevisiae.
101. Cherest, H., Surdin-Kerjan, Y., Exinger, F., and Lacroute, F. (1978) S-adenosyl methionine requiring mutants in Saccharomyces cerevisiae: evidences for the existence of two methionine adenosyl transferases, *Molecular and General Genetics MGG 163*, 153-167.
102. Thomas, D., and Surdin-Kerjan, Y. (1997) Metabolism of sulfur amino acids in Saccharomyces cerevisiae, *Microbiology and Molecular Biology Reviews 61*, 503-532.
103. Klockenbusch, C., and Kast, J. (2010) Optimization of Formaldehyde Cross-Linking for Protein Interaction Analysis of Non-Tagged Integrin *BioMed Research International 2010*.
104. Guerrero, C., Tagwerker, C., Kaiser, P., and Huang, L. (2006) An Integrated Mass Spectrometry-based Proteomic Approach Quantitative Analysis of Tandem Affinity-purified in vivo Cross-linked Protein Complexes (qtax) to Decipher the 26 s Proteasome-interacting Network, *Molecular & Cellular Proteomics 5*, 366-378.
105. Vasilescu, J., Guo, X., and Kast, J. (2004) Identification of protein-protein interactions using in vivo cross-linking and mass spectrometry, *Proteomics 4*, 3845-3854.
106. Tardiff, D. F., Abruzzi, K. C., and Rosbash, M. (2007) Protein characterization of Saccharomyces cerevisiae RNA polymerase II after in vivo cross-linking, *Proceedings of the National Academy of Sciences 104*, 19948-19953.
107. Orlando, V., Strutt, H., and Paro, R. (1997) Analysis of Chromatin Structure by< i> in Vivo</i> Formaldehyde Cross-Linking, *Methods 11*, 205-214.
108. Ethier, M., Lambert, J.-P., Vasilescu, J., and Figeys, D. (2006) Analysis of protein interaction networks using mass spectrometry compatible techniques, *Analytica chimica acta 564*, 10-18.
109. Metz, B., Kersten, G. F., Hoogerhout, P., Brugghe, H. F., Timmermans, H. A., De Jong, A., Meiring, H., ten Hove, J., Hennink, W. E., and Crommelin, D. J. (2004) Identification of formaldehyde-induced modifications in proteins reactions with model peptides, *Journal of Biological Chemistry 279*, 6235-6243.
110. Metz, B., Kersten, G. F., Baart, G. J., de Jong, A., Meiring, H., ten Hove, J., van Steenbergen, M. J., Hennink, W. E., Crommelin, D. J., and Jiskoot, W. (2006) Identification of formaldehyde-induced modifications in proteins: reactions with insulin, *Bioconjugate chemistry 17*, 815-822.
111. Sutherland, B. W., Toews, J., and Kast, J. (2008) Utility of formaldehyde cross-linking and mass spectrometry in the study of protein–protein interactions, *Journal of mass spectrometry 43*, 699-715.
112. Klopotowski, T., and Wiater, A. (1965) Synergism of aminotriazole and phosphate on the inhibition of yeast imidazole glycerol phosphate dehydratase, *Archives of Biochemistry and Biophysics 112*, 562-566.
113. Falco, S., and Dumas, K. (1985) Genetic analysis of mutants of Saccharomyces cerevisiae resistant to the herbicide sulfometuron methyl, *Genetics 109*, 21-35.

114. Romanos, M. A., Scorer, C. A., and Clare, J. J. (1992) Foreign gene expression in yeast: a review, *Yeast 8*, 423-488.
115. Terpe, K. (2003) Overview of tag protein fusions: from molecular and biochemical fundamentals to commercial systems, *Applied microbiology and biotechnology 60*, 523-533.
116. Hitzeman, R. A., Clarke, L., and Carbon, J. (1980) Isolation and characterization of the yeast 3-phosphoglycerokinase gene (PGK) by an immunological screening technique, *Journal of Biological Chemistry 255*, 12073-12080.
117. Vasilescu, J., Guo, X., and Kast, J. (2004) Identification of protein-protein interactions using in vivo cross-linking and mass spectrometry, *Proteomics 4*, 3845-3854.
118. Trinkle-Mulcahy, L., Boulon, S., Lam, Y. W., Urcia, R., Boisvert, F.-M., Vandermoere, F., Morrice, N. A., Swift, S., Rothbauer, U., and Leonhardt, H. (2008) Identifying specific protein interaction partners using quantitative mass spectrometry and bead proteomes, *The Journal of cell biology 183*, 223-239.
119. Maere, S., Heymans, K., and Kuiper, M. (2005) BiNGO: a Cytoscape plugin to assess overrepresentation of gene ontology categories in biological networks, *Bioinformatics 21*, 3448-3449.
120. Ben-Shem, A., de Loubresse, N. G., Melnikov, S., Jenner, L., Yusupova, G., and Yusupov, M. (2011) The structure of the eukaryotic ribosome at 3.0 Å resolution, *Science 334*, 1524-1529.
121. Kressler, D., Hurt, E., and Baβler, J. (2010) Driving ribosome assembly, *Biochimica et Biophysica Acta (BBA)-Molecular Cell Research 1803*, 673-683.
122. Rotenberg, M. O., Moritz, M., and Woolford, J. (1988) Depletion of Saccharomyces cerevisiae ribosomal protein L16 causes a decrease in 60S ribosomal subunits and formation of half-mer polyribosomes, *Genes & development 2*, 160-172.
123. Enyenihi, A. H., and Saunders, W. S. (2003) Large-scale functional genomic analysis of sporulation and meiosis in Saccharomyces cerevisiae, *Genetics 163*, 47-54.
124. Haarer, B., Viggiano, S., Hibbs, M. A., Troyanskaya, O. G., and Amberg, D. C. (2007) Modeling complex genetic interactions in a simple eukaryotic genome: actin displays a rich spectrum of complex haploinsufficiencies, *Genes & development 21*, 148-159.
125. Komili, S., Farny, N. G., Roth, F. P., and Silver, P. A. (2007) Functional specificity among ribosomal proteins regulates gene expression, *Cell 131*, 557-571.
126. Naora, H., and Naora, H. (1999) Involvement of ribosomal proteins in regulating cell growth and apoptosis: translational modulation or recruitment for extraribosomal activity?, *Immunology and cell biology 77*, 197-205.
127. Jang, C.-Y., Lee, J. Y., and Kim, J. (2004) RpS3, a DNA repair endonuclease and ribosomal protein, is involved in apoptosis, *FEBS Letters 560*, 81-85.
128. Kim, J., Chubatsu, L. S., Admon, A., Stahl, J., Fellous, R., and Linn, S. (1995) Implication of mammalian ribosomal protein S3 in the processing of DNA damage, *Journal of Biological Chemistry 270*, 13620-13629.

129. Neumann, F., and Krawinkel, U. (1997) Constitutive Expression of Human Ribosomal Protein L7 Arrests the Cell Cycle in G< sub> 1</sub> and Induces Apoptosis in Jurkat T-Lymphoma Cells, *Experimental cell research 230*, 252-261.
130. Lindström, M. S. (2009) Emerging functions of ribosomal proteins in gene-specific transcription and translation, *Biochemical and Biophysical Research Communications 379*, 167-170.
131. Deane, C. M., Salwiński, Ł., Xenarios, I., and Eisenberg, D. (2002) Protein interactions two methods for assessment of the reliability of high throughput observations, *Molecular & Cellular Proteomics 1*, 349-356.
132. Ramirez, M., Wek, R. C., Vasquez de Aldana, C. R., Jackson, B. M., Freeman, B., and Hinnebusch, A. G. (1992) Mutations activating the yeast eIF-2α kinase GCN2: Isolation of alleles altering the domain related to histidyl-tRNA synthetases, *Molecular and cellular biology 12*, 5801-5815.
133. Wek, R. C., Ramirez, M., Jackson, B. M., and Hinnebusch, A. G. (1990) Identification of positive-acting domains in GCN2 protein kinase required for translational activation of GCN4 expression, *Molecular and cellular biology 10*, 2820-2831.
134. Zhu, S., and Wek, R. C. (1998) Ribosome-binding domain of eukaryotic initiation factor-2 kinase GCN2 facilitates translation control, *Journal of Biological Chemistry 273*, 1808-1814.
135. Sattlegger, E., and Hinnebusch, A. G. (2005) Polyribosome binding by GCN1 is required for full activation of eukaryotic translation initiation factor 2α kinase GCN2 during amino acid starvation, *Journal of Biological Chemistry 280*, 16514-16521.
136. Muhs, M., Yamamoto, H., Ismer, J., Takaku, H., Nashimoto, M., Uchiumi, T., Nakashima, N., Mielke, T., Hildebrand, P. W., and Nierhaus, K. H. (2011) Structural basis for the binding of IRES RNAs to the head of the ribosomal 40S subunit, *Nucleic acids research*, gkr114.
137. Meskauskas, A., and Dinman, J. D. (2007) Ribosomal protein L3: gatekeeper to the A site, *Molecular Cell 25*, 877-888.
138. Folley, L. S., and Fox, T. D. (1994) Reduced dosage of genes encoding ribosomal protein S18 suppresses a mitochondrial initiation codon mutation in Saccharomyces cerevisiae, *Genetics 137*, 369-379.
139. Bommer, U., Lutsch, G., Stahl, J., and Bielka, H. (1991) Eukaryotic initiation factors eIF-2 and eIF-3: interactions, structure and localization in ribosomal initiation complexes, *Biochimie 73*, 1007-1019.
140. Westermann, P., Heumann, W., Bommer, U.-A., Bielka, H., Nygard, O., and Hultin, T. (1979) Crosslinking of initiation factor eIF-2 to proteins of the small subunit of rat liver ribosomes, *FEBS Letters 97*, 101-104.
141. Xue, S., and Barna, M. (2012) Specialized ribosomes: a new frontier in gene regulation and organismal biology, *Nature reviews Molecular cell biology 13*, 355-369.
142. Planta, R. J., and Mager, W. H. (1998) The list of cytoplasmic ribosomal proteins of Saccharomyces cerevisiae, *Yeast 14*, 471-477.
143. Sattlegger, E., and Hinnebusch, A. G. (2005) Polyribosome binding by GCN1 is required for full activation of eukaryotic translation initiation factor 2{alpha} kinase GCN2 during amino acid starvation, *The Journal of biological chemistry 280*, 16514-16521.

144. Sickmann, A., Reinders, J., Wagner, Y., Joppich, C., Zahedi, R., Meyer, H. E., Schönfisch, B., Perschil, I., Chacinska, A., and Guiard, B. (2003) The proteome of Saccharomyces cerevisiae mitochondria, *Proceedings of the National Academy of Sciences 100*, 13207-13212.
145. Ferguson, L. R., and Von Borstel, R. (1992) Induction of the cytoplasmic 'petite'mutation by chemical and physical agents in< i> Saccharomyces cerevisiae</i>, *Mutation Research/Fundamental and Molecular Mechanisms of Mutagenesis 265*, 103-148.
146. Lam, K., and Marmur, J. (1977) Isolation and characterization of Saccharomyces cerevisiae glycolytic pathway mutants, *Journal of Bacteriology 130*, 746-749.
147. Lu, Z., Xu, X., Fassett, J., Kwak, D., Liu, X., Hu, X., Wang, H., Guo, H., Xu, D., and Yan, S. (2013) Loss of the Eukaryotic Initiation Factor 2α Kinase General Control Nonderepressible 2 Kinase Protects Mice From Pressure Overload–Induced Congestive Heart Failure Without Affecting Ventricular Hypertrophy, *Hypertension*, HYPERTENSIONAHA. 113.02313.
148. Parsons, A. B., Brost, R. L., Ding, H., Li, Z., Zhang, C., Sheikh, B., Brown, G. W., Kane, P. M., Hughes, T. R., and Boone, C. (2004) Integration of chemical-genetic and genetic interaction data links bioactive compounds to cellular target pathways, *Nat Biotechnol 22*, 62-69.
149. Izumi, H., Torigoe, T., Ishiguchi, H., Uramoto, H., Yoshida, Y., Tanabe, M., Ise, T., Murakami, T., Yoshida, T., Nomoto, M., and Kohno, K. (2003) Cellular pH regulators: potentially promising molecular targets for cancer chemotherapy, *Cancer Treat Rev 29*, 541-549.
150. Lam, K. K., Davey, M., Sun, B., Roth, A. F., Davis, N. G., and Conibear, E. (2006) Palmitoylation by the DHHC protein Pfa4 regulates the ER exit of Chs3, *The Journal of cell biology 174*, 19-25.
151. Skube, S. B., Chaverri, J. M., and Goodson, H. V. (2010) Effect of GFP tags on the localization of EB1 and EB1 fragments in vivo, *Cytoskeleton 67*, 1-12.
152. Dong, J., Qiu, H., Garcia-Barrio, M., Anderson, J., and Hinnebusch, A. (2000) Uncharged tRNA activates GCN2 by displacing the protein kinase moiety from a bipartite tRNA-binding domain, *Molecular Cell 6*, 269-279.
153. Dever, T. E., Chen, J.-J., Barber, G. N., Cigan, A. M., Feng, L., Donahue, T. F., London, I. M., Katze, M. G., and Hinnebusch, A. G. (1993) Mammalian eukaryotic initiation factor 2 alpha kinases functionally substitute for GCN2 protein kinase in the GCN4 translational control mechanism of yeast, *Proceedings of the National Academy of Sciences 90*, 4616-4620.
154. Hannig, E., and Hinnebusch, A. (1988) Molecular analysis of GCN3, a translational activator of GCN4: evidence for posttranslational control of GCN3 regulatory function, *Molecular and cellular biology 8*, 4808-4820.
155. Collart, M. A. (2003) Global control of gene expression in yeast by the Ccr4-Not complex, *Gene 313*, 1-16.
156. Coller, J., and Parker, R. (2004) Eukaryotic mRNA decapping, *Annual review of biochemistry 73*, 861-890.
157. Houseley, J., and Tollervey, D. (2009) The many pathways of RNA degradation, *Cell 136*, 763-776.

158. Sun, M., Schwalb, B., Pirkl, N., Maier, K. C., Schenk, A., Failmezger, H., Tresch, A., and Cramer, P. (2013) Global analysis of eukaryotic mRNA degradation reveals Xrn1-dependent buffering of transcript levels, *Mol Cell 52*, 52-62.
159. Frischmeyer, P. A., van Hoof, A., O'Donnell, K., Guerrerio, A. L., Parker, R., and Dietz, H. C. (2002) An mRNA surveillance mechanism that eliminates transcripts lacking termination codons, *Science 295*, 2258-2261.
160. Kim, J., Ljungdahl, P., and Fink, G. (1990) kem mutations affect nuclear fusion in Saccharomyces cerevisiae, *Genetics 126*, 799.
161. Bashkirov, V. I., Solinger, J. A., and Heyer, W.-D. (1995) Identification of functional domains in the Sep1 protein (= Kem1, Xrn1), which is required for transition through meiotic prophase in Saccharomyces cerevisiae, *Chromosoma 104*, 215-222.
162. Cambiaghi, T. D., Pereira, C. M., Shanmugam, R., Bolech, M., Wek, R. C., Sattlegger, E., and Castilho, B. A. (2014) Evolutionarily conserved IMPACT impairs various stress responses that require GCN1 for activating the eIF2 kinase GCN2, *Biochemical and Biophysical Research Communications 443*, 592-597.
163. Beck, J., RIPKA, S., SIEGNER, A., SCHILTZ, E., and SCHWEIZER, E. (1990) The multifunctional 6-methylsalicylic acid synthase gene of Penicillium patulum, *European Journal of Biochemistry 192*, 487-498.
164. Alberts, A., Strauss, A., Hennessy, S., and Vagelos, P. (1975) Regulation of synthesis of hepatic fatty acid synthetase: binding of fatty acid synthetase antibodies to polysomes, *Proceedings of the National Academy of Sciences 72*, 3956-3960.
165. Wakil, S. J., Stoops, J. K., and Joshi, V. C. (1983) Fatty acid synthesis and its regulation, *Annual review of biochemistry 52*, 537-579.
166. Dudek, S. M., and Semenkovich, C. F. (1995) Essential amino acids regulate fatty acid synthase expression through an uncharged transfer RNA-dependent mechanism, *Journal of Biological Chemistry 270*, 29323-29329.
167. Alepuz, P. M., Matheos, D., Cunningham, K. W., and Estruch, F. (1999) The Saccharomyces cerevisiae RanGTP-binding protein Msn5p is involved in different signal transduction pathways, *Genetics 153*, 1219-1231.
168. Yoshida, K., and Blobel, G. (2001) The karyopherin Kap142p/Msn5p mediates nuclear import and nuclear export of different cargo proteins, *The Journal of cell biology 152*, 729-740.
169. Takano, A., Endo, T., and Yoshihisa, T. (2005) tRNA actively shuttles between the nucleus and cytosol in yeast, *Science 309*, 140-142.
170. Murthi, A., Shaheen, H. H., Huang, H.-Y., Preston, M. A., Lai, T.-P., Phizicky, E. M., and Hopper, A. K. (2010) Regulation of tRNA bidirectional nuclear-cytoplasmic trafficking in Saccharomyces cerevisiae, *Molecular Biology of the Cell 21*, 639-649.
171. Pathak, R., Bogomolnaya, L. M., Guo, J., and Polymenis, M. (2005) A role for KEM1 at the START of the cell cycle in Saccharomyces cerevisiae, *Current Genetics 48*, 300-309.